CHLORINATION KINETICS OF ZrO_2 IN AN RF PLASMA TAILFLAME

A

THESIS

by

OMER BICEROGLU, B.Sc., M.Sc.

Department of Chemical Engineering - McGill University

Under the Supervision of Dr. W.H. Gauvin

Submitted to the Faculty of Graduate Studies
and Research of McGill University in partial
fulfilment of the requirements for the
degree of Doctor of Philosophy

McGill University
MONTREAL, Canada

August 1978

CHLORINATION KINETICS OF ZrO_2

IN AN RF PLASMA TAILFLAME

ABSTRACT

The chlorination kinetics of ZrO_2 with and without a reducing agent was studied in a single stationary particle reactor system. A plasma of pure chlorine generated by an induction torch provided both the high-enthalpy field and the reacting gas. The influence on the rate of conversion of such parameters as temperature, chlorine concentration (in the presence of argon), particle diameter and porosity, were investigated. Based on experimental and theoretical studies, rate equations were developed for each reaction system under different rate-controlling mechanisms.

The chlorination of ZrO_2 with chlorine alone in the temperature range of 1540 - 2480 K obeyed a shrinking-core reaction model. The reaction was chemically-controlled below 1950 K and above this temperature both chemical and mass transfer resistances were important. The experimental results confirmed the theoretical analysis.

The reaction in the presence of carbon was studied in the temperature range of 1400 - 1950 K, and the rate was influenced by the separation distance between ZrO_2 and carbon particles, hence the shrinking-core model was not obeyed. A different conversion-time model was proposed. The rate was lower than the model predictions above a certain conversion, the level of which increased with both temperature and carbon content. The experimental results provided adequate information for the selection of optimum conditions with respect to reactor type, temperature and carbon content.

RESUME

La cinétique de chloration de ZrO_2 avec et sans agent réducteur a été étudiée en exposant une particule stationnaire à un plasma de chlore pur dans un réacteur, le plasma étant engendré par une torche à induction. L'influence sur le taux de conversion de paramètres tels que la température, la concentration du chlore (quand de l'argon était ajouté), le diamètre de la particule et sa porosité, a été étudiée. Basées sur les études théoriques et expérimentales, des équations cinétiques ont été développées pour les différents mécanismes de contrôle de la réaction.

La chloration de ZrO_2 avec du chlore pur dans l'intervalle de température de 1540 à 2480 K obéit au modèle "shrinking core." Le taux de conversion est contrôlé par la réaction chimique à moins de 1950 K, tandis qu'au dessus de cette température la résistance créée par le transfert de masse devient également importante. Les résultats expérimentaux confirment cette analyse théorique.

En présence de carbone, la réaction a été étudiée dans l'intervalle 1400 - 1950 K. Dans ces conditions la cinétique est influencée par la distance entre les particules de ZrO_2 et de carbone. Un nouveau modèle est proposé. Au-dessus d'un certain niveau de conversion, les résultats expérimentaux sont inférieurs à ceux prédits par le modèle, ce niveau croissant avec la température et la teneur en carbone. Les données expérimentales sont suffisantes pour permettre de choisir les conditions optimales pour la réaction en rapport avec le type de réacteur, le niveau de température et la teneur en carbone.

To my Mother

ACKNOWLEDGEMENTS

The author wishes to express his sincere thanks and his gratitude to all those who, in various ways, contributed to the work presented in this thesis.

To the members of the Plasma Technology Group, in particular, to Professor R.J. Munz and Dr. N.N. Sayegh, for many useful discussions and suggestions, and to fellow graduate students, Mr. M.T. Mehmetoglu for his generous help in the experimental work and in the final preparation of the thesis, and Mr. R. Reydon for providing stand-by safety assistance.

To fellow graduate students, Mr. B.Z. Uysal and Mr. E. Bayramli, for many interesting and fruitful discussions.

To Mr. A. Krish and the staff of the Chemical Engineering Workshop, and to Mr. R. Malboeuf of the Noranda Research Centre Workshop for prompt construction of essential items of the equipment; to the McGill University Mining and Metallurgical Engineering Department for the use of their facilities, and to Mr. J. Nesset, a graduate student of that department, for his help in the use of an X-ray Sedimentometer-Particle Size Analyzer; to the Noranda Research Centre for assistance with chemical analyses.

To the Safety Committee of the Chemical Engineering

Department for their assistance and efforts in making the experimental work safe.

To the National Research Council of Canada for their financial support in the form of a post graduate scholarship for a period of two years.

To Mrs. B. Toivanen for her patience and excellent typing of the manuscript, and to Mr. I. Sabadin for the preparation of the drawings.

Finally, the author extends his gratitude to his wife, Guler, and the rest of his family for their understanding, patience and encouragement, and to his little daughter, Ceyda, for contributing to the completion of this work at its earliest possible date.

Moreover, the author gives an expression of thanks to God, whose strength he always relies on.

TABLE OF CONTENTS

EXPERIMENTAL SECTION

APPENDICES

LIST OF FIGURES

PART II

LIST OF TABLES

GENERAL INTRODUCTION

GENERAL INTRODUCTION

To a far greater extent than for any other metal, with the exception of uranium, it can be said that zirconium, in its present highly-purified form, is truly a product of the nuclear age. No other metal offers such an unmatched combination of high-temperature strength, corrosion resistance, and unusually low neutron capture cross-section which have made the high performance of the Canadian CANDU reactor possible. Because of its high reactivity, the chemistry of zirconium has attracted researchers ever since it was discovered in the late eighteenth century, but it is only since the end of the Second World War that determined efforts have been made to separate the many impurities with which the native ore, zircon, is contaminated, in order to produce the high-purity metal required for nuclear applications in commercial quantities. Of these, hafnium is particularly difficult to eliminate because of its unusual chemical similarity with zirconium, in spite of the fact that its atomic weight is double that of zirconium.

The production methods currently used by Industry to produce the pure metal are both extremely complex (upward of forty process steps) and very costly. Typically, a modern plant

to produce three million pounds of pure zirconium annually would involve a capital expenditure of upward of 30 million dollars, with an operating cost of around $15 per kilo in the form of a sponge and $25 to $30 per kilo in semi-finished shapes. It is not surprising, therefore, that a considerable effort is currently being made to simplify the production process and lower its cost. The research project discussed in this thesis is an example of such an effort.

Without going into any of the details of zirconium production (this will be fully covered in the Literature Review section of this thesis), suffice to say that zirconium tetrachloride is an important intermediate not only in the current conventional process, but also in many of the newer processes which have recently been proposed. The direct high-temperature chlorination of zirconia (ZrO_2) to produce the tetrachloride may offer distinct advantages in the elaboration of future, more efficient production processes. This possibility is further enhanced if the use of a plasma flame is considered to generate the high temperature field necessary.

The literature on the chlorination of zirconia is scarce and is further limited to low temperatures (<1400 K). The primary objective of the present work was therefore to investigate the chlorination of zirconium oxide with and without carbon as a reducing agent at high temperatures (>1400 K). A chlorine plasma generated by an induction torch provided both the high-enthalpy

field and the reacting gas. It should be added that, to the author's knowledge, this is the first time that the generation of a plasma of pure chlorine and a kinetic study of this kind have been mentioned in the literature. As part of the project, a reactor system, complete with all auxiliary units, was designed and constructed to handle the hot and extremely corrosive chlorine gas, and to dispose of the off-gases safely. Measurement techniques had similarly to be developed to provide the required kinetic data. It is gratifying to report that the design of the reactor system proved to be so versatile that it will be used in other kinetic studies which will be undertaken in this laboratory in the near future.

In accordance with current practice, this thesis has been written as a number of individual sections which are complete in themselves, in that they each have a separate Introduction, Conclusion, Nomenclature and Bibliography. Thus, the experimental part of the thesis can be submitted for publication with little modification.

The thesis is divided into three main parts:

1. A Literature Review to provide the necessary background information on all related subjects: zirconium and its production methods; published kinetic studies on the chlorination of metal oxides relevant to this work; theoretical treatments of non-catalytic gas-solid reactions; and finally a description of

pertinent plasma phenomena and plasma gas-solid reactions.

2. A report on the theoretical and the experimental work related to the chlorination of zirconium oxide in the absence of a reducing agent.

3. A report of the work on the chlorination of zirconium oxide-graphite mixtures.

LITERATURE REVIEW

INTRODUCTION

The Review of the Literature is presented under the following four main headings:

1. Zirconium and Its Production Developments

2. Chlorination Kinetics of Metal Oxides

3. Mathematical Treatments of Non-Catalytic Gas-Solid Reactions

4. Plasma Phenomena and Plasma Gas-Solid Reactions

Since the chlorination of zirconium dioxide is an integral part of zirconium production techniques, the first section is aimed at providing background information on zirconium and its present and potential production methods, as well as related developments, including plasma applications. The second section presents a critical discussion of published works on the kinetics and reaction mechanisms of zirconium dioxide chlorination, as well as the chlorination of other metal oxides which might shed some additional light on this reaction. Due to the fact that understanding and interpretation of the mechanism of a gas-solid reaction is best obtained from its mathematical

representation, the third section is intended to give a fairly detailed overall view of the theoretical models representing non-catalytic gas-solid reactions, using a different - and hopefully novel - approach in classification. In an attempt to make the treatment as complete as possible, a full discussion of the inherent assumptions made in these models, of their mathematical complexities and of their potential fields of application, is also given.

Finally, since a plasma was used to generate the high-temperature heat source in the experimental part of this study, the last section of the Literature Review represents an attempt to provide a brief background on plasma-generating devices, on their operation and characteristics, and on their field of application in gas-solid reactions.

ZIRCONIUM AND ITS PRODUCTION DEVELOPMENTS

Although zirconium metal was discovered in 1789, its industrial uses have had a relatively short life, which began with the discovery of its nuclear properties during the late 1940's. Because of its low neutron absorption cross-section, its low radioactivity after radiation exposure plus its resistance to corrosion in high purity water, zirconium and its alloys (zircaloys) are used for the cladding of uranium dioxide fuel and for the permanent reactor core structural components in the pressurized

and boiling water reactors (Miller, 1954), (Shelton et al., 1956), (Kirk and Othmer, 1963). This initial major use stimulated the production of zirconium in the form of sponge and semi-finished shapes and it is now beginning to find increasing use in non-nuclear applications. A small quantity of commercial-grade zirconium metal is used as a corrosion-resistant construction material in the chemical industry (Stamper and Chin, 1970). Another small but growing market for commercial-grade zirconium is in the form of a very fine powder as a "getter" in vacuum tubes, as an ignition source in photo-flash and detonator applications and in the form of thin foils in flash bulbs (Sundaram et al., 1967). It is replacing tantalum in surgical applications (Reno, 1956).

Zirconium, formerly considered a rare element, is now known to be more plentiful in the earth's crust than nickel, copper, lead and zinc (Shelton et al., 1956). Zircon ($ZrSiO_4$) is the most widely distributed and most important source of the metal. A less important source mineral, because of its restricted occurrence, is baddeleyite, another form of zirconium oxide (Miller, 1954). Hafnium is almost invariably associated with zirconium minerals and the commercial zirconium (as opposed to nuclear-grade) will always contain hafnium in concentrations related to the Hf/Zr ratios of the source mineral. These Hf/Zr ratios vary from 0.017 to 0.049 for zircon and from 0.008 to 0.014 for baddeleyite (Ryan, 1968). Certain varieties of zircon

containing as much as 17 percent hafnia are the richest sources of hafnium.

The stability of the zirconium-oxygen bonding in zirconium silicates and zirconium oxide and the reactivity of zirconium towards the common gases, such as oxygen, nitrogen and hydrogen, even at moderate temperatures, make the production of the metal in a pure state a difficult task (Miller, 1954). This may be the reason for the passage of 130 years from the discovery of zirconium metal to the first production of pure metal by the iodide dissociation method of van Arkel and de Boer in 1925. For the first time, these workers obtained malleable metal that displayed the real properties of the element (Kroll and Schlechten, 1946). Following this development, it was recognized that a minute amount of gases like oxygen and nitrogen was the main cause for the embrittlement observed in previous works.

The U.S. Bureau of Mines initiated a research program in 1945 under the direction of W.J. Kroll in an attempt to develop a large-scale nuclear grade zirconium production method to supply the metal to the U.S. Navy. In the course of this work, Kroll and Schlechten (1946) published a critical survey of the literature on the metallurgy of zirconium, ranging from the ore to the metal product. The process finally developed by Kroll to produce zirconium metal free from most of the naturally-occurring contaminants, including hafnium, is covered extensively in the literature (Kroll et al., 1948, 1950), (Miller, 1954), (Shelton

et al., 1956) and became the major production technique, which it remains basically to this day. The overall process as originally conceived consisted of the following steps:

- reaction of zircon with carbon in an electric arc furnace to form zirconium carbide or carbonitride and volatile silicon monoxide;

- chlorination of the carbide to form zirconium tetrachloride;

- removal of hafnium and other contaminants by solvent extraction, to form high-purity zirconium oxide;

- chlorination of the pure zirconium oxide with carbon, to form the tetrachloride;

- further purification of zirconium tetrachloride and reduction with molten magnesium, and

- removal of magnesium chloride by vacuum distillation to produce zirconium sponge which, following vacuum remelting, was converted to ductile zirconium metal.

Figure 1 (from Noranda, 1977) summarizes the conventional Kroll Process, essentially used by Wah-Chang and Pechiney Ugine Kuhlmann. The actual production process entailed upward of 40 processing steps with corresponding high cost in material and chemicals, equipment and labour. Any reduction in the number of

FIGURE 1

THE CONVENTIONAL KROLL PROCESS

ESSENTIALLY AS USED BY WAH-CHANG

AND PECHINEY UGINE KHULMANN

(NORANDA, 1977)

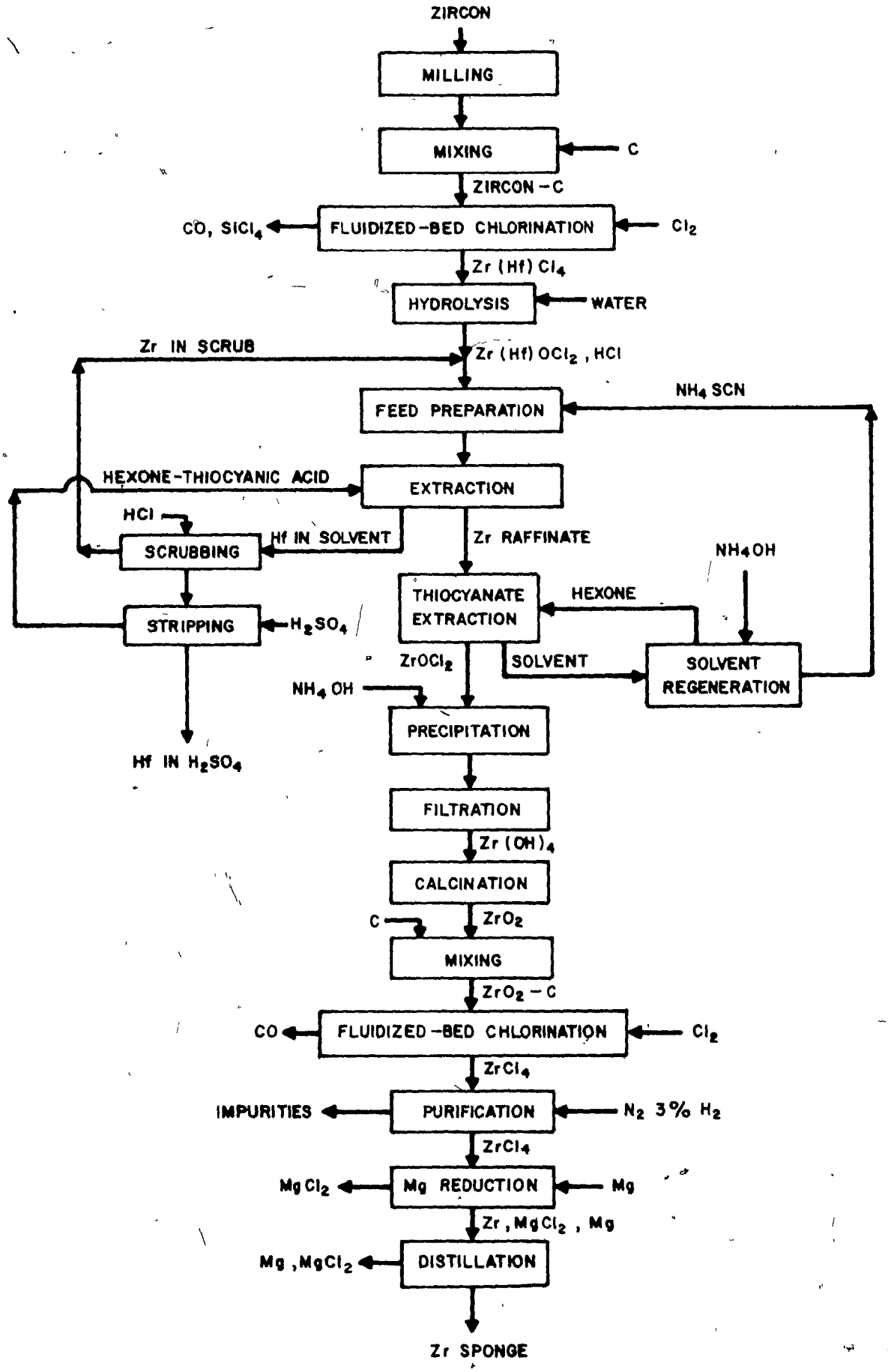
ZIRCON
MILLING
MIXING
C
ZIRCON – C
CO, $SiCl_4$
FLUIDIZED-BED CHLORINATION
Cl_2
Zr (Hf) Cl_4
HYDROLYSIS
WATER
Zr IN SCRUB
Zr (Hf) OCl_2 , HCl
NH_4 SCN
FEED PREPARATION
HEXONE-THIOCYANIC ACID
EXTRACTION
HCl
SCRUBBING
Hf IN SOLVENT
Zr RAFFINATE
NH_4OH
THIOCYANATE EXTRACTION
HEXONE
STRIPPING
H_2SO_4
$ZrOCl_2$
SOLVENT
SOLVENT REGENERATION
NH_4 OH
PRECIPITATION
Hf IN H_2SO_4
FILTRATION
Zr $(OH)_4$
CALCINATION
C
ZrO_2
MIXING
ZrO_2 – C
CO
FLUIDIZED-BED CHLORINATION
Cl_2
$ZrCl_4$
IMPURITIES
PURIFICATION
N_2 3% H_2
$ZrCl_4$
$MgCl_2$
Mg REDUCTION
Mg
Zr , $MgCl_2$, Mg
Mg , $MgCl_2$
DISTILLATION
Zr SPONGE

process steps or improvements in their respective efficiencies would not only reduce the cost, but also reduce the potential for impurities to enter into the system. The latter consideration is of considerable importance, since the purity specifications for the nuclear grade are extremely rigid. Hence, considerable research and development efforts have been devoted to virtually every step in the entire production spectrum.

The first step in recovering metallic zirconium is to "open" the ore, that is to break down the crystalline structure into its two oxide constituents. Zircon, like the silicates of most metals, is characterized by its relative chemical inertness. The various methods of "opening" zircon were summarized by Marden and Rich (1971), Kroll and Schlechten (1946) and also by Miller (1954). Chlorination constitutes one of these methods and has been well accepted by industry. As a matter of fact, the modern processes used by both Pechiney, Ugine Kuhlmann and by Teledyne-Wah Chang use it in preference to carbide formation.

Kroll, Carmody and Schlechten (1952) compared carbide (two steps) and zircon (one-step) chlorinations in reporting many sidelines that they investigated during the development of the Kroll process. Their recommendation was in favour of the two-step chlorination, based on the following factors. For the same output, the chlorinator needed for direct chlorination of zircon in the presence of carbon was about five times as large as the one used for the chlorination of carbide. Zircon powder (size less

than 200 mesh) and a large excess of carbon had to be used for effective chlorination of zircon. Furthermore, the zirconium loss in direct chlorination was higher than that of the carbide route and extra heat was required for the endothermic reaction.

Stephens and Gilbert (1952), although taking note of these disadvantages, nevertheless found carbide chlorination inefficient and less satisfactory. Instead, they proposed direct chlorination of pure zirconium dioxide which presented much less difficulty and lower operating costs than either the chlorination of zircon or that of zirconium carbide. Pilot plant studies and design for full-scale production equipment were described in their paper. Almond-shaped briquettes with dimensions of approximately 1-3/8 x 1 x 3/4 in. made up of 81 percent (-200 mesh) zirconium dioxide, 15 percent carbon black and 4 percent dextrine as a binder were chlorinated in a vertical shaft furnace reactor at 1173 - 1423 K. The source of pure zirconium dioxide was not reported.

Several patents on the subject of zircon and zirconia chlorination were issued. Anderson (1960) described the chlorination of -8 +200 mesh agglomerates of zircon and carbon in a fluidized bed at 973 - 1273 K. Wigton (1960) chlorinated a -65 +200 mesh zircon and carbon mixture in a fluidized bed at 1300 - 1423 K. Heat was supplied through the combustion of part of the carbon in the bed with oxygen. Callow and Bernard (1968) suggested the addition of 0.5 - 2 wt percent KCl together with coke to

chlorinate zircon. Ayukawa (1975) used pellets made up of -150 mesh zircon and petroleum coke for the chlorination of zircon.

McCord (1966) described chlorination of zirconium dioxide pelletized with a stoichiometric amount of carbon in a vertical shaft reactor at 1073 - 1273 K. Reaction was reported to be self-sustaining when the temperature in the reaction zone reached the operating temperature, after which external heat was discontinued.

Although reducing agents containing hydrogen are not recommended for the chlorination of zirconia and zircon due to the possibility of water formation which would in turn convert zirconium tetrachloride into the oxychloride in the condenser, in the patents claimed by George (1967) acetylene was suggested as the reducing agent, and more recently, Wilhelm (1974) proposed chlorohydrocarbons as the chlorinating and reducing agents for zirconia chlorination.

Sehra (1974) studied the chlorination of zirconium oxide with carbon monoxide and chlorine in batch and semi-continuous fluidized bed reactors. He reported 1023 K as an optimum operating temperature, above which reaction rate did not increase appreciably. Obviously, this temperature is not the optimum one, since a transition region occurs at about 900 - 1300 K in which the rate of chlorination stays constant and above which the reaction rate increases again (Landsberg et al., 1971). Sehra suggested that a

fluidized bed was more attractive than the industrial practice of using shaft furnace chlorination.

Recently, zircon chlorination was discussed by Manieh and Spink (1973), and Manieh, Scott and Spink (1974). They studied the chlorination in the presence of petroleum coke, both in static boat and in an electrothermal fluidized bed reactor. In the former, the individual effects of temperature, carbon/zircon ratio and chlorine concentration, and in the latter the influence of temperature, gas velocity and bed depth on chlorine utilization were evaluated. Sufficient fluidization of the bed was provided by the amount of chlorine used and the gaseous reaction products produced, thus, no diluting gas was required. The electrothermal fluidized bed reactor which was recommended by the authors as the only practical apparatus available for the chlorination of zircon sand on a commercial basis was described and the data needed to design such a reactor were given in their papers.

A somewhat different method of removing silica from zircon was proposed by White and Richmond (1972). Zircon was reacted with sulphur or other sulphur compounds at 1473 - 1673 K in the presence of hydrogen or carbon as reducing agent. Silica was removed as volatile SiS_2. Later Motoi and Kurita (1973) claimed removal of silica as the volatile halide and leaving zirconium dioxide as residue by reacting zircon with alkali earth halide and carbon at 1873 - 2173 K.

It was reported as early as 1923 (Kroll and Schlechten, 1946) that silica could be removed by dissociation of zircon at 2070 - 2400 K without the aid of carbon. But the mechanism and temperature of the dissociation process have been the subject of much discussion. Utseki et al. (1972) reviewed the previous work and studied the mechanism of this reaction. They concluded that fine zircon powder started to decompose at temperature as low as 1473 K, accompanied by sintering, but crystallization of zirconium dioxide (following dissociation) began at 1973 K.

For the last stages of zirconium production, the magnesium or magnesium-sodium reduction and vacuum distillation processes (Kroll process) have also been the topics of many studies and patent claims. Klimaszewski (1967), Ishizuka (1972), Kanji (1973a, 1973b) and recently Spink (1976) and Ishimatsu et al. (1976) described different equipment designs and modifications, suggesting improvements over the original Kroll process. In his latest patents, Ishizuka (1975a, 1975b) claimed a reduction in processing time, which was reported to be 1/3 that of the ordinary method.

Starrat (1959) gave detailed information on the production of nuclear-grade zirconium at the Ashtabula plant of Mallory Shanon Metals Corporation which used impure zirconium tetrachloride as raw material. The method of production was the same as the Kroll process except that instead of magnesium reduction, Ashtabula made use of what was claimed to be a lower cost reduction with sodium. Elger (1962) investigated the advantages

of using different reductants in the Kroll process and concluded that the use of a mixture of sodium and magnesium resulted in advantages such as higher purity, lower reaction temperature, easier separation and higher yield. These findings were later confirmed by Babu et al. (1969) and Chintamani et al. (1972) who carried out pilot plant work over the complete range from ore to metal to establish suitable equipment design and process conditions for large-scale operations in India.

Very recently, Spink (1977b) reviewed the historical development of the zirconium market in conjunction with the conventional production method and concluded that, due to the uncertainties and large fluctuations in zirconium demand caused by governmental policies, very little research and development work had been done in this highly demanding technological area over the last 20-25 years. As a consequence, the zirconium industry had changed very little from the original post-war operations installed years ago, despite the need for improvements or changes in these operations. In the same article, he described a new process ("The Spink Process") for the preparation of nuclear-grade zirconium and reasonably pure hafnium. The proposed process was claimed to be relatively pollution-free and more economical than the conventional process currently practised. A recent calculation by Spink (1977a) has showed that chemical costs associated with the new process are less than $1.00 per pound of zirconium sponge versus an estimated $3.23 for the

conventional process. The Spink process still uses the original concept of the Kroll process (magnesium reduction and vacuum distillation), the differences being due to improvements in individual operations (electrothermal fluidized bed chlorination of zircon, removal of hafnium in the tetrachloride form, etc.) and equipment designs, plus additional $SiCl_4$, Mg and chlorine recovery processes.

Among other production methods, the metallo-thermic reduction of zirconium oxide has found industrial use in the preparation of zirconium metal powder to be used as "getter" in vacuum tubes and as ignition source in photo-flash and detonator applications. This type of reduction is possible at a temperature of 1073 - 1273 K only in the presence of calcium (Roy 1964) which is the costliest among the metallic reducing agents (Ca, Mg, Al). While magnesium does not possess as high an affinity for oxygen as calcium, aluminum on the other hand creates difficulties due to the formation of solid aluminum-zirconium intermetallic compounds. Sandaram et al. (1967) investigated the preparation of micron size zirconium metal powder by the calciothermic reduction of zirconium dioxide at 1073 - 1223 K. Since the reaction of zirconium oxide with calcium is highly exothermic, it was found necessary to incorporate in the reaction charge a definite proportion of a heat-sink material such as $CaCl_2$ to minimize the sintering of the charge, which created difficulties in subsequent leaching treatments for the complete removal of calcium. They obtained a metal yield above 90 percent of theoretical in two-micron size range

using -325 mesh ZrO_2 with 50 percent excess Ca and half a mole of $CaCl_2$ per mole of ZrO_2. The residual oxygen content in the metal powders after reduction decreased from 2.34 percent to 0.10 percent by increasing the reaction temperature from 1073 K to 1223 K.

In his patent, Gallay et al. (1971) described the reduction of oxide with calcium in CaF_2 melt using a furnace heated by induction.

Another method which may have potential for the industrial production of zirconium is fused-salt electrowinning of the metal from zirconium tetrachloride. Martinez and Couch (1972) obtained high-purity zirconium on a laboratory scale by electrowinning from $ZrCl_4$, using a NaCl-NaF electrolyte which contained 2 wt. percent zirconium as $ZrCl_4$. The process temperature was 1073 K. Later, Martinez et al. (1976) proposed a twin cell design for large-scale operation. Zirconium metal meeting ASTM standards was produced only in electrolytes with a relatively low zirconium concentration (about 3 wt. percent). The rate of removal of chlorine from the anode was found to be limiting the rate of anodic reaction. They concluded that additional development work was still needed for this approach to gain commercial acceptance.

In parallel with the rapid advances which have been made in plasma technology over the last fifteen years, there has been a considerable number of investigations on the use of this technology in zirconium production. Brown (1967) presented a paper concerning

his work on the reduction of zirconium dioxide and zirconium tetrachloride to zirconium with the use of an arc plasma jet. His thermodynamic analysis showed that metal production by dissociation of zirconium dioxide in the absence of a reducing agent was not feasible. Zirconium dioxide partially dissociates on vaporizing to give the monoxide and atomic oxygen above 4300 K. Figure 2 from Brown's paper shows the stability of zirconium monoxide at quite high temperatures. Upon quenching, the products are Zr, ZrO and oxygen. But in the condensed phase, the monoxide is not stable and yields Zr and ZrO_2. In attempting to reduce zirconium dioxide to zirconium using carbon, Brown found that the residence time and particle size of the ZrO_2 were more important than the method of introducing carbon. Using 10-micron size ZrO_2 powder and a carbon tube to lengthen the plasma section, he reported an increase in zirconium content from 66.5 percent in the feed to 70 percent in the product. In the case of the decomposition of zirconium tetrachloride in an argon plasma, using a hydrogen dilution quench and also straight thermal quench, he reported an increase in zirconium content from 38.2 percent in the feed to 58.4 percent in the product. The products were not identified.

In their article concerning the state of the art in plasma chemistry, Vurzel and Polak (1970) indicated that they had had some success in reducing zirconium dioxide to zirconium in a hydrogen plasma. However, no further information was available concerning this work. The investigation of Matsumoto and Miyazaki (1971) on the reaction of zirconium dioxide with graphite

FIGURE 2

DISSOCIATION BEHAVIOUR OF ZrO_2

(BROWN, 1967)

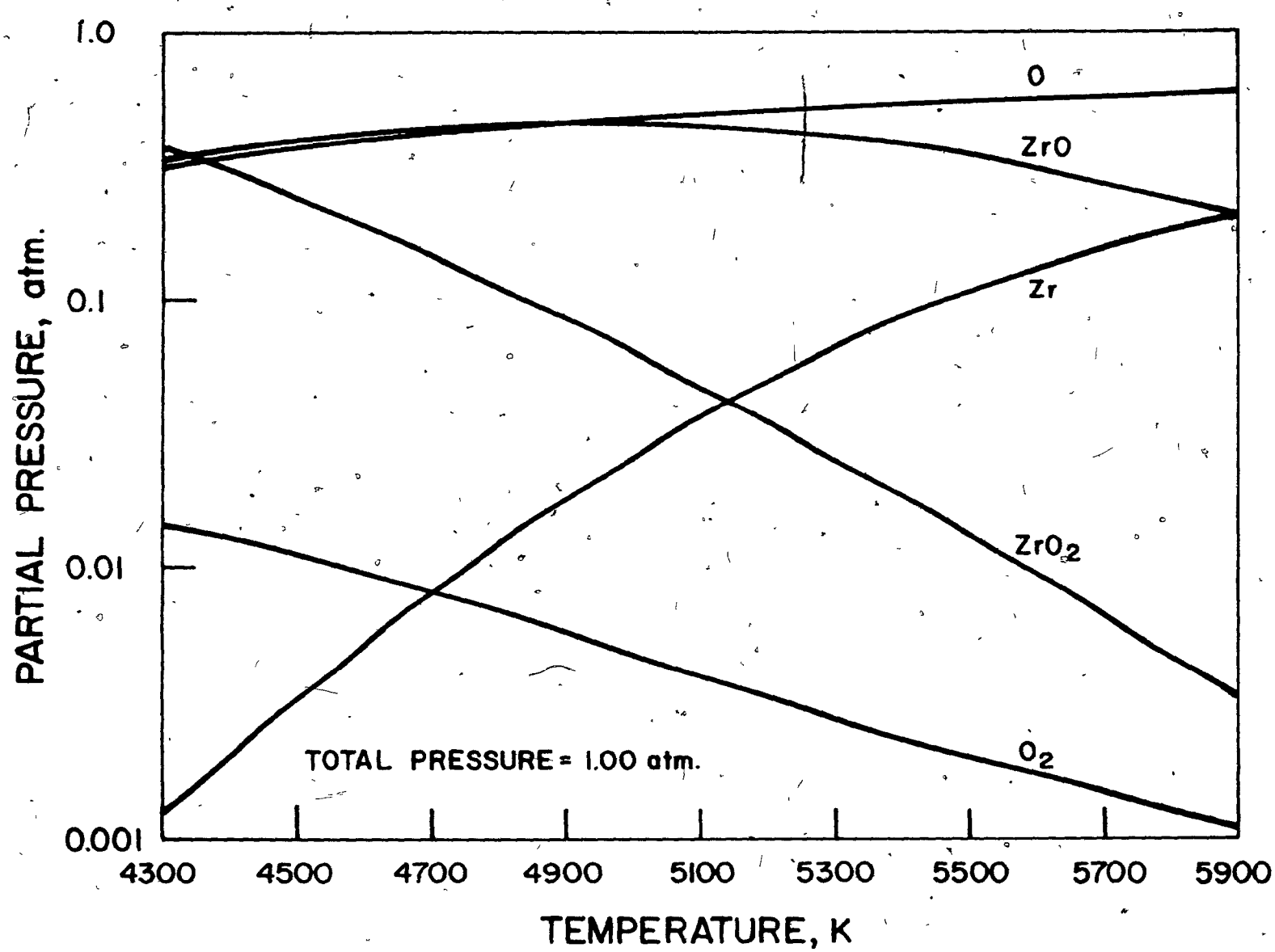
1.0
0.1
0.01
0.001
PARTIAL PRESSURE, atm.
4300
4500
4700
4900
5100
5300
5500
5700
5900
TEMPERATURE, K
O
ZrO
Zr
ZrO_2
O_2
TOTAL PRESSURE = 1.00 atm.

in argon and argon-hydrogen plasma jets showed that the final product composition was affected critically by the initial C/ZrO_2 ratio. The product consisted of Zr and ZrO_2 when the ratio C/ZrO_2 was one, and Zr, ZrC when the ratio was two.

Becherescu, Winter and Cicoare (1967) studied the reaction of ZrO_2 with metallic iron in a plasma jet supplied from a 60-kW unit. Their feed consisted of briquettes of ZrO_2 + Fe, with an iron content ranging from one to seventy percent. In each case, the final products consisted of a mixture of Zr, ZrO_2, Fe, FeO and Fe_3O_4. This was attributed to the short residence time in the plasma, in addition to the reaction condition.

Despite the earlier work of DiPietro and Findlay as reported by Abshire (1958) and of Kroll, Carmody and Schlechten (1952), some recent studies showed that the reduction or thermal decomposition of zirconium tetrachloride in argon or argon-hydrogen plasmas could be successful. Chizhikov, Deineka and Makarova (1969) and Chizhikov et al. (1971) reported the production of pyrophoric metal powders by reduction of $ZrCl_4$, WCl_6, $MoCl_3$ and $NbCl_5$ in an argon-hydrogen plasma. They also produced the respective oxides from the chlorides in an argon-oxygen plasma. Semenenko et al. (1975) studied the reduction of zirconium tetra and lower halides in a hydrogen plasma. The products contained the respective halogens and hydrogen in small quantities.

In his Ph.D. work, Gragg (1973) investigated the

feasibility of the thermal dissociation of zirconium tetrachloride in a radio-frequency argon plasma, produced from a 25-kW, 4-mHz generator. He collected the metallic zirconium at the centreline of the plasma by means of a water-cooled probe. The percent of feed collected ranged from 1.9 to 47.4. The percent conversion of $ZrCl_4$ to Zr based on the amount of metal collected ranged from 3.7 to 89.6. No information was given about the portion which was not collected. Quenching efficiency, position of the collecting probe in the plasma and the feed rate influenced the conversion. Gragg concluded that this process was technically feasible but not economical with the apparatus he used. This was due to the low efficiency which was reported to be 20% of the power input to the generator. The cost of production of zirconium from pure $ZrCl_4$ was estimated to be 5.3 cents per kg of zirconium which seems to be very unrealistic.

A patent by Little and Wentzell (1965) claims the use of Na or Mg in a plasma process to reduce chlorides of Zr, Ti, Nb and Mo. The process uses a transferred-arc plasma where the upper surface of a movable bar of the respective metal (which slides in a vertical water-cooled mold) acts as the anode. Chlorides are introduced into the plasma jet together with liquid sodium or powdered magnesium as the reducing agent. Pure metal is said to form as a molten pool at the anode. The process is attractive in that it produces not sponge but bulk metal.

Another patent (Ciba, 1966) disclosed the production of

non-pyrophoric powders of zirconium and some other metals by introduction of the chlorides with argon as a carrier gas into a hydrogen plasma.

The plasma dissociation of zircon into its component oxides was proposed as a preliminary route to zirconia and zirconium chemicals by Warren and Shimizu (1965). It has recently been the subject of a series of publications and patents as the basis for the Ionarc Process, which has enabled the manufacture of substantial quantities of plasma-dissociated zirconia with a high degree of conversion and low electrical energy requirement (Thorpe and Wilks, 1971), (Wilks et al., 1972, 1974), (Scammon et al., 1973). In this process, the finely-powdered zircon sand (<150 microns) is introduced with nitrogen as a carrier gas into the plasma flame of an Ionarc carbon arc furnace where it is melted and quickly quenched upon leaving the flame. Air jets introduced in the tailflame oxidize the carbon contaminants. This produces a product with high surface area from which the silica can easily be removed by a caustic leach. The purity of the final product depends on the number of leaching steps. The process is non-polluting in that there are no unwanted byproducts.

Very recently, Bayliss, Bryand and Sayce (1977) surveyed the earlier work on the thermal dissociation of zircon and described the development of a new form of arc heater which had the advantages of using non-consumable electrodes and permitted operation under carbon-free or oxidizing conditions.

CONCLUSION

Zirconium is proving to be a very useful metal but its use has so far been restricted by its relatively high price, due to the difficulties encountered in its production. Currently, research work is aimed at improving the efficiency of existing production methods and/or at finding alternative methods which would be less costly.

The review of both present industrial and potential production methods indicated the importance of zirconium tetrachloride as the intermediate product between the starting material zircon and the zirconium metal product. Development of the plasma process for the thermal dissociation of zircon into zirconia, plus the disadvantages of direct or indirect zircon chlorinations, may make the chlorination of zirconia more attractive than that of zircon. Depending upon the methods of removal of hafnium from zirconium, the chlorination of pure zirconium oxide becomes an essential part of the overall process when solvent extraction is used.

CHLORINATION KINETICS OF METAL OXIDES

CHLORINATION OF ZIRCONIUM DIOXIDE

Published works on the chlorination kinetics of zirconium dioxide are rather scarce. Two comprehensive kinetic studies (Landsberg et al., 1972), (O'Reilly et al, 1972) have

appeared in the literature recently, both of them covering temperature below 1400 K.

O'Reilly, Doig and Ratcliffe (1972) studied the reaction between zirconium dioxide, carbon and chlorine in a static bed in the temperature range of 940 to 1100 K using uncompacted, intimately mixed zirconium dioxide powder (15-micron particles, average) and petroleum coke (1 micron) in a weight ratio of one to four. It was reported that the reaction was chemically controlled and was taking place at the surface of the oxide particles. For conversions up to 30-80 percent, the time - vs - conversion data was correlated by the expression (shrinking-core):

$$1 - (1 - X)^{1/3} = Kt \qquad (1)$$

where $\underline{X}$ is the fraction of oxide reacted at time $\underline{t}$, and $\underline{K}$ is the overall rate constant. The activation energy and the order of reaction with respect to chlorine concentration were 230.7 kJ/mole and 0.64, respectively. Dependence of the reaction rate on the fractional power of chlorine concentration was attributed to the dissociation of chlorine molecules at the surface of the oxide.

The data of these authors showed that, at high conversions, the rate of reaction decreased significantly and conversion - vs - time deviated from the correlation predicted by the shrinking core model. The level of conversions at which this deviation occurred increased with increase in reaction temperature (for temperatures of 940 and 1100 K, deviations began to occur at

30 and 80 percent conversions, respectively). No explanation was given for this behaviour, beyond the mention that it was the subject of further investigation. The reason for such a reduction in the reaction rate, in the opinion of the present author, may be the change in the degree of contact between oxide and coke particles, which decreases as the reaction progresses. The importance of this intimate contact is less at high temperatures.

In their kinetic study, Landsberg, Hoatson and Block (1972) chlorinated both compacted powder and opaque single crystals of zirconium dioxide with carbon and carbon monoxide as reductants. They also investigated the chlorination of ZrO_2 single crystals with chlorine alone, these authors being the first to do so. Despite the fact that chlorination of ZrO_2 without reducing agent is thermodynamically not feasible, they managed to measure an appreciable rate of chlorination in the temperature range of 1320 to 1420 K and obtained an activation energy of 166.2 kJ/mole. They reported that the reaction rate was influenced by the total gas flow rate, at rates below 800 cc/min in a 25-mm reactor tube, suggesting a mass transfer effect.

The chlorination experiments with carbon were carried out between 1120 and 1320 K with disk pellets of zirconium dioxide surrounded by a loosely packed bed of carbon powder. The pellets, 15 mm in diameter and 5 mm in thickness, were compacted from ZrO_2 powder and sintered at 1273 K for one hour; they had a porosity of about 51 percent. In their work, the rate of chlorination in the

presence of carbon was found to be directly proportional to chlorine concentration which did not agree with the findings of O'Reilly et al. (1972) who reported proportionality to the 0.64 power of chlorine concentration. This may suggest that the manner of introducing the carbon and the reaction temperature may influence the reaction mechanism. As a matter of fact, the authors investigated the effect of carbon particle size on the reaction rate and found that coarser carbon particles resulted in lower reaction rates, which indicated the importance of oxide-carbon contact. Reaction was reported to be taking place at the surface and it was chemically controlled yielding an activation energy of 127.7 kJ/mole as opposed to 230.7 kJ/mole found by O'Reilly et al. Conversion - vs - time data were not correlated, nor were they presented.

Chlorination in the presence of carbon monoxide was studied by Landsberg et al. with compacted disk pellets of ZrO_2 at 675 - 1375 K and with single crystals of ZrO_2 at 875 - 1375 K. The chlorination rate with compacted samples was almost ten times that of single crystals at the same temperature of 1275 K. It was reported that reaction occurred within the entire porous structure of compacts exposed to carbon monoxide and chlorine, and the initial reaction rate showed a direct relationship to sample volumes and weight, irrespective of geometric surfaces. However, the change in reactivity observed by these authors as the reaction proceeded, for both types of samples, indicated that the available

surface area for the reaction played an important role in the reaction rate. The relationship between the rate of chlorination and the gas concentrations, as well as the activation energies, were found to be different at high and low temperatures. A transition zone in the temperature range of 900 - 1200 K was observed with both types of samples. In this zone, the rate either decreased or remained almost constant. This was explained by the transition in the carbon monoxide-carbon dioxide equilibrium and its resulting effect on the reaction mechanism. The same phenomenon was observed by Dunn (1960) in the chlorination of TiO_2 with phosgene ($COCl_2$) and with carbon monoxide plus chlorine.

The order of carbon monoxide reaction with respect to chlorine and carbon monoxide at 1273 K was reported as 0.6 and 0.5, respectively. The corresponding activation energy was about 96.3 kJ/mole.

On the basis of a thermodynamic analysis, Vasilenko and Vol'skii (1958) concluded that chlorination of ZrO_2 by chlorine alone was ineffective, even at temperatures between 1273 and 1773 K. At equilibrium, the product (zirconium tetrachloride) concentration in the gaseous phase was low and with a rise of temperature in the indicated limits, it increased insignificantly from 0.2 to 2.7 volume percent. They also showed that, at temperatures below 973 K, chlorination of ZrO_2 in the presence of solid carbon took place according to the reaction

$$ZrO_2 + C + 2\ Cl_2 \rightarrow ZrCl_4 + CO_2 \qquad (2)$$

while above 1300 K, it took place entirely according to:

$$ZrO_2 + 2\ C + 2\ Cl_2 \rightarrow ZrCl_4 + 2CO \qquad (3)$$

A recent work by Sehra (1974) reports on the fluidized-bed chlorination of nuclear-grade zirconium dioxide with carbon monoxide and chlorine. He did not carry out a kinetic study in the strict sense of the term, but rather investigated the effects of operating variables such as flow rates of CO and Cl_2, bed-height, temperature and residence time on the percent chlorination, in order to establish the optimum operating conditions. Sehra reported a linear relationship between percentage chlorination of ZrO_2 and reaction time at 1073 K up to 40 percent conversion, above which the rate dropped off. He interpreted this effect on the premise that, in the initial stages, with the generation of surface pores, the effective surface area remained constant; at a certain stage of the chlorination, the effective surface area and hence the rate of chlorination must begin to decrease. This explanation may be appropriate, however, it is known that the rate in gas-solid non-catalytic reactions generally varies with time and is basically transient (Szekely et al., 1976), since the amount of reactant surface and its availability changes with the extent of reaction. The conversion - versus - time data reported by Sehra was re-analysed by the author of this thesis. A plot of fractional conversion of ZrO_2 in the form of $[1 - (1 - x)^{1/3}]$ versus time resulted in a straight line at all conversion levels, suggesting that chlorination of ZrO_2 with carbon monoxide

and chlorine was a chemically-controlled surface reaction described by a shrinking-core model. Hence, the drop in the reaction rate mentioned by Sehra was really due to a decrease in geometrical surface area resulting from the shrinking of the reacting particles.

Sehra (1974) also concluded that a temperature of 1073 K was an optimum reaction temperature since the rate of reaction above this temperature did not increase much. This may not be true in the light of the results reported by Landsberg et al. (1972) who observed a transition region centered at about 1073 K in the ($CO + Cl_2$) chlorination of ZrO_2. In this region, the rate of the reaction was almost constant, but above 1173 K the rate started to increase again.

The paper published by Pogonina and Ivashentsev (1974) was very brief and was concerned with the chlorination of ZrO_2, HfO_2 and TiO_2 with and without carbon monoxide as reductant. The activation energy of 425.8 kJ/mole for the $ZrO_2 + Cl_2$ reaction reported by the authors seems to be very high. It appears to be based on only two experimental data points in a narrow temperature range (1173 - 1273 K).

CHLORINATION OF OTHER METAL OXIDES

A large number of publications have been accumulated in the literature on the chlorination of different ores and metal oxides. While a complete review is outside the scope of this

thesis, a brief discussion of some selected papers relevant to this study will be useful, on the premise that most of the metal oxide chlorination reactions may show at least similar qualitative behaviour.

The most controversial subject in this field has been the mechanism of the reaction. It has found the least agreement among different investigators, particularly among those who have studied the same system. The paper published by Seryakov et al. (1967) is concerned with the mechanism of chlorination of titanium dioxide by chlorine in the presence of carbon. The existing views on this matter at that time, as reported by the authors, were:

1. The metal oxide is first reduced by carbon or carbon monoxide to a lower oxide, which in turn reacts with chlorine to form the tetrachloride.

2. Chlorine reacts with the metal oxide to form the tetrachloride and elemental oxygen. The latter combines with carbon to form carbon dioxide or carbon monoxide.

3. The metal oxide is chlorinated by carbonyl chloride (phosgene $COCl_2$) formed as a result of the reaction of chlorine either with carbon monoxide or carbon dioxide in the presence of carbon.

4. Chlorination takes place with the aid of chlorocarbons formed on the surface of carbon due to the adsorbtion of

chlorine. It necessitates contact between the oxide and the carbon particles.

5. Chlorination proceeds through the formation of COCl-type of radicals. This occurs in the absence of direct contact between the particles of metal oxide and carbon.

On the basis of their experimental evidence, Seryakov et al. (1967) concluded that the chlorination of titanium dioxide by chlorine and carbon in the temperature range of 626 to 777 K proceeds without the participation of such intermediates as elemental oxygen, oxides of titanium in a lower valency, or phosgene.

Bergholm (1961) investigated the chlorination of rutile (TiO_2) in various ways and provided valuable information on the mechanism of the reaction and the parameters influencing the rate of the chlorination. In an attempt to establish the importance of contact between the oxide and the carbon particles, the author chlorinated a rutile tablet placed on top of a cubic carbon pellet. The rutile tablet had two small holes (450-micron deep) on the surface in contact with the carbon pellet. It was reported that the rutile reacted only where the two pieces had been in contact with one another. Almost no reaction took place in the bottom of the holes in spite of the fact that they must have been filled with carbon monoxide (produced during the reaction) and chlorine. From microscopic examination of the contact surfaces, Bergholm concluded that the reaction was strongly promoted by carbon if the distance

between the carbon and the rutile was less than 200 microns or so. He indicated that the points of contact did not react faster than surfaces 50 microns apart. Hence, the distance rather than the direct contact between the rutile and the carbon grains was found to be important. These findings were confirmed by chlorinating mixtures of the rutile and the carbon in pellet and loose forms. He found that the rate of dense pellets at 973 K was ten times higher than that of the loose mixture but the difference between the chlorination rates was less pronounced at 1120 K.

Another evidence showing the importance of the degree of contact between the carbon and the rutile grains was obtained from further treatment of residues of previous experiments in which the reaction almost stopped after 70 percent conversion. The residue was chlorinated once more after it had been thoroughly mixed. It was found that 60 percent of the residue could be further chlorinated. In another experiment, the residue was mixed with more carbon, but this addition did not cause a greater increase in the reaction rate than did mixing of the residue without new carbon. This important observation shows that the reaction slows down or stops after a certain amount of conversion not because of carbon deficiency or a loss of reactivity of constituents, but rather because of a decrease in the degree of contact between the rutile and the carbon grains.

Bergholm suggested that the reaction probably proceeded through the formation of an intermediate unstable compound such as

COCl-radicals, and that the formation of phosgene was less probable due to its dissociation into CO and Cl_2 at the reaction temperatures. He also found that the chlorination rate below 1273 K in the presence of carbon was much higher than that with CO, and recommended the use of a static bed rather than that of a fluidized bed reactor for chlorination in the presence of carbon.

In their investigation of the chlorination kinetics and reaction mechanism of different minerals including zircon, Stefanyuk and Morozov (1965) suggested that phosgene was the most probable intermediate activator of the process, even though this suggestion was rejected earlier by Bergholm (1961). The authors did not deny the possibility of formation of carbon-chlorine compounds or COCl-type radicals, but preferred the following stepwise mechanism:

$$Cl_2 + CO_{ads} = COCl_2 \qquad (4)$$

$$2COCl_2 + MeO_2 = MeCl_4 + 2CO_2 \qquad (5)$$

$$CO_2 + C = CO_{ads} + CO \qquad (6)$$

According to this scheme, chlorine reacts with intermediate surface oxides of carbon to form phosgene, and carbon dioxide reacts with carbon and regenerates the surface carbon oxides. The proposed mechanism does not require a direct contact between the metal oxide and the carbon particles but omits an initiation step. Based on their experimental evidence, Seryakov et al. (1967) later rejected the participation of phosgene as an intermediate chlorinating agent in the chlorination of titanium dioxide.

Stefanyuk and Morozov chlorinated uncompacted mixtures of zircon and carbon powders in the temperature range of 973 - 1473 K and obtained an activation energy of 97.6 kJ/mole. The process was found to be one of chemically-controlled surface reaction for a shrinking particle.

A comprehensive study of the influence of carbon on the chlorination of titanium dioxide was reported by Seryakov et al. (1970). They chlorinated disk pellets made out of titanium dioxide and different carbonaceous materials such as lamp black, petroleum coke and carbon obtained from the pyrolysis of sugar. It was reported that the chlorination rate in a chemically-controlled region was limited by the area of direct contact between the metal oxide and the carbon particles. The increased contact area provided by the pyrolyzed sugar and by a high pellet-forming pressure resulted in higher chlorination rate. This limiting step, plus the activation energy of the chlorination (268 - 285 kJ/mole) and the order of the reaction with respect to chlorine concentration (0.63 - 0.71) remained almost the same for all three types of carbon. However, the pre-exponential factor in the Arrhenius equation was found to be different and the highest one was obtained with the pryolysed sugar.

As for the mechanism of chlorination, Seryakov et al. proposed that the reaction proceeded through the transfer of molecules of an intermediate product formed on the carbon particles to the surface of the titanium dioxide particles at the points of

direct contact. Accordingly, the first step was the interaction of chlorine with carbon. The transfer of the intermediate product was reported to be the rate-limiting step, but the nature of this intermediate product was not given. On the basis of this proposed mechanism, the authors derived the empirical equation:

$$\ln (1 - \Delta W/\Delta W_{\infty}) = -Kt \qquad (7)$$

reported by them earlier on an experimental basis (Seryakov et al., 1967a). They assumed that:

1. The rate was proportional to the available contact area between the oxide and the carbon particles ($dW/dt \alpha S$), and

2. the rate of decrease of the contact area was proportional to the available contact area ($dS/dt \alpha S$).

These two assumptions imply that the reaction decreases and eventually stops when the contact area diminishes and ΔW_{∞} becomes the maximum amount of metal oxide that can be chlorinated.

The theoretical treatment and the experimental results of Seryakov et al. (1970) confirm the observations of Bergholm (1961) except that Bergholm suggested the necessity of a close distance (less than 200 microns) rather than the direct contact between the oxide and the carbon particles. In a paper concerning the chlorination of zircon in the presence of carbon, Manieh, Scott and Spink (1974) suggested a reaction mechanism similar to that of Seryakov et al. (1970). They postulated that carbon-chlorine bonding was an initial rapid step since molecular or atomic chlorine

was readily and strongly chemisorbed on hot carbon surfaces. The reaction then had to proceed subsequently by a solid state reaction on the surface of the zircon between the chlorinated carbon and the zircon. The following formulation was given:

$$C_{(s)} + Cl_2 = C.Cl_{2(s)} \quad (8)$$

$$4(C.Cl_2)_{(s)} + ZrSiO_{4(s)} = ZrCl_4 + SiCl_4 + 4\ CO \quad (9)$$

This mechanism requires the existence of a direct contact area between the zircon and the carbon particles, and in the presence of excess carbon the rate-determining factor will probably be the surface area of the zircon on which the carbon coats and not the amount of carbon surface which is available for chlorine adsorbtion.

Using an electrothermally-heated fluidized bed, the author found the chlorination reaction of zircon to be of zero order with respect to chlorine concentration, first order with respect to the surface area of zircon particles and slightly dependent on the carbon/zircon molar ratio. The activation energy of the reaction was given as 44.4 kJ/mole, whereas it was reported to be 58.6 kJ/mole in their previous paper (Manieh and Spink, 1973).

Ketov et al. (1974) recommended two types of reaction mechanisms depending on whether the carbon played a role either as a catalyst or as an oxygen-binding compound. It was reported that the majority of metal oxide chlorinations proceeded first with the formation of Cl-C type radicals, which in turn react immediately

at the contact sites with the oxide. This was in agreement with Manieh et al. (1974) and Seryakov et al. (1970). In the case of the chlorination of alkaline earth oxides, $MeCl_2$ and oxygen were suggested to be formed in the first stage followed by reaction of the oxygen with carbon in the second stage.

In another zircon chlorination study, Sparling and Glastonbury (1973) proposed an entirely different reaction mechanism in which the metal oxychloride was the intermediate product. The following formulation was considered as possible:

At the zircon surface:

$$MeO_{2(s)} + MeCl_{4(g)} = 2\ MeOCl_{2(g)} \qquad (10)$$

At the carbon surface:

$$MeOCl_{2(g)} + C_{(s)} + Cl_{2(g)} = MeCl_{4(g)} + CO_{(g)} \qquad (11)$$

According to this mechanism, some initiation reaction must occur by direct reaction of chlorine with the metal oxide to produce small amounts of the product or of the intermediate phase. The reaction is self-sustaining once a small amount of $MeCl_4$ or $MeOCl_2$ is present in the system. The authors described the zircon chlorination according to two possible situations. For a carbon-deficient system (zircon surface present in excess) it was claimed that the rate-limiting step was diffusion of the intermediate (oxychloride) to the carbon particles through the boundary layer surrounding the carbon and the reaction occurred as soon as the

intermediate reached the carbon surface. In a zircon deficient system, however, the rate-limiting step was suggested as the diffusion of the intermediate away from the zircon particles through the boundary layer surrounding the zircon.

Sparling and Glastonbury claimed that the distance between the oxide and the carbon particles was not important, in contradiction to the previous investigators, (Bergholm, 1961), (Seryakov et al., 1970), (Manieh et al., 1974). The applicability of their proposed mechanism to the zirconium constituent of the zircon is questionable, due to the fact that zirconium oxychloride in anhydrous form is not known (Braver, 1965), (Venable, 1922) and there is no experimental evidence demonstrating the presence of the unstable zirconium oxychloride at the reaction temperatures. Based on their proposed mechanism, the authors further suggested that the rate was not only a function of zircon surface area for a particular system, but also of the product partial pressure, hence, as the reaction proceeded the amount of zircon chlorinated was reduced due to reduction in both the particle surface area and in the product partial pressure.

The authors chlorinated the zircon in the presence of carbon in a fixed-bed reactor. It was reported that both the carbon and the zircon particles shrunk as the reaction progressed, indicating a surface reaction. Two different activation energy values, 134 and 151 kJ/mole, were obtained for zircon and carbon-deficient systems, respectively.

Ivashentsev et al. (1975) suggested the formation of thorium oxychloride ($ThOCl_2$) as an intermediate in the chlorination of ThO_2 with $CHCl_3$ in the temperature range of 873 - 1073 K, but formulated a different reaction mechanism, compared to that of Sparling and Glastonbury (1973), as follows:

$$ThO_2 + 2\ C.Cl = ThOCl_2 + CO + C \qquad (12)$$

$$ThOCl_2 + 2\ C.Cl = ThCl_4 + CO + C \qquad (13)$$

$$2\ ThOCl_2 = ThO_2 + ThCl_4 \qquad (14)$$

The formation of C.Cl-type active radicals were confirmed later by Gol'tsova et al. (1976) in the chlorination of TiO_2, ZrO_2 and HfO_2 with $CHCl_3$ above 800 K, but no reference was made with respect to the metal oxychloride as being an intermediate in the chlorination reactions. These authors reported an activation energy of 125.6 kJ/mole, being the same for the three oxides.

Some of the investigators concerned themselves only with the kinetic aspects of metal oxide chlorination, without suggesting any reaction mechanism. Masterova and Levin (1973) chlorinated a titanium slag (TiO_2, SiO_2) in the form of spherical pellets containing 30 percent carbon, at 777 - 1273 K, using a chlorine gas velocity of 1 cm/sec. It was reported that the reaction, having an activation energy of 55.3 kJ/mole, proceeded throughout the pellet volume up to 900 K, and was controlled by chemical kinetics. Transition from this to ash diffusion region with pellets larger

than 3 mm in diameter took place at a lower temperature. The equation $\ln (1 - X) = -Kt$, used by these authors to correlate time - versus - conversion data, differed from that of Seryakov et al. (1967, 1970) in the definition of conversion. Here, X was the fraction of the oxide chlorinated at time t, based on the initial weight rather than the maximum amount that could be chlorinated, as defined by Seryakov et al. The rate of chlorination was found to be independent of the variation of chlorine concentration above 35-45 percent chlorine, the latter depending upon the diameter of the pellet, and at lower chlorine concentrations the order of the reaction with respect to chlorine also varied with the diameter (0.62 for 2 mm and 0.87 for 8 mm pellets).

Although no explanation was offered by these authors for this behaviour, the latter may be attributed to the mass transfer effect present in the larger pellets, in which case the order of reaction is equal to $(n + 1)/2$ (Seryakov et al., 1969) where n is the order of the reaction in the kinetic region. Hence, the exponent of the chlorine concentration with larger particles (0.87) is approximately equal to $(0.62 + 1)/2$. The former, however, may be explained by a strong adsorbtion of chlorine on the carbon surface at high chlorine concentration. In this case, the reaction behaves as zero order or low fractional order in chlorine (Manieh et al., 1974).

A somewhat similar observation was reported by Stefanyuk and Morozov (1964) in the chlorination of pyrochlore ore ($Ca_2Nb_2O_7$,

$ZrSiO_4$) where they found dilution of the chlorine with nitrogen had a significant influence on the rate only at a chlorine concentration less than 50 percent. But Seryakov et al. (1969) did not make any reference to this concentration behaviour in their paper concerning the chlorination of titanium concentrate (80% TiO_2, 20% oxides of Si, Fe, Al) in the form of spherical pellets (8-10 mm in diameter) containing 27 percent coke. The order of the reaction with respect to chlorine and the activation energy in the kinetic region were found to be 0.6 and 152.4 kJ/mole respectively. They observed a transition from chemical control to mass transfer (first ash and then gas film diffusion) at a chlorine gas velocity of 8 mm/sec and temperature of about 800 K. In the chlorination of titanium dioxide and niobium pentoxide with carbon and chlorine, Morozov and Stefanyuk (1958) earlier indicated a similar transition at 823 K and 16 cm/sec chlorine velocity. At 873 K the rate was directly proportional to the chlorine concentration above 30 percent chlorine and it decreased sharply below this level. The activation energy of the TiO_2 chlorination was 157 kJ/mole.

Feruhan and Martonik (1973) chlorinated Fe_2O_3, NiO and $NiFe_2O_4$ spherical pellets with chlorine (1073 to 1473 K) and with HCl (1073 to 1273 K) diluted with helium or argon, in the absence of a reducing agent. The rates obtained when argon was used as the diluent were found to be always about 50 percent slower than those obtained when helium was used. They explained this by considering the diffusivities through argon and helium, and

indicated that gas diffusion was affecting the rates. Also in accordance with the proper particle size dependency, the rates with both Cl_2 and HCl decreased as the reaction progressed. Following chlorination, the physical appearance of the oxides was reported to have changed significantly. Below 1273 K in chlorine, the presence of a thin fluffy layer of oxide at the surface led to the conclusion that there was no internal reaction. Above 1273 K, this layer was even thinner. The rate of chlorination in Cl_2 at temperatures less than 1273 K was reported to be proportional to the external surface area and to the chlorine partial pressure. The rate also had a significant temperature dependence (activation energy of ~167 kJ similar for all of the oxides) and increased with effective gas diffusivity. At high temperatures, the rate was primarily controlled by the diffusion of chlorine through the gas film boundary. The observed rates at 1473 K were found to be in good agreement with those calculated for boundary layer diffusion using the Ranz and Marshall (1952) equation for the mass transfer coefficient. It was concluded that mass transfer was affecting the rates for all cases.

Fruehan and Martonik found the rates to be considerably faster for the more porous oxides, by a factor of 30 in the case of NiO and by a factor of 15 for Fe_2O_3. The authors suggested that the reaction was confined primarily to the pore openings near the external surface.

Concerning the effect of porosity on the reaction rate,

Costa and Smith (1971) obtained a similar result in the hydrofluorination of uranium dioxide. They reported that the rate for sintered pellets of lower porosity was about three times higher, although the activation energy was unchanged. This difference was found to be much greater than expected from the area increase associated with the porosity change. It was suggested that the degree of compression of the uranium dioxide particles used in forming the pellets appeared to affect the reactivity of the solid surface. It is also probable that the sintering process also changed the surface to an extent dependent upon the initial porosity.

The chlorination kinetics of alumina and alumina-containing minerals in the presence of either carbon or carbon monoxide or carbon plus oxygen was studied recently by Landsberg (1975, 1976). The experimental results showed that a phase transformation from γ-alumina to α-alumina lowered the reaction rate, and changed the temperature dependency (activation energy) of the reaction. When carbon monoxide and chlorine were used, both α- and γ-aluminas yielded two traditional Arrhenius reaction areas separated by a transition zone, as was observed with other oxides (Landsberg et al., 1972, Dunn, 1960). With only carbon and chlorine, the γ-alumina chlorination rate was found to be directly proportional to the chlorine concentration at 1273 K, and this dependency changed to a square root one in the presence of carbon monoxide. The author found that the overall dimensions (5 to 10 mm) of rectangular and disc-shaped compacts did not

change appreciably during chlorination, and that the reaction appeared to occur throughout the entire porous volume. This was true both when the compact surrounded by -325 mesh carbon reacted with chlorine and when it was chlorinated in a chlorine-carbon monoxide atmosphere. In his second paper, Landsberg (1976) investigated the effects of NaCl additions and different types of reductants on the chlorination of kaolin. Charcoal gave a much higher reaction rate than did petroleum coke or graphite. This was attributed to the greater surface area and hence greater contact available with the charcoal. The presence of NaCl salt in a ratio of 10 to 1 (clay/NaCl) enhanced the chlorination rate, and more particularly the reactivity of the alumina component.

A recent study on the chlorination of Australian rutile (~96% TiO_2) was published by Morris and Jensen (1976). The authors used both carbon monoxide and petroleum coke as reducing agents in a fluidized-bed reactor at temperatures in the range of 1143 to 1311 K. It was reported that the reaction occurred exclusively at the surface of the oxide particles, at a rate proportional to the receding surface area. The conversion - versus - time data were correlated by Equation (1) which assumed a chemically controlled surface reaction with shrinking particle. A comparison between the two reductants showed the energy of activation for the coke system to be much less than for the carbon monoxide, 45.2 versus 158 kJ/mole. The partial pressure of the chlorine had similar exponents (~0.665) for both systems. The coke was found

to be a more effective chlorination promoter than the carbon monoxide. At 1273 K, the rate with coke was nineteen times that with carbon monoxide as reducing agent. At higher temperature, this difference was less pronounced.

In the chlorination with coke, the rate was increased with coke/ore ratio (0.33 - 1.0 by weight) with an exponent of 0.376. However, as noticed by the authors, for a fixed bed volume the amount of ore should decrease correspondingly, so that there should exist an optimum coke/ore ratio above which the rate will drop.

In a similar but earlier study, Dunn (1960) found a semilogarithmic relationship between the amount of remaining unchlorinated titanium dioxide ore and the reaction time.

$$\ln (1 - W) = -Kt \qquad (15)$$

He also reported a surface reaction where the rate decreased with time. The rate was found to be directly proportional to both carbon monoxide and chlorine partial pressures, and the activation energy of the reaction was 87.5 kJ/mole. These results were not in agreement with those of Morris and Jensen (1976).

CONCLUSION

Studies of the chlorination kinetics of zirconium dioxide have been limited to temperatures below 1400 K and only reported in two papers neither of which suggested any mechanism nor agreed

on kinetic parameters. The reaction of chlorine with zirconium dioxide in the absence of a reducing agent has not been investigated fully.

Although a large number of publications have appeared in the literature on the chlorination of different metal oxides with different reducing agents, no agreement was found on the subject of reaction mechanisms and their activation energy values. Most of the proposed mechanistic models have been nearly entirely speculative. However, the importance of the degree of contact between the oxide and the carbon particles was indicated by several investigators.

The conversion-time relationships in the chlorination of oxides with gaseous reducing and chlorinating agents was successfully correlated by a shrinking core model, while in the case of the chlorination of carbon-oxide pellets with chlorine a homogeneous model was proven to be adequate in analyzing the experimental data in the absence of diffusional resistance.

MATHEMATICAL TREATMENTS OF NON-CATALYTIC GAS-SOLID REACTIONS

GENERAL CONSIDERATIONS

While there exists a close parallel between heterogeneous catalytic reaction systems and gas-solid non-catalytic reactions, the latter systems are rather more complicated because

of the direct participation of the solid in the overall reaction. As the solid is consumed or undergoes chemical change, its structure also changes continuously, making the system inherently transient in nature. It follows that the analysis of gas-solid reactions involves an additional dimension, namely that of time, which is not necessarily required in the study of heterogenous catalytic reactions (Szekely et al., 1976).

A general equation for these reactions may be written as follows:

$$A(gas) + bB(solid) \rightarrow cC(gas) + dD(solid) \qquad (16)$$

The products comprise either solids or fluids, or a combination of both. Halogenation of metal oxides, gasification or combustion of some carbonaceous materials are examples where only fluid products are encountered. A few examples of gas-solid reactions where both solid and fluid products are present and in which the solid does not change appreciably in size during the reaction are the decomposition of molybdenite, the reduction of metallic oxides and the roasting of ores.

The overall rates of gas-solid reactions are generally dependent on both the chemical kinetics and on the mass transfer characteristics of the system. The reaction is said to be under kinetic control when diffusion of the gaseous reactant into the solid is unhindered. However, as the temperature and hence the intrinsic kinetics of the chemical reaction increase, the mass

transfer characteristics become rate-controlling. When both the chemical kinetics and physical diffusion phenomena play a significant role in the overall rate control, the reaction is said to be in the intermediate region.

A large number of mathematical representations of the progress of gas-solid reactions have appeared in the literature under different names, sometimes with the same meanings. These are:

1. Sharp interface shrinking-core model (Yagi and Kunii, 1953).
2. Finite thickness, shrinking-core model (Bowen and Cheng, 1969), (Chettigar and Hughes, 1972).
3. General model (Ishida and Wen, 1968).
4. Diffusion with simultaneous reaction model (Calvelo and Cunningham, 1970).
5. Pore model (Peterson, 1957), (Hashimoto and Silveston, 1973a,b), (Ramachandran and Smith, 1977).
6. Grain model (Szekely and Evans, 1970, 1971a,c).
7. Particle-pellet model (Sempath et al., 1975).
8. Crackling-core model (Park and Levenspiel, 1975, 1977).
9. Volume-reaction model (Wen and Wu, 1976).
10. Homogenous (uniformly reacting pellet) model.

All these models were either related to a conceptual picture of the progress of the reaction or to a structural consideration of the reacting solid, or sometimes to a combination of both. Hence, to present a clear-cut classification is very difficult and such a classification has not appeared in the literature yet. However, they can be discussed under two general categories:

1. Surface reaction (shrinking-core) models, in which the reaction is considered to occur either at a sharp interface or in a very narrow zone near the interface.

2. Diffuse zone-reaction models, in which the reaction is considered to take place in a zone of substantial thickness. These models are either based on a volumetric reaction (that is, they consider the solid to be a continuous phase and use volumetric rate constant), or on a structural consideration (grain, particle-pellet and pore models).

Homogenous reactions may be considered as special cases of either one of the two diffuse zone-reaction models, when chemical kinetics are the rate-controlling step and the gaseous reactant diffuses throughout the pellet where reaction occurs uniformly. They will be discussed in connection with the diffuse zone-reactions models.

A recent text by Szekely, Evans and Sohn (1976) provided a comprehensive description of gas-solid non-catalytic systems and

their mathematical treatments under various conditions, with particular emphasis on the structural viewpoint. Review articles in the field include the work of De Wet (1970) who discussed the kinetics and mechanism of gas-solid reactions of interest to the chemical and metallurgical industries; Sampath and Hughes (1973) who compared the mathematical properties of the volumetric, the sharp interface and the finite thickness shrinking core models; Roy and Luthra (1974) who discussed the various kinetic equations available for different rate-controlling mechanisms. Also, Munz (1974) reviewed the works under the topics of "shrinking-core" and "general" models.

An attempt will now be made to provide an updated comprehensive review of the field with a more specific classification and definition of the various models than have appeared in the literature todate. The major applications, simplifications and complexities associated with each development will be emphasized, and experimental verification will be pointed out whenever possible. As a result, it is hoped that the reader will be provided with a broader view of the field, in a condensed form, and will be in a better position to ascertain where the treatment of the present kinetic study fits in these highly diverse approaches.

SURFACE REACTION (SHRINKING-CORE) MODEL

Due to the mathematical simplicity of this approach, the majority of the models for gas-solid reactions have been based

on the assumption of a non porous solid reactant - even when the latter exhibits considerable porosity. It is convenient to classify gas-solid reactions according to the geometry of the system undergoing reaction. The reaction of non porous solids can be divided into two types of geometrical groups:

1. A shrinking particle, which results from the products being gaseous, or from a solid product flaking off the surface of the reactant as soon as it is formed (shrinking-particle).

2. A particle whose overall size is unchanged, with a product or 'ash' layer remaining around the unreacted core(hence the term 'shrinking unreacted core' model).

The shrinking-core model was first developed by Yagi and Kunii (1953, 1955a, 1955b) who visualized the following steps occurring in succession during reaction:

Step 1 - Diffusion of gaseous reactant through the film surrounding the particle to the surface of the solid.

Step 2 - Penetration and diffusion of gaseous reactant through the blanket of ash to the surface of the unreacted core.

Step 3 - Reaction of the gaseous reactant with the

solid at this reaction surface.

Step 4 - Diffusion of the gaseous products through the ash, back to the exterior surface of the solid.

Step 5 - Diffusion of gaseous products through the gas film back into the main body of the fluid.

If the reaction is irreversible or if no gaseous product is formed, Steps 4 and 5 and, in the absence of an ash layer, Steps 2 and 4, do not contribute directly to the resistance to reaction. Also, the resistances of the different steps usually vary greatly from each other; in such cases, the step with the highest resistance is considered to be rate-controlling. Yagi and Kunii derived expressions for the rate of conversion of a spherical pellet where boundary layer diffusion, ash diffusion or a first order chemical reaction at the interface was the rate controlling step, as well as cases where the control was mixed. To overcome mathematical difficulties, a pseudo-steady state was assumed, according to which the rate of movement of the reaction interface was considered to be small with respect to the velocity of diffusion of the reactant through the product layer, with the result that the concentration of gaseous reactant in the particle was considered to be time-invariant. The validity of this assumption has been examined by several investigators (Bischoff, 1965), (Bowen, 1965), (Luss, 1968), and it has been concluded that the pseudo-steady state solution is a good approximation for most of the gas-solid reaction systems, except for systems under

extremely high pressures or in the case of very low solid reactant concentrations.

The sharp interface shrinking-core model has also been discussed by Levenspiel (1972) for the general case of a spherical particle and for the three special cases in which gas film diffusion, ash diffusion or chemical reaction is the rate controlling step. However, Szekely, Evans and Sohn (1976) presented a more complete view on this subject and derived equations in generalized forms applicable to different particle geometries. Their conversion-versus-time relationships are summarized below.

For a shrinking particle (no ash layer) under chemical reaction control:

$$t/\tau = 1 - (1 - X)^{1/F_p} \tag{17}$$

where $$\tau = \rho_s (F_p V_p / A_p) / b k_s [C_{A0} - (C_{C0}/K_E)] \tag{18}$$

$\underline{F_p}$ is the shape factor, which takes the values 1, 2 and 3 for flat plates, long cylinders and spheres, respectively.

$\underline{A_p}$, $\underline{V_p}$ are the original surface area and volume of the particle, respectively.

If the particles are too small to be easily observed visually, F_p can be obtained as the value that gives a straight line between the experimental values of $[1 - (1 - X)^{1/F_p}]$ and the reaction time, $\underline{t}$.

The relationship for a shrinking particle under gas film diffusion control is not straightforward. It requires a knowledge of the mass transfer coefficient and is dependent on particle size. For a spherical particle, using the Ranz and Marshall correlation for the mass transfer coefficient for a first order reaction and for equimolar counter diffusion, the conversion-time relationship becomes:

$$t/\tau = \frac{4}{3a}[1-(1-X)^{1/2}] - \frac{2}{a^2}[1-(1-X)^{1/3}] + \frac{4}{a^3}[1-(1-X)^{1/6}] - \frac{4}{a^4}\ln[\frac{1+a}{1+a(1-X)^{1/6}}] \quad (19)$$

where $$\tau = \rho_s R^2/2bD_e(C_{AO}-C_{CO}/K_E)(\frac{K_E}{1+K_E}) \quad (20)$$

and $$a = 0.3\ N_{Sc}^{1/3}\ (N_{Re}^{0})^{1/2} \quad (21)$$

In the systems displaying a shrinking unreacted-core (overall size unchanging) the relationships are:

a) for gas film diffusion control:

$$t/\tau = X$$

where $$\tau = \rho_s/(A_P/V_P)bk_m(C_{AO}-C_{CO}/K_E)(K_E/1+K_E) \quad (22)$$

b) for ash diffusion control:

$$2t/\tau = X^2 \quad (23)$$

$$4t/\tau = X+1(1-X)\ln(1-X) \quad (24)$$

and $$6t/\tau = 1-3(1-X)^{2/3} + 2(1-X) \quad (25)$$

for infinite slabs, long cylinders and spheres, respectively where

$$\tau = \rho_s/bD_e(A_P/F_PV_P)^2(C_{AO}-C_{CO}/K_E)(K_E/1+K_E) \quad (26)$$

For chemical reaction control, the conversion-time relationship is the same as that given by Equation (17). All these treatments were based on an isothermal particle.

Shen and Smith (1965) extended the sharp interface shrinking-core model to include a reversible reaction where both diffusion and reaction resistances are important under isothermal conditions. Based on equimolar counter diffusion and constant effective diffusivities in the gas film and within the product layer, the degree of conversion was expressed as an analytical function of dimensionless time and of two parameters depending upon the relative resistances of internal and external diffusion and chemical reaction. The model was applied to the hydrogen reduction of FeS_2, and reasonable agreement with the experimental data was obtained. They also developed a different model to account for nonisothermal effects for a first order irreversible reaction. Radiation effects, variation of concentration and of diffusion coefficient with temperature were neglected, and the overall particle size was assumed to be constant. In this case, three additional parameters which included the relative resistances to heat transfer in the boundary film and in the ash layer, and

the heat and activation energy of the reaction, were required in order to solve the model equations numerically. Analytical solutions could not be obtained. This model was later applied to the hydrofluorination of uranium dioxide by Costa and Smith (1971) with minor modifications (the particle size was allowed to change and a different method of solution was employed). An intrinsic rate equation for the chemical step at the reacting interface was obtained from an initial time period where diffusion effects were unimportant. The temperature and the reaction rate data were used to calculate the effective diffusivity and thermal conductivity of the product layer under actual reaction conditions. Predictions of conversion-versus-time curves from the nonisothermal model and from the derived properties compared well with the experimental results. However, predictions of temperature profile in the product layer were found to be unsatisfactory under a pseudo-steady state assumption with respect to the reaction interface, because of heat transfer into the unreacted core of the pellet. An unsteady state method corrected much of the error in the predicted temperature. It was concluded that, while a pseudo-steady state assumption is valid for mass transfer, the same assumption is less suitable for the calculation of the temperature profile in the product layer.

Ishida and Wen (1968a) introduced the concept of the effectiveness factor (actual reaction rate/rate obtainable when the reaction site is exposed to the concentration and temperature

of the bulk gas) to examine three types of instabilities: the geometrical instability, the thermal instability due to metastable temperatures, and the instability resulting from sudden shiftings of the rate controlling regions. The geometrical instability (uneven surface growth) is due to the increase in rate per unit area as the reaction progresses and is indicated by an increase in effectiveness factors with an increase in the conversion of the solid reactant. This may take place in both isothermal and non-isothermal reactions, independent of the transition between the rate-controlling regions. However, the second and third kinds of instabilities occur only when the reaction is exothermic and depend upon the heat generation and heat loss processes. A metastable reaction temperature was reported to exist when the following conditions were satisfied:

$$Q_{gen} = Q_{loss} \tag{27}$$

$$\frac{\partial Q_{gen}}{\partial T_c} > \frac{\partial Q_{loss}}{\partial T_c} \tag{28}$$

It was pointed out that, because the unreacted core shrinks during the reaction, the shapes and slopes of heat generation and heat loss curves will change for a given system, even when the surrounding conditions are kept constant. This, in return, causes a sudden transition of the rate-controlling steps.

Based on a shrinking-core model and constant particle size during an irreversible chemical reaction, Ishida and Wen solved

the heat and mass balance equations analytically, under pseudo-steady state assumption. The influence of various factors on the effectiveness factor was investigated and conditions of optimum reaction rate were postulated. When the reaction temperature must be fixed within a certain range to avoid side reactions, the reaction should be carried out in a region where chemical reaction is controlling, in which case the effectiveness factor is about unity. On the other hand, if the range of reaction temperature is unlimited, it is more advantageous to select a temperature at which the transition from chemical controlling region to ash diffusion controlling region would take place. Under such conditions, a higher reaction rate can be achieved at a lower surrounding gas temperature particularly for highly exothermic reactions.

A graphical analysis of the effects of diffusion and heat transfer on solid-gas reactions based on a shrinking-core model was reported by Ishida and Shirai (1969a). An irreversible reaction with constant particle size and with pseudosteady state heat and mass transfer was considered. Two types of nomographs were presented: one was to determine the temperature at the reacting core surface for both exothermic and endothermic reactions; the other was to predict whether or not thermal or transitional instabilities existed in an exothermic reaction. In a second paper, Ishida and Shirai (1969b) reported an experimental study of the oxidation of a carbon-cement sphere in a hot air stream. The sample burned homogenously under the control of chemical reaction at relatively

lower temperatures. Under diffusion-controlled conditions, however, an interface between the reacted shell and the unreacted core was quite distinct. The temperature of the reacting core surface was almost constant and the temperature profile in the ash layer was linear in terms of a reduced diameter. An arithmetic-mean temperature of bulk and core surface was suggested as the representative temperature for the estimation of the effective diffusivity in nonisothermal systems.

The instability problem associated with gas-solid reactions based on a shrinking-core model was further discussed by Wen and Wang (1970) in a paper concerning the thermal and diffusional effects associated with this model. The governing equations were solved numerically for an irreversible reaction with equimolar counter-diffusion. It was pointed out that when geometrical instabilities occur, the reaction interface is no longer smooth and the mathematical model becomes a poor approximation. The validity of the pseudosteady state assumption for heat transfer was also investigated; it was reported that this approximation may become inaccurate at large values of heat capacity of the solid and large temperature gradients in the reacting pellet. The pseudosteady state model was extended to include multiple reactions in the sphere. This was also reported by Wen and Wei (1970) where three types of simultaneous reactions, independent, parallel, and consecutive, were examined in terms of the selectivity and the effectiveness factor, based on the

shrinking core model under isothermal conditions. Effects of diffusion and chemical reaction were discussed. In a subsequent paper by Wen and Wei (1971) simultaneous mass and heat transfer were treated in the same model, to examine the nonisothermal behaviour.

Wang and Wen (1972) investigated the combustion of a single agglomerated carbon-fire clay sphere in a thermobalance to test the nonisothermal shrinking-core model, using expressions for unsteady state heat transfer developed earlier by them (Wen and Wang, 1970). The initial porosities of the samples were quite high (40 - 50%) and the particles were about 1 cm in diameter. Visual examination of the partially-reacted spheres showed that, above a temperature of 800 K, the reaction interface was sharp, while below this value a reaction zone was formed. Conversion-time curves predicted by the shrinking core model and accounting for both heat and mass transfer agreed well with the experimental data where the carbon content of the spheres was low, and to a lesser degree for high carbon content. This deviation was greater in the initial stages of the reaction, due to the fact that the reacting spheres were not preheated to the gas temperature. Hence the assumption that the unreacted core was at a constant temperature equal to that of the reaction front was not valid in the initial stages of the reaction. The variations of the surface reaction rate with the fractional conversion of carbon calculated from both the unsteady and pseudosteady state conditions for heat

transfer agreed well with the experimental results, although the latter assumption overestimated conversion rates during the early stages of reaction. At a solid conversion of about 95% for the high-carbon run, a transition from a diffusion-controlled regime to a chemical reaction-controlled one occurred.

Bowen and Cheng (1969) modified the sharp interface shrinking core model to suit the intermediate region of reaction control. They suggested that it is more realistic to assume a narrow but finite thickness reaction zone between the product layer and the unreacted core, instead of one with a sharp interface. This in effect means that the diffusing gas does not get consumed immediately on contact with the reaction zone but only after penetration of a small but finite length into the unreacted core. Reaction occurs all over this finite length. Under extreme conditions of total kinetic or diffusion control, this reaction zone either extends all over the particle or contracts to give a sharp interface. Bowen and Cheng formulated a model for an irreversible gas-solid reaction which was $\underline{n^{th}}$ and $\underline{m^{th}}$ order with respect to fluid and solid reactant, respectively. It was assumed that the reaction zone was thin with respect to the radius of the unreacted core and that the variation of concentration through the zone was linear. An expression was derived for the thickness of the reaction zone and it was shown that if the reaction was first order with respect to the gas or under kinetic control, the reaction zone thickness would be constant throughout the reaction.

For the case of chemical reaction control, the rate was given as:

$$r_A = 4\pi r_c^2 \, (\nu D_e k_s \Psi)^{1/2} \, C_{AO}^{(n+1)/2} \, C_{BO}^{m/2} \tag{29}$$

while for the sharp interface model, the case of chemical reaction control would be written as:

$$r_A = 4\pi r_c^2 \, k_s' \, C_{AO}^n \, C_{BO}^m \tag{30}$$

where

$$\Psi = \frac{1}{n+1} - \frac{m}{n+2} + \frac{m(m-1)}{2\,!(n+3)} - \frac{m(m-1)(m-2)}{3\,!(n+4)} \tag{31}$$

and ν is the ratio of the gaseous reactant concentration gradient at the product interface to the mean linear gradient across the zone, D_e is the effective diffusivity of the reactant in the reaction zone, and k_s, k_s' are the rate constants in the finite thickness and sharp interface models, respectively. It is apparent that an order of reaction n, m becomes an apparent order $(n+1)/2$, $m/2$ and apparent activation energy becomes one half of the intrinsic activation energy.

Further development of the finite thickness reaction zone unreacted shrinking core model was carried out by Shettigar and Hughes (1972) who extended the model to include nonisothermal situations. An expression, including both the chemical and the mass transfer resistances, was developed for the rate of advance of the reaction zone. This was coupled with the energy balance equation to calculate the transient temperature in the pellet. It was found that neglecting the chemical resistance would lead to

the prediction of an excessive maximum temperature rise in the pellet. The model also predicted that a change in mechanism from chemical control to diffusional control may occur, especially during the early stages of the reaction, and this may give rise to thermal instabilities.

The concept of reaction order with respect to the solid reactant in a reaction between gas and a porous solid was analysed by Cunningham and Calvelo (1970). Considering the rate equation:

$$r_A = k_s \, C_{AO}^n \, C_{BO}^m \tag{32}$$

it was found that the reaction order with respect to the solid was a function of the porous structure of the solid and might vary as the solid was being consumed. The exponent m was suggested to be lower than unity for all practical cases. In the case of a solid obtained by compaction of nonporous particles, the value of m should be 2/3 while in the case of a solid matrix containing a network of uniform, randomly-connected cylindrical pores (Peterson Model; Peterson, 1957), the value of m would vary with the degree of conversion. It was concluded that whether or not the above equation could be used to express the rate of porous solid-gas reactions depended on the pore structure model.

The majority of the models proposed for the interpretation of non-catalytic gas-solid reactions were based on the assumption that the reaction was of first order with respect to the gaseous reactant, for mathematical convenience. Shon and Szekely (1972a)

showed that use of first order kinetics for other reaction orders may introduce a serious error if the overall rate is determined by both chemical reaction and diffusion.

The concept of shrinking core has been used for various types of processes. In the reduction of spherical ferrous chloride particles by hydrogen in the temperature range of 720 - 900 K for particle diameters 0.7 - 2.0 cm, Yannapoulos and Themelis (1965) showed that the rate of reduction could be expressed by a shrinking core model. When both chemical reaction and boundary layer diffusion were controlling factors, a single rate equation was developed by combining the respective contributions of each resistance.

Munz and Gauvin (1975) found that the decomposition of molybdenite in solid state was controlled by the diffusion of sulphur through the product layer and the shrinking core model described the overall reaction.

Morris and Jensen (1976) reported that in the chlorination of titanium dioxide with chlorine and carbon monoxide in a fluidized bed reactor, the reaction occurred exclusively at the surface of the oxide particles and exhibited shrinking particle behaviour under chemical reaction control. The conversion-time relationship was expressed by a shrinking core model. Earlier, Fruehan and Martonik (1973) made a similar observation in the chlorination of porous NiO spheres by chlorine above 1473 K, except that the reaction was found to be controlled by gas-film diffusion. The rate was proportional to the mass transfer

coefficient of chlorine calculated from the Ranz and Marshall (1952) correlation.

Recently, the shrinking core model was applied to another gas-solid reaction of metallurgical interest. Fahim and Ford (1976) studied the hydrogen reduction of cobalt sulphide. It was pointed out that the reaction was reversible and that the evolution of small amounts of hydrogen sulphide would be sufficient to keep the reduction reaction at equilibrium. In order to carry out the reaction under conditions approaching irreversibility, a high hydrogen flow rate was used to sweep the hydrogen sulphide formed away from the vicinity of the solid. The unreacted shrinking core behaviour was tested by sectioning a partially-reduced spherical pellet, and a finite thickness reaction zone rather than a sharp interface was observed. However, the time-conversion data fitted well with the sharp-interface shrinking core model under chemical reaction control. An attempt was made to evaluate the true intrinsic kinetic parameters of the reaction by using nonporous cobalt sulphide powder rather than compacted porous pellet. The powders showed a sharp interface type of reaction. Although the activation energies found in both cases (pellet = 113.5 kJ/mole, powder = 116.1 kJ/mole) were identical, the frequency factors in the Arrhenius equation were different and in the case of the porous pellet this factor was overestimated. This was attributed to differences in the reacting areas, which was the geometrical area in the case of powders, and the surface area in the diffuse

reaction zone in the case of the pellet.

DIFFUSE ZONE-REACTION MODELS

When a porous solid particle reacts with a gas at low temperatures, the reactant gas can diffuse easily into the interior of the porous solid and the reaction takes place in zones of substantial width. These models consider either a particular solid structure (pore-model, grain-model) or simply a porous solid volume (volumetric-reaction model). Figure 3, from Ishida and Wen (1971) illustrates the description of these models. The diffuse zone-reaction models reduce to the uniform reacting pellet (homogenous) model at one extreme (kinetic control) and to the shrinking-core model at the other extreme (diffusion control).

a- Volumetric-Reaction Model

Ausman and Watson (1962), using a pseudosteady state approximation for gas concentration distribution and a first order reaction with respect to the gaseous reactant, obtained a general solution under isothermal condition for the combustion of carbon in porous spherical catalyst particles based on the volumetric-reaction model. The reaction process was broken into two distinct stages, the first of which was a constant-rate period which ended when the outside layer of material was completely reacted. The second stage was a falling-rate period during which the reaction boundary receded towards the centre of the spherical pellet. Carbon and oxygen concentration profiles in the pellet

FIGURE 3

SCHEMATIC DIAGRAM OF CONCENTRATION PROFILE

AND SOLID STRUCTURE IN THE PARTICLE

(ISHIDA AND WEN, 1971)

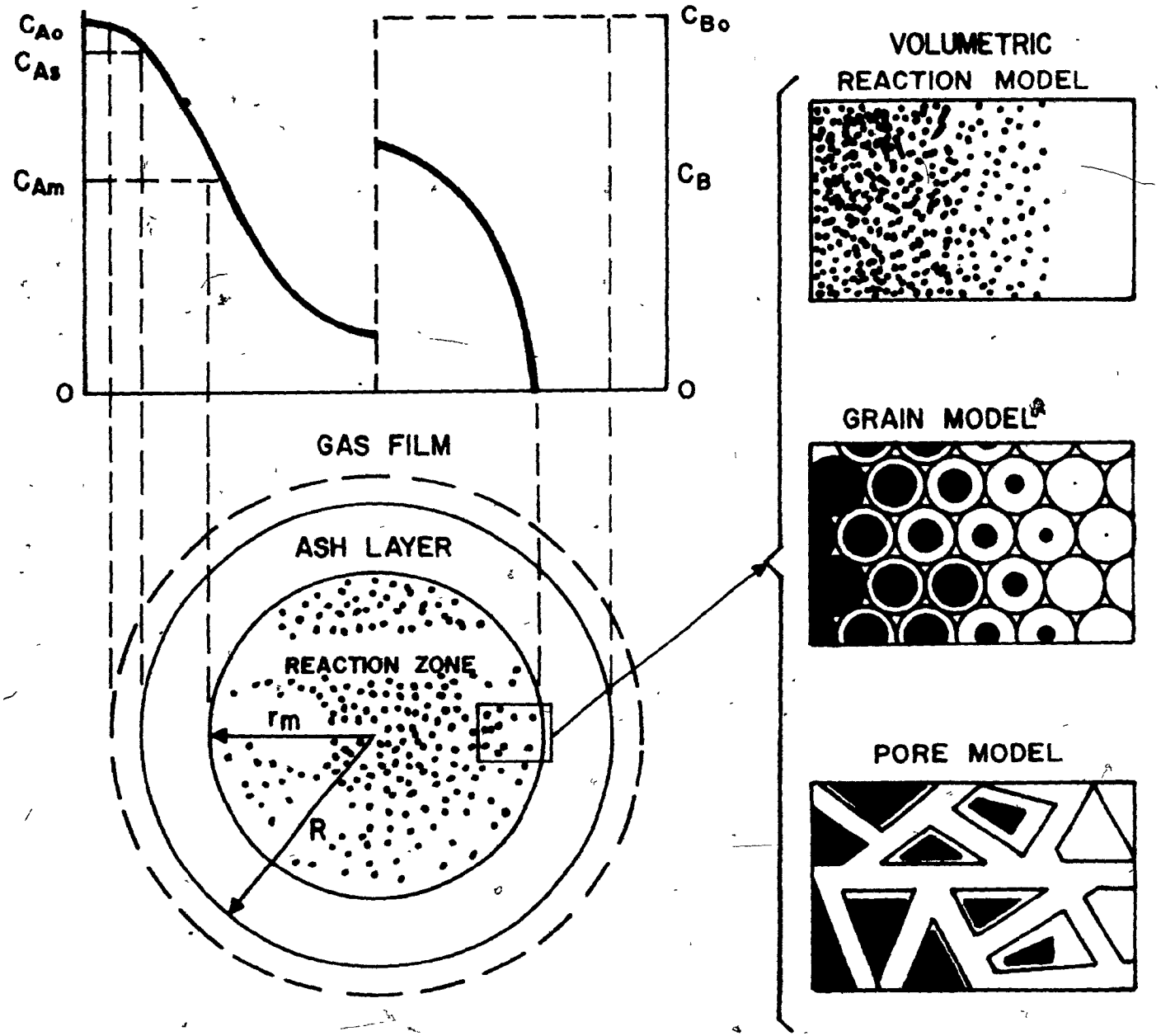
C_{Ao}
C_{As}
C_{Am}
0
C_{Bo}
C_B
0
GAS FILM
ASH LAYER
REACTION ZONE
rm
R
VOLUMETRIC
REACTION MODEL
GRAIN MODEL
PORE MODEL

carbon and oxygen concentration profiles in the pellet were obtained as a function of time, from which the overall carbon burning rate equations for the pellet were obtained.

A similar stagewise treatment for an isothermal, irreversible spherical porous pellet-gas reaction was presented by Ishida and Wen (1968b) and Wen (1968) with pseudosteady state approximation. The rate was assumed to be independent of the solid reactant concentration but first order with respect to the gaseous reactant. The reaction was investigated in two stages: considering the reaction as being faster near the surface than in the interior of the pellet, after a certain time the solid reactant near the surface would be completely consumed, thus forming an inert product layer. The period of reaction prior to the formation of the ash layer was designated as the first stage and the period following the ash layer formation as the second stage. The diffusion in the ash layer and in the solid volume was considered to be different but constant throughout the reaction. Two different conversion-time analytical equations were derived: one for the first stage in terms of a Thiele modulus based on diffusivity in the reacting volume, the other for the second stage in terms of a Sherwood number and Thiele modulus based on diffusivities in the ash layer and in the reacting volume. These were then combined to give a single time-conversion relationship. When the effective diffusivities (ash and reacting volume) were assumed to be the same and in the absence of gas-film resistance, the time-conversion relationship for the high Thiele modulus

(diffusion of the gas through the solid becomes rate-controlling) was exactly equal to that predicted by the shrinking-core model. When the chemical reaction was very slow and was the rate-controlling factor (low Thiele modulus) the model became similar to that of a homogenous reaction, but a plot of conversion-versus-time data was again very similar to that predicted by the shrinking core model. This indicates that determination of a correct model from the experimental data is rather difficult. On the other hand, if the ash diffusivity was much greater than the reacting volume diffusivity, it was shown that the equations were equivalent to the ones derived on the basis of a shrinking-core model, as was expected. It was further pointed out that, the rate constant based on surface (shrinking-core) is proportional to the square root of that based on volume (volumetric-reaction); therefore, the activation energy obtained from the shrinking-core model could be as small as one half of the true value.

Wen (1968) extended this anlysis to an irreversible reaction of first order with respect to solid and second order with respect to gaseous reactant. An empirical equation relating the effective diffusivity to the conversion was included and the governing equations were solved numerically with a pseudosteady state assumption.

Calvelo and Cunningham (1970) presented another method of approximation, in which the concentration profile of the solid reactant was obtained from a volumetric-reaction model. The main

application of this work is the inclusion of transient behaviour of the solid structure with respect to porosity, and hence surface area, and of the effective diffusivity of the gaseous reactant in the porous pellet. The model assumed that the gaseous reactant was consumed completely inside the pellet at a distance from its outer surface, and that the pseudosteady state approximation was valid. The relationship between the surface area and porosity (hence the solid concentration) was obtained from a structural model (Peterson, 1957) and the variation of the effective diffusivity with porosity was estimated from:

$$D_e = D_{eo} \, (\varepsilon/\varepsilon_o)^2 \tag{33}$$

The influences of the variation of surface area and effective diffusivity on conversion-time relationships of an isothermal, irreversible, first order reaction involving diffusional resistances of both the gas film and the ash layer were then taken into account through a correction modulus of the effectiveness factor. The model was called by these authors the "diffusion with simultaneous reaction model." This was later compared by Lemcoff et al. (1971) with those of Ausman and Watson (1962), Ishida and Wen (1968b), Bowen and Cheng (1969), taking the predicted conversion-time relationship as a reference for their comparison, and by Calvelo and Cunningham (1972) with the shrinking core model. Later Williams, Calvelo and Cunningham (1972) applied their model to the two-stage analysis proposed by Ishida and Wen (1968b).

Recently, Wen and Wu (1976) developed a volume-reaction

model for a slow isothermal porous solid-gas reaction, having first order dependence on the solid and gaseous reactants. An average bulk solid concentration was used to approximate the local solid concentration. The gas concentration profile and the effectiveness factor (η_o) were derived under the assumptions of pseudo-steady state of gaseous components within the solid particle, and with constant effective diffusivity. These were given as:

$$C_A/C_{AO} = (\sinh Mr/R)/(r/R) \sinh M \tag{34}$$

$$\eta_o = (1-X)(3/M)(1/\tanh M - 1/M) \tag{35}$$

where

$$M = R(k_v C_{BO}/D_e)^{1/2} (1-X)^{1/2} \tag{36}$$

The overall rate was expressed as:

$$dX/dt = \eta_o k_v C_{AO} \tag{37}$$

and in the case of chemical-reaction control (homogenous model) the rate was suggested to be:

$$-dX/dt = (1-X) k_v C_{AO} \tag{38}$$

The model was tested experimentally on a carbon-carbon dioxide reaction system, and close agreement was obtained between the experimental and calculated time-conversion relationships. When the observed rate (dX/dt) was plotted against 1/T at 20 percent conversion from 1160 to 1365 K, a straight line was obtained in the low-temperature region, leaving the points in the high-temperature region below the straight line. This was ascribed

to the intraparticle diffusion which affected the overall reaction rate significantly at high temperatures. However, when the effectiveness factor was used to convert the observed fractional rate into the intrinsic chemical reaction rate, the plots of $(dX/dt)/(\eta_0)$ versus $1/T$ yielded a straight line passing through all the points. This model provides a simplified interpretation of the experimental results and takes into account the intraparticle diffusion for the reactions which are not exceedingly rapid and assumes that the porous structure remains essentially unchanged.

The chlorination of metal oxide-carbon compacted porous pellets represents a different type of gas-solid reaction involving two solid components. Seryakov et al. (1970) analyzed this problem using a volumetric-reaction model and assuming homogenous reaction where the contact area between the solid constituents was the rate-determining factor, since the reaction was assumed to be limited by the step involving the transfer of an intermediate product from the surface of one solid phase to the other. The rate equation was given as:

$$-dW/dt = S\, f_1\,(C^*,T) \tag{39}$$

and

$$-dS/dt = S\, f_2\,(C^*,T) \tag{40}$$

hence

$$dW/dS = f_1(C^*,T)/f_2(C^*,T) \tag{41}$$

where, C^* is the concentration of the intermediate product on the carbon surface in the thermodynamic equilibrium with the chlorinating gas, S is the contact area between the solid phases, T is the

reaction temperature, W is the weight of metal oxide.

Integration of Equation (41) yields:

$$W_o - W = (S_o - S)\ f_1\ (C^*,T)/f_2\ (C^*,T) \tag{42}$$

As the contact area approaches zero, the maximum amount of the oxide that can be reacted from Equation (42) becomes:

$$W_o - W_\infty = \Delta W_\infty = S_o\ f_1\ (C\ ,T)/f_2\ (C\ ,T) \tag{43}$$

Inserting this into the integrated form of Equation (40), which is:

$$\ell n\ (S/S_o) = t\ f_2\ (C^*,T) \tag{44}$$

yields:

$$-\ell n\ \{1 - \Delta W/[S_o\ f_1\ (C^*,T)/ f_2\ (C^*,T)]\} = t\ f_2\ (C^*,T) \tag{45}$$

and hence:

$$-\ell n\ (1 - \Delta W/\Delta W_\infty) = t\ f_2\ (C^*,T) \tag{46}$$

where $f_2\ (C^*,T)$ was taken by Seryakov et al. as the apparent rate constant. In terms of fractional conversion based on the maximum amount of oxide that can be reacted, the resulting conversion-time expression becomes:

$$-\ell n\ (1 - X) = Kt \tag{47}$$

This model fitted their experimental data reasonably well.

b- Pore Model

Macroscopic models are incapable of describing changes in porous solid structure or surface area through reaction, except with the aid of auxiliary empirical expression (Wen, 1968). Microscopic consideration of porous solid-gas reaction was undertaken by Peterson (1957) who provided one of the first models for the gasification of solids, in which account was taken of the changes in pore structure. Peterson considered a single cylindrical pore initially of uniform diameter, and a porous cylindrical pellet initially containing cylindrical pores. A model for the time rate of change of the average radius of a cylindrical pore was developed for a first order reaction with simultaneous mass transfer, assuming pseudosteady state. This model was extended to a network of intersecting pores by including expressions for the surface area and porosity as a function of the pore diameter and initial porosity. The governing equations were solved numerically and the solutions were used to interpret the experimental results reported in the literature on the gasification of graphite rods with carbon dioxide. Although the agreement between the estimated and observed rate was found to be satisfactory, the model underestimated the effective pore diffusivity. The latter was attributed to the fact that the real pore system containing pores of varying diameters was replaced by an idealized system of uniform cylindrical pores characterized by an average diameter.

Later, Szekely et al. (1976) applied Peterson's pore

structure model to a porous spherical pellet for the low-temperature region of a gasification-type reaction. It has been pointed out that (Walker et al., 1959) in the gasification reactions (where no solid residue remains) there are three somewhat distinct temperature regions with transition regimes between them. In Region I, the reaction temperature and the intrinsic reactivity of the solid are low, the gaseous reactant entering the solid has a high probability of diffusing deeply into the pellet. Also, the activation energy and all other kinetic parameters are the intrinsic values for the reaction, and the rate does not depend on the size. The intermediate temperature region, Region II, is one in which pore-diffusion is controlling, the concentration of the reactant species goes to zero at a distance from the exterior surface. In the high temperature zone, Region III, the rate becomes so great that the reaction is effectively localized at the external surface of the particle.

According to the three-temperature regions' theory, the treatment of Szekely et al. corresponds to Region I and it demonstrates the "homogenous reaction" version of the pore model. Considering that the reaction was under kinetic control, they obtained an analytical solution which provided an explicit relationship between the conversion (X) and time (t):

$$X = (\varepsilon_o/1 - \varepsilon_o)\{[(1 + t/\tau)^2(G - 1 - t/\tau)/(G - 1)] - 1\} \tag{48}$$

where

$$\tau = r_o\, \rho_s/b\, k\, C_A^n \tag{49}$$

and r_o is the initial pore radius, ε_o the initial porosity of the pellet, ρ_s the molar density of pore-free solid and b is a stoichiometric coefficient. The parameter G is a function only of ε_o and is obtained by solution of cubic equation:

$$(4/27)\ \varepsilon_o . G^3 - G + 1 = 0 \qquad (50)$$

This type of structural approach was found to be useful in describing the fact that the surface area per unit volume may increase, go through a maximum and then decrease.

Another gasification-type pore model was introduced by Hashimoto and Silveston (1973a, b) which allowed a pore size distribution and took into account pore growth, initiation and coalescence. The model considered cylindrical pores, uniform pore length, first order kinetics and an isothermal system, and required a large number of input parameters. In their first paper, they only concerned themselves with kinetic-control gasification (low-temperature region), and predicted the particle radius as a function of either time or the extent of reaction by means of numerical methods. The model was tested with the experimental data reported in the literature. The agreement between the experimental values and the predictions were usually very satisfactory. In their second paper, this model was extended to allow for mass transfer of gaseous reactant to the particle and for intraparticle diffusion which shifted the gasification to the outer surface of the particle. Hence reaction took place in a diffuse zone,

Gasification is a special type of porous solid-gas reaction where no ash or solid product forms; hence the diffusion of gaseous reactant through the ash layer has not been considered in the models which have just been discussed. Szekely and Evans (1970) included this additional parameter into their pore model, which considered a semi-infinite porous solid containing cylindrical pores of uniform size, spaced apart by a uniform distance and running normal to the reaction interface. It was assumed that the initial structure was maintained throughout and was unaffected by the progress of the reaction; the gaseous reactant diffusion in the pores was in the axial direction only, but the diffusion through the product layer in the solid was purely radial. With these assumptions, the conversion-time relations were calculated numerically in terms of an equivalent penetration of the reaction into the solid for a first order irreversible reaction involving equimolar counter diffusion, with no external mass transfer resistance. The influences of such parameters as pore radius, porosity, diffusivity through the product layer and gas phase, and intrinsic rate constant on the equivalent penetration, were demonstrated.

Chemical reaction may result in a more open pore structure when the molal volume of the product formed is less than that of the reactant. Alternatively, the effect of chemical reaction may be to form a denser pore structure, resulting in a decrease in porosity. Recently, Ramachandran and Smith (1977) proposed a

different type of pore model, which takes into account the structural changes due to reaction which were neglected by Szekely and Evans (1970). The model analyzed a single pore, as representative of the behaviour of the whole porous pellet. The solid was assumed to consist of parallel cylindrical macropores, each of finite length, and an associated concentric cylindrical solid reactant. The chemical reaction which occurred along the pore walls, resulting in a build-up of product layer, was irreversible and first order with respect to the gaseous reactant. Only axial diffusion in the pore and only radial diffusion in the product layer and a sharp interface reaction were considered. The main parameters of the model were the effective pore length, the effective diffusivity in the product layer and the ratio of the molal volume of the porous product to that of the reactant (γ), which accounted for the change in pore geometry. The governing equations were solved numerically and the effects of γ, the effective pore length, the effective diffusivity, and the reaction rate constant on the conversion were investigated. For $\gamma > 1$, the model predicted an asymptotic conversion less than 100 percent due to the closure of the pore mouths. The use of the proposed model for predicting conversion-time curves was illustrated by means of experimental data for the reduction of NiO pellets with carbon monoxide ($\gamma < 0$) and for the reaction of sulphur dioxide with calcium carbonate ($\gamma > 1$). In the former, reasonable agreement was obtained, and in the latter, the model predictions agreed well with the experimental data in the early

stages of the reaction, but overestimated the asymptotic conversion level. This was attributed to other possible structural changes, such as sintering, during the experiment.

c- Grain Model

Szekely and co-workers published a series of papers concerning the development of a structural model to describe the progress of a reaction in terms of the porosity, grain size, gas phase and solid state diffusivities, and a heterogenous reaction rate constant independent of the solid structure, as opposed to the rate constant of a shrinking-core model where structural parameters were incorporated into an empirical reaction rate constant.

The basic model (Szekely and Evans, 1970) was developed for a first order isothermal irreversible reaction, taking place in a semi-infinite porous solid, without external mass transfer resistances and with equimolar counter-diffusion in the solid. It was further assumed that the initial structure was maintained throughout the reaction and remained unaffected by the progress of the reaction. Two types of material were examined. The first was a continuous solid with uniform cylindrical pores normal to the reaction interface, the pore model which has already been discussed. The second was composed of spherical solid particles, each of which reacted according to the shrinking-core model. In this case, the gaseous reactant diffuses in the axial direction

through the interstices, and each horizontal row of grains is surrounded by a gas of uniform but time-dependent composition. Under pseudosteady state approximation, the time-conversion relations were calculated numerically in terms of an equivalent penetration similar to the pore model case. The influences of such parameters as the grain size, the porosity of the solid material, solid state and gas phase diffusivities and the reaction rate constant on the equivalent penetration-time relationships were demonstrated. Szekely and Evans recognized the fact that structural changes are likely to occur as the reaction proceeds, due to sintering, agglomeration or simply change in the molar density.

Later, Szekely and Evans (1971 a, c) extended the plain grain model to a spherical geometry with the additional assumption that the reacted layer surrounding each grain presents no diffusional resistance. The model incorporated parameters such as porosity and grain size, and allowance was made for the role played by these quantities in affecting both the pore diffusivity and the reaction of individual grains. The overall rate of reaction was computed by summing up the contributions of all the individual grains that made up the porous solid matrix. A solution was obtained numerically and presented in the paper by Szekely and Evans (1971 a).

Experimental measurements (Szekely and Evans, 1971 b, c) on the reaction of nickel oxide pellets with hydrogen were in-

terpreted on the basis of this grain model. The photographs of sectioned partially-reduced pellets showed that, at the lowest temperatures, the reaction extended throughout the pellet volume. Increasing temperatures led to progressively narrower reaction zones and the pellet reacted at 1173 K exhibited a very sharp interface between the reduced and unreduced regions of the pellet. Good agreement between the predicted and measured overall reduction rates was obtained for different pellet sizes and porosities. The agreement was less satisfactory at low temperatures, where chemical kinetics played a predominant role, and also at high temperature where structural changes (sintering) occurred, which was neglected in the model. Both the predictions and the experimental data indicated the existence of an optimal condition in terms of grain size, porosity and temperature, for the reaction of single spherical porous pellets. The proposed scheme would converge to the shrinking-core model at high temperature (diffusion control) and would approach the behaviour of a homogenous reaction model at low temperatures, where chemical reaction control takes place.

Sohn and Szekely (1972 b) generalized their grain model to allow for spherical and flat plate-like pellets made up of spherical or flat plate-like grains. The governing equations, under the same assumptions which were applied to the previous model, were non-dimensionalized and solved numerically for a number of situations. The solution resulted in a plot of

dimensionless time to achieve complete reaction against a generalized gas-solid reaction modulus (σ) which incorporated both structural and kinetic parameters, and was valid for all geometries. The generalized reaction modulus was defined as:

$$\sigma = V_p/A_p\,[(1 - \varepsilon)\, k_s\, C_{A0}^{n-1}\, F_p\, A_g / 2\, D_e\, F_g\, V_g]^{1/2} \tag{51}$$

where, F_p and F_g are shape factors for the pellet and the grains, respectively. A is the initial surface area and V is the initial volume.

As σ approaches zero, the overall rate is controlled by chemical kinetics and the diffusion within the pellet is rapid compared with the rate of chemical reaction and a homogenous reaction model with respect to the pellet results. As σ approaches infinity, the overall rate is controlled solely by the diffusion of the gaseous reactant within the pellet and the model reduces to the shrinking-core model.

Szekely, Lin and Sohn (1973) further investigated the reduction of porous nickel oxide pellets with hydrogen within the temperature range of 500 - 685 K, and interpreted the experimental results using their recent generalized model. A set of experimental runs on thin discs at different temperatures was performed to obtain information on the intrinsic kinetic parameters and on the shape of the solid grains under conditions where diffusional effects were negligible. The shape factor F_g was obtained by

plotting $1 - (1 - X)^{1/F_g}$ versus time (chemical control) for various trial values of F_g; the value of 2 was then selected for F_g as it provided the best straight line relationship. Reaction rates at the same temperature but for different pellet sizes allowed the evaluation of the intrinsic rate constant. The plots of conversion-versus-time which were predicted by the model to be linear showed deviation from a straight line towards the end of the conversion. This was attributed to the possibility of a diffusional resistance in the individual grains and also to the non-uniformity of the grain size. The intrinsic kinetic data obtained at lower temperatures agreed well with the literature data, while that at high temperatures was less satisfactory, due to the fact that diffusional effects could not be properly excluded. The data taken using larger pellets allowed the determination of the diffusional parameters. The kinetic and diffusional parameters obtained in the two asymptotic regions were then used to predict the conversion-time curves for reaction in the intermediate region (diffuse zone-reaction) where both the kinetic and diffusional resistances were important. The predictions were found to be reasonable in most cases, where an appreciable induction period did not occur. However, the time predicted for complete conversion of the pellets over and under estimated randomly. This was suggested to be due to some structural changes in the reacting pellet during the course of the reaction.

The grain-pellet model developed by Szekely and co-

workers considered the pellet to be isothermal and neglected the diffusion-resistance through the ash layer of the grain. Recently, Sampath et al. (1975) made a transient non-isothermal analysis of the same model with the inclusion of an ash layer diffusion resistance but called their treatment a "particle-pellet" model. The solid was taken as an assembly of relatively non-porous spherical particles of uniform size compressed into a spherical pellet. Their mathematical model assumed: (i) both pellets and constituent particles did not change in size during the reaction; (ii) particles were at a uniform temperature, but the pellet was large enough to permit both concentration and temperature profiles to exist; (iii) the chemical reaction was first order and irreversible with respect to the gaseous reactant; (iv) the reaction occurred at a sharp interface in the particle; (v) the effective diffusivity of the gas in the pellet and of the product layer in the particle, and the mass and heat transfer coefficients in both gaseous and solid phases remained invariant with temperature and concentration changes throughout the reaction. This model also neglected the structural changes. A single particle rate equation was incorporated with the initial porosity and particle diameter to evaluate the rate based on the pellet volume. This was then coupled with the transient mass and heat balance equations on the pellet. The resulting non-linear parabolic partial differential equations were reduced to systems of simultaneous first order ordinary differential equations by means of the "Orthogonal Collocation" method, which

were then solved numerically. The Orthogonal Collocation method is a special case of the collocation method and of the method of weighted residuals, and it was first reported by Villadsen and Stewart (1967) and further discussed by Ferguson and Finlayson (1970) and Finlayson (1972, 1974). In this method, the unknown solution is expanded in a series of known functions (orthogonal polynomials) with arbitrary coefficients and the solution is obtained at the collocation points which are the roots of the orthogonal polynomials. Sampath et al. investigated the effects on the temperature profile and overall conversion of such parameters as the particle and pellet radii, the effective diffusivity in the product layer and in the pellet and the thermal conductivity in the pellet. The inadequacy of the pseudosteady state assumption for heat transfer was confirmed. The model approximated the homogeneous, shrinking-core and diffuse zone-reaction models for the pellet as a whole, depending upon the physical characteristics of the pellet and the intrinsic kinetics of the reaction.

All of the diffuse zone-reaction models discussed until now viewed the pellet as originally porous and having diffusional gradients. The majority of them required computer solutions. Park and Levenspiel (1975) introduced a distinctly different kind of model which was called the "crackling-core model." The pellet was assumed to be initially non porous. Under the action of the reactant gas, the pellet then transformed itself progressively

from the outside in, by crackling and fissuring, to form an easily penetrated (no diffusional resistance) grainy material, which then reacted away to the final product according to a shrinking-core model with either reaction or ash-diffusion control. The diffusion resistance within the attacked porous structure was neglected in order to avoid the need for a numerical solution. The rate of reaction of the virgin core and of the grains was first order with respect to gaseous reactant and the system was isothermal. Figure 4 from Park and Levenspiel illustrates the different stages through which a pellet passes according to this model, in relation to the relative values of the time needed for complete disappearance of the virgin core (τ_c) and the time for complete conversion of a grain (τ_g). Analytical expressions for the time-conversion relationships were presented for various stages of conversion: initiation, propagation and termination. For the reaction control of grains the analysis yielded explicit solutions, while for the ash-diffusion control in the grain the expressions could not be obtained in explicit forms. This model is an extension of the shrinking-core model, involving one additional parameter (τ_c/τ_g). The evaluation of this parameter which was described in the paper required conversion-time experiments with different pellet size and fitting the data for the best values of τ_g and τ_c.

At one extreme ($\tau_g \ll \tau_c$), the proposed model reduces to the simple shrinking-core model, while at the other extreme (τ_g

FIGURE 4

PROGESSIVE STAGES IN CONVERSION OF A PELLET

ACCORDING TO THE CRACKLING CORE MODEL

TWO PROGRESSIONS ARE POSSIBLE DEPENDING ON WHETHER

$\tau_g > \tau_c$ or $\tau_g < \tau_c$

(Park and Levenspiel, 1975)

THE CRACKLING CORE MODEL FOR THE REACTION OF SOLID PARTICLES

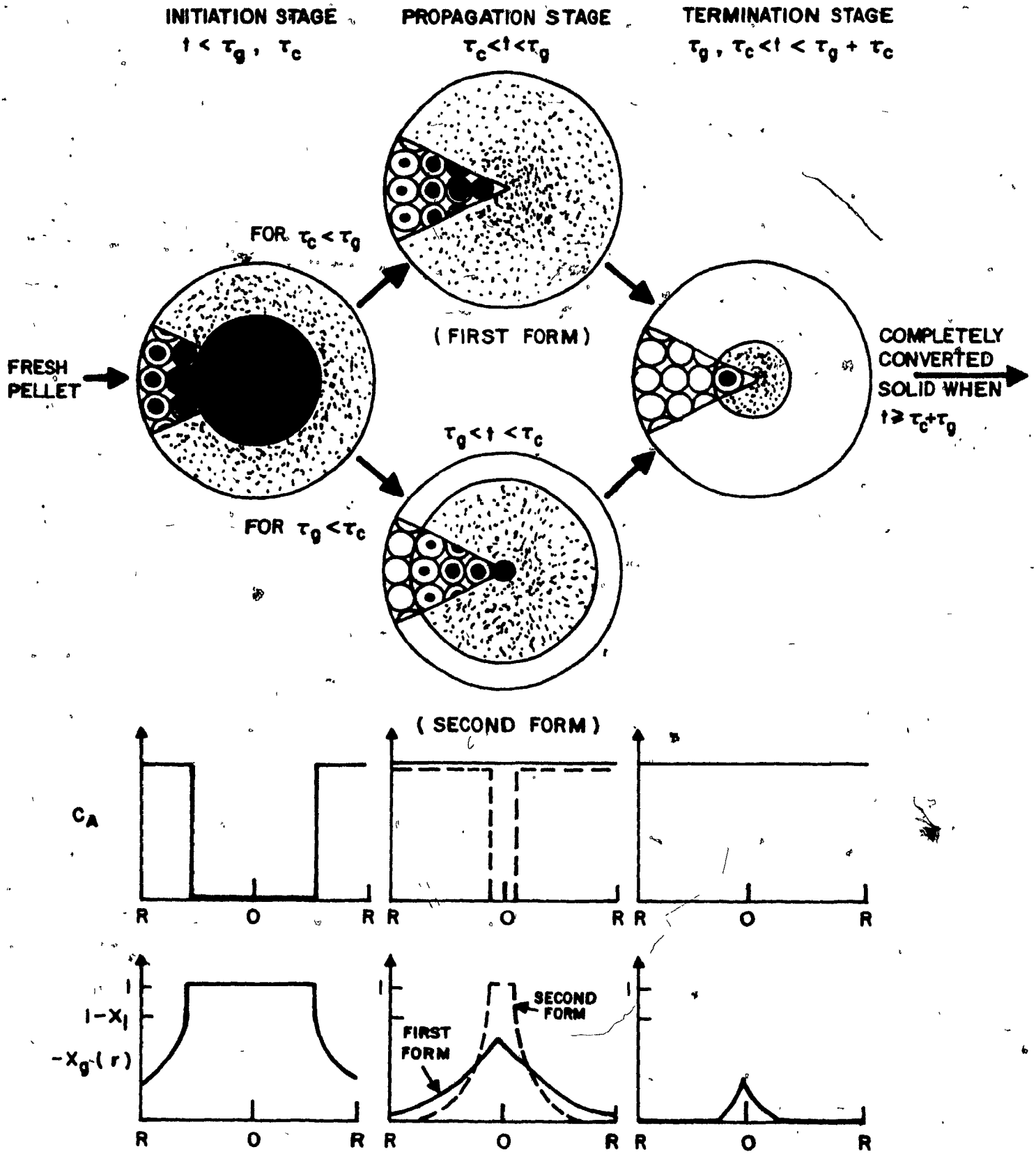

$\gg \tau_c$), it predicts a uniformly reacting pellet. Application of the crackling core model to the experimental conversion-time data of the reduction of magnetite with CO, resulted in a close agreement, better than with the shrinking-core model. Recently, Park and Levenspiel (1977) suggested the use of this model in gas-solid reactions involving multisteps, such as the reduction of hematite through magnetite, then wüstite and finally to iron (Tsay et al., 1976).

The interrrelationships between the three types of diffuse zone-reaction models (volumetric, pore and grain models) was discussed by Ishida and Wen (1971a). By introducing the concept of an equivalent rate constant based on the surface reaction model, each diffuse zone-reaction model was shown to be represented in terms of equivalent characteristic parameter of the shrinking-core model. Later, this isothermal analysis was extended to nonisothermal cases (Ishida and Wen 1971b). It was shown that nonisothermal diffuse zone-reaction model could also be approximated by the shrinking-core model, by considering the heat effect on the equivalent rate constant. However, since the temperature profile in the solid did not normally reach steady state, the equivalent rate constant approach for the nonisothermal case tended to be more in error than that for the isothermal case.

CONCLUSION

The noncatalytic gas-solid reaction models for a single

particle (pellet) were reviewed under two headings: the surface reaction models and the diffuse zone-reaction models. The latter were discussed with respect to the volumetric-reaction model, pore model and grain model, together with their "uniformly-reacting pellet" applications. The isothermal shrinking-core model in the presence of individual rate-controlling mechanisms (kinetic, ash-diffusion, film-diffusion) is the simplest and the most widely used for the interpretion of experimental data. The non-isothermal case of the shrinking-core model with a pseudosteady state approximation gives an analytical solution, but this assumption has been found not to be valid for most cases. On the other hand, a transient approach requires a computer solution.

The majority of the diffuse zone-reaction models necessitate numerical solution plus a large number of input parameters, depending upon the specific model they are based on. Uncertainties in the physical and kinetic input parameters usually reduce the accuracy gained from the mathematically-complex treatments, and the predictions become no more accurate than those obtained from analytical expressions of simpler models. In any event, the works in the field seem to be divided in two groups, the first with a primary interest in mathematical modelling, and the second mainly concerned with experimental measurements and the interpretation of the data.

Almost all of the proposed models consider the presence of a single solid component in the pellet, although practical

situations arise where more than one component is involved, such as the chlorination of a metal oxide in the presence of carbon. Russian workers treated this problem as a homogeneous reaction version of the volumetric-reaction model. Although the shrinking-core model assumes a non-porous solid, it has been applied to porous solid reactions successfully.

Finally, it is important to note that the use of a particular model can only be justified if it fits the specific gas-solid reaction involved, if it agrees with the conceptual representation of the progress of the reaction, and if the reliability and accuracy of the experimental data are good enough to take into account the complexities of the more sophisticated models.

PLASMA PHENOMENA AND GAS-SOLID REACTIONS IN PLASMAS

DEFINITIONS

A plasma may be defined as a gas that is sufficiently ionized to be electrically conductive, although, as a whole, it is electrically neutral. For the ionized gas (composed of free electrons, positive ions, neutral atoms and molecules) to be properly termed a plasma, it must satisfy the requirement that the concentrations of positive and negative charge carriers are approximately equal (Hollahan and Bell, 1974). Depending upon the conditions under which it is formed, the plasma may be

either hot (operating at and above atmospheric pressure) or cold (operating under vacuum, in which case the molecules are at a low temperature and the electrons at a high temperature). It is generally considered that plasmas operating at and above atmospheric pressure, the "thermal plasmas," are locally in thermal equilibrium (Reed, 1967). This assumption of local thermal equilibrium (LTE) is of fundamental importance from a theoretical and analytical point of view. Thermal plasmas formed by electrical discharges are those most relevant to high-temperature chemical and metallurgical processing and, for the purpose of this thesis, discussion will be limited to this type of plasmas.

PLASMA GENERATION

A plasma is generated whenever sufficient energy is transmitted to a gas to cause at least partial ionization. The electrons accelerated by the initiation of a plasma will collide with and excite the atoms or molecules in the gas. This excitation can cause complete ionization, orbital displacement of one or several electrons or simply increased kinetic energy of the various species involved. The electrons freed by ionization are also accelerated and cause more collisions and further ionization, resulting in an energy transfer from the electric field to the gas, which is accompanied by a rise in the latter's temperature. Once a plasma is formed, energy must be continuously added to make up for thermal conduction and radiation losses and to prevent immediate reattachment and recombination.

A thermal plasma formed by electrical discharges can be generated either with electrodes (arc discharges) or without electrodes, as in inductance or capacitance-generated plasma from a high-frequency source. Arc discharges, on the other hand, are produced either as non-transferred (stationary) arc or as transferred arc. Depending upon the method of arc stabilization (which is defined as the process by which the arc column is positioned or localized within the region between the electrodes), the non-transferred arc is further subdivided into different categories. Baddour and Timmins (1967) and Gerdeman and Hecht (1972) have described these in detail.

In the transferred arc, the arc is struck between the cathode and the external workpiece which acts as the anode. This type is used for welding, cutting or other processing requiring high workpiece temperature, and also for the spraying of protective coatings. New and important applications for transferred arcs have recently been found in the field of extractive metallurgy, when the anode consists of a molten metal.

In the non-transferred arc, such as in a d.c. torch, the cathode is surrounded by an annular anode, the outer end of which consists of a constricting nozzle. An arc is struck between the electrodes and is blown through the nozzle by the plasma-forming gas.

In the electrodeless plasma generator, the energy is

transferred from the high frequency source to the gas by either a coil or a set of capacitor plates, resulting in an inductive or capacitive coupling between the electric and magnetic fields. Elimination of the presence of electrodes from the plasma chamber avoids contamination of the working system with material which may evaporate or be eroded from the electrodes, and permit the use of even quite corrosive gases like chlorine as plasma-forming gases. Application of a radio-frequency energy source to sustain a plasma was first described by Reed (1961) and further covered by Baddour and Timmins (1967) and Hollahan and Bell (1974).

In his Ph.D. thesis, Munz (1974) made an extensive review of plasma devices, both those which were useful in small laboratory experiments, and those which were considered for commercial operations. He described in detail the operations of different torches and compared them with respect to their areas of application. Also, in a number of review papers, Kubanek and Gauvin (1967), Ibberson and Thring (1969), Landt (1970), Sayce (1971, 1976), Rykalin (1977) and Hamblyn (1977) described various types of plasma devices and/or furnaces.

Both d.c. plasma and R.F. induction torches have been used in this laboratory for a number of studies on heat and momentum transfer to small particles (Kubanek and Gauvin, 1968), (Kubanek et al., 1968), (Chevalier et al., 1970), (Lewis and Gauvin, 1973), (Katta et al., 1973), (Katta and Gauvin, 1973a, 1973b), (Sayegh, 1977). An induction torch was also used in a study of

high-temperature reaction kinetics (Munz and Gauvin, 1975). Currently, work is continuing on heat transfer and diagnostics of a transferred arc plasma.

PLASMA GAS-SOLID REACTIONS

Considerable research effort has been devoted over the past twenty years in the development of new chemical and metallurgical processing technologies, based on plasma devices. Several recent review articles cover much of the progress to date. The most important of these will now be briefly summarized.

Vurzel and Polak (1970) covered a wide range of chemical reactions which have been studied in various plasma devices, with particular emphasis on homogenous reactions and on the importance of quenching. The review by Landt (1970) was devoted to a description of inorganic reactions that have been carried out in arc plasma jets. Sayce (1971) and Waldie (1972a, 1972b) concentrated on heterogenous reactions in plasma, with particular emphasis on metallurgical processes. Hamblyn and Reuben (1975) reviewed the use of radio-frequency plasmas in chemical synthesis, covering both organic and inorganic reactions and their prospects for commercial applications.

In his recent review, Sayce (1976) discussed the current status of plasma processes involving heat and mass transfer with particular reference to chemical reaction and processes of vaporization and condensation. Rykalin (1976) presented a survey of

the work done in the U.S.S.R. on the generation of thermal plasmas generated by d.c. jets. More recently, Polak (1977) gave an account of various plasma reactions that have been reported mostly by Russian workers. Hamblyn (1977) presented a brief survey of typical applications of plasma technology in metallurgical processing and discussed the work carried out on ferroalloy applications in South Africa.

The first comprehensive study of heterogeneous chemical kinetics in a plasma flame was reported by Munz and Gauvin (1975). They investigated the decomposition kinetics of molybdenite in the tailflame of a radio-frequency induction plasma. A reactor system was developed to allow kinetic measurements in both the solid and the molten state, using single stationary spherical pellets pressed from naturally-occurring thin flakes of molybdenite. It was concluded that the solid state reaction was controlled by the diffusion of sulphur vapour through the product layer. The shrinking-core model described the overall reaction which led to a time-versus-conversion equation of the form:

$$t/\tau = 1 - 3\ (1 - X)^{2/3} + 2\ (1 - X) \qquad (52)$$

where, X is the fractional conversion to metal, τ is the time for complete conversion and t is the reaction time. The influence of particle diameter and void fraction on the rate of reaction confirmed the existence of ash diffusion control.

The liquid state reaction was found to be governed by the

rate of heat transfer to the reacting particles, which was in turn influenced by the mass transfer of sulphur vapour from the molten molybdenite. For the heat transfer calculations, the temperatures and velocities of the plasma jet at the position of the reacting particles were estimated by the authors from the mean nozzle exit values, which were obtained from experimental calorimetric studies (Munz, 1974), using the predictions of Boulos and Gauvin (1974).

Earlier studies of the thermal decomposition of molybdenite in plasma were reported by Huska and Clump (1967) and Charles et al. (1970). Huska and Clump injected fine (-200 mesh) molybdenite particles directly into an R.F. argon plasma fireball through a water-cooled probe and collected the product both from the quartz tube which contained the plasma and from a water-cooled quench chamber. They obtained conversions as large as 70 percent, although most of the conversions ranged from 30 to 50 percent, with feed rates ranging from 0.67 to 2.5 gm/hr. The degree of conversion was found to be a linear function of the power transferred to the plasma flame.

Charles et al. (1970) injected molybdenite powder (50 micron in average diameter) through a water-cooled probe into the upper surface of plasma fireball. Molybdenum was collected from the fireball on a water-cooled surface. They obtained 60-70 percent conversions at a feed rate up to 60 gm/hr.

Bhattacharyya and Gauvin (1975) used the thermal

decomposition of molybdenite particles as a specific application of their theoretical model which was developed to simulate a plasma jet reactor for the treatment of fine particles. They considered a three-dimensional, non-isothermal, turbulent, compressible swirling confined flow. Velocity profiles of the plasma jet were calculated from the equations given by Chigier and Chervinsky (1967) and similar profiles were assumed for temperature. Particle size, injection velocity and location, swirl parameter and angle of injection of the feed were found to be the important parameters. While high solid loadings quenched the gas and lowered the reaction rate, lower solid loadings (wt. solid/ wt. gas < 0.25) had insignificant effects on the overall conversion provided that sufficient residence time was available.

Recently, Bonet (1976) made a theoretical analysis of heterogenous reactions taking place in plasma systems. Using a shrinking-core model, he showed that, in general, the progress of reaction in fine particles (or in larger ones, as soon as they have reached a high temperature) was controlled mainly by a heat transfer mechanism. In view of this fact, he emphasized the importance of transport phenomena in the development and design of plasma reactors, particularly for the processing of refractory metals and their compounds.

Among the several papers published by Matsumoto and coworkers (Matsumoto, 1968, 1969), (Matsumoto and Shirato, 1970), (Matsumoto and Kawai, 1972), (Matsumoto et al., 1972) concerning

the synthesis of refractory metal nitrides and oxides in transferred arc plasma, only in the two most recent papers were some kinetic data reported. The reaction was usually carried out between plasma gas and a disk-like pellet mounted on a water-cooled copper anode.

In the reaction between a nitrogen plasma and zirconium metal (Matsumoto and Kawa, 1972), the rate of nitridation followed a parabolic law, which was attributed to the diffusion of nitrogen into liquid zirconium as the rate limiting step. In the reaction between an air plasma and zirconium (Matsumoto et al., 1972), nitrogen and oxygen atoms in the air plasma jet were shown to react independently with zirconium to form ZrN and ZrO_2. It was reported that the dissolved amount of oxygen increased linearly with increasing reaction time and air flow rate and stayed in the surface region, while that of nitrogen increased parabolically and penetrated into the inner regions of the metal. Their thermodynamic analysis showed that, while the nitriding of ZrO_2 by nitrogen was impossible, the oxidation of ZrN might take place. This was in fact confirmed experimentally, since the ZrN formed was oxidized by oxygen in the air plasma jet.

The mechanism of the reaction between zircon-graphite mixtures and a nitrogen plasma jet was studied by Matsumoto and Shirato (1970). They reported that zircon was first decomposed, following which reaction between nitrogen and ZrO_2, SiO_2 and graphite took place. The $C/ZrSiO_4$ ratio influenced the composition

of the final product and the optimum nitriding condition for zircon was obtained with a $C/ZrSiO_4$ ratio of 3. The overall reaction was suggested as:

$$ZrSiO_4 + 3C + N \rightarrow ZrN + SiO + 3CO \qquad (53)$$

When the ratio $C/ZrSiO_4$ exceeded 4, ZrC and SiC were also formed.

Particulate systems have also been used to synthesize nitrides. Stokes (1969) reported the production of nitrides of titanium, magnesium and tungsten by injecting the powdered metal into a nitrogen plasma. Complete conversion was obtained with titanium, while the conversions of magnesium and tungsten were 40 and 25 percent, respectively.

Plasma reduction of metal oxides has been attempted by several investigators (Gilles and Clump, 1970), (Rains and Kadlec, 1970), (Stokes, 1969), (Brown, 1967). However, in all of these works, as in most other investigations, the intention was to determine important process parameters and assess their quantitative effects, rather than to make a detailed kinetic study.

Rains and Kadlec (1970) investigated the feasibility of reducing a stable refractory oxide, such as aluminum oxide, in an argon induction plasma. Alumina powder (26 - 45 microns) was fed into the fireball and the product was collected on the water-cooled reactor wall. Conversions ranging from 3 to 30 percent were reported in the absence of reducing agent and at power levels

of 5.03 - 6.69 kW, corresponding to argon temperatures of 10 900 - 11 200 K. Conversions increased with increasing power input, and with decreasing alumina flowrate and particle size. The use of a water-cooled probe placed directly in the plasma allowed the recovery of additional aluminum at higher conversions. Doubling and quadrupling of the conversion were obtained by using CO and CH_4 as reducing agents, in the plasma, and by quenching with cold gases introduced into the lower section of the plasma core, counter-current to the plasma flow. It is interesting to note that the use of hydrogen as a reductant showed almost no effect on the conversion. The conversion data presented by Rains and Kadlec were based only on the material collected, and as such may not represent a realistic sample. Extrapolation of their analysis to all the alumina in the feed may not be justified, as material bypassing the flame would not deposit on the walls and would probably show a much lower degree of conversion.

Using a direct current arc plasma jet, Gilles and Clump (1970) attempted to reduce iron ore with hydrogen. They injected the iron ore powder into the nozzle (anode) exit plane at a 45-degree angle through two ports spaced 180 degrees apart, thus permitting the ore particles to leave the torch without coming into contact with the anode wall. The product was quenched and collected on a water-cooled copper plate assembly. Their conversions were up to 69 percent with a 100-percent hydrogen plasma, and at a feed rate of 1 gm/min. It was again found that the

extent of conversion to iron increased with an increase in power and a decrease in powder size. In addition, conversion was higher at the lower plasma gas flow rates for the same amount of energy per unit volume of plasma gas. This was attributed to a longer residence time.

Stokes (1969) reported complete conversion of ferric oxide to iron metal with hydrogen in a helium plasma jet. No conversions were obtained in the reduction of titanium dioxide and zirconium dioxide with hydrogen in the same work.

Although Brown's (1967) attempt to reduce zirconium dioxide to the metal by passing powdered (10-micron particles) zirconia through a d.c. plasma flame in a carbon reaction chamber resulted in an increase in the zirconium content of the product, his work was not conclusive in that the presence of metallic zirconium was not clearly identified and the small differences in zirconium content between the reactants and the products might have been due to experimental error.

Recently, Gold et al. (1977) reported the development of a single-step plasma reactor system to convert iron oxide directly to molten iron in a hydrogen-natural gas mixture. The iron ore powder was pneumatically conveyed to the plasma reactor and injected into the hot reducing gases produced by a d.c. arc. Molten iron and slag were collected in a holding crucible, which was poured intermittently. The electrical energy consumed was given as 9.5 MJ/kg of iron (not including energy losses from the

reactor) at a hydrogen-natural gas ratio of two. This value compared favourably with a minimum thermodynamic process energy requirement of about 7.9 MJ/kg of iron. It was suggested that the specific energy requirement would be decreased by a reactor scale-up from 100 kW to 1 MW, by the use of finer powder and by an increase in the natural gas-hydrogen ratio.

Again recently, Mac Rae et al. (1977) described a commercial-scale plasma reactor that has been developed for the production of ferrovanadium. The operation involved the injection of a mixture of vanadium oxide and coke powders into a transferred arc plasma (falling-film plasma reactor) where the oxide was reduced by carbon, and the vanadium thus produced was combined with an initial charge of iron in a receiving crucible below the reactor. The design of the falling-film plasma reactor developed by Mac Rae and his co-workers is rather unique, in that the arc is transferred from a single cathode to the lower portion of the cylindrical reactor wall which acts as the anode. By the use of a strong swirling action in the injected reducing gas (hydrogen mixed with argon) the particles are flung against the anode walls where they melt and flow down in the form of a film, which accounts for the name given to this type of system.

The molten ferrovanadium produced contained 40 - 90 percent vanadium, and the energy consumption was reported to be 32 MJ/kg of vanadium. The reactor was developed at a nominal 100 kW level and then scaled-up to 500 kW.

PLASMA CHLORINATION OF METAL OXIDES

The use of plasma technology in metal oxide chlorination was suggested in the paper published by Warren and Shimizu (1967). Aside from this, the literature on the subject of plasma chlorination is limited to a few patents issued after 1950. Two of these were granted to Sheer and Korman (1952a, 1952b) in which the high-intensity transferred arc was one of the first techniques to be employed for the purpose of vapor phase halogenation or reduction of metal oxides. In the first process described by Sheer and Korman (1952a) a mixture of the metal oxide and carbon in stoichiometric proportions was compacted into a hard cylindrical bar and was fed into the reaction chamber as the core of a carbon shell. The core acted as a consumable anode and was evaporated in an atmosphere of chlorine, thereby producing chlorides of all the metal constituents by vapor phase reaction. In an inert atmosphere, the reduction of the oxide to the metal was also claimed.

In the case of silicates, Sheer and Korman (1952b) suggested that partial chlorination was possible by recycling the silicon tetrachloride formed to the reaction chamber, thus preventing further halogenation of the silicon dioxide in the ore and conserving carbon and chlorine. Using their high intensity arc, the core made out of a mixture of the silicate with carbon was vaporized at the rate of several feet per minute at 1500 amp., and reacted with the chlorine plasma at a temperature of 7000 -

10 000 K.

Orbach et al. (1968) have patented a plasma process with non-consumable electrodes for the chlorination of beryllium oxide. The process used a d.c. plasma jet (55 - 60 kW) of nitrogen (as arc stabilizer) to heat a stream of chlorine containing a mixture of finely ground beryllium oxide (68 percent) and petroleum coke (32 percent by wt.). Using feed rates of 16 kg of ore-carbon mixtures, 28 kg chlorine and 6.22 m^3 nitrogen per hour, a conversion of 62.6 percent was obtained in a single pass at an energy consumption of 417 MJ/kg of beryllium. The arc temperatures and reaction times for halogenation were reported to be 2000 - 10 000 K and 1/1000 second, respectively. Reduction of $BeCl_2$ with sodium to obtain metallic beryllium was also included in their patent claims.

A very recent patent granted to Davis et al. (1976) described the use of plasma method to chlorinate the oxides of Nb, Mo and Ta with carbon-chlorine or carbon tetrachloride. In their description, the metal oxide and the chlorinating agent were introduced into the reaction zone downstream of the anode of the d.c. jet device, where the temperature was 2000 - 5000 K. The products were passed from this zone through a restricted passageway into a collection zone while maintaining a pressure differential of 0.5 - 5 psig between the reaction and collection zones by varying the size of the restricted passageway during the course of the reaction. No operating data was reported. The main

thrust of this patent was the agglomeration of very fine product powders into larger particles in the collection zone.

CONCLUSION

The selected articles on plasma gas-solid reactions and some of the review papers discussed in this section indicate that the majority of the investigations were designed to evaluate the importance of relevant operating parameters and their quantitative effects on the performance of the plasma system, rather than to do a fundamental kinetic study. The reason for this trend may be attributed to the nature of plasma systems, namely the high initial cost of plasma devices and attendant electrical controls, the complexity of their operation under laboratory conditions, not to mention the difficulties of obtaining reliable measurements under a very difficult experimental situation. The important kinetic parameters such as residence time, particle temperature, gas velocity, gas concentration and gas temperature may not be varied independently. Furthermore, conventional measurement techniques in most cases may not be used; simple measurements, such as gas and particle temperatures and velocities, usually require the development of sophisticated and often indirect techniques.

In the case of a chlorine plasma, such a study becomes an even more difficult task. The highly corrosive nature of hot chlorine creates serious problems of materials of construction,

and its toxicity necessitates extreme care in the handling of the gas streams. Finally, the stability of plasma operation may limit the concentration of chlorine gas that may be used in the plasma. All these limitations are most probably responsible for the absence of any plasma chlorination kinetic studies on a laboratory scale in the literature.

In recent years, the increase in the market value of fossil fuels and the experience with larger-scale plasma operations seems to have improved the prospects for their industrial commercialization considerably. However, to attain this objective, a much better understanding of the fundamental principles underlying their operation must first be obtained, particularly in the area of transport phenomena. In addition, it is now quite clear that different reactions will require different, unique design characteristics. Before the design of a plasma system can be undertaken, it is imperative to obtain the necessary kinetic data, which in turn will govern the design of virtually every component in the plasma.

In conclusion, it is now apparent that a plasma system every component of which is closely tailored to the exigencies of the proposed process, can effect the desired physical and chemical changes under unique conditions of extremely high reaction rates, resulting in high throughput per unit time, small equipment and continuous operation susceptible to excellent control. Because of high capital cost considerations, their

domain of application, at least for the present, should be restricted to high-temperature reactions yielding a product of high unit value. Because of the growing demand of our society for high-purity metals, metallic compounds and refractory materials, this domain is sufficiently vast to ensure this new technology a very bright future.

NOMENCLATURE

NOMENCLATURE

A	-	Gaseous reactant in Equation (16)
A_g	-	External surface area of the grain
A_p	-	External surface area of particle (or pellet)
a	-	Constant defined by Equation (21)
B	-	Solid reactant in Equation (16)
b, c, d	-	Stoichiometric coefficients
C	-	Gaseous product in Equation (16)
C_i	-	Molar concentration of species i
C_{AO}	-	Bulk concentration of gaseous reactant A
C_{BO}	-	Initial concentration of solid in the pellet
C_{CO}	-	Bulk concentration of gaseous product C
C^*	-	Concentration of intermediate product on the carbon surface
D_e	-	Effective diffusivity
D_{eo}	-	Effective diffusivity based on initial porosity
F_g	-	Shape factor for grain
F_p	-	Shape factor for particle (or pellet)
f_1, f_2	-	Functions of rate constants in Equations (39), (40)
G	-	Constant defined by Equation (50)
K	-	Overall rate constant
K_E	-	Equilibrium constant
k_s	-	Rate constant based on surface
k_m	-	Mass transfer coefficient

k_v	-	Rate constant based on volume
M	-	Modified Thiele modulus defined by Equation (36)
m	-	Order of reaction for solid reactant
N_{Re}	-	Reynolds number
N^o_{Re}	-	Reynolds number based on initial particle diameter
N_{Sc}	-	Schmidt number
n	-	Order of reaction for gaseous reactant
Q_{gen}	-	Rate of heat generation
Q_{loss}	-	Rate of heat loss
R	-	Initial particle radius
r	-	Particle or pore radius
r_A	-	Rate of reaction
r_C	-	Radius of unreacted core
r_o	-	Initial pore radius, Equation (49)
S	-	Contact area between metal oxide and carbon particles in the pellet
S_o	-	Initial contact area between metal oxide and carbon particles in the pellet
T	-	Reaction temperature
T_c	-	Temperature of unreacted core
t	-	Time
V_g	-	Volume of grain
V_p	-	Volume of particle (or pellet)
W	-	Weight of metal oxide in the pellet
W_∞	-	Weight of metal oxide for S = 0
ΔW	-	Amount of metal oxide reacted at time t
ΔW_∞	-	Maximum amount of metal oxide that can be reacted

X	-	Fractional conversion of the solid
γ	-	Ratio of molal volume of porous product to that of solid reactant
η_o, η	-	Effectiveness factor
ε	-	Porosity of solid reactant
ε_o	-	Initial porosity of solid reactant
ρ_s	-	Molar concentration of solid reactant
σ	-	Generalized gas solid reaction modulus, Equation (51)
τ	-	Time for complete conversion
τ_c	-	Time for complete disappearance of virgin core in the crackling-core model
τ_g	-	Time for complete conversion of any grain in the crackling-core model
ψ	-	Constant defined by Equation (31)

REFERENCES

REFERENCES

Abshire, E., Bibliography of Zirconium, U.S. Bureau of Mines I.C. 7830, U.S. Government Printing Office, Washington, (1958)

Anderson, J.W., 'Zirconium Tetrachloride,' U.S. Patent: 2,940,826, (1960)

Ausman, J.M. and Watson, C.C., 'Mass Transfer in a Catalyst Pellet During Regeneration,' Chem. Eng. Sci., 17, 323 (1962)

Ayukawa, B., 'Zirconium Chloride and Silicon Chloride from Zircon Sand,' Japan. Kokai Patent: 7,591,592, (1975)

Babu, R.S., Chintamani, Vijay, P.L. and Subramanyam, R.B., 'Production of Nuclear-Grade Zirconium Sponge from Pure Zirconium Oxide,' India, At. Energy Comm., Bhabha At. Res. Cent., BARC-427, (1969)

Baddour, R.F. and Timmins, R.S., The Application of Plasmas to Chemical Processing, The MIT Press, Cambridge, Massachusetts, (1967)

Bayliss, R.K., Bryant, J.W. and Sayce, I.G., 'Plasma Dissociation of Zircon Sand,' 3rd International Symposium on Plasma Chemistry, Paper No. S.5.2, Limoges, France, (1977)

Becherescu, D., Winter, Fr. and Cicoare, L., 'Reaction of ZrO_2 with Metallic Fe at High Temperatures,' Bul. Stiint. Teh. Inst. Politeh. Timisoara (Rom.), 12, (1), 37 (1967); Chem. Abst., 68:74782

Bergholm, A., 'Chlorination of Rutile,' Trans. Metall. Soc. AIME, 221, 1121 (1961)

Bhattacharyya, D. and Gauvin, W.H., 'Modeling of Heterogenous Systems in a Plasma Jet Reactor,' AIChE J., 21, (5), 879 (1975)

Bischoff, K.B., 'Further Comments on the Pseudo-Steady State Approximation for Moving Boundary Diffusion Problems,' Chem. Eng. Sci., 20, 783 (1965)

Bonet, C., 'Thermal Plasma Processing,' CEP, 72, 63 (Dec., 1976)

Boulos, M.I. and Gauvin, W.H., 'Powder Processing in a Plasma Jet: A Proposed Model, 'Can. J. Chem. Eng., 52, 355 (1974)

Bowen, J.R., 'Comment on the Pseudo-Steady State Approximation for Moving Boundary Problems, 'Chem. Eng. Sci., 20, 712 (1965)

Bowen, J.H. and Cheng, C.K., 'A Diffuse Interface Model for Fluid-Solid Reaction, 'Chem. Eng. Sci., 24, 1829 (1969)

Braver, G., Handbook of Preparative Inorganic Chemistry, Academic Press, New York, N.Y., 2nd. Ed., 1210 (1965)

Brown, R.A.S., 'Reaction of Some Zirconium Compounds in a Plasma Jet,' Presented at the CIMM Conference of Metallurgists, Kingston, Ontario, August 28-30 (1967)

Callow, A.E. and Bernard, H., 'Preparation of Zirconium and Silicon Tetrachloride,' German Patent: 1,268,603, (1968)

Calvelo, A. and Cunningham, R.E., 'Kinetics of Gas-Solid Reaction-Influence of Surface Area and Effective Diffusivity Profile,' J. Catalysis, 17, 1 (1970)

Calvelo, A. and Cunningham, R.E., 'Criticism of the Shrinking Core Model Used for Gas-Porous Solid Noncatalytic Reactions', Lat. Am. J. Chem. Eng. Appl. Chem., 2, 77 (1972)

Charles, J.A., Davies, G.J., Jervis, R.M. and Thursfield, G., 'Mineral Processing and Extractive Metallurgy,' Trans. Sect. C. Inst. Min. Met., 79, 54 (1970)

Chevalier, P.H., Kubanek, G.R. and Gauvin, W.H., 'Heat Transfer to Cylinders in a Confined Jet at High Temperature,' AIChE J., 16, 520 (1970)

Chigier, N.A. and Chervinsky, A., 'Experimental Investigation of Swirling Vortex Motion in Jets,' Trans. ASME J. Appl. Mech., 34, 443 (1967)

Chintamani, Vijay, P.L., Subramanyam, R.B. and Sundaram, C.V., Further Studies on the Pilot Plant Production of Reactor-Grade Zirconium Sponge,' India, At. Energy Comm., Bhabha At. Res. Cent., BARC-607, (1972)

Chizhikov, D.M., Deineka, S.S. and Makarova, V.N., 'Use of Plasmas in Chloride Metallurgy,' in Manual Investigations of Processes in Metallurgy of Nonferrous and Rare Metals, Naulca, Moscow, 136 (1969); Chem. Abst., 73:90192

Chizhikov, D.M., Tsvetkov, Yu.V., Panfilov, S.A., Deineka, S.S., and Tagirov, I.K., 'Use of a Low-Temperature Plasma in the

Metallurgy of Nonferrous and Rare Metals,' Nizkotemp. Plasma Tekhnol. Neorg. Veshchestv, Tr. Vses. Semin., 2nd 1970, 86 (1971); Chem. Abst., 80:147764

Ciba Ltd., 'Finely Divided, Nonpyrophoric Metals,' Neth. Patent Appl. 6,608,844, (1966)

Costa, E.C. and Smith, J.M., 'Kinetics of Noncatalytic, Non-isothermal, Gas-Solid Reactions: Hydro-fluorination of Uranium Dioxide,' AIChE J., 17, (4), 947 (1971)

Cunningham, R.E. and Calvelo, A., 'Kinetic Expressions for Reaction Rate in Noncatalytic Solid-Gas Systems,' Ind. Eng. Chem. Fundam., 9, (3), 505 (1970)

Davis, R.D., Meyer, T.N. and Blizzard, R.L., 'Plasma Method and Apparatus for Carrying Out High Temperature Chemical Reactions,' U.S. Patent: 3,954,954, (1976)

De Wet, J.F., 'The Kinetics and Mechanism of Solid-Gas Reactions,' Minerals Sci. Eng., 2, (2), 35 (1970)

Dunn, W.E., Jr., 'High Temperature Chlorination of TiO_2 Bearing Minerals,' Trans. Metall. Soc. AIME, 218, 6 (1960)

Elger, G.W., Quality of Zirconium Prepared by Different Reductants, U.S. Bureau of Mines R.I. - 5933, U.S. Government Print. Office, Washington, (1962)

Fahim, M.A. and Ford, J.D., 'Kinetics of Hydrogen Reduction of Cobalt Sulfide,' Can. J. Chem. Eng., 54, 578 (1976)

Ferguson, N.B. and Finlayson, B.A., 'Transient Chemical Reaction Analysis by Orthogonal Collocation,' Chem. Eng. J. Lausanne, 1, 372 (1970)

Finlayson, B.A., Method of Weighted Residuals and Variational Principles, Academic Press, New York, NY, (1972)

Finlayson, B.A., 'Orthogonal Collocation in Chemical Reaction Engineering,' Catal. Rev. Sci. Eng. 10, (1), 69 (1974)

Fruehan, R.J. and Martonik, L.J., 'The Rate of Chlorination of Metals and Oxides: Part III. The Rate of Chlorination of Fe_2O_3 and NiO in Cl_2 and HCl,' Metall. Trans., 4, 2793 (1973)

Gallay, J.J., Helary, J.L. and Graviere, M.J., 'Bulk Uranium, Titanium and Zirconium from their Oxides,' German Patent: 2,034,385, (1971)

George, A.,'Chlorination of Refractory Metal Oxides with Acetylene as Reducing Agent,' U.S. Patent: 3,320,023, (1967)

Gerdeman, D.A. and Hecht, N.L., Arc Plasma Technology in Materials Science, Springer-Verlag, New York, (1972)

Gilles, H.L. and Clump, C.W., 'Reduction of Iron Ore with Hydrogen in a Direct Current Plasma Jet,' Ind. Eng. Chem. Process Des. and Dev., 9, (2) 194 (1970)

Gold, R.G., Sandall, W.R., Cheplick, P.G. and Mac Rae, D.R., 'Plasma Reduction of Iron Oxide with Hydrogen and Natural Gas at 100 kW and 1 MW,' Ironmaking and Steelmaking, (1), 10 (1977)

Gol'tsova, T.F., Ivashentsev, Ya. I., Bezgreshnaya, N.P. and Skipor, L. Ya., 'Kinetic Study of Reductive Chlorination of Titanium Subgroup Oxides,' Uchebn. Zaved. Khim Khim Tekhnol., 19, (1), 169 (1976)

Gragg, F.M., 'Production of Pure Zirconium by Use of a Radio Frequency Plasma,' Ph.D. Dissertation, The University of Arizona, (1973)

Hamblyn, S.M.L. and Reuben, B.G., 'Use of Radio-Frequency Plasma in Chemical Synthesis,' in Advances in Inorganic Chemistry and Radio Chemistry, 17, Academic Press, 89 (1975)

Hamblyn, S.M.L., 'A Review of Application of Plasma Technology with Particular Reference to Ferro-Alloy Production,' National Institute for Metallurgy Report No. 1895, (1977)

Hashimoto, K. and Silveston, P.L., 'Gasification: Part I. Isothermal, Kinetic Control Model for a Solid with a Pore Size Distribution,' AIChE J., 19, (2), 259 (1973a)

Hashimoto, K. and Silveston, P.L., 'Gasification: Part II. Extension to Diffusion Control,' AIChE J., 19, (2), 268 (1973b)

Hollahan, J.R. and Bell, A.T., Edit., Techniques and Applications of Plasma Chemistry, John Wiley & Sons, (1974)

Huska, P.A. and Clump, C.W., 'Decomposition of Molybdenum Dilsufide in an Induction-Coupled Argon Plasma,' Ind. Eng. Chem. Process Des. and Dev., 6, (2), 238 (1967)

Ibberson, V.J. and Thring, M.W., 'Plasma Chemical and Process Engineering,' Ind. Eng. Chem., 61, (11), 48 (1969)

Ishida, M. and Shirai, T., 'Graphical Representation of Solid-Gas Reactions Based on Unreacted Core Model,' J. Chem. Eng. Japan, 2, (2), 1975 (1969a)

Ishida, M. and Shirai, T., 'Non-Isothermal Analysis of Unreacted Core Model for the Burning Rate of Single Carbon-Cement Spheres,' J. Chem. Eng. Japan, 2, (2), 180 (1969b)

Ishida, M. and Wen, C.Y., 'Effectiveness Factors and Instability in Solid-Gas Reactions,' Chem. Eng. Sci., 23, 125 (1968a)

Ishida, M. and Wen, C.Y., 'Comparison of Kinetic and Diffusional Models for Solid-Gas Reactions,' AIChE J., 14, (2), 311 (1968b)

Ishida, M. and Wen, C.Y., 'Comparison of Zone-Reaction Model and Unreacted Core Shrinking Model in Gas-Solid Reactions - Isothermal Analysis,' Chem. Eng. Sci., 26, 1031 (1971)

Ishida, M. and Shirai, T., 'Comparison of Zone-Reaction Model and Unreacted Core Shrinking Model in Gas-Solid Reactions - Non-isothermal Analysis,' Chem. Eng. Sci., 26, 1043 (1971)

Ishimatsu, K., Akira, M. and Masami, K., 'Manufacture of Zirconium Sponge by Reduction of Zirconium Tetrachloride and Its Apparatus,' Japan. Kokai Patent: 76 92 711, (1976)

Ishizuka, H., 'Zirconium Tetrachloride Reduction to the Metal; German Patent: 2 100 498, (1972)

Ishizuka, H., 'Preparation of Metal from Volatile Chloride,' Japan. Kokai Patent: 75 80 909, (1975a)

Ishizuka, H., 'Zirconium Metal,' Japan. Kokai Patent: 75 109 108, (1975b)

Ivashentsev, Ya. I., Gol'tsova, T.F. and Bezgreshaya, N.P., 'Chlorination of Thorium Dioxide in Trichloromethane Vapor,' J. Appl. Chem. USSR, 48, (11), 2543 (1975)

Kanjii, E., 'Titanium and Other Metals,' Japan. Kokai Patent: 73 63 914, (1973a)

Kanjii, E., 'Tatanium and Zirconium Manufacture,' Japan. Kokai Patent: 73 103 409, (1973b)

Katta, S. and Gauvin, W.H., 'Local and Overall Heat Transfer to Spheres in a Confined Plasma Jet,' AIChE E. Symposium Series No. 131, Heat Transfer: Fundamentals and Industrial Applications, 69, 174 (1973a)

Katta, S. and Gauvin, W.H., 'The Effect of Local Gas Velocity and Temperature on the Local Heat Transfer to a Sphere in a High Temperature Jet,' Can. J. Chem. Eng., 51, (3), 307 (1973b)

Katta, S., Lewis, J.A. and Gauvin, W.H., 'A Plasma Calorimetric Probe,' Rev. Sci. Istrum., 44, (10), 1519 (1973)

Ketov, A.N., Gaisinovich, M.S., Burmisurova, E.V. Fedorov, A.A., Shlingerskii, A.S., 'Mechanism of Chlorination of Metal Oxides in the Solid State,' Chem. Abst., 83: 103 907, (1974)

Kirk, R.E. and Othmer, D.F., Encyclopedia of Chemical Technology, 2nd Ed., 22, Wiley (Interscience), New York, (1963)

Klimaszewski, I.C., 'Zirconium Metal Production,' U.S. Patent: 3 318 688, (1967)

Kroll, W.J. and Schlechton, A.W., Survey of Literature on the Metallurgy of Zirconium, U.S. Bureau of Mines I.C. - 73 41, U.S. Government Printing Office, Washington, (1946)

Kroll, W.J., Anderson, C.T., Holmes, H.P. Verkes, L.A. and Gilbert, H.L., 'Large Scale Laboratory Production of Ductile Zirconium,' Trans. Electrochem. Soc., 94, 1, (1948)

Kroll, W.J., Hergert, W.F. and Gerkes, L.A., 'Improvements in Methods for the Reduction of Zirconium Chloride with Magnesium,' Trans. Electrochem. Soc., 97, 305 (1950)

Kroll, W.J., Carmody, W.R. and Schlechton, A.W., High Temperature Experiments with Zirconium and Zirconium Compounds, U.S. Bureau of Mines R.I. - 4915, U.S. Government Printing Office, Washington, (1952)

Kubanek, G.R. and Gauvin, W.H., 'Recent Developments in Plasma Jet Technology,' Can. J. Chem. Eng., 45, 251 (1967)

Kubanek, G.R. and Gauvin, W.H., 'Plasma Research Facility for Solid-Gas Heat Transfer Studies,' The Chemical Engineer (U.K.) No. 222, 332 (1968)

Kubanek, G.R., Chevalier, P. and Gauvin, W.H., 'Heat Transfer to Spheres in a Confined Plasma Jet,' Can. J. Chem. Eng., 46, (2), 101 (1968)

Landsberg, A., 'Chlorination Kinetics of Aluminum Bearing Minerals,' Metall. Trans., 6B, 207 (1975)

Landsberg, A., 'Some Factors Affecting the Chlorination of Kaolinic Clay,' Metall. Trans., 8B, 435 (1977)

Landsberg, A., Hoatson, C.L. and Block, F.E., 'The Chlorination Kinetics of Zirconium Dioxide in the Presence of Carbon and Carbon Monoxide,' Metall. Trans., 3, 517 (1972)

Landt, U., 'Developments in Inorganic Arc Plasma Chemistry,' Angew. Chem. Internat. Edit., 9, (10), 780 (1970)

Lemcoff, N.O., Calvelo, A. and Cunningham, R.E., 'Models of Diffusion with Simultaneous Reaction in Noncatalytic Gas-Solid Systems - A Critical Review,' Lat. Am. J. Chem. Eng. Appl. Chem., 1, 3 (1971)

Levenspiel, O., Chemical Reaction Engineering, 2nd Ed., John Wiley and Sons, New York, 357 (1972)

Lewis, J.A. and Gauvin, W.H., 'Motion of Particles Entrained in a Plasma Jet,' AIChE J., 19, (5), 982 (1973)

Little, J.E. and Wentzell, J.M., 'Reduction to a Refractory Metal by a Plasma Jet,' Belgium Patent: 668 600, (1965)

Luss, D., 'The Pseudo Steady State Approximation for Gas-Solid Reactions,' Can. J. Chem. Eng., 46, (3), 154 (1968)

Mac Rae, D.R., Gold, R.G., Thompson, C.D. and Sandall, W.R., 'Ferrovanadium Production by Plasma Carbothermic Reduction of Vanadium Oxide,' Presented at 3rd. Internat. Symp. on Plasma Chem., Paper No. S.5.1, Limgoes, France, (1977)

Manieh, A.A. and Spink, D.R., 'Chlorination of Zircon Sand,' Can. Met. Quart., 12, (3), 331 (1973)

Manieh, A.A., Scott, D.S. and Spink, D.R., 'Electrothermal Fluidized Bed Chlorination of Zircon,' Can. J. Chem. Eng., 52, 507 (1974)

Marden, J.W. and Rich, M.N., Investigation of Zirconium, with Special Reference to the Metal and Oxide, U.S. Bureau of Mines Bulletin 186, U.S. Government Printing Office, Washington, (1921)

Martinez, G.M. and Couch, D.E., 'Electrowinning of Zirconium from Zirconium Tetrachloride,' Metall. Trans. 3, 571 (1972)

Martinez, G.M., Shanks, D.E., Woodyard, J.R. and Wong, M.M., Investigation of a Cell Design for Electrowinning Zirconium Metal from Zirconium Tetrachloride, U.S. Bureau of Mines R.I. - 8125, U.S. Government Printing Office, Washington (1976)

Masterova, A.P. and Levin, M.I., 'Study of Kinetic Relationships in Chlorination of Granules made from Titanium-containing Concentrate and Coke,' J. Appl. Chem. USSR, 46, (6), 1286 (1973)

Matsumoto, O., 'Formation of Titanium Nitride by Means of a Transferred Arc Plasma Jet,' J. Electrochem. Soc. Japan, 36, (3) 1953 (1968)

Matsumoto, O., 'Oxidation of Titanium by Means of an Argon Oxygen Plasma Jet,' J. Electrochem. Soc. Japan, 37, (4), 200 (1969)

Matsumoto, O. and Shirato, Y., 'Nitrization of Zirconium Silicate by Means of Nitrogen Plasma Jet,' Denki Kagaku, 38, (3), 168, (1970)

Matsumoto, O. and Miyazaki, T., 'Carburization of Zirconium Oxide by Means of Plasma Jet,' Denki Kagaku, 39, (5), 388, (1971)

Matsumoto, O., Tsuda, T., Mukunoki, A. and Hayakawa, Y., 'Reaction Between Air Plasma Jet and Zirconium,' Denki Kagaku, 40, (5), 352, (1972)

Matsumoto, O. and Kawai, Y., 'Nitriding Reaction of Zirconium by Nitrogen Plasma Jet,' Denki Kagaku, 40, (4), 271 (1972)

McCord, A.T., 'Process for Chlorinating Refractory Oxides,' U.S. Patent: 3 293 005, (1966)

Miller, G.L., Metallurgy of the Rarer Metals-2, Zirconium, Butterworths Scientific Publications, London, (1954)

Morozov, I.S. and Stefanyuk, S.L., 'Kinetics of Chlorination of Titanium Dioxide and Niobium Pentoxide,' Russian J. Inorg. Chem., 3, (10), 2366 (1958)

Morris, A.J. and Jensen, R.F., 'Fluidized Bed Chlorination Rates of Australian Rutile,' Metall. Trans., 7B, 89 (1976)

Motoi, S. and Kurita, H., 'Dry Process for Producing Zirconia,' Japan Patent: 73 17 993, (1973)

Munz, R.J., 'The Decomposition of Molybdenum Disulphide in an Induction Plasma Tailflame,' Ph.D. Thesis, McGill University, Montreal, Canada, (1974)

Munz, R.J. and Gauvin, W.H., 'The Decomposition Kinetics of Molybdenite in an Argon Plasma,' AIChE J. 21, 6, 1132 (1975)

Noranda, Internal Report on Zirconium Sponge Production, Noranda Research Centre, Montreal, Canada, (October 27, 1977)

Orbach, H.K., Bedjai, J.G., Martindill, R.E. and Kritchevsky, J., 'Plasma Jet Halogenation of Beryllium,' U.S. Patent: 3 390 380, (1968)

O'Reilly, A.J., Doig, I.D. and Ratcliffe, J.S., 'The Kinetics of the Chlorination of Zirconium Dioxide in a Static Bed with Carbon and Chlorine,' Inorg. Nucl. Chem., 34, 2487 (1972)

Park, J.Y. and Levenspiel, O., 'The Crackling Core Model for the Reaction of Solid Particles,' Chem. Eng. Sci., 30, 1207 (1975)

Park, J.Y., 'The Crackling Core Model for the Multistep Reaction of Solid Particles,' Chem. Eng. Sci., 32, 233 (1977)

Peterson, E.E., 'Reaction of Porous Solids,' AIChE J., 3, (4), 443 (1957)

Pogonina, L.N. and Ivashentsev, Ya. I., 'Investigation of the Chlorination of Titanium Dioxide, Zirconium Dioxide and Hafnium Dioxide by Chlorine,' Voprosy Khimii, (2), 47 (1974)

Polak, L.S., 'Prospects and Development Ways of Plasma Chemistry,' Presented at World Electrochemical Congress, June 21-25, Paper No. 29, Moscow, (1977)

Rains, R.G. and Kadlec, R.H., 'The Reduction of Al_2O_3 to Aluminum in a Plasma,' Metall. Trans., 1, 1501 (1970)

Ramachandran, P.A. and Smith, J.M., 'A Single-Pore Model for Gas-Solid Noncatalytic Reactions,' AIChE J., 23, (3), 353 (1977)

Ranz, W.E. and Marshall, W.R., 'Evaporation from Drops,' CEP, 48, (3), 141 (1952)

Ray, H.S. and Luthra, K.L., 'Kinetic Aspects of Noncatalytic Gas-Solid Reactions,' J. Inst. Eng. (India), Part MM, 54, (3), 76 (1974)

Reed, T.B., 'Induction-Coupled Plasma Torch,' J. Appl. Phys., 32, 821 (1961)

Reed, T.B., 'Plasma for High Temperature Chemistry,' Advances in High Temp. Chem., 1, Academic Press, New York, 259 (1967)

Reno, H.T., Zirconium Mineral Facts and Problems, U.S. Bureau of Mines Bulletin 556, U.S. Government Printing Office, Washington, (1956)

Roy, S., 'Thermodynamics of Metallo-Thermic Reduction of Oxides of Zirconium and Titanium in Different Gaseous Media,' Trans. Indian Inst. Metals, 17, 122 (Sept. 1964)

Ryan, W., Non-Ferrous Extractive Metallurgy in the United Kingdom, The Institution of Mining and Metallurgy, London, 222 (1968)

Rykalin, N.N., 'Plasma Engineering in Metallurgy and Inorganic Materials Technology,' Pure and Appl. Chem., 48, 179 (1976)

Sampath, B.S. and Hughes, R., 'A Review of Mathematical Models in Single Particle Gas-Solid Noncatalytic Reactions,' The Chemical Engineer, (278), 485 (1973)

Sampath, B.S., Ramachandran, P.A. and Hughes, R., 'Modeling of Noncatalytic Gas-Solid Reactions - I. Transient Analysis of the Particle-Pellet Model,' Chem. Eng. Sci., 30, 125 (1975)

Sayce, I.G., 'Plasma Processes in Extractive Metallurgy,' Conf. Advances in Extractive Metallurgy and Refining, Paper No. 27 (October 1971)

Sayce, I.G., 'Heat and Mass Transfer in Thermal Plasmas,' Pure and Appl. Chem., 48, 215 (1976)

Sayegh, N.N., 'Variable-Property Flow and Heat Transfer to Single Spheres in High Temperature Surroundings,' Ph.D. Thesis, McGill University, Montreal, Canada (1977)

Scammon, L.W., Jr., Grant, C.L. and Wilks, P.H., 'Silicate Ore Products,' German Patent: 2 238 277, (1973); U.S. Patent: 3 811 907 (1974)

Sehra, J.C., 'Fluidized Bed Chlorination of Nuclear Grade ZrO_2 with CO and Cl_2,' Trans. Indian Inst. Metals, 27, (2), 93 (1974)

Semenenko, K.N., Felin, M.G. and Kostenko, A.L., 'Reaction of Atomic Hydrogen with Zirconium Halides in a Glow Discharge Plasma,' Vestn. Mosk. Univ. Khim., 16, (1), 39 (1975)

Seryakov, G.V., Baks, S.A., Zheltova, V.V. and Strashun, E.P., 'Mechanism of the Chlorination of Titanium Dioxide by Chlorine in the Presence of Carbon,' Russian J. Inorg. Chem., 12, (1), 3 (1967)

Seryakov, G.V., Baks, S.A., Strashun, E.P. and Tulyakov, N.V., 'Kinetics of the Chlorination of Briquettes from a Mixture of Titanium Concentrate and a Carbonaceous Reducing Agent,' J. Appl. Chem. USSR, 42, (1), 150 (1969)

Seryakov, G.V., Baks, S.A., Strashun, E.P. and Tulyakov, N.V., 'Nature of Limiting Step in the Chlorination of Titanium Dioxide Briquetted with Carbon,' J. Appl. Chem. USSR, 43, (8), 1653 (1970)

Sheer, C. and Korman, S., 'Arc Process for the Reduction of Metals,' U.S. Patent: 2 616 843, (1952a)

Sheer, C. and Korman, S., 'Arc Process for the Selective Recovery of Metals,' U.S. Patent: 2 617 761, (1952b)

Shelton, S.M., Kauffman, A.J., Roberson, A.H., Dilling, E.D., Beall, R.A., Hayes, E.T., Kato, H., McClain, J.H. and Halbrook, F., Zirconium - Its Production and Properties, U.S. Bureau of Mines Bulletin 561, U.S. Government Printing Office, Washington, (1956)

Shen, J. and Smith, J.M., 'Diffusional Effects in Gas-Solid Reactions,' Ind. Eng. Chem. Fundam., 4, (3), 293 (1965)

Shettigar, U.R. and Hughes, R., 'Prediction of Transient Temperature Distribution in Gas-Solid Reactions,' Chem. Eng. J., 3, 93 (January 1972)

Sohn, H.Y. and Szekely, J., 'The Effect of Reaction Order in Non-catalytic Gas-Solid Reactions,' Can. J. Chem. Eng., 50, 674 (1972a)

Sohn, H.Y. and Szekely, J., 'A Structural Model for Gas-Solid Reactions with a Moving Boundary - III. A General Dimensionless Representation of the Irreversible Reaction Between a Porous Solid and a Reactant Gas,' Chem. Eng. Sci., 27, 763 (1972b)

Sparling, D.W. and Glastonbury, J.R., 'Kinetics and Mechanism of Zircon Chlorination,' Pap. West. Aust. Conf., Australas. Inst. Min. Metall., May 10, 455 (1973)

Spink, D.R., 'Reduction of Hafnium and Zirconium Tetrachloride by Magnesium,' U.S. Patent: 3 966 460, (1976)

Spink, D.R., Memorandum to Ad Hoc Committee on the Extractive Metallurgy of Zirconium, June 17, (1977a)

Spink, D.R., 'Extractive Metallurgy of Zirconium and Hafnium,' CIM Bulletin, 70, (787), 145 (1977b)

Stamper, W.J. and Chin, E., Zirconium, U.S. Bureau of Mines Mineral Year Book, 1, U.S. Government Printing Office, Washington, 825 (1970)

Starrat, F.W., 'Zirconium by Sodium Reduction,' J. Metals, 11, 441 (1959)

Stefanyuk, S.L. and Morozov, I.S., 'The Kinetics of the Chlorination of Complex Pyrochlore Concentrates,' J. Appl. Chem. USSR, 37, (8), 1665 (1964)

Stefanyuk, S.L. and Morozov, I.S., 'Kinetics and Mechanism of Chlorination of Minerals, Loparite, Pyrochlore, Zircon and Euxenite,' J. Appl. Chem. USSR, 38, (4), 729 (1965)

Stephens, W.W. and Gilbert, H.L., 'Chlorination of Zirconium Oxide,' Trans. AIME J. Metals, 194, 733 (1952)

Stokes, C.S., 'Chemistry in High Temperature Plasma Jet,' Adv. Chem. Ser. 80, Section 33, American Chemical Society, Washington (1969)

Sundaram, C.V., Chaudhuri, P.K.R., Raman, L.V.P. and Krishnan, T.S., 'Preparation of Zirconium Metal Powder by Calciothermic Reduction of Zirconium Oxide,' Trans. Indian Inst. Metals, 20, 187 (December 1967)

Szekely, J. and Evans, J.W., 'A Structural Model for Gas-Solid Reactions with a Moving Boundary,' Chem. Eng. Sci., 25, 1091 (1970)

Szekely, J. and Evans, J.W., 'Studies in Gas-Solid Reactions: Part I. A Structural Model for the Reaction of Porous Oxides with a Reducing Gas,' Metall. Trans., 2, 1691 (1971a)

Szekely, J. and Evans, J.W., 'Studies in Gas-Solid Reactions: Part II. An Experimental Study of Nickel Oxide Reduction with Hydrogen,' Metall. Trans., 2, 1699 (1971b)

Szekely, J. and Evans, J.W., 'A Structural Model for Gas-Solid Reactions with a Moving Boundary - II. The Effect of Grain Size, Porosity and Temperature on the Reaction of Porous Pellets,' Chem. Eng. Sci., 26, 1901 (1971c)

Szekely, J., Lin, C.I. and Sohn, H.Y.,'A Structural Model for Gas-Solid Reaction with a Moving Boundary - V. An Experimental Study of the Reduction of Porous Nickel Oxide Pellets with Hydrogen,' Chem. Eng. Sci., 28, 1975 (1973)

Szekely, J., Evans, J.W. and Sohn, H.Y., Gas-Solid Reactions, Academic Press, New York, (1976)

Thorpe, M.L. and Wilks, P.H., 'Electric-Arc Furnace Turns Zircon Sand to Zirconia,' Chem. Eng., 78, 117 (November 15, 1971)

Tsay, Q.T., Ray, W.H. and Szekely, J., 'The Modeling of Hematite Reduction with Hydrogen Plus Carbon Monoxide Mixtures: Part I. The Behaviour of Single Pellets,' AIChE J., 22, (6), 1064 (1976)

Uetsuki, T., Tanaka, K. and Nakazawa, Y., 'Decomposition and Dissociation of Zircon,' Memoirs Fac. Ind. Arts, Kyoto Tech. Univ., Sci. Tech., 21, 59 (1972)

Vasilenko, D.B. and Vol'skii, A.N., 'The Thermodynamics of Reactions of Chlorination of Zirconium Dioxide by Gaseous Chlorine,' Russian J. Inorg. Chem., 3, (7), 32 (1958)

Venable, F.P., Zirconium and Its Compounds, The Chemical Catalog Comp. Inc., New York, 66 (1922)

Villadsen, J.F. and Stewart, W.E., 'Solution of Boundary Valve Problems by Orthogonal Collocation,' Chem. Eng. Sci., 22, 1483 (1967)

Vurzel, F.B. and Polak, L.S., 'Plasma Chemical Technology - The Future of the Chemical Industry,' Ind. Eng. Chem., 62, (6), 8 (1970)

Waldie, B., 'Review of Recent Work on the Processing of Powders in High Temperature Plasmas - Part I. Processing and Economic Studies,' The Chemical Engineer, (259), 92 (1972a)

Waldie, B., 'Review of Recent Work on the Processing of Powders in High Temperature Plasmas - Part II. Processing and Economic Studies,' The Chemical Engineer, (261), 188 (1972)

Walker, P.L., Jr., Rusinko, F., Jr. and Austin, L.G., 'Gas Reactions of Carbon,' in Advances in Catalysis, Academic Press, New York, 2, 133 (1959)

Wang, S.C. and Wen, C.Y., 'Experimental Evaluation of Nonisothermal Solid-Gas Reaction Model,' AIChE J. 18, (6), 1231 (1972)

Warren, I.H. and Shimizu, H., 'Applications of Plasma Technology in Extractive Metallurgy,' Trans. Can. Inst. Min. Metall., 58, 169 (1965)

Wen, C.Y., 'Noncatalytic Heterogenous Solid Fluid Reaction Models,' Ind. Eng. Chem., 60, (9), 34 (1968)

Wen, C.Y. and Wang, S.C., 'Thermal and Diffusional Effects in Non-Catalytic Solid Gas Reactions,' Ind. Eng. Chem., 62, (8), 30 (1970)

Wen, C.Y. and Wei, L.Y., 'Simultaneous Noncatalytic Solid-Fluid Reactions,' AIChE J., 16, (5), 849 (1970)

Wen, C.Y. and Wei, L.Y., 'Simultaneous Nonisothermal Noncatalytic Solid-Gas Reactions,' AIChE J., 17, (2), 272 (1971)

Wen, C.Y. and Wu, N.T., 'An Analysis of Slow Reactions in a Porous Particle,' AIChE J., 22, (6), 1012 (1976)

White, J. and Richmond, C., 'Removal of Silicon Dioxide in the Manufacture of Zirconium Dioxide and Nickel from Silicates,' German Patent: 2 311 213, (1974)

Wilks, P.H., Ravinder, P., Grant, C.L., Pelton, P.A., Downe, R.R.J. and Talbot, M.C., 'Plasma Process for Zirconium Dioxide,' CEP, 68, 82 (April, 1972)

Wilks, P.H., Ravinder, P., Grant, C.L., Pelton, P.A., Downe, R.R.J. and Talbot, M.C., 'Commercial Production of Submicron Zirconium Dioxide via Plasma,' Chem. Eng. World, 9, (3) Section 1, 59 (1974)

Williams, R.J.J., Calvelo, A. and Cunningham, R.E., 'A General Asymptotic Analytical Solution for Noncatalytic Gas-Solid Reactions,' Can. J. Chem. Eng., 50, 486 (1972)

Wington, H.F., 'Chlorides of Zirconium and Silicon,' U.S. Patent: 2 952 513, (1960)

Yagi, S. and Kunii, D., 'Proposed Theory of Fluidized Roasting of Sulfide Ore with Uniform Size. I - Single Particle of Ore in the Fluidized Bed,' J. Chem. Soc. Japan. Ind. Chem. Sect., 56, 131 (1953)

Yagi, S. and Kunii, D., 'Fluidized-Solid Reactors for Particles with Decreasing Diameters,' Chem. Eng. Japan., 19, 500 (1955a)

Yagi, S. and Kunii, D., 'Combustion of Carbon Particles in Flames and Fluidized Beds,' Symp. Combustion, 5th, Pittsburgh, 1954, Reinhold, New York, 231 (1955b)

Yannopoulos, J.C. and Themelis, N.J., 'A Rate Equation for the Reduction of Ferrous Chloride by Hydrogen,' Can. J. Chem. Eng. 43, 173 (1965)

EXPERIMENTAL SECTION

GENERAL INTRODUCTION

The chlorination of zirconium oxide may be considered as an integral part of the overall process for the production of nuclear-grade zirconium. The latter's commercial production is currently based on the Kroll Process (Miller, 1954), (Shelton et al., 1956), (Starrat, 1959), (Elger, 1962), (Babu et al., 1969), (Chintamani et al., 1972), (Spink, 1977) which uses hafnium-free, pure zirconium tetrachloride as the feed material. Newer processes which have been proposed to replace the conventional commercial method of production also use zirconium tetrachloride as the starting material. These include plasma decomposition of zirconium tetrachloride (Chizhikov, Deineka and Makarova, 1969), (Chizhikov et al., 1971), (Semenenko et al., 1975), (Gragg, 1973), (Little and Wentzell, 1965), (CIBA, 1966) and electrowinning of the metal from fused salts containing zirconium tetrachloride (Martinez and Couch, 1972), (Martinez et al., 1976).

Zircon, the main source of the metal, may be either chlorinated directly (Manieh and Spink, 1973), (Manieh, Scott and Spink, 1974) or through a two-step process, namely the

carburization of zircon followed by the chlorination of zirconium carbide or carbonitride (Kroll, Carmody and Schlechton, 1952), (Stephens and Gilbert, 1952), (Shelton et al., 1956). The former requires a larger reactor volume, extra chlorine and carbon for the SiO_2 constituent of the ore, for the same throughput of zirconium tetrachloride. Furthermore, it necessitates the separation, handling and disposal of $SiCl_4$. On the other hand, the two-step process has been shown to be less efficient than ZrO_2 chlorination (Stephens and Gilbert, 1952). The recent development of a plasma process for the dissociation of zircon into its two constituent oxides, ZrO_2 and SiO_2, (Wilks et al., 1972, 1974), (Bayliss, Bryant and Sayce, 1977) followed by leaching of the silica may lead in future to the direct chlorination of zirconia rather than that of zircon.

For the production of nuclear-grade zirconium, the near-complete separation of hafnium, which is always associated with zirconium in the ore, is necessary due to hafnium's high neutron absorption cross-section. In the present conventional process, hafnium separation is effected by means of solvent extraction, to yield purified $Zr(OH)_4$. The latter is then calcined to yield de-hafniated ZrO_2. The subsequent chlorination of the dioxide to produce the tetrachloride feed for the Kroll Process is thus an essential processing step in the overall complex production scheme.

The Literature Review chapter showed that the kinetics

of the chlorination of zirconium oxide have not received much attention. The available publications in the field are limited to those of O'Reilly et al. (1972), Landsberg et al. (1972) for the kinetic study; to those of Stephen and Gilbert (1952) and Sehra (1974) for vertical shaft furnace and fluidized-bed chlorination operation, respectively, and to that of Vasilenko and Volskii (1958) for thermodynamic analysis. All of these studies are concerned with temperatures below 1400 K.

In the present work, it was intended to study the kinetics of zirconium oxide chlorination at high temperatures (1400 - 2480 K). A chlorine induction plasma reactor system was used to provide both the high-temperature field and the reactant gas. To the author's knowledge, the generation of a plasma of pure chlorine has never been attempted before, nor has the use of a plasma system for chlorination kinetic studies. With the exception of the work of Munz and Gauvin (1975) on the decomposition of molybdenite in an argon plasma tailflame, most of the other published plasma gas-solid reactions (Huska and Clump, 1967), (Gilles and Clump, 1970), (Rains and Kadlec, 1970) have not been studies in chemical kinetics proper, but were rather intended to evaluate the effects of operating parameters on the degree of conversion.

To achieve the objectives of the study, a special reactor system had to be designed and developed to handle hot chlorine and control and measure all parameters affecting the rate of the heterogeneous ZrO_2 chlorination. A theoretical analysis

was carried out along with the experimental work. The work is reported in two parts, due to the differences in reaction conditions and consequent differences in the analytical interpretation of the results. The first part is concerned with the chlorination of ZrO_2 with chlorine alone, while in the second, graphite was added as a reducing agent for the chlorination. Each part is intended to be complete in itself for the purpose of presentation and eventual publication.

PART I - CHLORINATION OF ZIRCONIUM DIOXIDE IN THE ABSENCE OF REDUCING AGENT

INTRODUCTION

Normally, chlorination of zirconium dioxide necessitates the presence of a reducing agent due to the lower affinity of zirconium for chlorine than for oxygen. The free energy of the chlorination reaction:

$$ZrO_2 + 2\ Cl_2 = ZrCl_4 + O_2 \qquad (1)$$

remains positive up to quite high temperatures as shown in Figure 1, for which the free energy data were extracted from the JANAF Thermochemical Tables (1967). Landsberg et al. (1972) studied this reaction in a very preliminary way at temperatures in the range 1320 - 1420 K. The reaction could take place only when the chlorine gas velocity was high enough to eliminate the accumulation of the products near the reacting particle, and even

FIGURE 1

FREE ENERGIES OF

ZrO_2 CHLORINATION REACTIONS

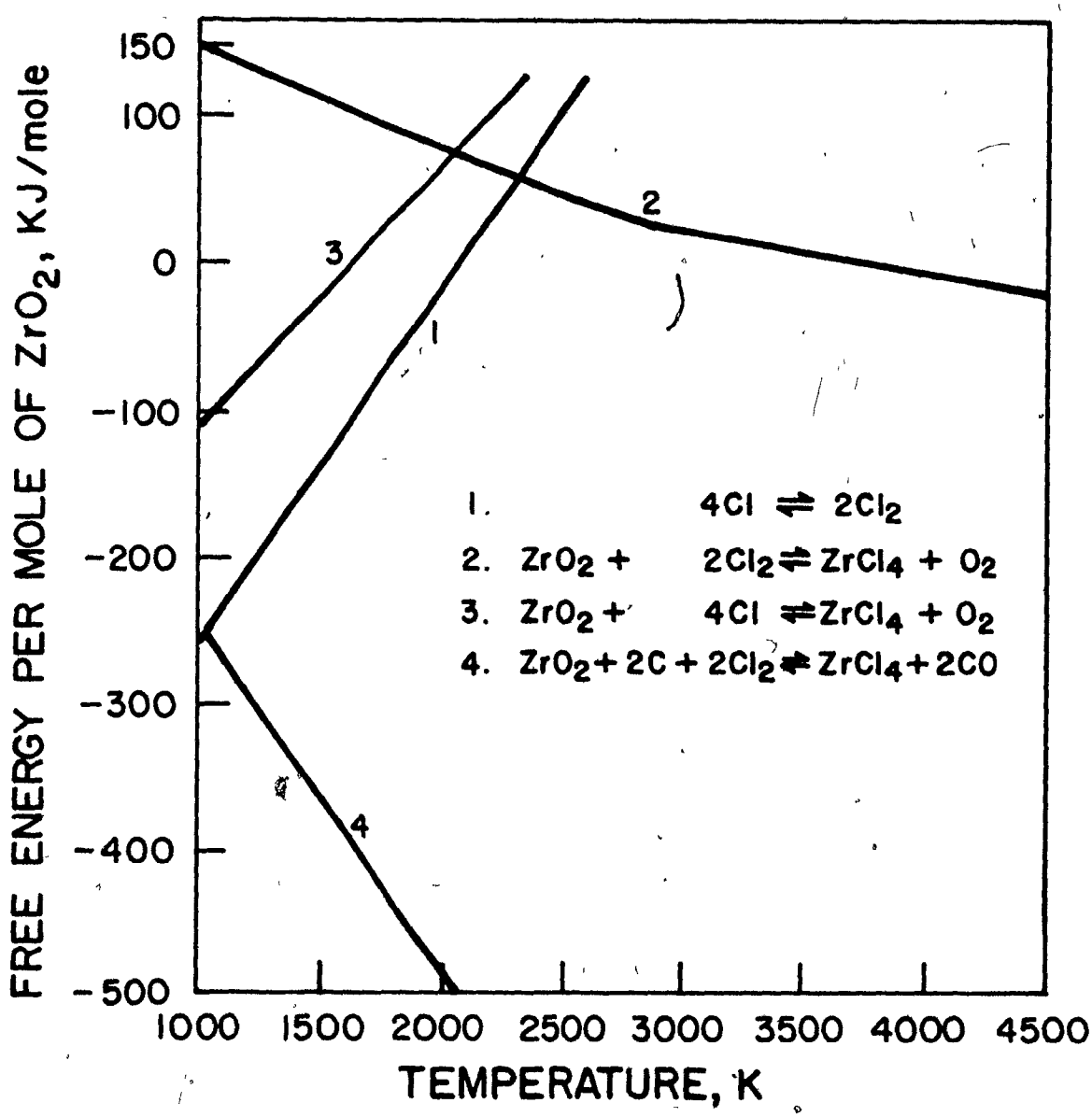
FREE ENERGY PER MOLE OF ZrO_2, KJ/mole
150
100
0
-100
-200
-300
-400
-500
1000
1500
2000
2500
3000
3500
4000
4500
TEMPERATURE, K
1
2
3
4
1. $4Cl \rightleftharpoons 2Cl_2$
2. $ZrO_2 + 2Cl_2 \rightleftharpoons ZrCl_4 + O_2$
3. $ZrO_2 + 4Cl \rightleftharpoons ZrCl_4 + O_2$
4. $ZrO_2 + 2C + 2Cl_2 \rightleftharpoons ZrCl_4 + 2CO$

then at a slow rate. Recently, Pogonina and Ivashentsev (1974), in a very short paper, reported 8.1 per cent conversion in 50 minutes at 1273 K. Earlier, Vasilenko and Vol'skii (1958) showed on the basis of a thermodynamic analysis that the equilibrium concentration of zirconium tetrachloride in the gaseous phase increased insignificantly from 0.2 to 2.7 volume percent with a rise of temperature from 1273 to 1773 K. However, all these works were based on the reaction of molecular chlorine with ZrO_2 (Equation 2 in Figure 1).

In plasma systems, the temperature difference between the reacting particle and the ambient gas is usually quite large. In the present case, it was of the order of 2000 - 3000 K, with the ambient gas temperature in the range 3500 - 6000 K. The equilibrium concentrations of molecular and atomic chlorine, as calculated from the data in the JANAF Tables at different temperatures, are given in Table I. It is seen that, at the experimental gas temperature levels (3500 - 6000 K) used in this work, the chlorine gas will be in the atomic form. Thus, the following reactions may take place on the zirconium dioxide surface:

$$4\ Cl = 2\ Cl_2 \tag{2}$$

$$ZrO_2 + 2\ Cl_2 = ZrCl_4 + O_2 \tag{3}$$

$$ZrO_2 + 4\ Cl = ZrCl_4 + O_2 \tag{4}$$

Reaction (3) is possible, depending upon whether atomic

TABLE I

EQUILIBRIUM CONCENTRATIONS OF ATOMIC CHLORINE

$1/2\ Cl_2 = Cl$

T, °K	log K_E [1]	y_{Cle}
1500	-1.226	0.0577
2000	-0.128	0.5174
2500	0.536	0.9272
3000	0.982	0.9894
3500	1.303	0.9980
4000	1.545	0.9992
4500	1.734	0.9997
5000	1.886	0.9998

(1) From JANAF Thermochemical Tables

chlorine associates to form molecular chlorine at the oxide surface. Although the reaction temperature of ZrO_2 pellet is lower than the bulk gas temperature and permits the formation of molecular chlorine, the extent of Reaction (2) may not be large due to very short residence time. In any event, Reaction (4) represents both the summation of Reactions (2) and (3) and also the direct action of atomic chlorine on zirconium dioxide. Hence, regardless of what happens on the pellet surface, Reaction (4) may be considered as representing the chlorination of ZrO_2 in the absence of reducing agent in the chlorine plasma. This reaction is also a reversible one and it is thermodynamically more favourable than that with molecular chlorine below about 2050 K, as indicated in Figure 1.

The purpose of this section is to investigate fully the possibility of direct chlorination of ZrO_2 with chlorine alone and to study its kinetics. A theoretical analysis was carried out along with the experimental work in order to obtain a time-conversion relationship and to compare the experimental data with those of theoretical predictions of this work when gas film diffusion becomes important.

THEORETICAL ANALYSIS

MATHEMATICAL MODELING OF THE REACTION

The review on the mathematical treatments of gas-solid reactions in the Literature Review showed that every conceptual

picture or model for the progress of a heterogeneous reaction was accompanied by its specific mathematical representation. The published treatments either assumed a surface reaction which was expressed by a shrinking core model (Yagi and Kunii, 1953, 1955a, 1955b), (Shen and Smith, 1965), (Levenspiel, 1972), (Szekely et al., 1976), or a diffuse-zone reaction model. The latter either viewed the reacting pellet as a homogenous matrix-volumetric reaction model (Ishida and Wen, 1968), (Wen, 1968), (Calvelo and Cunningham, 1970), (Williams et al., 1972), or considered a pore structure (Peterson, 1957), (Ramachandran and Smith, 1977) or envisaged a grain structure (Szekely and Evans, 1970, 1971), (Sohn and Szekely, 1972), (Sampath et al., 1975). The uniform-reacting-pellet model was treated as a special case of diffuse-zone reaction models. Except for the isothermal shrinking-core model, the majority of the treatments required a numerical solution. Generally, the modeling works seemed to be divided in two groups: for the first, the primary interest was in mathematical modeling, while for the second the main concern was experimental measurements and the interpretation of data. With respect to the second group, the shrinking-core model was found useful in analysing many solid-gas reactions including porous solids, due to its mathematical simplicity (Costa and Smith, 1971), (Wang and Wen, 1972), (Munz and Gauvin, 1975), (Morris and Jensen, 1976), (Fahim and Ford, 1976).

In the light of the experimental observations, the theoretical analysis of the reaction between ZrO_2 and atomic

chlorine will be based on surface reaction of the shrinking pellet, and it will be carried out for chemical reaction and for gas film diffusion controlling mechanisms, separately. Then an approximate solution will be obtained for the intermediate case where both the chemical reaction and the gas film diffusion resistances contribute.

For the purpose of a compact generalized presentation and as a convenience for computer programming, the following general gas-solid reaction is first considered:

$$a_1 A_{1(gas)} + B_{(solid)} = a_2 A_{2(gas)} + a_3 A_{3(gas)} \tag{5}$$

and the final results are then applied to the specific chlorination reaction. The treatment assumes a shrinking isothermal spherical pellet, a reversible surface reaction and a nonlinear dependency of the reaction rate on the gaseous reactant concentration. A schematic representation of the reacting system is given in Figure 2.

Chemical Reaction Control

The overall rate of the reaction (Equation 5) may be expressed as the rate of disappearance of the gaseous reactant A_1 by the surface chemical reaction according to the expression:

$$-N_1 = k_s \, f(y_1) \tag{6}$$

where N_1 is the rate of reaction (moles per unit time, per unit

FIGURE 2

SCHEMATIC DRAWING OF REACTING SYSTEM

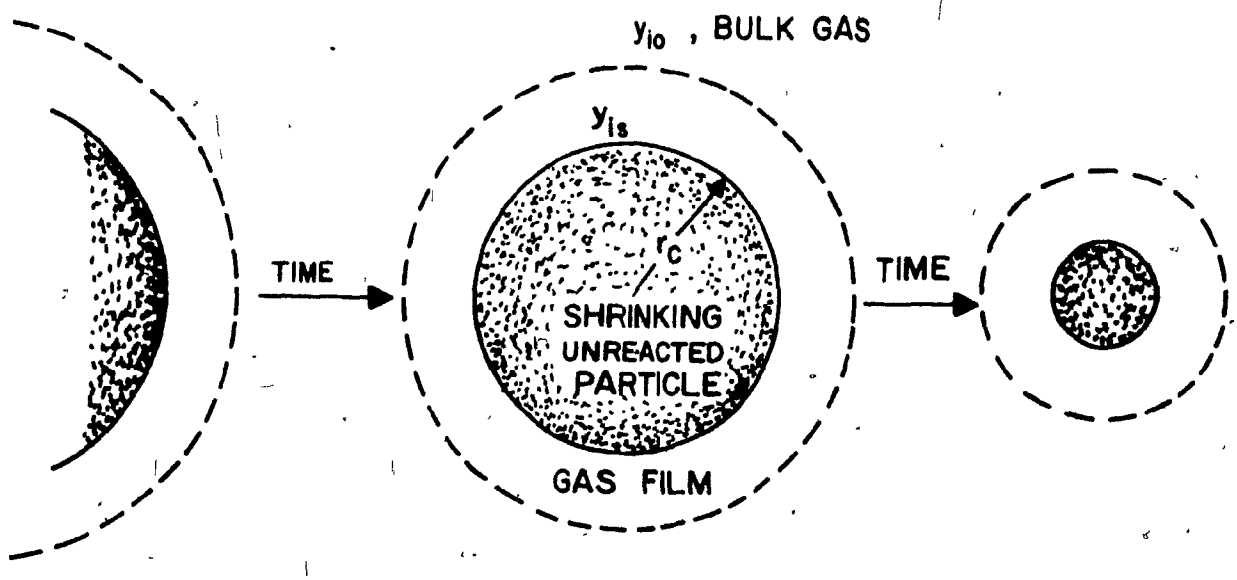
y_{io} , BULK GAS
y_{is}
r_c
TIME
SHRINKING
UNREACTED
PARTICLE
GAS FILM
TIME

surface area), k_s is the surface reaction rate constant and $f(y_1)$ is the concentration dependence. Equation (5) may be related to the disappearance of solid reactant (B) as:

$$-(a_1/4\pi r_c^2)(dw/dt)(1/M) =$$

$$-N_1 = k_s\, f(y_1)(1/M) \qquad (7)$$

or

$$-(a_1/4\pi r_c^2)(4\pi r_c^2 \rho_s)(dr_c/dt) = k_s\, f(y_1) \qquad (8)$$

and Equation (8) becomes:

$$-(dr_c/dt) = (k_s/a_1\rho_s)\, f(y_1) \qquad (9)$$

where, a_1 is the stoichiometric coefficient in Equation (5), r_c the radius of the shrinking spherical solid, t the reaction time, w the weight of solid and ρ_s the molar density of the solid in the pellet. Integrating Equation (9):

$$-\int_R^{r_c} dr_c = (k_s/a_1\rho_s)\, f(y_1) \int_0^{t_r} dt \qquad (10)$$

yields:

$$1 - (r_c/R) = (k_s/a_1\rho_s R)\, f(y_1)\, t_r \qquad (11)$$

This can be written in terms of fractional conversion (X) of solid reactant by noting that X = (Initial Weight − Weight of Unreacted Pellet)/Initial Weight. Hence:

$$X = 1 - \frac{4}{3}\pi r_c^3 / \frac{4}{3}\pi R^3 = 1 - (r_c/R)^3 \qquad (12)$$

Therefore:

$$r_c/R = (1-X)^{1/3} \tag{13}$$

Then Equation (11) becomes:

$$1 - (1-X)^{1/3} = (k_s/a_1\rho_s R)\ f(y_1)\ t_r \tag{14}$$

where, R is the initial radius of the reacting pellet.

Concentration dependence on reaction rate is usually expressed as an exponent of concentration. In accordance with the experimental data, the dependence of the chlorination rate on the concentration of atomic chlorine is written as:

$$f(y_1) \propto y_{1s}/(2-y_{1s}) \tag{15}$$

The mathematical convenience of this expression will be seen later. In addition, for a reversible reaction, the equilibrium concentration should also be included. Hence the concentration function $f(y_1)$ is defined as:

$$f(y_1) = (y_{1s}-y_{1se})\ /(2-y_{1s}) \tag{16}$$

where y_{1s} is the mole fraction of the reactant gas (atomic chlorine) at the reaction surface, and y_{1se} is that of reactant gas at equilibrium with the concentrations of product gases at the reaction surface. It is assumed that porosity, particle size, sintering and structural changes have no effect.

If the reaction is controlled solely by chemical reaction, the gas film diffusion resistance is considered to be negligible,

hence the concentrations at the reaction surface are the same as in the bulk of the gas stream. Therefore, for chemical reaction control, the concentration function becomes:

$$f(y_1) = (y_{1o}-y_{1oe}) / (2-y_{1o}) \tag{17}$$

where the subscript o denotes the bulk condition. The final form of the conversion-time relationship from Equation (14) is:

$$1 - (1-X)^{1/3} = t_r(k_s/a_1\rho_s R)(y_{1o}-y_{1oe}) / (2-y_{1o}) \tag{18}$$

where a_1 is equal to 4 from the stoichiometry of the chlorination reaction (Equation 4).

Mass Transfer Control

Equation (4) and similarly Equation (5) involve multicomponent nonequimolar counter diffusion. Bird, Stewart and Lightfoot (1960) have shown that mass transfer rates through a gas film in multicomponent systems can be predicted by using analogous binary formulae if an effective binary diffusivity D_{im} for the diffusion of the i-th component in a mixture can be defined so that species i behaves as if it were in a binary mixture of diffusivity D_{AB} equal to the prevailing D_{im}. The requirements for such a treatment are that the mass transfer rates should be low and the physical properties, including the effective diffusivities, should be constant. It is obvious that the physical properties generally vary from point to point, and this variation is more significant in the case of plasma systems, owing to the large

temperature gradients. For an approximate calculation, Sayegh (1977) pointed out that these variations can be handled by using average fluid properties evaluated at the mean of the reaction surface and plasma gas temperatures. This, together with an arithmetic mean average film composition, is assumed to permit the use of binary diffusion formulae and mass transfer coefficient correlations by introducing the effective binary diffusivity D_{im}.

The molar flux of component i (N_i) by analogy with the binary formulae, is the sum of the diffusional contribution and of the bulk flow contribution. That is:

$$N_i = k_{mi} (y_{is} - y_{io}) + y_{is} \sum_{j=1}^{n} N_j \tag{19}$$

where k_{mi} is the mass transfer coefficient, y_i is the mole fraction for component i, subscript s denotes the reaction surface while o denotes the bulk condition. n is the total number of gaseous components. Equation (19) can be simplified by using the stoichiometric relationships of Equation (5):

$$N_2 = -(a_2/a_1)\ N_1 \tag{20}$$

$$N_3 = -(a_3/a_1)\ N_1 \tag{21}$$

or, in a general form:

$$N_j = (\phi_j/\phi_i)(a_j/a_i)\ N_i \tag{22}$$

$$\phi_j = 1 \text{ for the reactants}$$

$$\phi_j = -1 \text{ for the products} \tag{23}$$

where, a_i is the stoichiometric coefficient and ϕ_i the index for the stoichiometric coefficient for component i.

Insertion of Equation (22) into Equation (19) yields:

$$N_i = k_{mi}(y_{is}-y_{io})/[1-y_{is}\sum_{j=1}^{n}(\phi_j/\phi_i)(a_j/a_i)] \tag{24}$$

Equation (24) may be related to the disappearance of solid reactant (B):

$$N_i = (\phi_i a_i/4\pi r_c^2)(4\pi r_c^2 \rho_s)(dr_c/dt) \tag{25}$$

or:

$$N_i = \phi_i a_i \rho_s \, (dr_c/dt) \tag{26}$$

Equating Equations (24) and (26) and rearranging gives:

$$dr_c/dt = k_{mi} \, (y_{is}-y_{io})/$$
$$\{[1-y_{is}\sum_{j=1}^{n}(\phi_j/\phi_i)(a_j/a_i)]\phi_i a_i \rho_s\} \tag{27}$$

Equation (27) cannot be integrated directly since k_{mi} is a function of r_c.

For a spherical pellet, the mass transfer coefficient k_{mi} may be calculated from the Ranz and Marshall (1952) correlation:

$$N_{Sh} = 2 + 0.6 \, N_{Sc}^{1/3} \, N_{Re}^{1/2} \tag{28}$$

Equation (28) can be rewritten for a reacting pellet of radius r_c as:

$$\frac{k_{mi}(r_c/R)R}{c\ D_{im}} = 1 + 0.3\left(\frac{\mu}{\rho\ D_{im}}\right)_f^{1/3}\left(\frac{2U\ \rho R}{\mu}\right)_f^{1/2}\left(\frac{r_c}{R}\right)^{1/2} \tag{29}$$

Rearranging Equation (29) gives:

$$k_{mi} = (c\ D_{im}/r_c) + (0.3\ c\ D_{im}/r_c)\ N_{Sc}^{1/3}\ N_{Re}^{o\ 1/2}\ (r_c/R)^{1/2} \tag{30}$$

where, $\underline{c}$ is the total concentration of gas (moles per unit volume), $\underline{N_{Sc}}$ the Schmidt number, $\underline{N_{Re}^{o}}$ the Reynolds number based on initial pellet radius $\underline{R}$, $\underline{N_{Sh}}$ the Sherwood number, $\underline{U}$ the bulk gas velocity, $\underline{\mu}$ the viscosity and $\underline{\rho}$ the density of the fluid at average gas film conditions.

Equation (30) can be written as:

$$k_{mi} = \beta/(z_c R) + \alpha\ \beta\ z_c^{1/2}/(z_c R) \tag{31}$$

where:

$$z_c = r_c/R \tag{32}$$

$$\alpha = 0.3\ N_{Sc}^{1/3}\ N_{Re}^{o\ 1/2} \tag{33}$$

$$\beta = c\ D_{im} \tag{34}$$

Inserting Equations (31) and (32) into Equation (27) yields:

$$z_c dz_c/(1 + \alpha\ z_c^{1/2}) = \gamma\ dt \tag{35}$$

where:

$$\gamma = (y_{is} - y_{io})cD_{im}/\{R^2\phi_i a_i \rho_s[1 - y_{is}\sum_{j=1}^{n}(\phi_j/\phi_i)(a_j/a_i)]\} \tag{36}$$

Integration of Equation (35), for $1 \leq z_c \leq z$, and $0 \leq t \leq t_m$ is given in Appendix I. The final form of the conversion-time relationship is thus:

$$t_m = -(1/\gamma)[2/3\alpha(1-z^{3/2})-\alpha^{-2}(1-z) + 2\alpha^{-3}(1-z^{1/2})-2\alpha^{-3}(1-z^{1/2})-2\alpha^{-4}\ln\frac{(1+\alpha)}{(1+\alpha z^{1/2})} \quad (37)$$

where:

$z = r_c/R = (1-X)^{1/3}$ as given by Equation (13)

The concentration driving force in the treatment up to now was taken to be the difference between that at the reaction surface and that in the bulk gas. For a purely gas-film diffusion-controlled reaction, a good approximation to the reaction surface gas concentration may be obtained by assuming that chemical equilibrium exists at the reaction surface. Then the chemical equilibrium relationship may be written as:

$$K_E = y_2^{a_2}\, y_3^{a_3}/y_1^{a_1} \quad (38)$$

or in general form:

$$K_E = y_1^{-\phi_1 a_1}\, y_2^{-\phi_2 a_2} \;\ldots\; y_n^{-\phi_n a_n} \quad (39)$$

where, $\underline{K_E}$ is the equilibrium constant and $\underline{n}$ the total number of gaseous components. For an $\underline{n}$ component system, the summation of mole fractions is unity, or:

$$\sum_{i=1}^{n} y_i = 1 \quad (40)$$

For a three-gaseous component system, a set of three equations is needed to evaluate the three unknowns (y_1, y_2, y_3). So one more relationship is required in addition to Equations (39) and (40). It should be noted that due to the existence of a diffusional process, the surface concentrations are not stoichiometric, but the molar fluxes are. That is, Equations (20), (21) and (22) must be true. Then the molar fluxes of the second and third components may be related as:

$$N_2 = (a_2/a_3)(a_2/a_3)\, N_3 \tag{41}$$

Inserting Equation (24) for i = 2 and i = 3 into Equation (41) gives:

$$\frac{k_{m_2}\,(y_{2se}-y_{2o})}{1-y_{2se}\sum_{j=1}^{n}(\phi_j/\phi_2)(a_j/a_2)} = \frac{(\phi_2/\phi_3)(a_2/a_3)k_{m_3}(y_{3se}-y_{3o})}{1-y_{3se}\sum_{j=1}^{n}(\phi_j/\phi_3)(a_j/a_3)} \tag{42}$$

or after rearranging:

$$y_{3se}/y_{2se} = (k_{m_2}/k_{m_3})(\phi_3/\phi_2)(a_3/a_2)\,\cdot$$

$$(1-y_{2o}/y_{2se})\,\frac{1-y_{3se}\sum_{j=1}^{n}(\phi_j/\phi_3)(a_j/a_3) + y_{3o}}{1-y_{2se}\sum_{j=1}^{n}(\phi_j/\phi_2)(a_j/a_2)\quad y_{2se}} \tag{43}$$

The mass transfer coefficients k_{mi} can be calculated from Equation (30) by inserting $r_c/R = (1-X)^{1/3}$ as given by Equation (13). Then Equation (30) yields:

$$Rk_{mi} = cD_{im}/(1-X)^{1/3} + 0.3\; cD_{im}\, N_{Sc}^{1/3}\, N_{Re}^{0.1/2}\, (1-X)^{1/6} \tag{44}$$

Since the fluid density, viscosity and effective diffusion coefficient are all functions of the gas film composition, the mass transfer coefficient $\underline{k_{mi}}$ is also composition-dependent. Hence the calculation of $\underline{y_{1se}}$ requires the use of an iteration technique for Equations (38), (40), (43) and (44). The procedure may be as follows:

1. Assume a value for y_{3se}/y_{2se}:

$$y_{3se}/y_{2se} = C \text{ (a constant)} \tag{45}$$

2. Calculate $\underline{y_{1se}}$ using Equations (38), (40), (44), and (45).

3. Calculate y_{3se}/y_{2se} from Equation (43).

4. Compare the value of y_{3se}/y_{2se} found at step 3 with that at step 1. If the calculated y_{3se}/y_{2se} value is not acceptable, using a convergence criterion (Carnahan, Luther and Wilkes, 1969) repeat steps 2-4 until a convergence is obtained.

Using the stoichiometric coefficients of Equation (4) (chlorination reaction: $a_1 = 4$, $a_2 = 1$, $a_3 = 1$ and $\phi_1 = 1$, $\phi_2 = -1$, $\phi_3 = -1$) in Equation (36) and applying it to Equation (37) yields the reaction time-conversion relationships for the chlorination reaction as:

$$t_m = \frac{2R^2\rho_s''/\beta}{(y_{1o}-y_{1se})/(2-y_{2se})}\left[\frac{2}{3\alpha}(1-z^{2/3})-\alpha^{-2}(1-z) + 2\alpha^{-3}(1-z^{1/3}) + 2\alpha^{-4}\ln\frac{(1+\alpha)}{(1+\alpha z^{1/3})}\right] \tag{46}$$

Combined Mass Transfer and Chemical Reaction Control

When chemical reaction and mass transport present comparable resistances to the progress of a reaction, the contribution of these processes must be considered simultaneously. A pseudo-steady state assumption, stating that the rate of movement of the reaction surface, dr_c/dt, is small with respect to the velocity of the gaseous components through the gas film, has been shown to be a good approximation for most of the gas-solid reaction systems, except for those under extremely high pressures and very low solid reactant concentration (Bischoff, 1965), (Bowen, 1965), (Luss, 1968). Then the overall rate is identical to the rate of interfacial chemical reaction and also to that of mass transport.

Using the stoichiometric coefficients in Equation (4) ($a_1 = 4$, $a_2 = 1$, $a_3 = 1$ and $\phi_1 = 1$, $\phi_2 = -1$, $\phi_3 = -1$) Equation (27) can be rewritten for component 1 (chlorine) as:

$$dr_c/dt = k_{m1}(y_{1s}-y_{1o})/2\rho_s(2-y_{1s}) \tag{47}$$

It should be noted that the subscript e in the surface concentration terms is not used, due to the fact that the system is not purely mass transfer controlled, hence chemical equilibrium at the reaction surface may not be assumed to exist. Equation (9) for the chemical reaction can be rewritten as:

$$-dr_c/dt = (k_s/4\rho_s)(y_{1s}-y_{1se})/(2-y_{1s}) \tag{48}$$

In Equation (48), surface instead of bulk gas concentrations were

used since, in the presence of diffusional resistance, the concentrations at the bulk are not the same as those at the surface any more, as was the case in purely chemical reaction control. Solving Equation (47) for the term $y_{1s}(2-y_{1s})$ and substituting it into Equation (48) yields:

$$-(4\rho_s/k_s)dr_c/dt - (2\rho_s/k_{m_1})dr_c/dt = (y_{1o}-y_{1se})/(2-y_{1s}) \qquad (49)$$

Here, $\underline{y_{1s}}$ is the concentration of chlorine at the reaction surface and it is not known. A total elimination of the $\underline{y_{1s}}$ term results in a nonlinear differential equation which creates considerable mathematical complexities in handling. For the purpose of practicality and mathematical convenience, the term $\underline{y_{1s}}$ is left on the right hand side of Equation (49) to eliminate the handling of a nonlinear differential equation. Keeping this consideration in mind, derivation is continued leaving the $\underline{y_{1s}}$ term as unknown. Insertion of Equations (31) and (32) into Equation (49) after rearrangement gives:

$$-\frac{(4\rho_s R/k_s)dz_c}{(y_{1o}-y_{1se})/(2-y_{1s})} - \frac{2R^2\rho_s\beta}{(y_{1o}-y_{1se})/(2-y_{1s})}\left(\frac{z_c dz_c}{1+\alpha z_c^{1/2}}\right) = dt \qquad (50)$$

where $\underline{\alpha}$ and $\underline{\beta}$ are given by Equations (33) and (34). Integration of Equation (50) gives:

$$t = \frac{4\rho_s R(1-z)}{(y_{1o}-y_{1se})/(2-y_{1s})} + \frac{2R^2\rho_s/\beta}{(y_{1o}-y_{1se})/(2-y_{1s})}\left[\frac{2}{3\alpha}(1-z^{2/3}) - \alpha^{-2}(1-z) + 2\alpha^{-3}(1-z)^{1/2} + 2\alpha^{-4}\ln\left(\frac{1+\alpha}{1+\alpha z^{1/2}}\right)\right] \qquad (51)$$

Comparison of Equation (51) with Equation (18) and (46) reveals that the first term in Equation (51) represents the chemical reaction contribution and the second term the mass transfer contribution. If the y_{1s} term in the first term is approximated by y_{1o} (that is by the bulk gas concentration) then the first term becomes the time for purely kinetic control as given by Equation (18). Similarly, if the y_{1s} term in the second term is approximated by y_{1se} (that is, the equilibrium concentration at the reaction surface) then the second term yields the time for purely mass transfer control as given by Equation (46). So when the reaction is under intermediate control, both the kinetic and the gas film diffusion resistances are contributing, the total time can be approximated by the summation of two terms: the time required to reach the same conversion (or $z = (1-X)^{1/3}$, Equation 12) in the absence of mass transfer resistance as given by Equation (18) and that for pure mass transfer control as given by Equation (46). As will be shown later, the experimental data obtained in this study were in reasonable agreement with these theoretical formulations.

PREDICTION OF TRANSPORT PROPERTIES

Diffusion Coefficient

In accordance with the concept of using analogous binary formulae for multicomponent diffusion, Hsu and Bird (1960) and also Bird, Stewart and Lightfoot (1960) obtained an equation for the effective binary diffusivity based on the Stefan-Maxwell equation:

$$\nabla y_i = \sum_{j=1}^{n} (1/D_{ij})(y_i N_j - y_j N_i) \tag{52}$$

which describes the diffusion in an n-component mixture of ideal gases at constant temperature and pressure. The effective binary diffusivity D_{im} for the diffusion of i in a mixture is defined by analogous binary relation as:

$$N_i = -cD_{im} \nabla y_i + y_i \sum_{j=1}^{n} N_j \tag{53}$$

Insertion of Equation (52) into (53) and solving for D_{im} gives:

$$D_{im} = (N_i - y_i \sum_{j=1}^{n} N_j) / \sum_{j=1}^{n} (1/D_{ij})(y_j N_i - y_i N_j) \tag{54}$$

where, D_{ij} is the binary diffusion coefficient for the components i and j, y_i is the mole fraction of component i in the gas film and N_i is the molar flux of component i. Equation (54) can be simplified by using stoichiometric requirements on molar fluxes as given by Equation (22). Then the effective diffusion coefficient becomes:

$$D_{im} = [1 - y_i \sum_{j=1}^{n} (\phi_j a_j)/(\phi_i a_i)] / \sum_{j=1}^{n} (1/D_{ij}) [y_j - (y_i \phi_j a_j)/(\phi_i a_i)] \tag{55}$$

A direct replacement of the binary diffusion coefficient by the effective diffusivity D_{im} in binary formulae assumes that D_{im} is almost independent of the changes in concentration or position in the gas film. Hsu and Bird (1960) discussed the assumption of linear variation with composition for systems in which the variation of D_{im} is considerable and showed that the D_{im} approach in solving multicomponent diffusion problems gives reasonable

results for mass transfer rates, but a less satisfactory description of the concentration profiles. The problem of defining an average diffusion coefficient has also been discussed by Wilke (1950a), Sahin (1961) and Tureuskii et al. (1971). The latter made a comparison of the calculation methods.

Reid and Sherwood (1966) recommended the expression:

$$D_{ij} = 0.001858\ T^{3/2}[(M_i+M_j)/M_iM_j]^{1/2}/P\sigma_{ij}^2\Omega_D \tag{56}$$

for the estimation of binary diffusion coefficients D_{ij} at low pressure. In this equation, M is the molecular weight, P the system pressure in atmospheres, T the temperature in Kelvin, σ_{ij} the Lennard-Jones force constant for the mixture, Ω_D the collision integral which is a function of the dimensionless temperature $T/(\varepsilon/k)_{ij}$ where ε is the energy potential-parameter and k is the Boltzmann constant. The parameters σ_{ij} and ε_{ij} are estimated from the force constants for the pure gases by use of the combining rules (Reid and Sherwood, 1966):

$$\sigma_{ij} = 1/2\ (\sigma_i + \sigma_j) \tag{57}$$

$$\varepsilon_{ij}/k = [(\varepsilon_i/k)(\varepsilon_i/k)]^{1/2} \tag{58}$$

Usually, the values of the collision integrals Ω_D are given in tabular form (Hirschfelder, Curtiss and Bird, 1954) which have to be interpolated for general applicability. The available values were correlated by Hattikudur and Thodos (1970) to produce a functional relationship which is more convenient for computerized

calculations. The expression was given as:

$$\Omega_D = 1.069/T^{*0.1580} + 0.3445/\exp(0.6537T^*) + 1.556/\exp(2.099T^*) + 1.976/\exp(6.488T^*) \quad (59)$$

where,

$$T^* = T/(\varepsilon/k) \quad (60)$$

Viscosity

The semi-empirical formula of Wilke (1950b) has been recommended by Reid and Sherwood (1966) and also by Bird, Stewart and Lightfoot (1960) for the estimation of multicomponent gas mixture viscosities at low pressures and it was given as

$$\mu_{mix} = \sum_{i=1}^{n} (y_i \mu_i / \sum_{j=1}^{n} y_j \Psi_{ij}) \quad (61)$$

in which

$$\Psi_{ij} = (1/\sqrt{8})(1+M_i/M_j)^{-1/2}[1+(\mu_i/\mu_j)^{1/2}(M_j/M_i)^{1/4}]^2 \quad (62)$$

Here n is the number of chemical species in the mixture, y_i and y_j are the mole fractions of species i and j, μ_i and μ_j are the viscosities of species i and j at the system temperature and pressure, and M_i and M_j are the corresponding molecular weights. Ψ_{ij} is dimensionless and, when $i = j$, $\Psi_{ij} = 1$. The data required for Wilke's method are more readily available, and the latter has been found to be reliable in almost all the cases in which it has been used (Reid and Sherwood, 1966).

For the estimation of pure gas viscosity the following equation has been recommended:

$$\mu_i = 2.669 \times 10^{-5} \sqrt{M_i T}/(\sigma^2_i \Omega_v), \text{ (Poise)} \qquad (63)$$

where $\underline{T}$ is the temperature in Kelvin, $\underline{\sigma}$ is the Lennard-Jones potential parameter ('molecular diameter') in Ångstroms and $\underline{\Omega_v}$ is the collision integral for the viscosity.

Hattikudur and Thodos (1970) provided an equation for $\underline{\Omega_v}$ in terms of the reduced temperature $T^* = T/(\varepsilon/k)$ similar to that of $\underline{\Omega_D}$. It was given as:

$$\Omega_v = 1.155/T^{*0.1463} + 0.3945/\exp(0.6672T^*) + 2.05/\exp(2.168T^*) \qquad (64)$$

Lennard-Jones Potential Parameters

The predictions of binary diffusion coefficients and viscosities from Equations (56) and (63) require the knowledge of the Lennard-Jones potential parameters $\underline{\sigma}$ and (ε/k). For chlorine and oxygen, these values were readily available (Svehla, 1962). However, no such data could be found in the literature for zirconium tetrachloride vapour. Hirschfelder, Curtiss and Bird (1954), Reid and Sherwood (1966) and Svehla discussed the different methods to evaluate these parameters. Some of the suggested prediction methods make use of either of the following information:

1. Experimental second virial coefficients, B(T), at two temperatures;

2. critical values, or
3. experimental viscosity or thermal conductivity data at two temperatures.

The procedure to determine the Lennard-Jones potential parameters from the experimental B(T) (second virial coefficient) values is given by Hirschfelder, Curtiss and Bird. First a quantity q is defined by:

$$q = [B(T_2)/B(T_1)]_{exptl} \tag{65}$$

and (ε/k) is determined by the trial-and-error solution of the equation:

$$q = B^*(T_2^*)/B^*(T_1^*) \tag{66}$$

where B^* is the Lennard-Jones second virial coefficients and is given in tabular form as a function of the reduced temperature $T^* = T/(\varepsilon/k)$. Once (ε/k) is estimated, the collision diameter, σ, is given by the relationship:

$$1.2615\ \sigma^3 = B(T_i^*)/B^*(T_i^*) \tag{67}$$

In order to carry out the calculations with reasonable accuracy, the tabular values of B^* (Hirschfelder, Curtiss and Bird, Table I-B) in the temperature region of interest were expressed by a set of equations obtained by curve-fitting. These are given in Table II. The second virial coefficients for zirconium tetrachloride reported by Denisova and Bystrova (1972) were

TABLE II

EQUATIONS FOR LENNARD-JONES SECOND VIRIAL COEFFICIENTS

$T^* = T/(\varepsilon/k)$	$B^*(T^*)$
$2.3 \leqslant T^* \leqslant 2.4$	$B^* = 0.26787 - 3.63713/T^{*2}$
$2.4 \leqslant T^* \leqslant 2.5$	$B^* = 0.28645 - 3.74417/T^{*2}$
$2.5 \leqslant T^* \leqslant 2.6$	$B^* = 0.30347 - 3.85055/T^{*2}$
$2.6 \leqslant T^* \leqslant 2.7$	$B^* = 0.31909 - 3.95612/T^{*2}$
$2.7 \leqslant T^* \leqslant 2.8$	$B^* = 0.33347 - 4.06092/T^{*2}$

used in connection with the equations of Table II. The results of the trial and error solution outlined above are summarized in Table III. The parameters based on the second virial coefficients were found to be:

$$\varepsilon/k = 301.5 \text{ K}$$

$$\sigma = 10.872 \text{ Å}$$

The second method uses the critical values for the estimation. The empirical equations:

$$\varepsilon/k = 0.75\ T_c \tag{68}$$

and

$$\sigma = 5/6\ V_c^{1/3} \tag{69}$$

suggested by Svehla (1962) were based on a large number of data. The critical parameters of zirconium tetrachloride (T_c = 776.5 K, V_c = 306 cm^3/mole, P_c = 57 atm) reported by Nisel'son et al. (1966) were used in Equations (68) and (69), and the following values were obtained:

$$\varepsilon/k = 582.4 \text{ K}$$

$$\sigma = 5.616 \text{ Å}$$

It is evident that the values based on the second virial coefficient and those based on the critical parameters are quite different. A comparison of these values with the Lennard-Jones parameters for other molecules listed by Svehla showed that $\underline{\sigma}$ =

TABLE III

LENNARD-JONES POTENTIAL PARAMETERS FOR $ZrCl_4$

AS CALCULATED FROM SECOND VIRIAL COEFFICIENTS

T (K)	B(T) [1] (cm^3/mole)	ε/k (K)	σ (A°)
713	-618		
		304.4	10.744
733	-562		
		298.9	10.984
753	-507		
		303.3	10.778
773	-457		
		299.2	10.983
793	-408		
		301.2	10.872
713	-618		
Average		301.5	10.872

[1] Denisova and Bystrova (1972)

10.872 (from the virial coefficient) may not be true. The highest value of $\underline{\sigma}$ among more than 200 compounds was about 6.5.

Experimental viscosity data for $ZrCl_4$ vapour at two temperatures were reported by Tsirel'nikov et al. (1961). The viscosity of $ZrCl_4$ was calculated from Equation (63) using both sets of the Lennard-Jones parameters predicted here, and the results are summarized in Table IV. As can be seen, the estimated viscosities using the parameters based on the critical properties gave an almost perfect agreement with the experimental data, while those based on the second virial coefficients were not even close. Hence the previous conclusion on the second virial coefficients is confirmed by viscosity data. Therefore, the values

$$\varepsilon/k = 528.4 \quad K$$

and

$$\sigma = 5.616 \quad A^{o}$$

evaluated from the critical parameters were chosen for the calculation of the binary diffusion coefficient and viscosity of zirconium tetrachloride.

PREDICTION OF GAS VELOCITY AND TEMPERATURE

Numerical solution of the mass transfer model developed in the previous sections requires a knowledge of the velocity and temperature of the gas. The problem of arcing between the plasma gas and a conducting object acting as a ground inside the plasma, plus the reaction of very hot chlorine with almost any material

TABLE IV

LENNARD-JONES POTENTIAL PARAMETERS (σ, ε/k) FOR $ZrCl_4$ - COMPARISON OF EXPERIMENTAL AND CALCULATED VISCOSITY DATA

Temperature (K)	573		973	
	Viscosity x 10^7 (poise)	% Δ	Viscosity x 10^7 (poise)	% Δ
Experimental	1970		3230	
From Equation (63) with, σ = 10.872, ε/k = 301.5	690	65%	871	73%
From Equation (63) with, σ = 5.616, ε/k = 582.4	1927	2.2%	3209	0.66%

made the experimental measurement of gas velocity and temperature by practical methods extremely difficult. For the purpose of the theoretical analysis of the experimental data, a set of empirical expressions was developed for the estimation of these values.

The reaction system in this work, as will be discussed later, involved a nonisothermal swirling confined chlorine plasma jet issuing from a round orifice. Since the reacting spherical pellet was small and was positioned along the centerline of the jet at some distance away from the nozzle exit, evaluation of the axial velocity and of the temperature only along the centerline of the plasma jet was considered.

Chigier and Chervinsky (1966, 1967) applied the principle of similarity to the integral form of the Reynolds equations of motion and obtained the following theoretical expression for the decay of the axial velocity in the fully developed region of the jet:

$$U/U_N = K_1[d/(x + x_0)]f_1^{1/2} \qquad (69)$$

where, d is the diameter of the nozzle, f_1 is the axial decay function expressed in terms of the degree of swirl, U is the local axial velocity along the centerline, U_N is that at the nozzle exit plane, x is the distance from the nozzle exit plane, and x_0 is the distance of the virtual origin of the fully developed jet from the nozzle exit plane. The x_0 is independent of the degree of swirl and is given as 2.3 times the diameter of the

nozzle. K_1 is the axial velocity decay constant expressed by an empirical equation of the form

$$K_1 = 6.8 \,/(1 + 6.8\, S^2) \tag{70}$$

where, S is the swirl number which is related to the maximum values of swirl and axial velocities at the nozzle exit. The foregoing relations were confirmed experimentally by Chigier and Chervinsky (1967) and by Pratte and Keffer (1972) who used (x_o/d) as 3 instead of 2.3. Also, Bhattacharyya and Gauvin (1975) used these relations incorporated with a density correction factor in their modeling studies of a plasma jet reactor. An expression used by Lilley (1974) was similar to Equation (69) but the axial decay function f_1 was eliminated by letting the virtual origin distance x_o vary with the swirl and it was given as:

$$U/U_N = K_1 \; (\rho_\infty/\rho)^{1/2} \; d/(x + x_o) \tag{71}$$

where

$$x_o/d = 35 + 100\, S \tag{72}$$

and

$$K_1 = 15 + 10\, S \tag{73}$$

ρ_∞ and ρ are the ambient and local centerline densities, respectively.

In the case of a plasma jet obtained from an induction torch, however, the plasma fireball formed between the gas dis-

tributor and the nozzle may affect the jet and furthermore the swirl number S as defined in the literature may not be the sole parameter to be considered. Experimentally, it was observed that, at a constant tangential and total gas flow rate, a change in input power may influence the behaviour of the jet. Hence an attempt was made to develop empirical expressions to predict the centerline axial velocity and temperature profiles in the fully developed region as well as in the transition one, based on the experimental data reported by Sayegh (1977) who used the same induction torch with argon gas.

Two parameters were defined to represent the operation of the induction torch with respect to the jet. The first one was the ratio of the flow rates of swirl to radial gas (S_R), and the second was the ratio of the power measured at the nozzle exit plane to that at the inlet (plate power), P_R. Sayegh provided the decay of axial velocity and temperature data along the centerline of the jet for four different conditions which are given in Table V.

A regression analysis was carried out on the experimental profile data, using a package statistical computer program, STATPK, of the McGill University Computing Centre, and the following expression were found to fit the data best:

TABLE V

PLASMA OPERATING CONDITIONS

(SAYEGH, 1977)

CONDITION	RATIO OF GAS FLOW RATES S_R = (SWIRL/RADIAL)	RATIO OF POWERS P_R = (NOZZLE EXIT/PLATE)
I	0.381	0.500
II	0.434	0.450
III	0.333	0.642
IV	0.266	0.666

i) for the fully-developed region

axial velocity decay:

$$U/U_N = A_v \, (\rho_\infty/\rho)^{1/2} [1/(x/d + 2.3)] \tag{74}$$

axial temperature decay:

$$T/T_N = A_T [1/(x/d + 2.3)]^2 \tag{75}$$

ii) for the core and transition region

axial velocity decay:

$$U/U_N = [A_v (\rho_\infty/\rho)^{1/2}]^{b_v} (x/d)^3 \tag{76}$$

axial temperature decay:

$$T/T_N = (A_T)^{b_T} (x/d)^2 \tag{77}$$

where A_v and A_T are the fully developed region velocity and temperature decay constants, respectively; b_v and b_T are the transition region velocity and temperature decay constants, respectively.

The values of the jet development parameters A_v, A_T, b_v and b_T resulting from the regression study are given in Table VI for four different torch operating conditions. A similar regression analysis was carried out on these data to find empirical expressions for the jet development parameters in terms of the operating variables, S_R and P_R, so that Equations (74) through (77) could be generalized and used in the present work. After a considerable search, the following empirical expressions were

found to fit the data best:

$$A_v = 1.826/[1 + 0.922\ S_R - 0.27(S_R/P_R)^2] \tag{78}$$

$$A_T = 9.364 + 0.567/P_R^2 \tag{79}$$

$$b_v \times 10^2 = 0.555 - 9.234\ S_R P_R \tag{80}$$

and

$$b_T \times 10^2 = 0.273 - 17.221\ P_R^2 - 2.360\ S_R^3 \tag{90}$$

The experimental induction torch operating data as given in Table V were used in Equations (74) through (90) and the calculated velocity and temperature profiles for each set of conditions were plotted in Figures 3 through 6, together with the experimental profiles. Inspection of the plots indicates that the empirical equations developed here fit the experimental data closely. It should be pointed out that, while the form of the expressions for the decay of axial velocity and temperature in both the developed and the transition regions of the plasma jet are proper, the empirical equations of the jet development parameters (A_V, A_T, b_v, b_T), [Equations (78) - (90)] by no means represent the behaviour of the jet in full confidence. This is due to the fact that they were based on a limited amount of experimental operating data which were not aimed at carrying out such an analysis when the original author (Sayegh, 1977) made his studies. Although Equations (78) through (90) are adequate for the purpose of their use in this work, they should be based on a larger number of experimental torch operating data (S_R, P_R) to ensure their general applicability.

TABLE VI

PLASMA JET DEVELOPMENT PARAMETERS

(FROM REGRESSION ANALYSIS)

CONDITION	A_V	$b_V \times 10^2$	A_T	$b_T \times 10^2$
I	1.279	-1.191	13.222	-2.509
II	1.327	-1.277	12.401	-3.198
III	1.227	-1.410	14.492	-2.248
IV	1.263	-1.075	17.375	-1.655

FIGURE 3

DECAY OF AXIAL GAS VELOCITY AND TEMPERATURE

ALONG THE CENTERLINE (CONDITION I)

(——) EXPERIMENTAL DATA FROM SAYEGH (1977)

(- -) DATA CALCULATED THROUGH EQUATIONS (74) - (90)

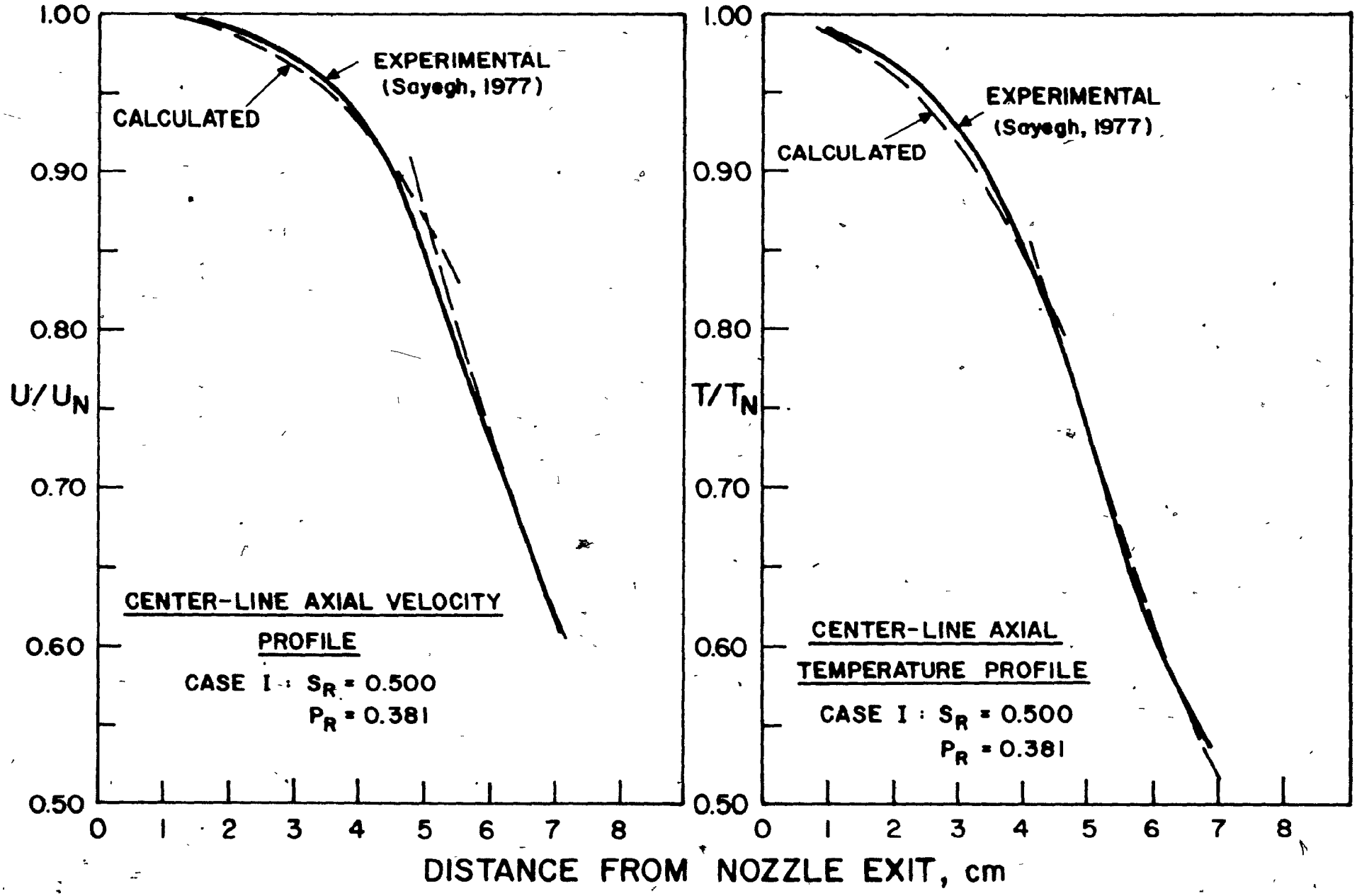
1.00
0.90
0.80
0.70
0.60
0.50
U/U_N
EXPERIMENTAL
(Sayegh, 1977)
CALCULATED
CENTER-LINE AXIAL VELOCITY
PROFILE
CASE I : S_R = 0.500
P_R = 0.381
T/T_N
EXPERIMENTAL
(Sayegh, 1977)
CALCULATED
CENTER-LINE AXIAL
TEMPERATURE PROFILE
CASE I : S_R = 0.500
P_R = 0.381
0 1 2 3 4 5 6 7 8
DISTANCE FROM NOZZLE EXIT, cm

FIGURE 4

DECAY OF AXIAL GAS VELOCITY AND TEMPERATURE

ALONG THE CENTERLINE (CONDITION II)

(——) EXPERIMENTAL DATA FROM SAYEGH (1977)

(- -) DATA CALCULATED THROUGH EQUATIONS (74) - (90)

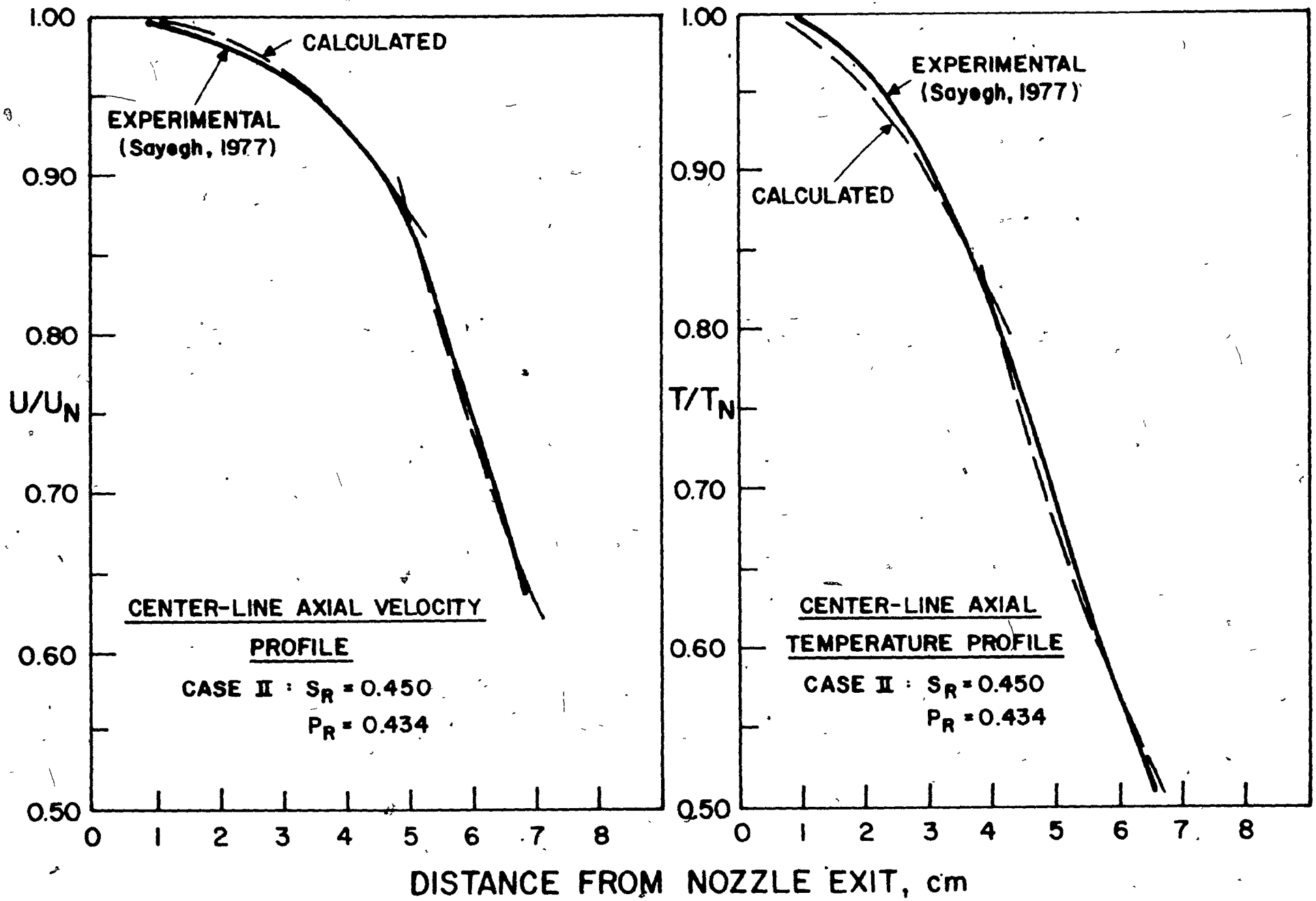
1.00
0.90
0.80
0.70
0.60
0.50
U/U_N
CALCULATED
EXPERIMENTAL
(Sayegh, 1977)
CENTER-LINE AXIAL VELOCITY
PROFILE
CASE II : S_R = 0.450
P_R = 0.434
T/T_N
EXPERIMENTAL
(Sayegh, 1977)
CALCULATED
CENTER-LINE AXIAL
TEMPERATURE PROFILE
CASE II : S_R = 0.450
P_R = 0.434
0 1 2 3 4 5 6 7 8
DISTANCE FROM NOZZLE EXIT, cm

FIGURE 5

DECAY OF AXIAL GAS VELOCITY AND TEMPERATURE

ALONG THE CENTERLINE (CONDITION III)

(——) EXPERIMENTAL DATA FROM SAYEGH (1977)

(- -) DATA CALCULATED THROUGH EQUATIONS (74) - (90)

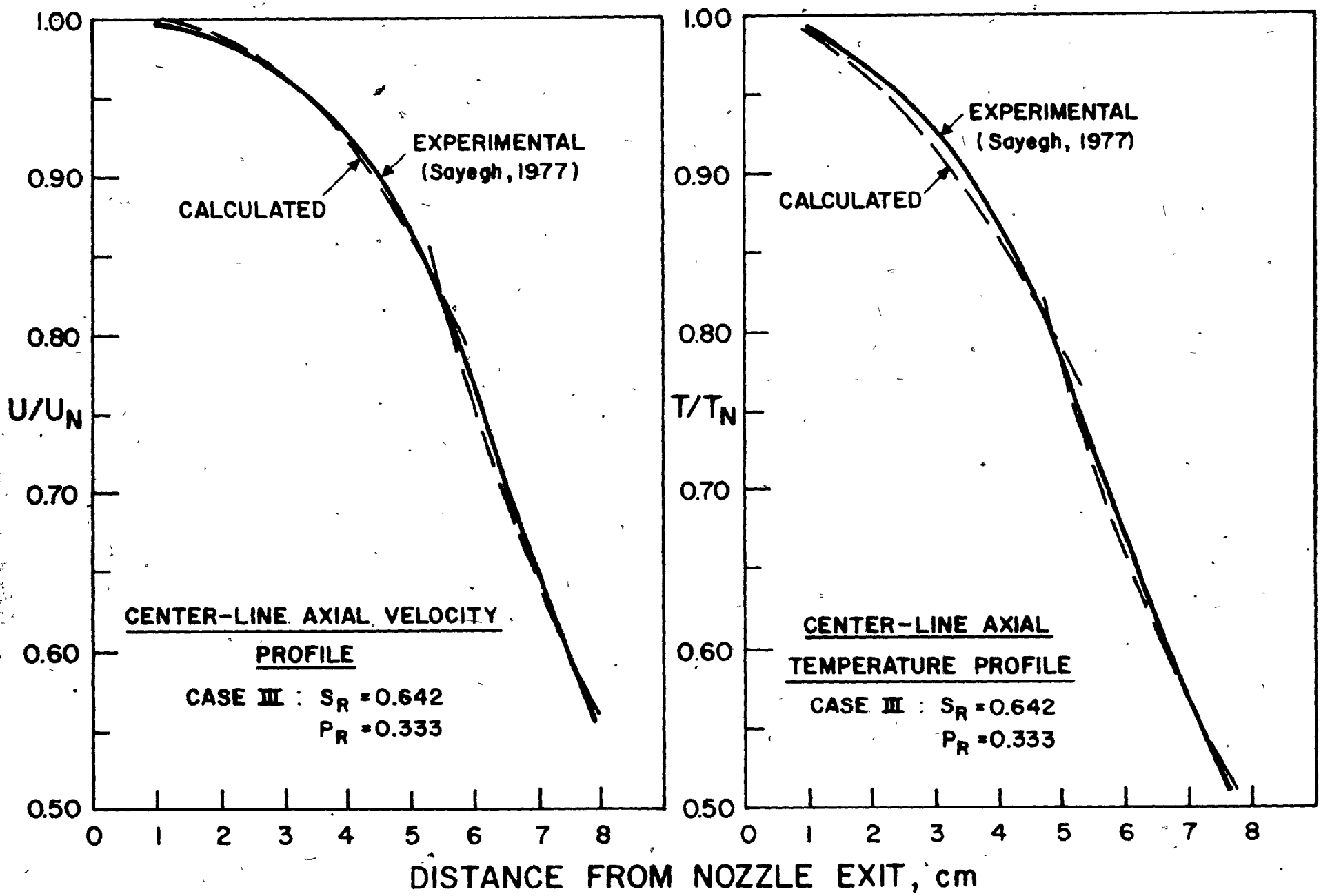
1.00
0.90
0.80
0.70
0.60
0.50
U/U_N
EXPERIMENTAL
(Sayegh, 1977)
CALCULATED
CENTER-LINE AXIAL VELOCITY
PROFILE
CASE III : S_R = 0.642
P_R = 0.333
T/T_N
EXPERIMENTAL
(Sayegh, 1977)
CALCULATED
CENTER-LINE AXIAL
TEMPERATURE PROFILE
CASE III : S_R = 0.642
P_R = 0.333
0 1 2 3 4 5 6 7 8
DISTANCE FROM NOZZLE EXIT, cm

FIGURE 6

DECAY OF AXIAL GAS VELOCITY AND TEMPERATURE

ALONG THE CENTERLINE (CONDITION IV)

(——) EXPERIMENTAL DATA FROM SAYEGH (1977)

(- -) DATA CALCULATED THROUGH EQUATIONS (74) - (90)

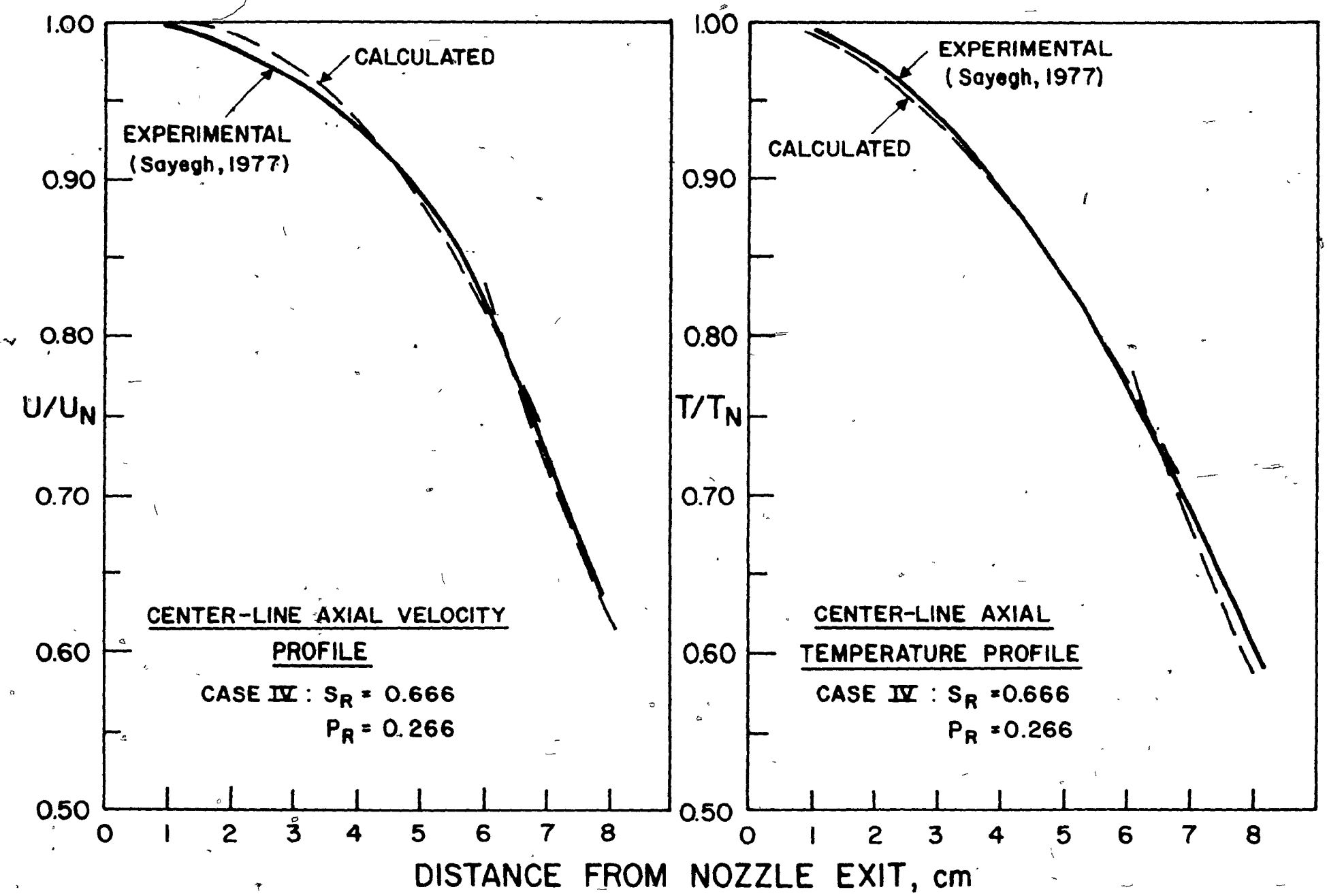
1.00
0.90
0.80
0.70
0.60
0.50
U/U_N
CALCULATED
EXPERIMENTAL
(Sayegh, 1977)
CENTER-LINE AXIAL VELOCITY
PROFILE
CASE IV : S_R = 0.666
P_R = 0.266
T/T_N
EXPERIMENTAL
(Sayegh, 1977)
CALCULATED
CENTER-LINE AXIAL
TEMPERATURE PROFILE
CASE IV : S_R = 0.666
P_R = 0.266
0 1 2 3 4 5 6 7 8
DISTANCE FROM NOZZLE EXIT, cm

NUMERICAL CALCULATIONS

The foregoing theoretical discussions were incorporated in a computer program for numerical calculations. The listing of the program is given in Appendix III. Briefly, the program uses the intrinsic kinetic data (activation energy, frequency factor), torch operating data (S_R, P_R), nozzle exit velocity (U_N) and temperature (T_N), stoichiometric coefficients (a_i) and indexes (ϕ_i), Lennard-Jones potential parameters (ε_i/k, σ_i), particle distance from the nozzle exit (x), bulk gas composition (y_{io}), and particle reaction temperature (T_R) as the input data for the calculations. The program may be considered to be a general one if the equations in SUBROUTINE THERMO calculating the free energy of the chlorination reaction are replaced with appropriate ones for the reaction under consideration. The free energy equations were developed from the data in the JANAF Tables by curve fitting and they are (in cal/mole):

For Equation (2), per mole of Cl_2,

$$\Delta F_1 = -59628.8 + 28.18\ T + 229.80 \times 10^{-6}\ T^2 \tag{91}$$

For Equation (3), per mole of O_2,

$$\Delta F_2 = 51625.92 - 15.98\ T + 203.48 \times 10^{-6}\ T^2 \tag{92}$$

For Equation (4)

$$\Delta F_3 = 2\ \Delta F_1 + \Delta F_2 \tag{93}$$

The output of the program which will be discussed at length later, includes the input data as well as the calculated values of the binary and effective diffusion coefficients, pure component and mixture viscosities, surface concentrations with associated degree of convergence, and the reaction times (chemical reaction and mass transfer).

EXPERIMENTAL

APPARATUS

The apparatus used in the experimental work consisted of two main systems: a plasma generation system including an induction torch, a power supply and a console, and a reactor system including a single-particle reactor, a set of heat exchangers to cool the reactor exhaust, and a chlorine absorption and disposal unit. A schematic drawing of the overall set up is given in Figure 7.

Plasma Generation System

The plasma was generated in a radio-frequency induction torch manufactured by TAFA (model 56), Concord, New Hampshire. A drawing of the torch is given in Figure 8. It consisted of a quartz tube surrounded by a copper induction coil immersed in cooling water, inside a Teflon body. Each end of the torch was constructed of metal. Tight seals were effected with O-rings, and the whole assembly could be easily dismantled to provide

FIGURE 7

SCHEMATIC DRAWING OF EQUIPMENT

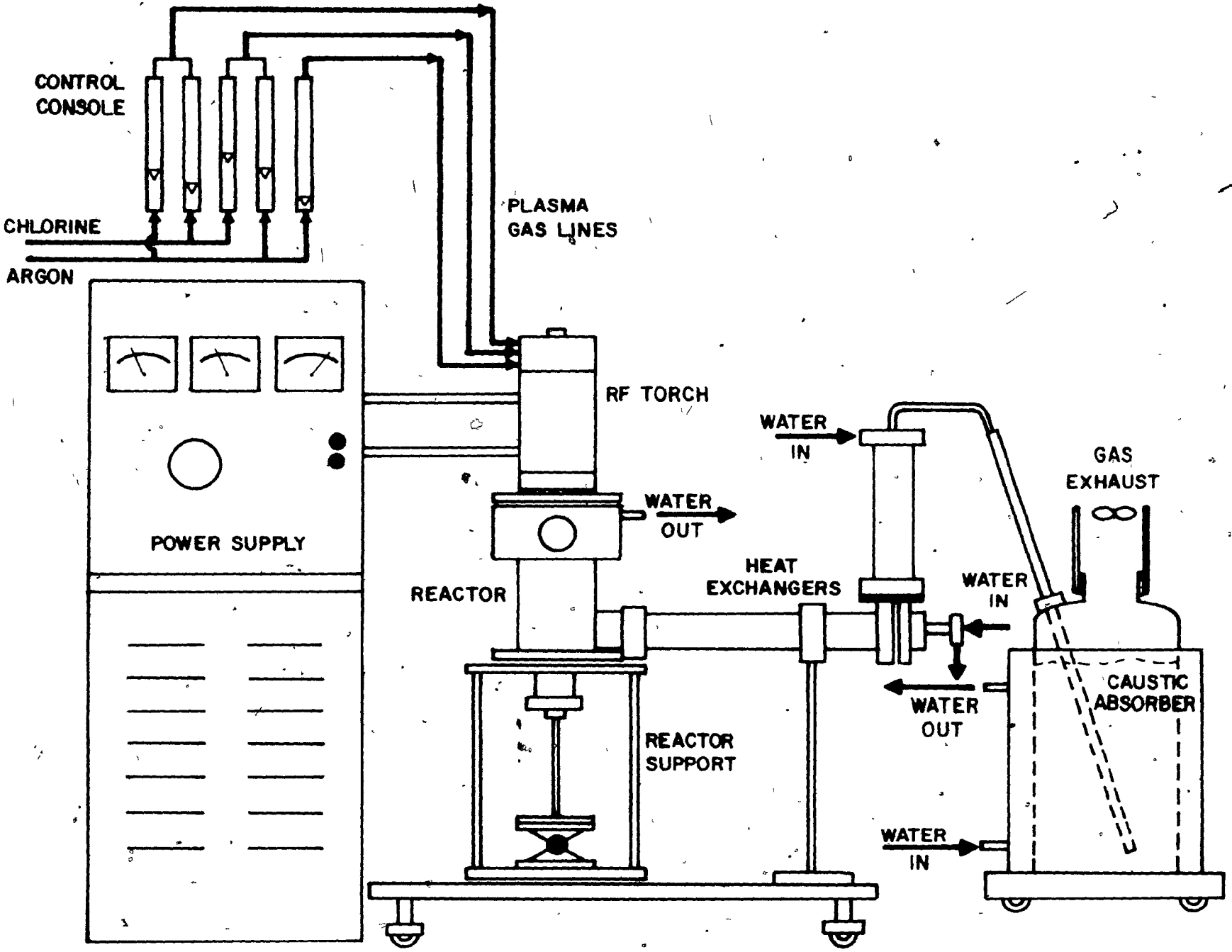
CONTROL
CONSOLE
CHLORINE
ARGON
PLASMA
GAS LINES
RF TORCH
POWER SUPPLY
WATER
IN
WATER
OUT
GAS
EXHAUST
REACTOR
HEAT
EXCHANGERS
WATER
IN
WATER
OUT
CAUSTIC
ABSORBER
REACTOR
SUPPORT
WATER
IN

FIGURE 8

SCHEMATIC DRAWING OF INDUCTION TORCH

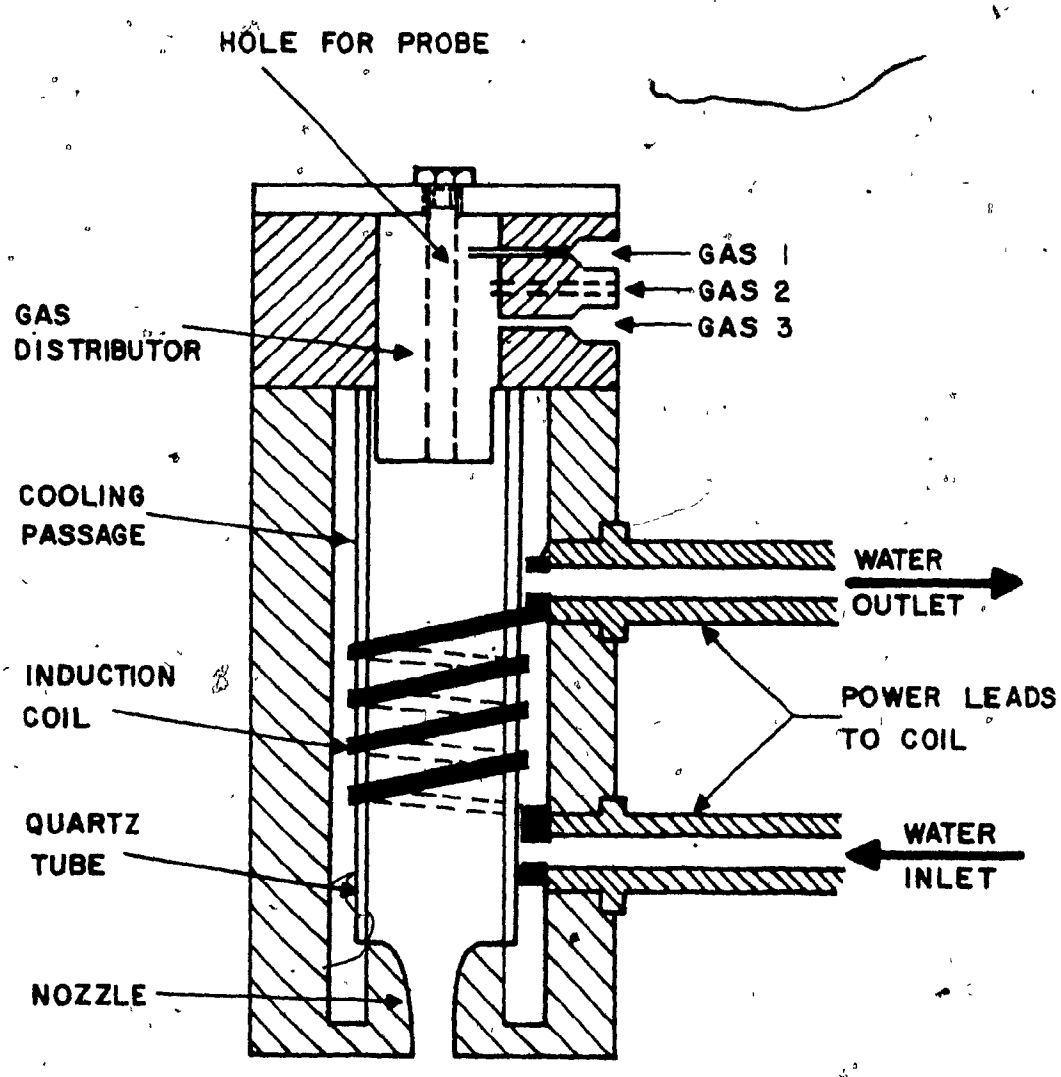
HOLE FOR PROBE
GAS 1
GAS 2
GAS 3
GAS DISTRIBUTOR
COOLING PASSAGE
WATER OUTLET
INDUCTION COIL
POWER LEADS TO COIL
QUARTZ TUBE
WATER INLET
NOZZLE

replacement of the quartz tube, as required. The cold plasma-forming gas entered the torch at the top, through a water-cooled gas distributor which allowed the introduction of the gas in axial, radial and tangential directions. The tangential (swirl) stream served the purpose of stabilizing the flow and preventing the hot plasma fire-ball, formed near the axis, from reaching the inner walls of the quartz tube. The axial flow was used for ignition only, and normal operation was in the radial and swirl modes. The plasma gas, heated up and ionized in the coil section, left the torch as a jet through a water-cooled monel nozzle which replaced the original copper one when chlorine was used. The nozzle was 25.4 mm in diameter. Water at a flow rate of 1.36 m^3/h and at 414×10^3 N/m^2 was required to cool the torch.

The torch had to be started with argon gas and, following ignition, chlorine gas could be introduced. Normally, with argon operation, the plasma flame was ignited by a spark produced by the coupling of a thin gold film on the inside surface of the quartz tube with the induction coil. However, once chlorine was introduced, it reacted with the gold film and subsequent ignition could not be achieved by this method. Hence a different ignition procedure was employed. A graphite rod, 6.4 mm in diameter, was inserted from the top through the center-hole of the torch. The tip of the rod did not enter the plasma but extended from the end of gas distributor. Ignition was obtained by contacting the other end of this rod intermittently with a grounded graphite probe,

while adjusting the input power. The operation of the torch with chlorine gas was not as smooth and as flexible as that with argon. It extinguished at low power levels (7-10 kW depending upon the gas flow rate) and it reacted with the water-cooled monel nozzle at high power levels (25-30 kW) due to insufficient cooling.

Power and cooling water entered the torch through two copper pipes connected directly to the power supply. The power supply was manufactured by Lepel High Frequency Laboratories Inc. It provided a maximum power of 30 kW in the plasma gas at 4 MHz, and required 3 m^3/h of cooling water at 414×10^5 N/m^2.

The standard control console, TAFA model 47-10A, metered and controlled the flow of gas to the plasma torch. It was modified to allow a smooth transfer of operation from pure argon to pure chlorine or to a mixture of both, while the inlet power was adjusted to compensate for the change of gas. A schematic drawing of the standard and of the modified flow connections are shown in Figure 9. No modification was made to the axial gas line, since it used argon only, as previously mentioned. The console consisted of five precision (2%) rotameters with check valves at the outlets to prevent back flow of chlorine, and with a safety interlock to the power supply to prevent operation under low gas pressure. An additional flowmeter was installed to regulate the flow of argon purge gas to the viewing port of the reactor.

Chlorine gas with a minimum of 99.9% purity was supplied

FIGURE 9

SCHEMATIC DRAWING OF GAS CONSOLE CONNECTIONS

a - Standard

b - Modified

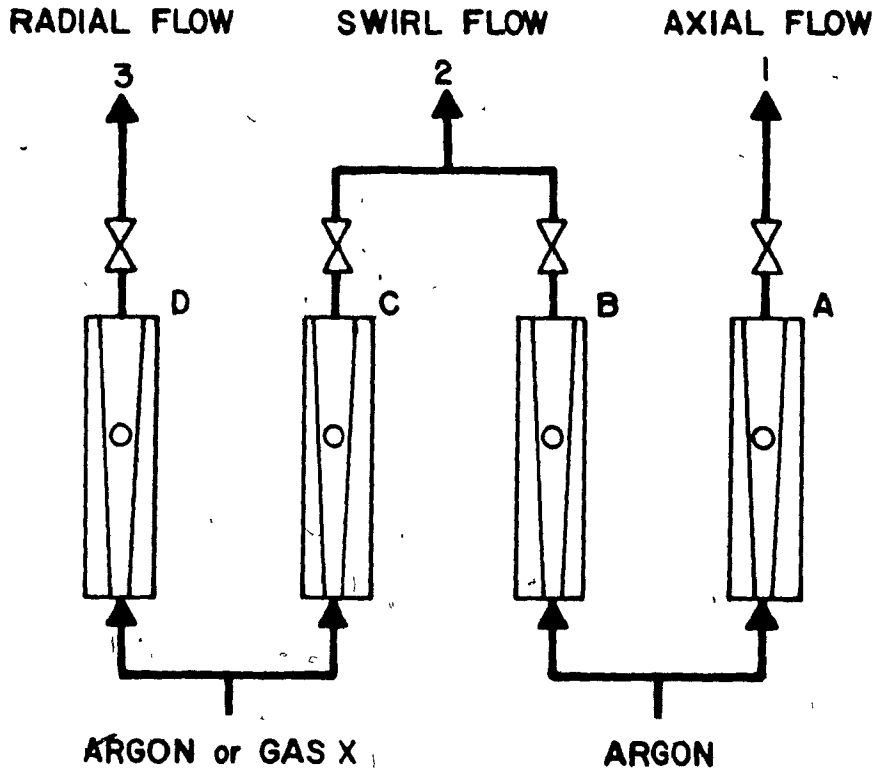

a – STANDARD D

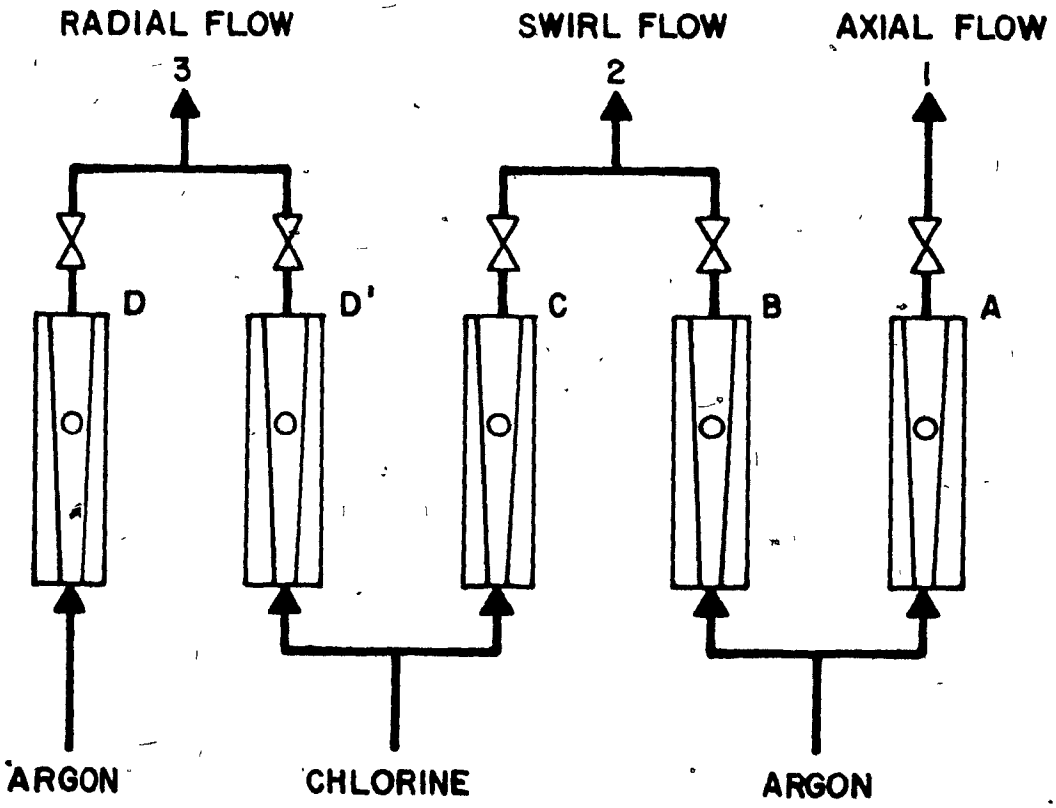

b – MODIFIED

from a commercial liquid chlorine cylinder (Canadian Industries Limited) and regulated by a single-stage monel regulator accompanied by a purge assembly and a check valve connected to an argon cylinder to purge the system from the regulator on. Argon gas was supplied from three cylinders joined to a common manifold and regulated by a two-stage pressure regulator.

The Reactor System

The reactor (Figure 10) was designed specifically to study the kinetics of gas-solid reactions of a single stationary particle and to meet the requirements of operation with hot chlorine.

The water-cooled inner part was machined from a single piece of monel -400 rod. The upper section (the reaction chamber) was 5.08 cm in diameter and 11.4 cm in length. The lower section (2.54 cm in diameter and 11.4 cm in length) housed the particle support system and provided a non-reactive area for the particle while steady plasma conditions were established. It also accommodated the reactor outlet (1.9 cm in diameter) without disturbing the symmetry of the flow in the reaction chamber. The effective length of the reaction chamber could be increased further (by 2.54 cm) by the installation of a water-cooled flange of the same diameter as the reactor at its upper end.

A single window was provided for visual observation and particle temperature measurements by means of optical pyrometry. The window was kept clear by the continuous injection of a small

FIGURE 10

SCHEMATIC DRAWING OF REACTOR

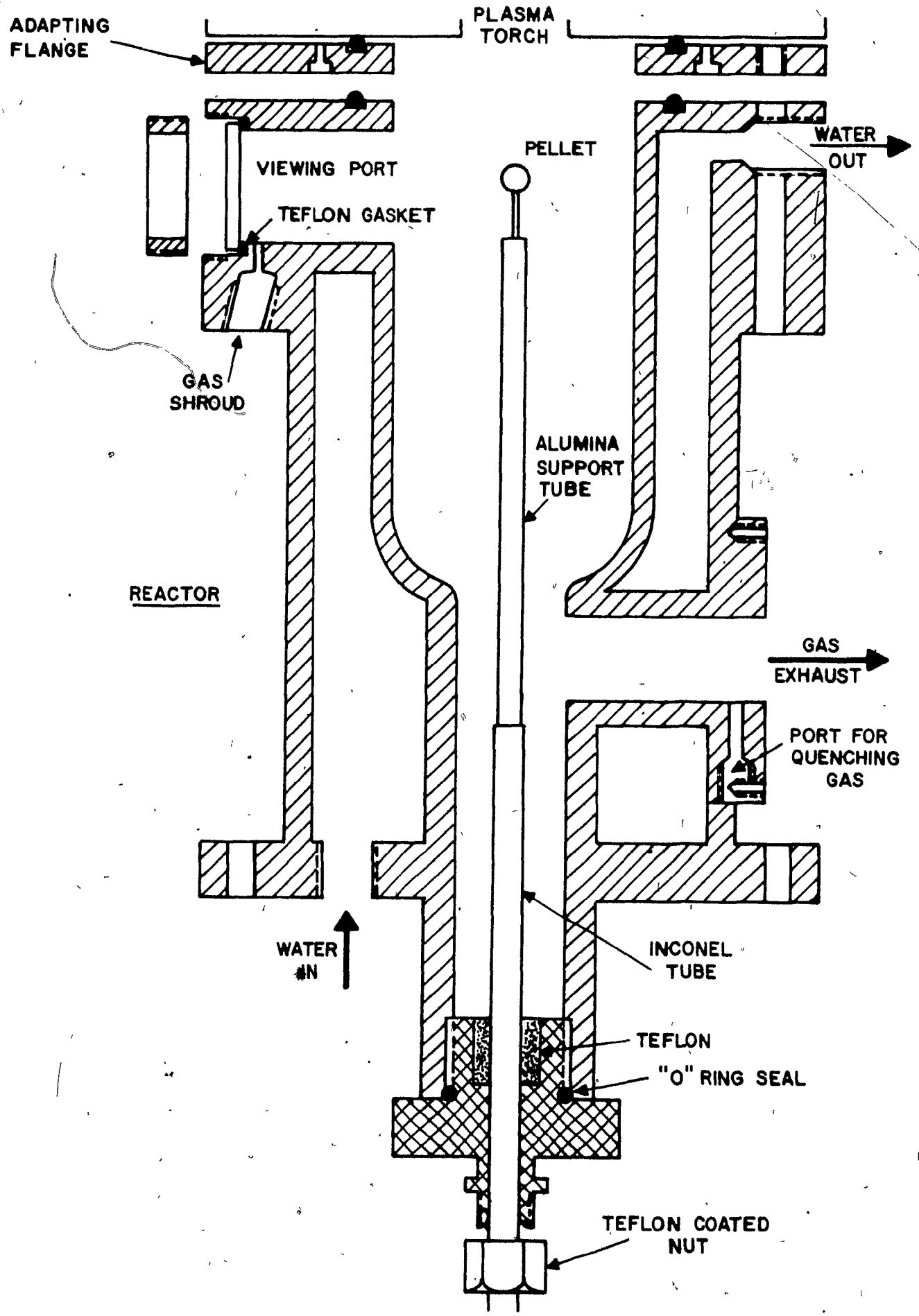
ADAPTING FLANGE
PLASMA TORCH
VIEWING PORT
TEFLON GASKET
PELLET
WATER OUT
GAS SHROUD
ALUMINA SUPPORT TUBE
REACTOR
GAS EXHAUST
PORT FOR QUENCHING GAS
WATER IN
INCONEL TUBE
TEFLON
"O" RING SEAL
TEFLON COATED NUT

amount of argon gas which prevented the condensation of zirconium tetrachloride on the pyrex glass. The design of the bottom part of the reactor allowed the particle supporting system to slide up and down under leak-proof conditions. The reactor was connected to the torch through a 0.63-cm thick uncooled stainless steel -304 flange which acted as an adaptor.

The particle was mounted on an alumina sting 0.08 cm in diameter and 1.0 cm in length which itself was mounted on a larger alumina rod 0.48 cm in diameter and 30.5 cm in length. The lower part of the alumina rod was sheathed by an inconel tube 0.64 cm in outside diameter and 15 cm in length, to provide strength and tight sealing at the bottom. When the particle was positioned at the level of the viewing port, the inconel tube remained below the level of the reactor outlet so that it was not affected by the hot chlorine. The inconel tube was connected to a laboratory jack through a male connector to allow positioning of the particle. Plexiglass was used to isolate the metal supports electrically from the jack and the table.

A cold gas injection port was provided at the outlet of the reactor to allow quenching if needed. The reactor outlet was equipped with an integral flange to connect with the heat exchanger shown in Figure 11. The inner part of the heat exchanger (50-cm long) was a water-cooled stainless steel -304 tube 2.54 cm in diameter with twenty internal longitudinal fins manufactured by the French Tube Division of Noranda Metal Industries Inc. in

FIGURE 11

SCHEMATIC DRAWING OF HEAT EXCHANGER

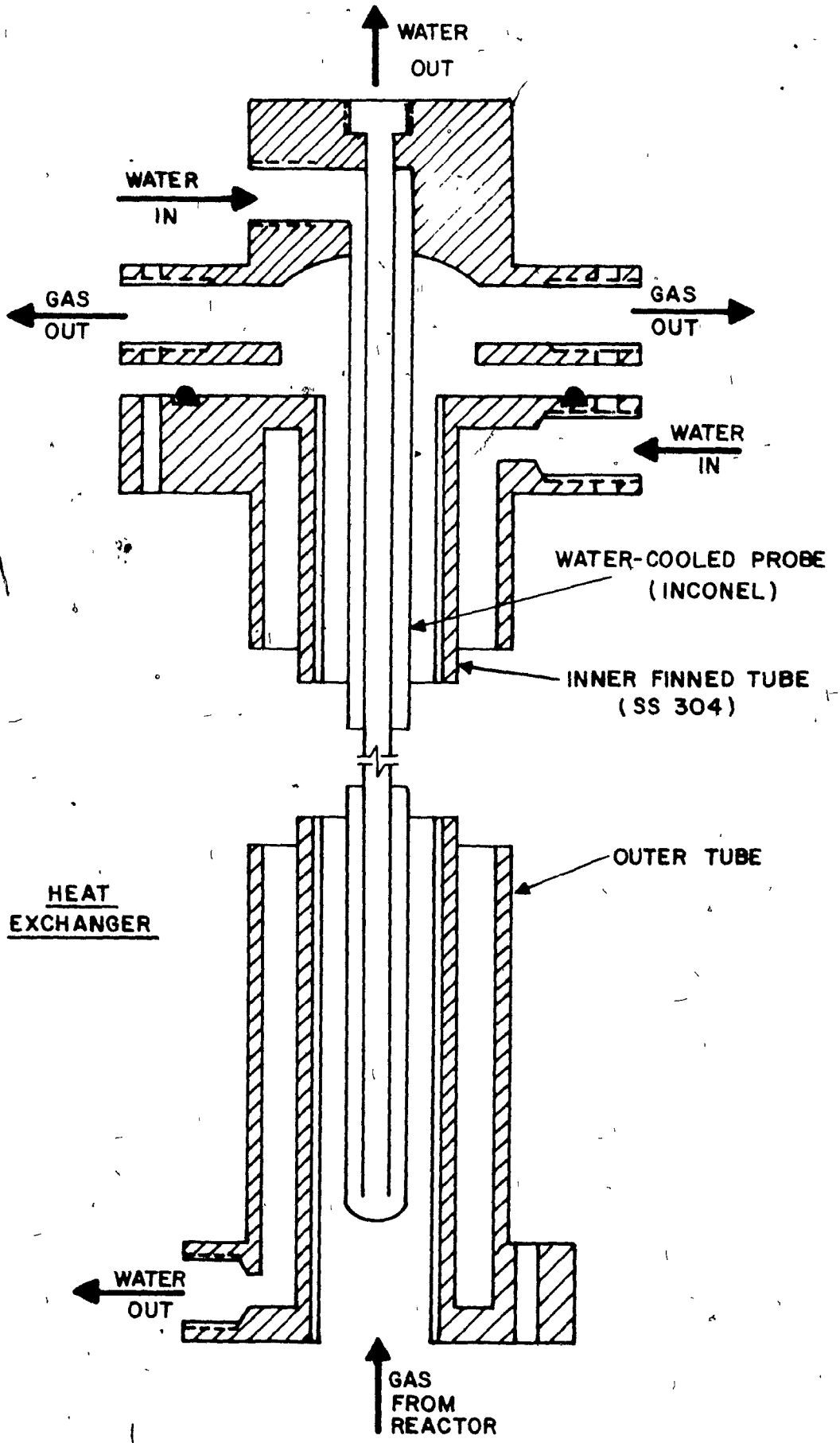
WATER
OUT
WATER
IN
GAS
OUT
GAS
OUT
WATER
IN
WATER-COOLED PROBE
(INCONEL)
INNER FINNED TUBE
(SS 304)
OUTER TUBE
HEAT
EXCHANGER
WATER
OUT
GAS
FROM
REACTOR

Newton, Connecticut. A water-cooled probe was placed inside the exchanger to provide extra cooling, while keeping the equipment size small enough not to act as a ground and to prevent arcing. The outside tube of the probe was inconel and 0.95 cm in outside diameter. The gas leaving this heat exchanger entered a second one of similar design, but shorter in length (30 cm).

The chlorine gas, cooled down to 350 - 500 K at the outlet of the cooling system, entered a caustic absorber through a Teflon pipe. The end of this pipe had a large number of small holes through which the chlorine gas was injected in the form of very fine bubbles into the caustic solution. The absorber consisted of a plastic tank 38 cm in diameter and 64 cm in length surrounded by a metallic jacket to provide water cooling. The NaOH solution (28% wt) was sufficient to absorb 7 - 8 kg of chlorine in one batch.

The outlet of the absorber was connected to a specially designed exhaust system through a 10-cm diameter neoprene-coated flexible hose. Great care was exercised in the design of the ventilation and exhaust system. Thus, three large flexible exhaust hoses (15.2 cm in diameter) were provided in key locations in the laboratory, in the chlorine cylinder area, over the control console, and over the reactor area. The laboratory atmosphere was monitored continuously for chlorine with an automatic detector (Toxgard, Mine Safety Appliances of Canada), backed up by a visual and sound alarm unit.

Since the entire reactor system had to be kept electrically

floating to prevent arcing, all the water and the gas lines connected to the system were of non-conducting material. Provisions were made in the design of the reactor and of the heat exchangers for calorimetric measurements, in order to predict the gas velocity and the temperature at the reactor inlet.

MEASUREMENT TECHNIQUES

Preparation of Spherical Pellets

The zirconium dioxide used in these experiments was optical grade, having a minimum purity of 99.8%, and was supplied by Atomergic Chemetals Corp., Plainview, New York. Analysis of the material was performed by the same company upon request and the results based on spectrographic methods are given in Table VII. Particle size was analyzed using an X-ray sedimentometer (SediGraph 5000D Particle Size Analyzer, Micromeritics Instrument Corp., Norcross, Georgia) which measured the sedimentation rates of the zirconium dioxide particles suspended in a 0.1% sodium silicate solution, and presented the data as a cumulative mass percent distribution in terms of equivalent spherical diameter. The result given in Figure 12 showed that about 96 mass percent of the particles had an equivalent diameter less than about 44 microns and the mass median diameter corresponded to 6.6 microns. The experimental measurements were carried out with spherical pellets of different diameters and porosities compacted from this powder.

A die compaction method with pressure applied to both ends

TABLE VII

ANALYSIS OF ZIRCONIUM DIOXIDE USED IN KINETIC STUDY

IMPURITY[1]	CONCENTRATION %
Al	<0.01
Fe	<0.01
Hf	<0.03
Mg	<0.01
Mn	<0.01
Si	<0.10

(1) The following elements were checked but not detected:

Ag, As, B, Ba, Bi, Ca, Cd, Co, Cr, Cu, Li, Mo, Na, Nb, Ni, Pb, Sb, Sn, Ta, Ti, V, W, Zn.

FIGURE 12

ZIRCONIUM DIOXIDE PARTICLE SIZE DISTRIBUTION

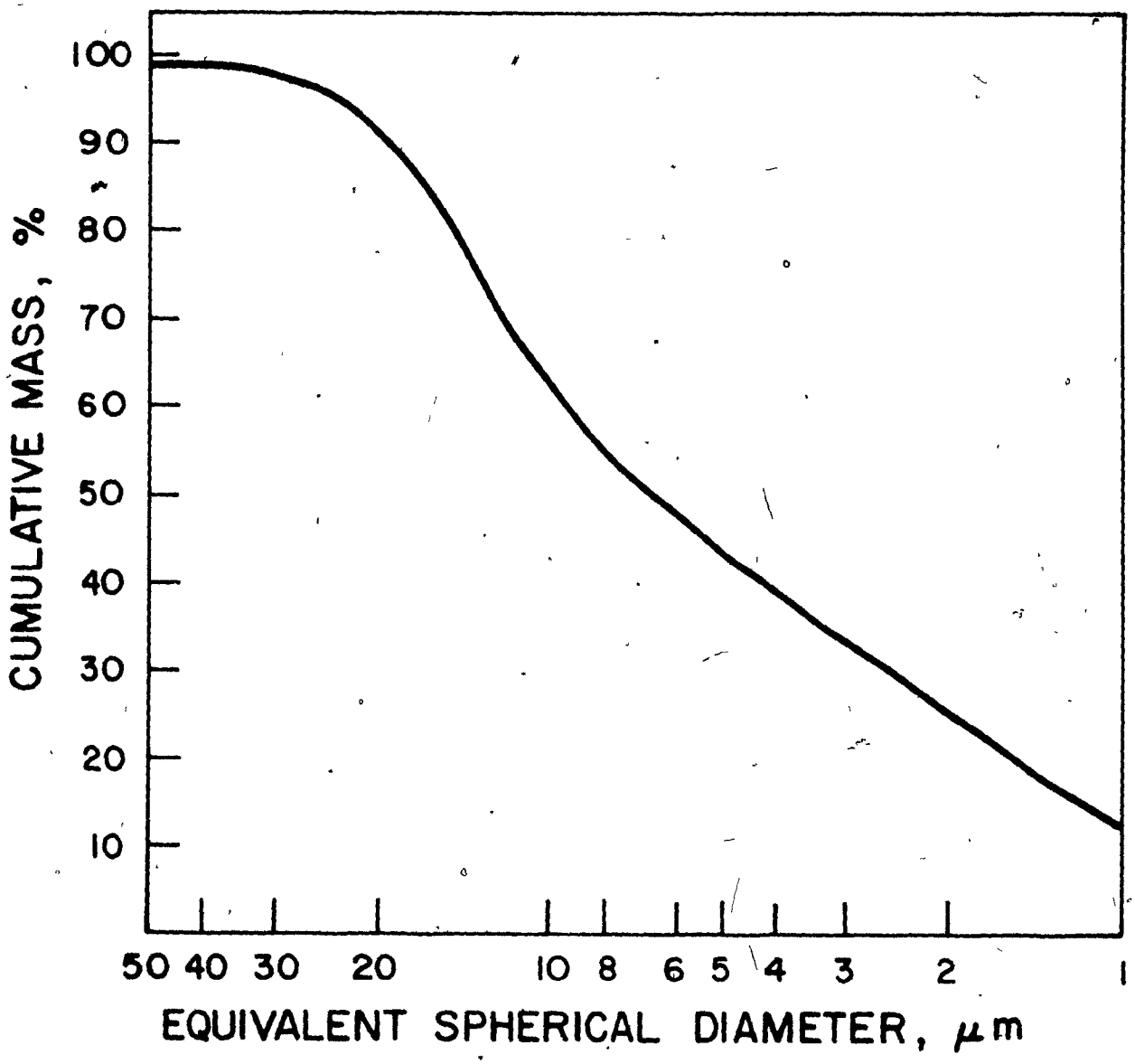
CUMULATIVE MASS, %
100
90
80
70
60
50
40
30
20
10
50 40 30 20 10 8 6 5 4 3 2 1
EQUIVALENT SPHERICAL DIAMETER, μm

of the powder mass was used to prepare the pellets. The zirconium dioxide powder did not possess any lubricant property, as for example in the case of molybdenite, and presented considerable frictional forces between adjacent particles and between particles and die surfaces. This made the ejection of compacted spheres from the die without breaking the pellet impossible. Following many unsuccessful trials, including the use of stearic acid as lubricant, a successful technique was developed when the hemispherical cavities were shortened from both sides of the equator by a total length of one third of the sphere diameter and the pieces containing the cavities were made separate from the cylindrical punches, as shown in Figure 13. This design resulted in a pellet of somewhat spherical shape having a disk portion around the equator. The pellet could be ejected easily if both the cavities and the die walls were polished with the stearic acid prior to the compaction process. Micrographs of two pellets are shown in Figure 14.

An attempt was made to form exact spherical shape and to obtain pellets of different diameter by tumbling in a cylinder lined with a very fine abrasive cloth, but this only led to breakage of the pellets.

The pellets were sintered in air atmosphere at 1400 K for four hours. Following the sintering process, a hole of 0.08 cm in diameter was drilled to mount the pellet on the particle supporting system.

FIGURE 13

SCHEMATIC DIAGRAM OF DIE COMPACTION SYSTEM

FOR A SPHERICAL PELLET

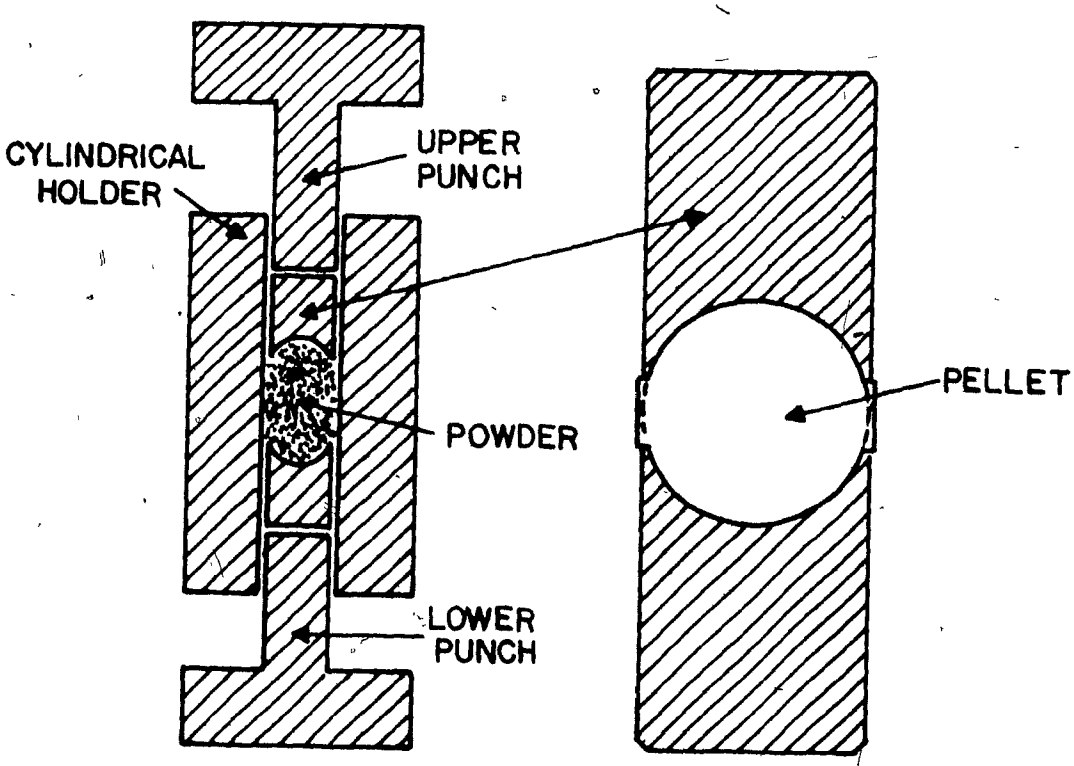
CYLINDRICAL
HOLDER
UPPER
PUNCH
POWDER
LOWER
PUNCH
PELLET

FIGURE 14

MICROGRAPHS (x 4) OF SINTERED UNREACTED PELLETS

a) DIAMETER - 0.826 cm

b) DIAMETER - 0.494 cm

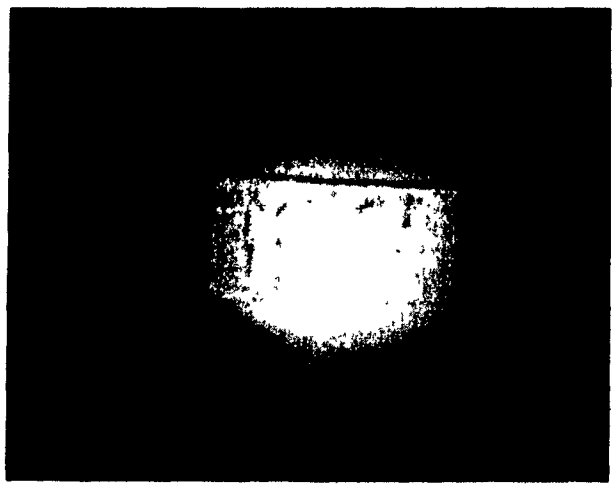

(a)

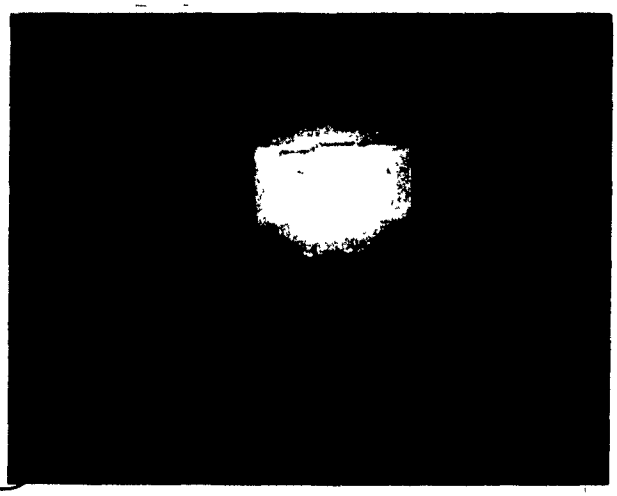

(b)

Pellets of three different void fractions with a diameter of 0.671 cm were produced by applying the appropriate pressure. The maximum density which could be produced in this way was 2.95 g/cm^3 which corresponded to a void fraction of 0.485. The minimum density was limited by the strength of the pellet and the lower limit of the press. The maximum porosity which could be obtained was 0.59. Pellet sizes ranged from a minimum of 0.494 cm to a maximum of 1.00 cm.

Measurement of Particle Temperature

Generally, thermocouples or optical pyrometry can be used to measure solid temperatures in the range between 1400 and 2500 K. In this work the latter was selected, since the measurements with the former were found impossible (Munz, 1974), (Sayegh, 1977) in the case of induction plasma systems where both the torch and the flame operated at a floating potential of several hundred volts. This is due to the fact that, when a gas having a fairly high electric potential comes in contact with a grounded object, a discharge between the object and the gas takes place. The higher the temperature of the gas, the easier it is to form a conductive path between the object and the high-potential region of the gas.

A high-resolution pyrometer (Pyro Micro-Optical Pyrometer, The Pyrometer Instrument Co., Inc., Northvale, N.J.) was used. The pyrometer was supplied with six interchangeable objective lenses that permitted measurements to be made at distances varying from 12 cm to infinity with object sizes as small as 0.01 cm. Temperatures in the range of 1000 - 3500 K could be measured.

Since the pyrometer ammeter readings are pre-calibrated with a standard light source to indicate the temperature of a black body that has the same brightness as that of the tungsten filament, and since radiance from real bodies and, consequently, their brightness temperature, are both lower than those from a black body, the value indicated by the pyrometer ammeter is less than the actual surface temperature of the object. Therefore, the ammeter readings should be corrected for the emissivity of the real object, in this case the zirconium dioxide pellet. The temperature correction for an optical pyrometer is given (Branstetter, 1966) as:

$$1/T - 1/T_b = (\lambda/1.438)\ \ell n\ e \qquad (94)$$

where, $\underline{e}$ is the spectral emissivity, $\underline{\lambda}$ is the wave length in angstroms x 10^{-8} (6500 x 10^{-8} for the present case), $\underline{T}$ and $\underline{T_b}$ are the black body and the brightness temperatures in degrees Kelvin, respectively.

The emissivity of solids depends to a large extent upon the roughness of the surface. Since the reacted pellets were compacted from zirconium dioxide powder, they had considerable surface roughness which changed during the sintering process and possibly during the reaction also. Therefore, a literature emissivity value would not represent the real situation. The actual emissivity values were measured by providing a blackbody hole on the reacting pellet. The results showed a dependence on the reaction temperature and, hence, on the speed of removal of zirconium dioxide as zirconium tetrachloride. A large number of blackbody experiments confirmed the trend shown in Figure 15.

This indicated that, during chlorination, the microscale surface roughness and, hence, the emissivity of the pellet, must change in a manner dependent upon the temperature. In a certain temperature range, the roughness was minimum and then increased slightly to a constant value which was no longer affected by the reaction rate. Such a behaviour introduced some degree of complexity in the evaluation of the temperature.

The temperatures of the reacting pellets were measured by focussing the pyrometer filament on the equator portion of the spheres. The brightness temperatures were then corrected by means of Equation (94) by using an appropriate emissivity value from Figure 15.

FIGURE 15

SPECTRAL EMISSIVITY OF REACTING

ZIRCONIUM DIOXIDE PELLET

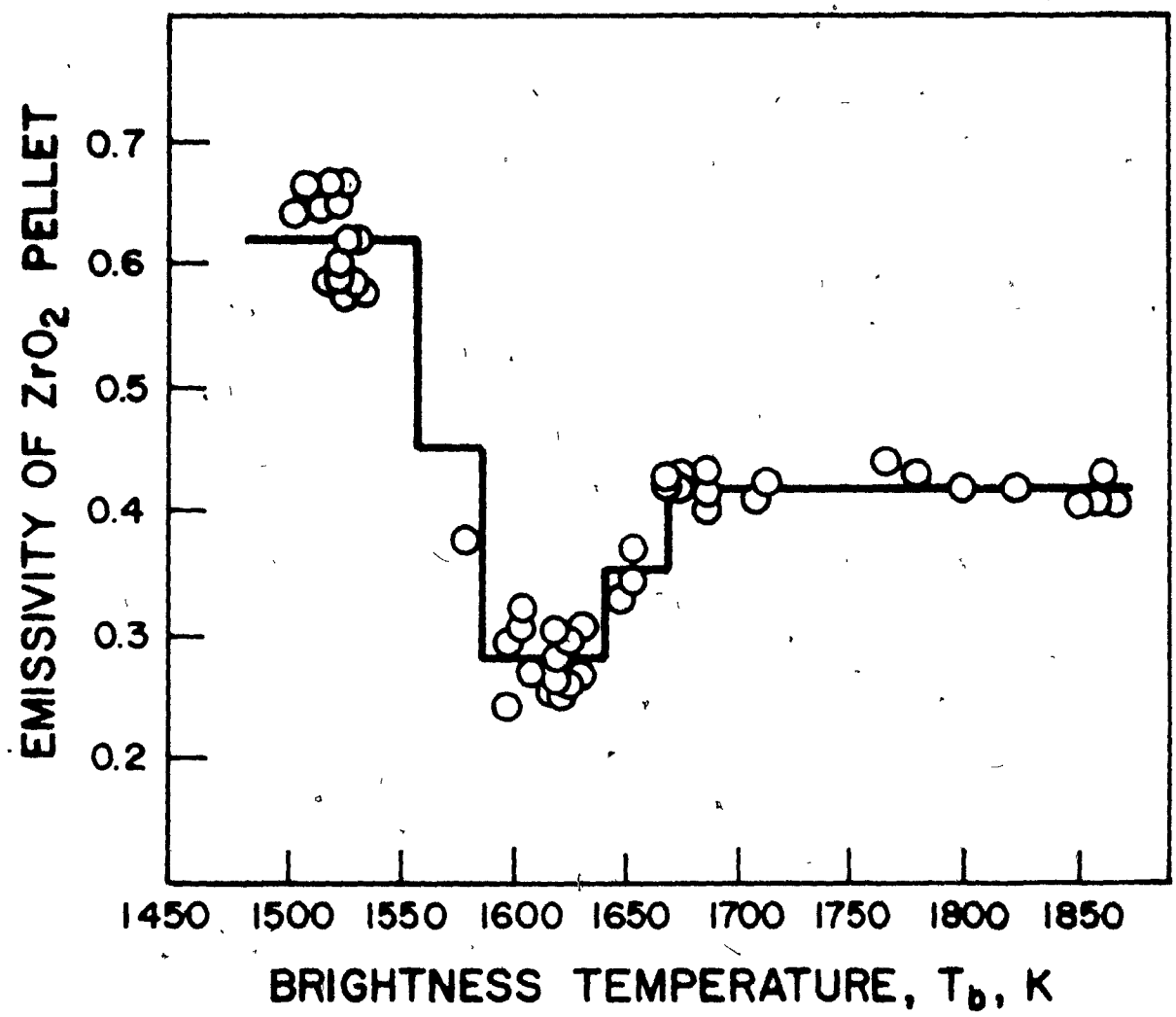
EMISSIVITY OF ZrO_2 PELLET
0.7
0.6
0.5
0.4
0.3
0.2
1450
1500
1550
1600
1650
1700
1750
1800
1850
BRIGHTNESS TEMPERATURE, T_b, K

Nozzle Exit Gas Temperature and Velocity

Predictions of temperature and velocity of the plasma gas at the position of a reacting pellet, as discussed in the Theoretical Analysis section, required a knowledge of the nozzle exit values. The reactor and the heat exchanger themselves could be used as a calorimeter to obtain the mean plasma enthalpy at the flow condition of the same kinetic experiment. Preliminary runs indicated that the cooling water outlet and the exhaust gas temperatures could reach a steady state condition in a very short time (about three minutes). Hence, operation of the system with argon for a few minutes and then taking the calorimetric data towards the end of the kinetic run with the chlorine plasma ensured that steady state conditions had been attained.

The inlet and outlet water temperatures were measured by bimetallic dial thermometers accurate to 0.25 K in the range 273 - 323 K. The gas exhaust temperature was measured with a similar type of thermometer accurate to 1.5 K in the range 273 - 523 K. Provisions were made in the design of the equipment for immersion of the thermometer stems of about 10 cm in the fluid, in order to meet their calibration. Water flow rate to the reactor system was metered, using precalibrated Brooks rotameters. For the purpose of computer calculations, an equation was developed for the enthalpy of molecular chlorine in the temperature range of 298 - 1000 K by curve fitting the tabular data of JANAF tables:

$$H_{Cl_2} = -2323.9 + 7.332\ T + 17.436 \times 10^{-4}\ T^2 - 636.27 \times 10^{-9}\ T^3 \qquad (95)$$

where, H_{Cl_2} is the enthalpy in cal/mole, and T is the temperature in degrees Kelvin. The mean plasma enthalpy at the nozzle exit was calculated by a simple heat balance, which also yielded the nozzle exit mean plasma temperature. Using the atomic chlorine density evaluated at this temperature, the mean plasma gas velocity at the nozzle exit could be calculated from the mass flow rate of the gas.

Amount of Reaction

The amount of reaction was measured by weight loss due to removal of zirconium tetrachloride as vapour. Pellets were weighed before and after the reaction on a Mettler H15 analytical balance which could give readings to within ±0.0001 gm. Several blank runs were carried out in argon plasma (hence, no reaction) to check losses to the pellets during handling, weighing, mounting the pellet on the supporting system and placing the 'pellet system' in and out of the reactor. The losses due to such processes were found to be negligible.

PROCEDURE

Before an experimental run, the sintered and drilled pellet was checked under a microscope for cracks and for its spheroidal shape. If the diameters measured along the two axes differed by more than three percent (which was set by the accuracy of press) of

the shortest diameter, the pellet was discarded.

Following weighing and mounting on the support, the pellet was placed in the lower cool portion of the reactor which was then closed and purged for several minutes to remove any residual oxygen. This was followed by start-up and operation of the torch with an argon plasma for about five minutes to ensure steady state conditions for the purpose of calorimetric data. Switching from pure argon to pure chlorine plasma was carried out by closing the swirl and the radial argon gas valves while opening those for the chlorine rotameters and at the same time adjusting the input power without extinguishing the plasma. Once operation of the torch with chlorine was adjusted to the appropriate conditions, the pellet supporting system was moved up to a predetermined reaction position and a stopwatch started. Visual observations and pyrometric measurements were made during the reaction. After a predetermined length of time, following the calorimetric measurements, the torch was turned off. Chlorine gas flow was stopped and the system was purged with cold argon to remove the remaining chlorine so that the reactor could be opened safely. Meanwhile, the partially-reacted pellet cooled down. This was followed by its final weight measurement, microscopic examination and micrographing.

The temperature of a reacting pellet in the chlorine plasma was controlled by its emissivity, its position below the torch nozzle and the power and gas flow rates of the plasma torch. For a given temperature, an attempt was made to keep all these

conditions constant. However, since the chlorine gas was withdrawn from a cylinder through evaporation of its liquid, the cylinder temperature and hence its pressure, changed during the reaction and also from one run to another. Furthermore, operation of the torch with chlorine, unlike that with argon, was very sensitive to the gas flow fluctuations especially at high powers which influenced the pellet temperature. These caused considerable experimental difficulties, mainly in designing experimental conditions. If a considerable temperature fluctuation occurred during a kinetic run (which happened in an appreciable number of experiments) the results of that run were ignored. In addition, since pure (non-stabilized) zirconium dioxide is less resistant to thermal shock, some pellets cracked and fell apart once the torch was extinguished. The experiments were designed to obtain conversion-time relationship as a function of the reaction temperature, the chlorine concentration and the porosity and the diameter of particle.

RESULTS AND DISCUSSION

Microscopic Examinations

Microscopic examinations of partially-reacted pellets revealed the presence of a thin fluffy layer at the surface. The thickness of this layer increased with an increase in pellet porosity and it decreased with an increase in reaction temperature. This may indicate that the reaction did not occur exactly on the geometrical surface, but was rather confined to the pore mouths

near the external surface, as had also been observed in the chlorinations of iron and nickel oxides with chlorine (Fruchan and Martonik, 1973). The core of a partially-reacted pellet beyond the fluffy layer was still hard and had almost the same density as that of an unreacted pellet, thus supporting a surface reaction model.

The majority of the partially-reacted pellets showed cracks which usually occurred at the base of the top and bottom spheroidal segments. These cracks were possibly caused by a large change in the volume (approximately 6 percent) of the zirconia during phase transformations as reported by Grain and Garvie (1965), Garvie (1970), and Neubauer and Romwalter (1977). The crystal structure of pure ZrO_2 is monoclinic under about 1423 K and then transforms over a 100 K temperature range to a tetragonal phase. The latter phase is stable up to about 2643 K, above which the zirconia adopts a cubic structure. A reverse transformation from the tetragonal to the stable monoclinic phase takes place, during cooling, over a temperature range of 450 K starting at about 1225 K.

The localization of the cracks, however, may be attributed to the characteristics of the zirconium dioxide powder which limited bulk movement and rearrangement of particles due to the frictional forces developed between neighbouring particles during the compaction process. The applied unidirectional force during compression may have induced different orientations of the particles in the spheroidal segments and in the disk portions, causing

a layer type of formations and weak spots in the pellet. Hence, the changes in the crystalline phases of ZrO_2 accompanied by the large volume change may have caused the pellets to crack at the localized weak points. Several pellets were treated in argon plasma at comparable temperatures for about ten minutes. Microscopic examinations of these blanks also showed the presence of similar type of cracks, although the pellets were denser and harder. This observation supports the reasoning above.

The cracks usually did not penetrate deep into the pellet volume, although they were more severe in the case of the less porous pellets. But at no time did they cause a pellet to react homogenously throughout its volume.

A comment should also be made regarding the shape of a partially-reacted pellet. The central disk of an unreacted pellet, as shown in Figure 14, disappeared after a certain amount of reaction, resulting in a nearly spherical appearance. The shape was not, however, entirely spherically-symmetrical, being reacted more at the upper surface of the reacting sphere where the temperature (and thus the reaction rate) was the highest.

Figures 16 and 17, which show micrographs (x 6.4) of typical partially-reacted pellets, illustrate the foregoing descriptions. The pellets (0.671-cm initial diameter) shown in Figure 16 were all reacted at 2210 K but to different conversions (Figure 16a to 51.2%, Figure 16b to 65.8% and Figure 16c to 82.6%).

FIGURE 16

MICROGRAPHS (X 6.4) OF PARTIALLY-REACTED

PELLETS OF THE SAME INITIAL DIAMETER

a) Conversion of 51.2% at 2210 K
b) Conversion of 65.8% at 2210 K
c) Conversion of 82.6% at 2210 K

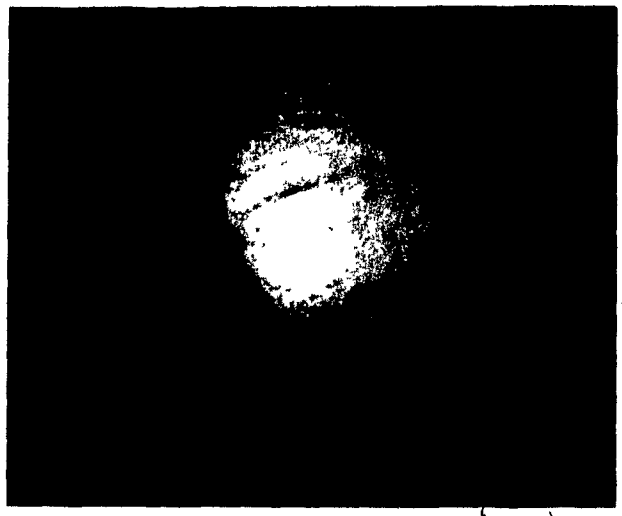

(a)

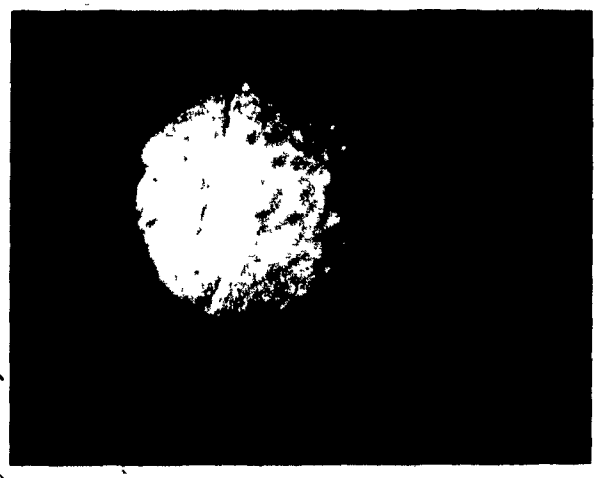

(b)

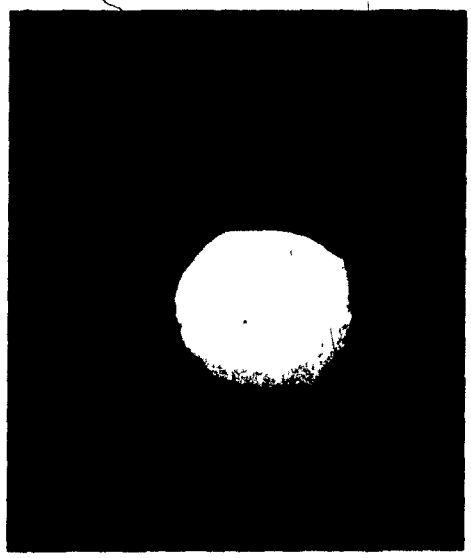

(c)

The pellets illustrated in Figure 17 had initially different diameters (Figure 17a - 1.00 cm, 17b - 0.826 cm, 17c - 0.494 cm), and were reacted at different temperatures (2175, 2015, 1885°K, respectively) to about the same conversion (50%, 56% and 54.9%, respectively).

Conversion-Time Relationship

Based on the microscopic examinations of partially-reacted pellets (which showed that the reaction was confined to the external surfaces) the conversion-time relationship can be expressed by the shrinking-core model of changing particle size. Thus, when the chlorination of zirconium dioxide is purely chemical reaction controlled, the overall consumption of ZrO_2 with time [as developed in the Theoretical Analysis part of this section, Equation (14)] can be written as

$$1 - (1 - X)^{1/3} = K\ t \qquad (96)$$

where, K is the phenomenological overall rate constant.

A number of pellets of equal diameter and porosity were reacted at a constant temperature for different lengths of time in order to check the fitness of Equation (96). The experimental results carried out at different temperature levels are given in Figures 18a and 18b for a pellet diameter of 0.671 cm and a void fraction of 0.481. It is seen that the plots of time versus $[1 - (1 - X)^{1/3}]$ yielded straight lines, in agreement with Equation

FIGURE 17

MICROGRAPHS (X 6.4) OF PARTIALLY-REACTED

PELLETS OF DIFFERENT INITIAL DIAMETERS

		a	b	c
Initial Diameter	(cm)	1.00	0.826	0.494
Temperature	(K)	2175	2015	1885
Conversion	(%)	50	56	54.9

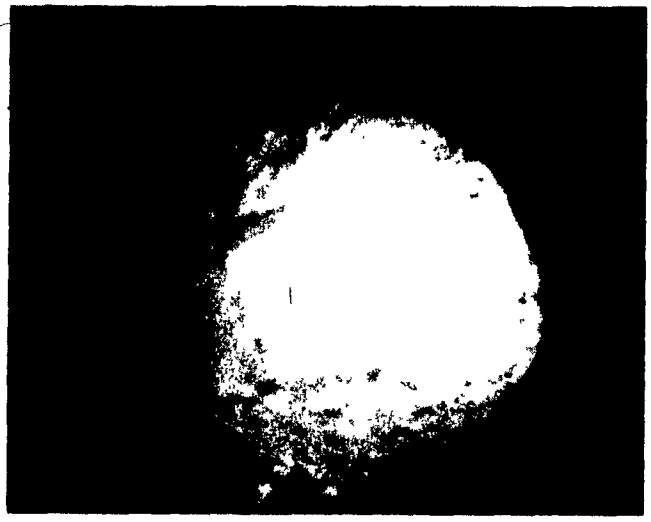

(a)

(b)

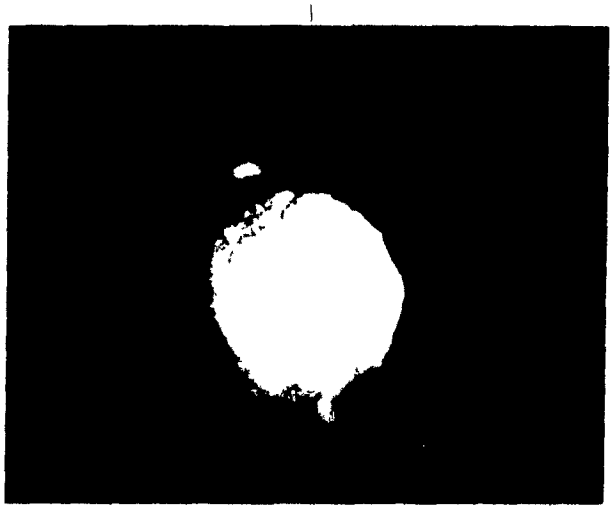

(c)

FIGURE 18a

CONVERSION VERSUS REACTION TIME

Void Fraction = 0.485
Pellet Diameter = 0.671 cm
Chlorine = 100 %

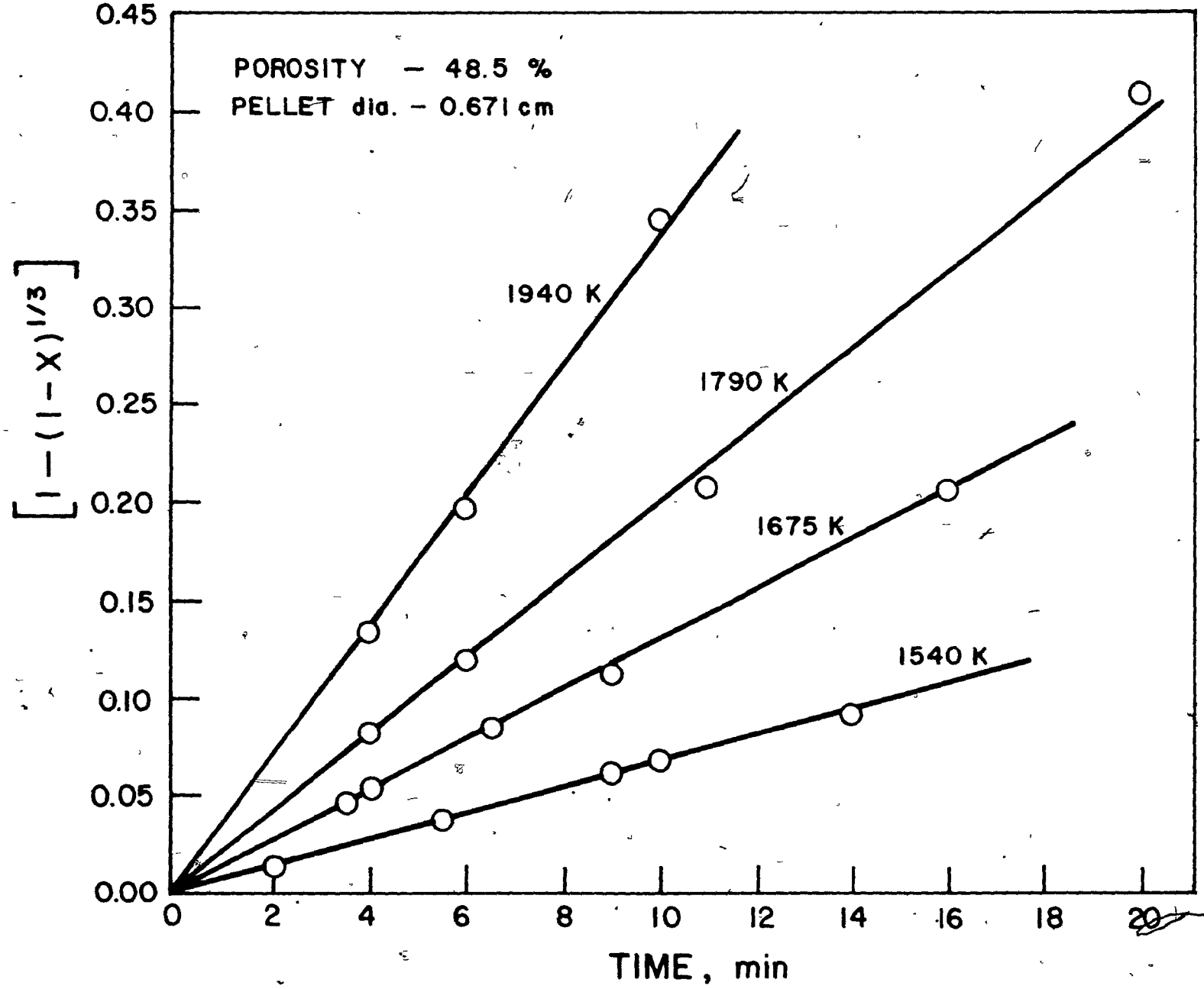
POROSITY — 48.5 %
PELLET dia. — 0.671 cm
1940 K
1790 K
1675 K
1540 K
$[1-(1-X)^{1/3}]$
0.45
0.40
0.35
0.30
0.25
0.20
0.15
0.10
0.05
0.00
0
2
4
6
8
10
12
14
16
18
20
TIME, min

FIGURE 18b

CONVERSION VERSUS REACTION TIME

Void Fraction = 0.485
Pellet Diameter = 0.671 cm
Chlorine = 100 %

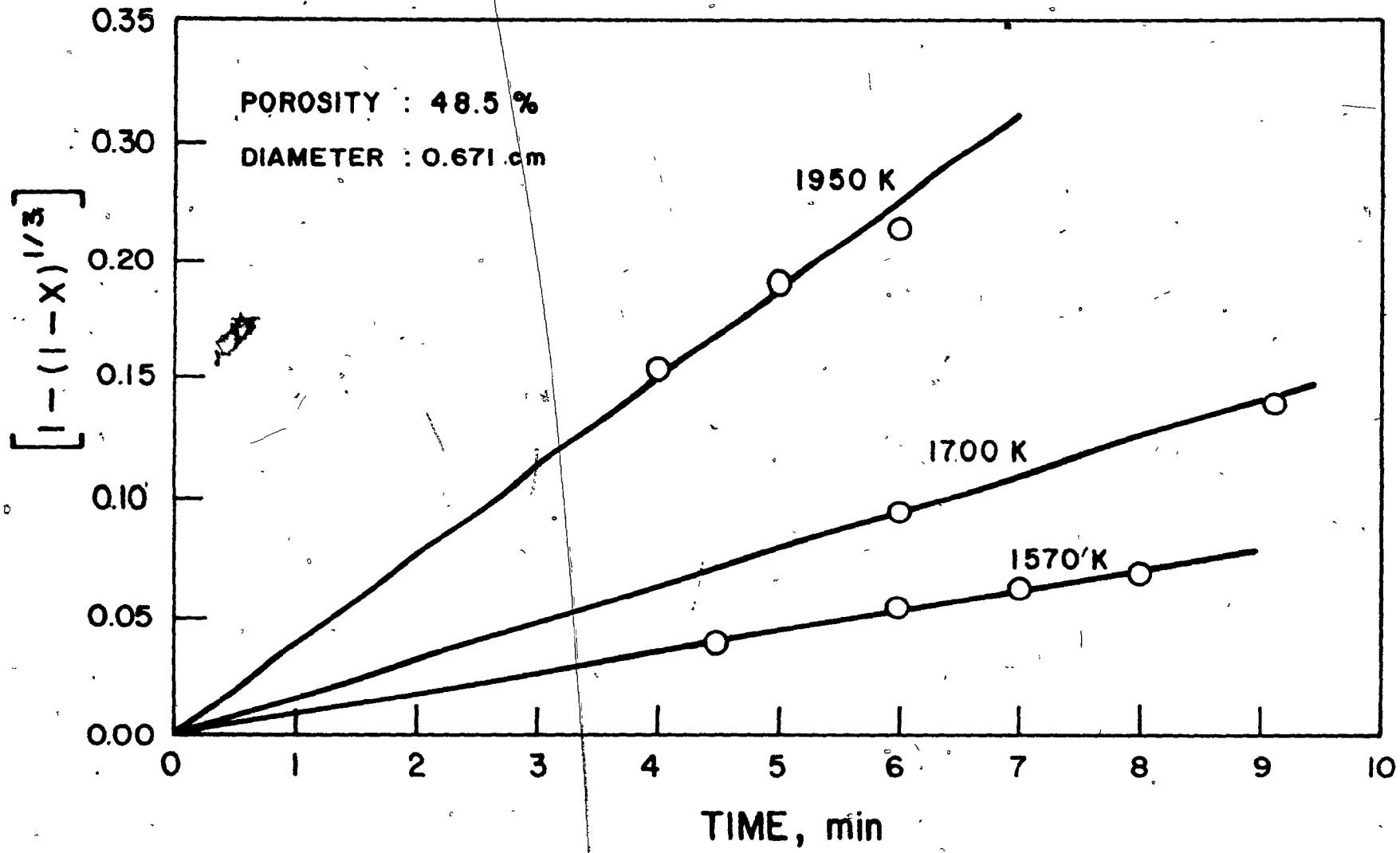
POROSITY : 48.5 %
DIAMETER : 0.671 cm
1950 K
1700 K
1570°K
$[1-(1-X)^{1/3}]$
0.35
0.30
0.20
0.15
0.10
0.05
0.00
0
1
2
3
4
5
6
7
8
9
10
TIME, min

(96). In order to confirm this straight-line relationship for the reaction of pellets of higher void fractions, similar experiments were carried out with pellets having porosities 54.9% and 59.0%. The results are given in Figures 19 and 20, respectively. In all cases the pellet diameter was 0.671 cm. The straight-line relationships obtained in the latter figures confirmed the results of microscopic examination to the effect that a higher void fraction did not cause a pellet to react uniformly throughout the pellet volume in the porosity range reported here. Hence Equation (96) was used in the calculation of overall rate constant (K) from the experimental conversion-time data in analyzing other reaction parameters (temperature, porosity, diameter and chlorine concentration). The complete experimental data are given in Appendix II.

Influence of Temperature

The effect of temperature on the reaction rate was studied in the range between 1540 and 2480 K. The upper temperature was limited by the maximum power to the torch, by the arcing that took place between the plasma and the torch nozzle, and also by the excessive heating of the nozzle with consequent attack by the hot chlorine. The lower temperature, on the other hand, was that at which the chlorine plasma could be maintained at a given gas flow rate with a minimum power input, for a maximum distance from the nozzle exit (about 6 cm) at which a pellet could be viewed.

The stability and reproducibility problem encountered with

FIGURE 19

CONVERSION VERSUS REACTION TIME

Void Fraction = 0.549
Pellet Diameter = 0.671 cm
Chlorine = 100 %

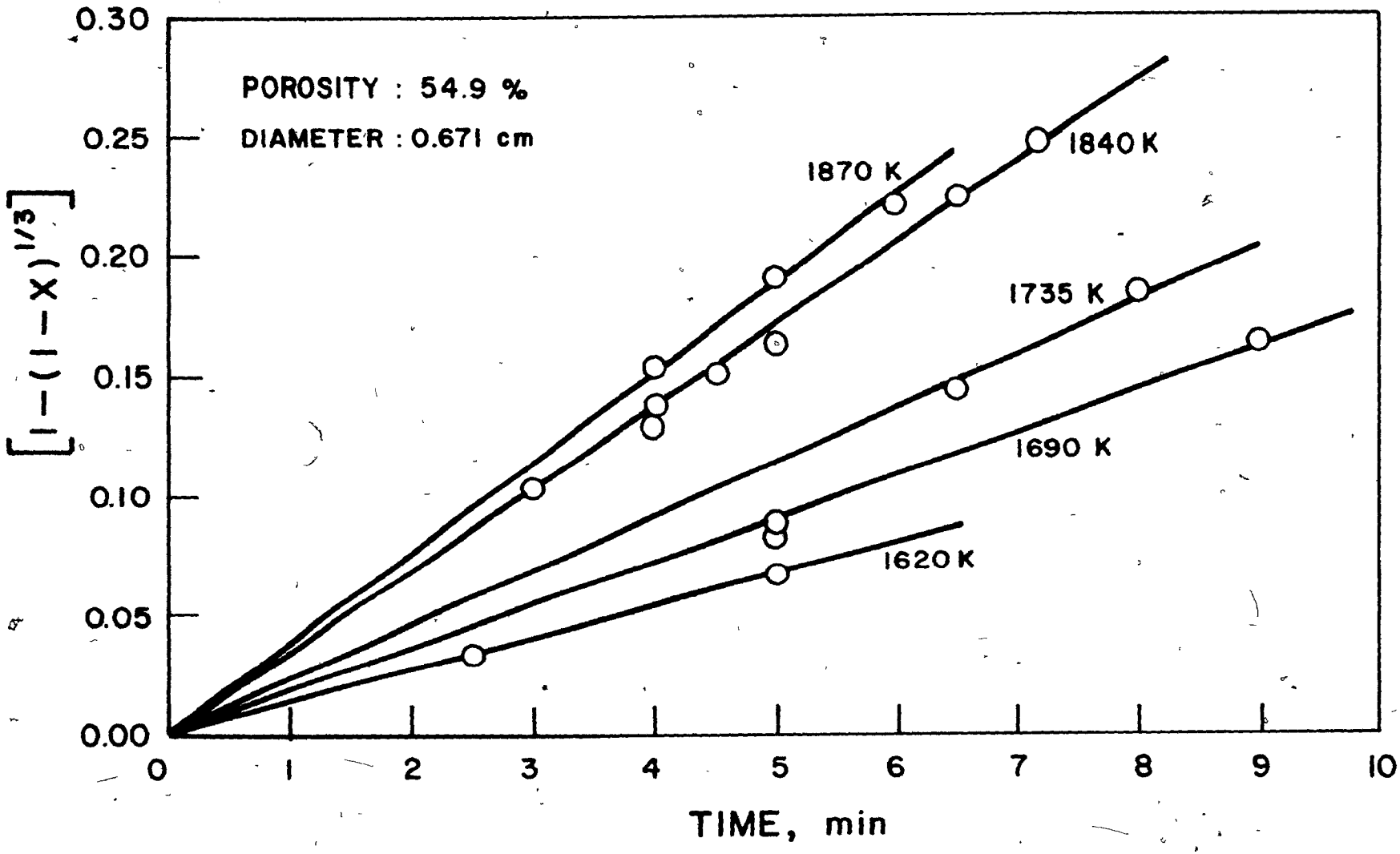
POROSITY : 54.9 %
DIAMETER : 0.671 cm
1870 K
1840 K
1735 K
1690 K
1620 K
$[1-(1-X)^{1/3}]$
0.30
0.25
0.20
0.15
0.10
0.05
0.00
0
1
2
3
4
5
6
7
8
9
10
TIME, min

FIGURE 20

CONVERSION VERSUS REACTION TIME

Void Fraction = 0.590

Pellet Diameter = 0.671 cm

Chlorine = 100 %

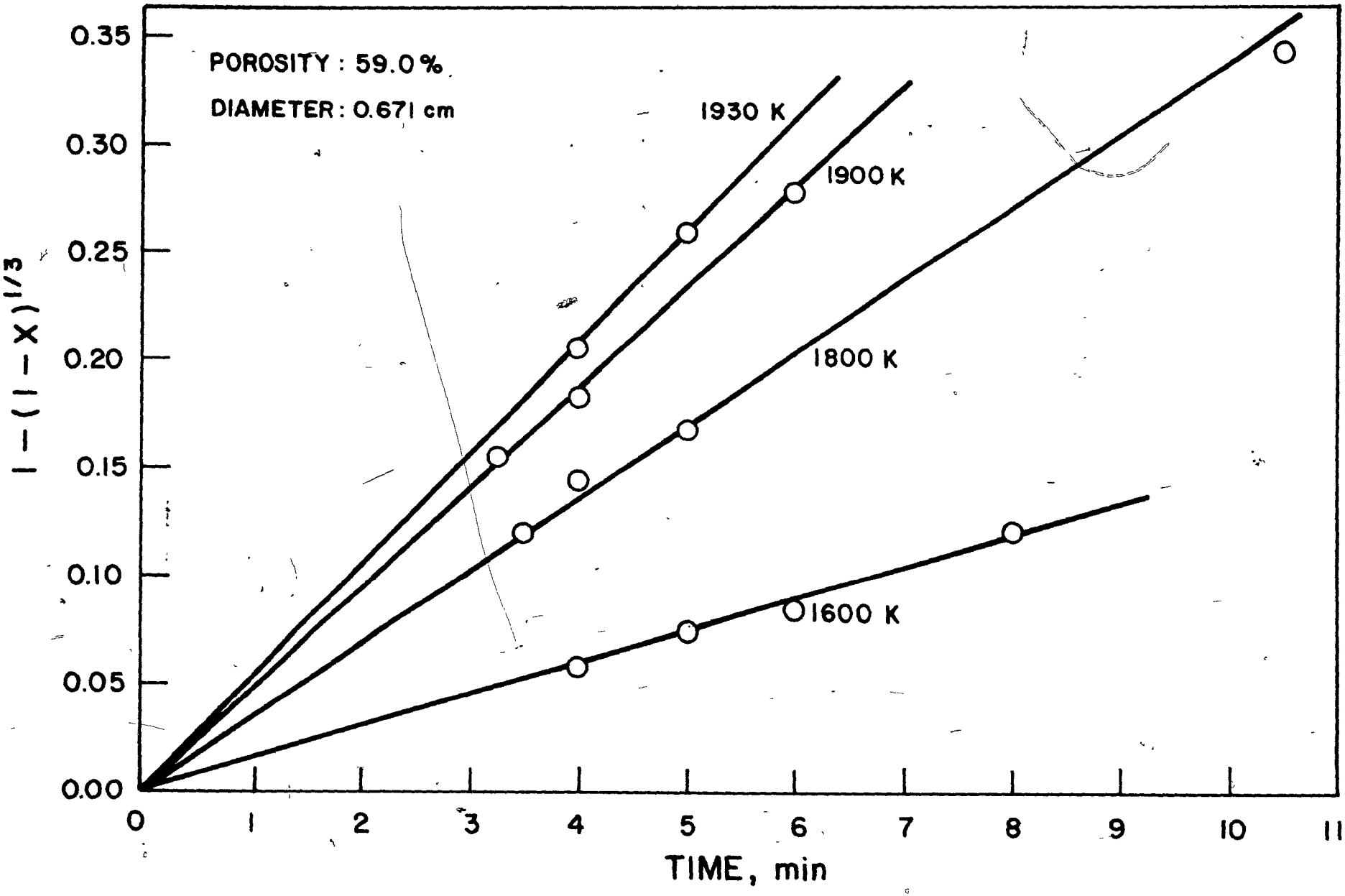
POROSITY : 59.0 %
DIAMETER : 0.671 cm
1930 K
1900 K
1800 K
1600 K
0.35
0.30
0.25
0.20
0.15
0.10
0.05
0.00
1 − (1 − X)^1/3
0
1
2
3
4
5
6
7
8
9
10
11
TIME, min

the generation of the chlorine plasma did not allow the experiments to be carried out systematically at originally-planned temperature intervals. As a result, the choice of temperature levels was dictated by the plasma behaviour, since the torch operated with chlorine very smoothly only in a certain range of operating conditions (relatively narrower than those with argon) for a given gas flow rate.

When more than one set of conversion-time data at a constant temperature was available (under reproducible plasma conditions), the overall rate constants were obtained from the slopes of straight lines, $[1 - (1 - X)^{1/3}]$ versus t, (Figures 18-20) by least-squares fit. The results of these analyses are given in Table VIII. These values together with the rest of the data (based on 123 experiments) were plotted according to an Arrhenius-type of relationship in Figures 21, 22 and 23 for pellets of three different void fractions, 0.485, 0.549 and 0.590, respectively. The experimental data for each case are presented in Tables A, B and C of Appendix II. In these experiments, the pellet diameter was 0.671 cm.

The plots in Figures 21-23 showed the existence of two distinct temperature regions. Up to about 1950 K (the straight line portion), the reaction rate was sensitive to temperature, thus suggesting a chemical reaction control region. At temperatures higher than this, the rate was relatively insensitive to the temperature rise showing that a physical step (gas-film diffusion)

TABLE VIII

OVERALL RATE CONSTANT FROM THE

SLOPE OF $[1 - (1 - X)^{1/3}]$ VERSUS t

POROSITY %	T K	NUMBER OF DATA POINTS	OVERALL RATE CONSTANT (K) ($minute^{-1}$)
48.5	1540	5	0.0065
48.5	1570	4	0.0083
48.5	1675	5	0.0127
48.5	1700	3	0.0155
48.5	1790	4	0.0201
48.5	1880	2	0.0295
48.5	1940	3	0.0339
48.5	1950	3	0.0376
54.9	1620	2	0.0134
54.9	1685	3	0.0180
54.9	1735	2	0.0228
54.9	1800	2	0.0292
54.9	1835	7	0.0341
54.9	1875	3	0.0375
59.0	1600	4	0.0146
59.0	1800	4	0.0337
59.0	1830	2	0.0385
59.0	1900	3	0.0464
59.0	1930	2	0.0514

FIGURE 21

ARRHENIUS PLOT OF REACTION BETWEEN

ZIRCONIUM DIOXIDE AND CHLORINE

Pellet Porosity = 48.5 %

Pellet Diameter = 0.671 cm

Chlorine = 100 %

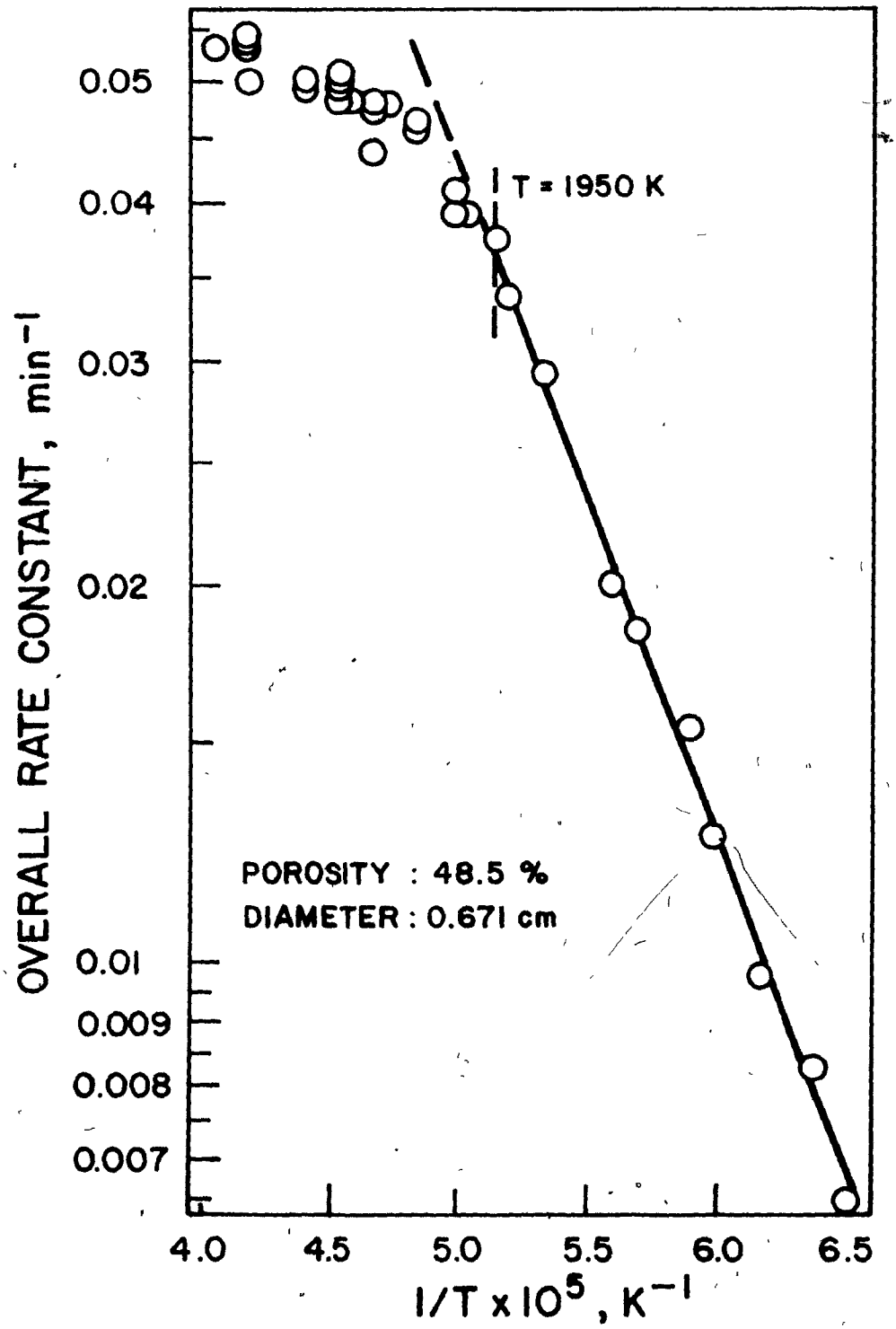
0.05
0.04
0.03
0.02
0.01
0.009
0.008
0.007
OVERALL RATE CONSTANT, min⁻¹
T = 1950 K
POROSITY : 48.5 %
DIAMETER : 0.671 cm
4.0
4.5
5.0
5.5
6.0
6.5
1/T x 10⁵, K⁻¹

FIGURE 22

ARRHENIUS PLOT OF REACTION BETWEEN

ZIRCONIUM DIOXIDE AND CHLORINE

Pellet Porosity = 54.9 %

Pellet Diameter = 0.671 cm

Chlorine = 100 %

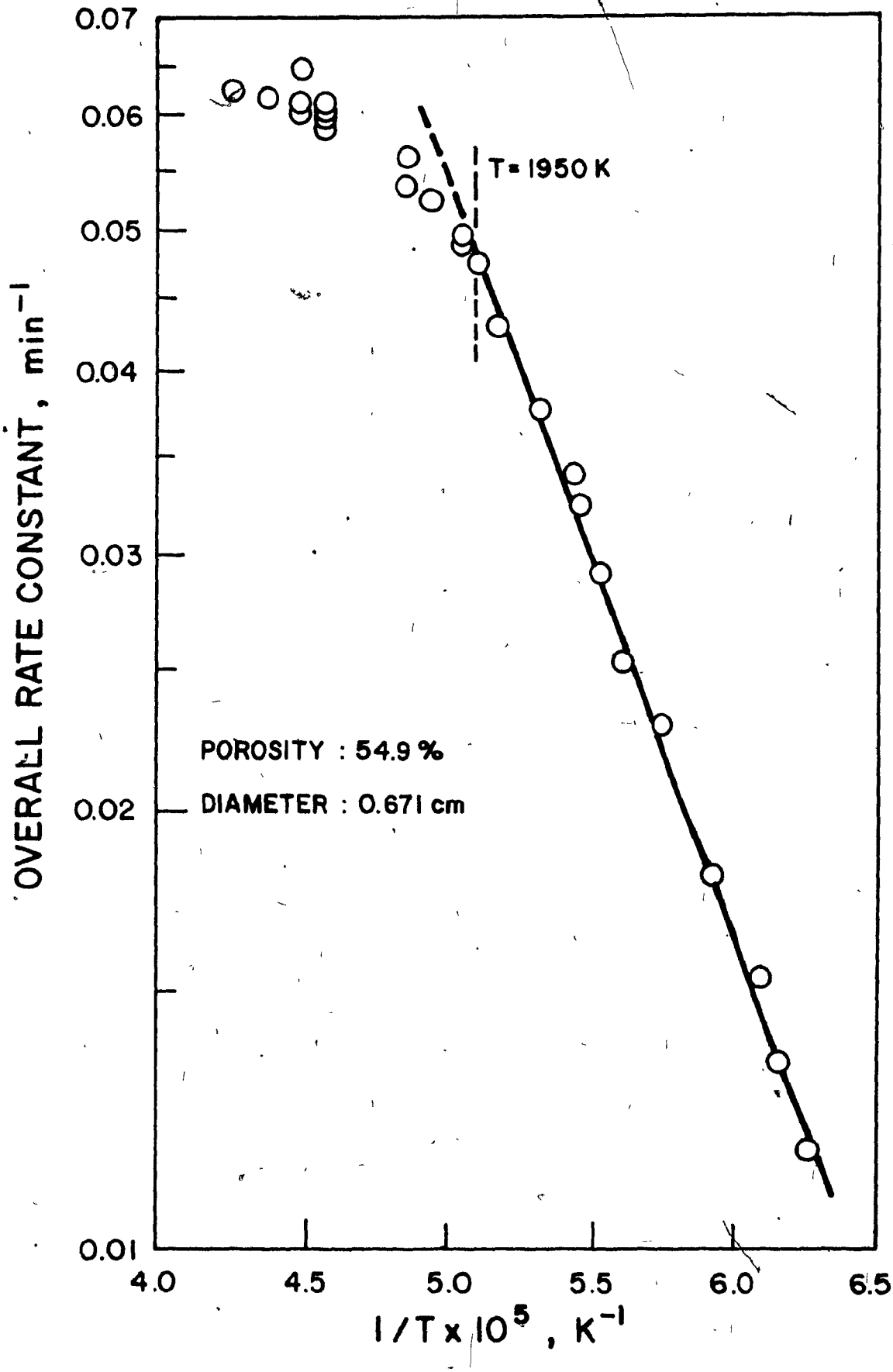
0.07
0.06
0.05
0.04
0.03
0.02
0.01
OVERALL RATE CONSTANT, min⁻¹
T = 1950 K
POROSITY : 54.9 %
DIAMETER : 0.671 cm
4.0
4.5
5.0
5.5
6.0
6.5
1/T x 10⁵ , K⁻¹

FIGURE 23

ARRHENIUS PLOT OF REACTION BETWEEN

ZIRCONIUM DIOXIDE AND CHLORINE

Pellet Porosity = 59.0 %

Pellet Diameter = 0.671 cm

Chlorine = 100 %

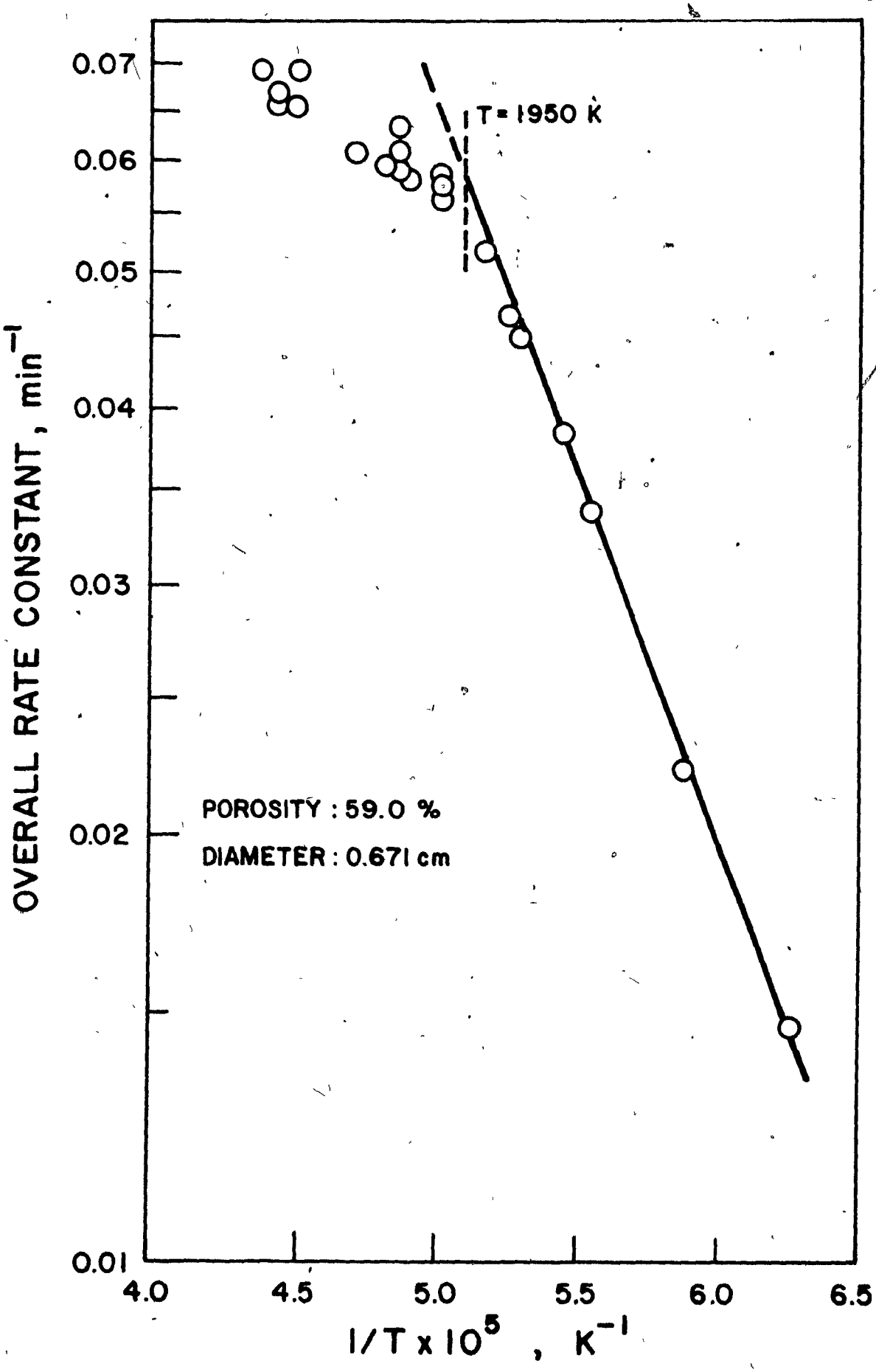
0.07
0.06
0.05
0.04
0.03
0.02
0.01
OVERALL RATE CONSTANT, min^{-1}
T = 1950 K
POROSITY : 59.0 %
DIAMETER : 0.671 cm
4.0
4.5
5.0
5.5
6.0
6.5
1/T x 10^5 , K^{-1}

started to influence the rate. The temperature at which both mass transfer and chemical reaction started to have a combined effect on the rate was almost the same with the three different pellet void fractions, as was expected. The data of these figures below about 1950 K were then used in a multiple regression analysis using a statistical package program (STATPK, McGill University Computing Centre) in order to obtain the value of the activation energy together with the porosity dependence which will be discussed subsequently. The least squares fit gave the following expression:

$$\ln K = 1.603 - (12162 \pm 176)/T - (1.993 \pm 0.081) \ln (1 - \varepsilon) \qquad (97)$$

with a multiple correlation coefficient of 0.998 and with a probability associated with 'F' being unity, (indicating that the excellent fit was not due to chance). From Equation (97), the regression analysis yielded an activation energy of 101.183 ± 1.465 kJ/mole (24.166 ± 0.350 kcal/mole). The partial correlation coefficient of activation energy was 0.997.

The overall rate constants (K) of the data at temperatures above 1950 K in Figures 21-23 were also based on chemical reaction control (Equation 96) in order to obtain the turning point with respect to temperature. The results of a more correct treatment of the data in this region will be presented later, by considering both mass transfer and reaction resistances together.

Influence of Pellet Porosity

The limited compactibility of zirconium dioxide powder did not allow a wide range of void fractions. The smallest porosity (48.5%) did not change much by increasing the applied die pressure, while with the lowest pressure (one-seventh of that of the smallest porosity) that could be used a maximum porosity of 59.0% was obtained. Therefore, only three different porosity values could be studied. However, a large number of experiments were carried out at each value, so that the porosity dependance of the overall rate constant could be evaluated with a relatively high degree of confidence. The experimental data are plotted in Figure 24, where each point represents the cumulative data (including their extent of scatter) at the corresponding solid volume fraction. The straight line in the same figure is the result of a regression analysis as given by Equation (97), which yielded the value of the exponent of the solid volume fraction, $(1 - \varepsilon)$, as about -2 (-1.993 ± 0.81 with a partial correlation coefficient of 0.979). Hence:

$$K \alpha (1 - \varepsilon)^{-2} \qquad (98)$$

On the other hand, the conversion-time relationship based on the shrinking-core model [as derived in the Theoretical Analysis section, Equation (14)] indicated that the overall rate constant, $\underline{K}$, [Equation (96)] was inversely proportional to the porous solid density, $\underline{\rho_s}$:

FIGURE 24

EFFECT OF POROSITY ON OVERALL RATE CONSTANT

Pellet Diameter = 0.671 cm
Chlorine = 100 %

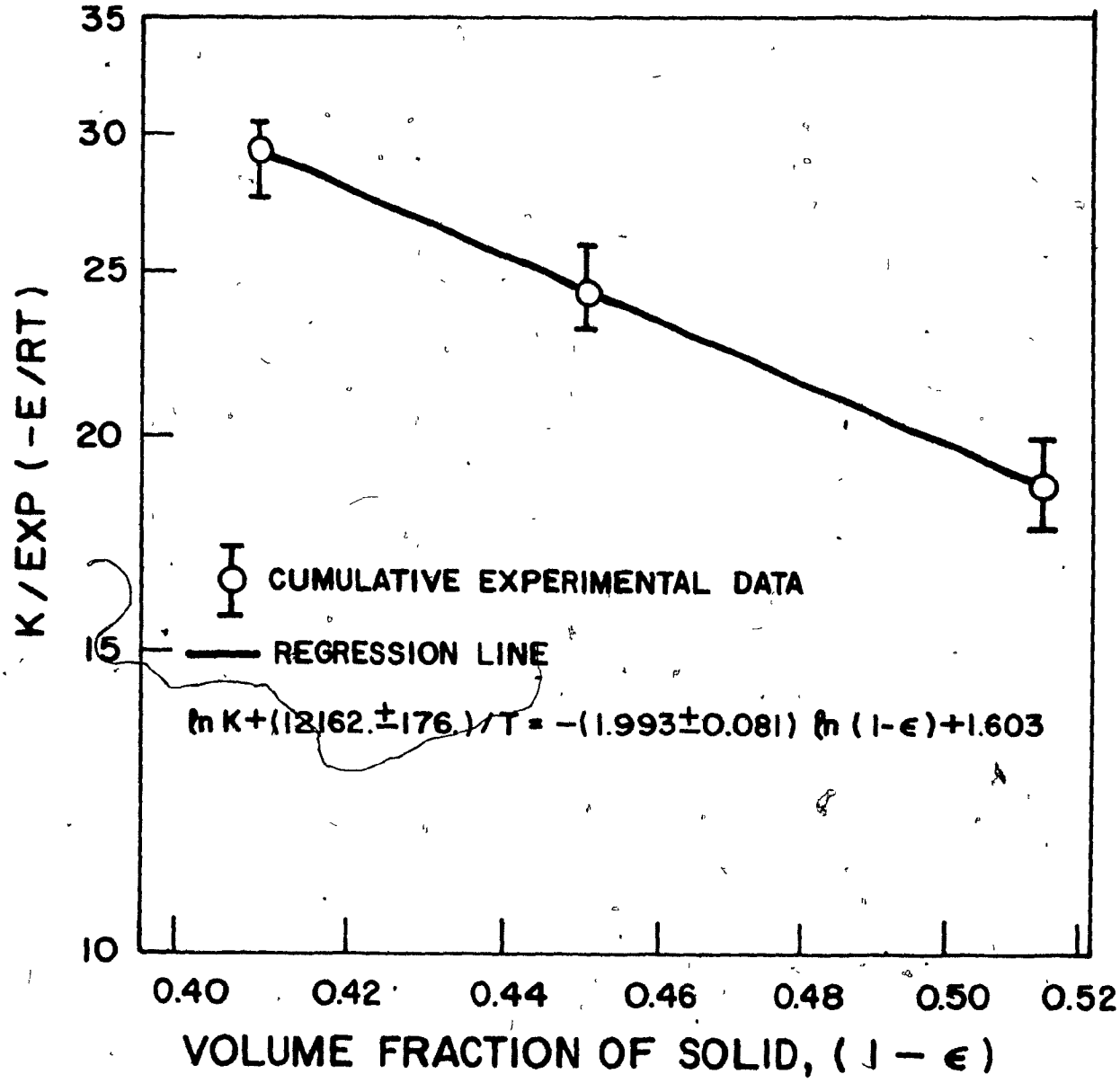
35
30
25
20
15
10
K / EXP (-E/RT)
CUMULATIVE EXPERIMENTAL DATA
REGRESSION LINE
ln K+(12162.±176.)/T = -(1.993±0.081) ln (1-ε)+1.603
0.40
0.42
0.44
0.46
0.48
0.50
0.52
VOLUME FRACTION OF SOLID, (1 − ε)

$$K \alpha 1/\rho_s \tag{99}$$

but:

$$\rho_s = \rho_t (1 - \varepsilon) \tag{100}$$

and, hence:

$$K \alpha (1 - \varepsilon)^{-1} \tag{101}$$

where, ρ_t is the theoretical density of the solid, and ε is the void fraction. Therefore, the overall rate constant was expected to be inversely proportional to $(1 - \varepsilon)$ if the assumption that a shrinking-core model could be used was truly met in the reaction of a zirconium dioxide pellet.

This contradictory conclusion, compared with the experimental result of Equation (98), may be explained by the fact that the reaction between a zirconium dioxide pellet and chlorine is not taking place truly on the geometrical surface area, but in a very thin layer on the exterior of the pellet, as observed from the microscopic examination of a partially-reacted pellet. Therefore, depending upon the void fraction of a pellet (probably also on the pore size and structure) the thickness of this layer and, consequently, the actual reacting area, changed in such a way as to result in a higher overall rate constant than could be accounted for by the simple dependence on the solid density, as given in Equations (99-101). It should be mentioned that Fruehan and Martonik (1973) in the chlorination of iron and nickel oxides, and

also Costa and Smith (1971) in the hydrofluorination of uranium dioxide, reported similar behaviour, but with a higher porosity dependence than in the present case. It should also be pointed out that the value of the activation energy did not change with the void fraction in the range studied here, indicating, therefore, that it should be representing an intrinsic activation energy. In this respect, Fahim and Ford (1976), in the reduction of cobalt sulphide in nonporous powder and porous pellet forms, also found the same activation energy for both cases, although in the latter a diffuse reaction front was observed and consequently a higher rate constant was obtained.

Influence of Pellet Diameter

All of the previous results were based on a pellet diameter of 0.671 cm. To evaluate the influence of the diameter on the overall rate constant, three other diameters were studied, giving a range diameter from 0.494 to 1.00 cm. The void fractions of these pellets varied to some extent depending upon the size. But, since the influence of porosity on the rate constant had already been determined, it was felt that such a restriction (truly constant porosity) was not necessary. A summary of the diameters and their corresponding porosities is given in Table IX and the experimental data are presented in Table D of Appendix II. These experiments were not carried out at a constant temperature (due to experimental difficulties), hence, the data of the chemical reaction controlled region (T<1950 K) were corrected for temperature (using the exper-

TABLE IX

SUMMARY OF PELLET DIAMETER AND POROSITY

DIAMETER cm	POROSITY %
0.494	50.5
0.671	48.5
0.671	54.9
0.671	59.0
0.826	50.0
1.000	49.8

imental value of the activation energy) and for porosity effects [using the form $(1 - \varepsilon)^{-2}$]. The results are shown in Figure 25. A multiple regression analysis, involving both the diameter and the chlorine concentration as independent variables, was carried out using the STATPK package program. The least square fit of the data gave:

$$\ln K + 12162.3/T + 2 \ln (1 - \varepsilon) = 1.198 - (1.047 \pm 0.041) \ln D + (0.992 \pm 0.011) \ln y_{Cl_2} \quad (102)$$

with a multiple correlation coefficient of 0.996 (partial correlation coefficients of 0.944 and 0.996, respectively), and the probability associated with 'F' being unity.

As seen in Figure 25 and Equation (102), the overall rate constant is found to be about inversely proportional to the diameter, which is in agreement with the theoretical result given in Equation (14). This finding confirms the fact that the rate was controlled by chemical reaction (otherwise the exponent would be between 1.5 and 2.0).

Influence of Chlorine Concentration

The experiments to determine the effect of chlorine partial pressure on the overall rate constants were performed with pellets of two different porosities (48.5% and 54.9%) and the same diameter (0.671 cm). Chlorine gas was diluted with argon in both the radial and the swirl flows of the torch in the same proportion to ensure a uniform mixing. A value lower than 20% chlorine could not be tried,

FIGURE 25

EFFECT OF PELLET DIAMETER ON

OVERALL RATE CONSTANT

Chlorine = 100%

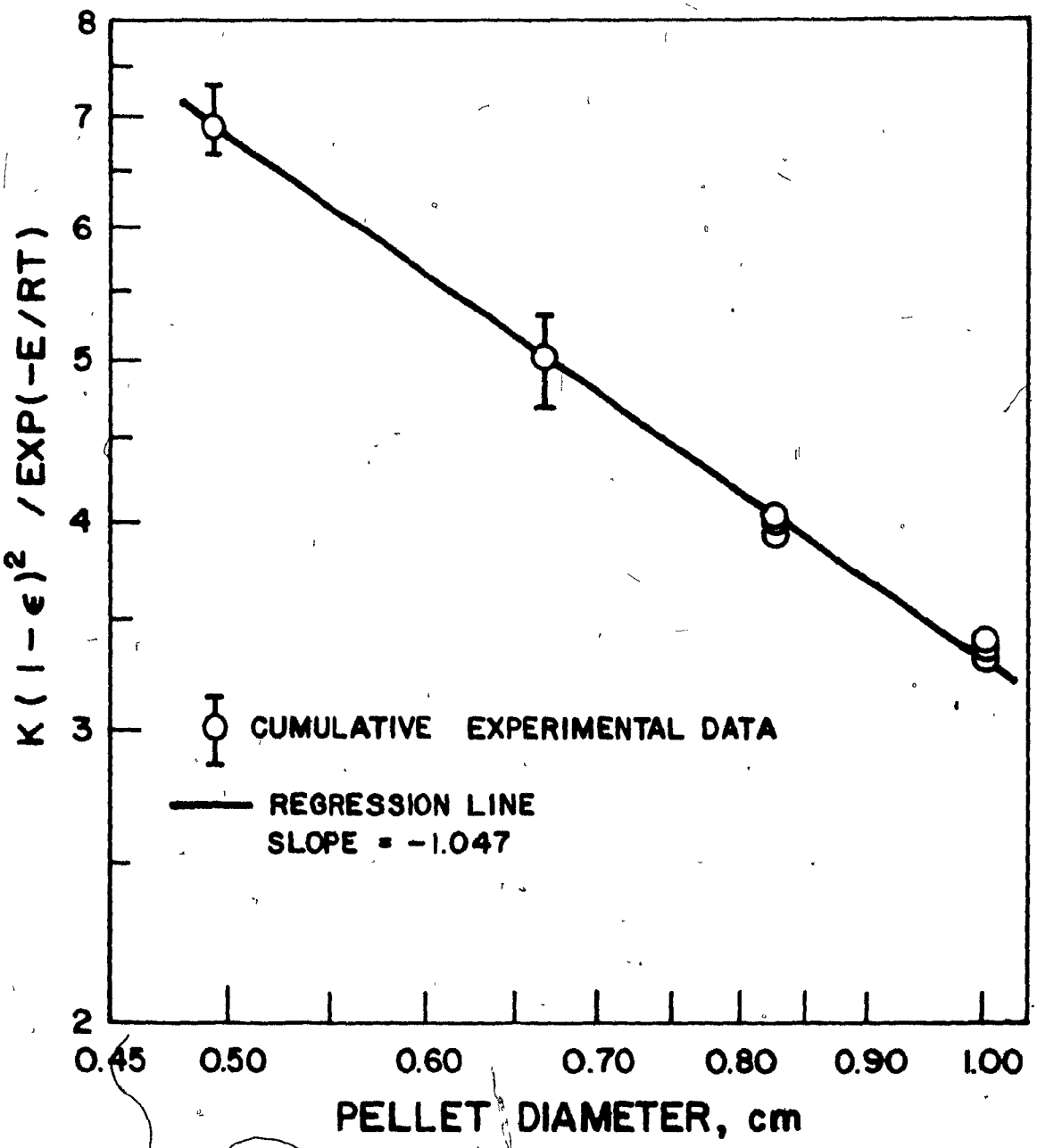
8
7
6
5
4
3
2
K (1 − ε)² / EXP(−E/RT)
CUMULATIVE EXPERIMENTAL DATA
REGRESSION LINE
SLOPE = −1.047
0.45
0.50
0.60
0.70
0.80
0.90
1.00
PELLET DIAMETER, cm

due to measurement difficulties. An attempt was made to react the pellets at the same temperature, but this required a considerable trial - and - error approach in finding the appropriate power input and pellet position at different concentration levels. Although this was achieved in some cases, the overall temperature varied from run to run, hence, the analysis was done by correcting the overall rate constant for the temperature by using the value of activation energy reported earlier. The experimental data are presented in Table E of Appendix II and in their corrected form in Figures 26 and 27.

The regression analysis of the data as given by Equation (102) resulted in an exponent of about one (0.992 ± 0.011) for the mole fraction of molecular chlorine, y_{Cl_2}. This shows that the reaction is first order with respect to chlorine when the concentration is expressed in terms of Cl_2. However, the thermodynamic analysis presented earlier indicated that chlorine should be present in the bulk gas in the atomic form, especially when the experimental conditions result in mass transfer effects (T>1950 K). Another regression analysis was therefore performed, this time based on the concentration expressed in terms of atomic chlorine, y_{Cl}. This yielded an exponent of about 1.53. But it can be shown that y_{Cl_2} and y_{Cl} are related by:

$$y_{Cl_2} = y_{Cl}/(2 - y_{Cl}) \tag{103}$$

A chlorine concentration dependence in terms of y_{Cl} as

FIGURE 26

EFFECT OF CHLORINE CONCENTRATION

Pellet Porosity = 48.5 %

Pellet Diameter = 0.671 cm

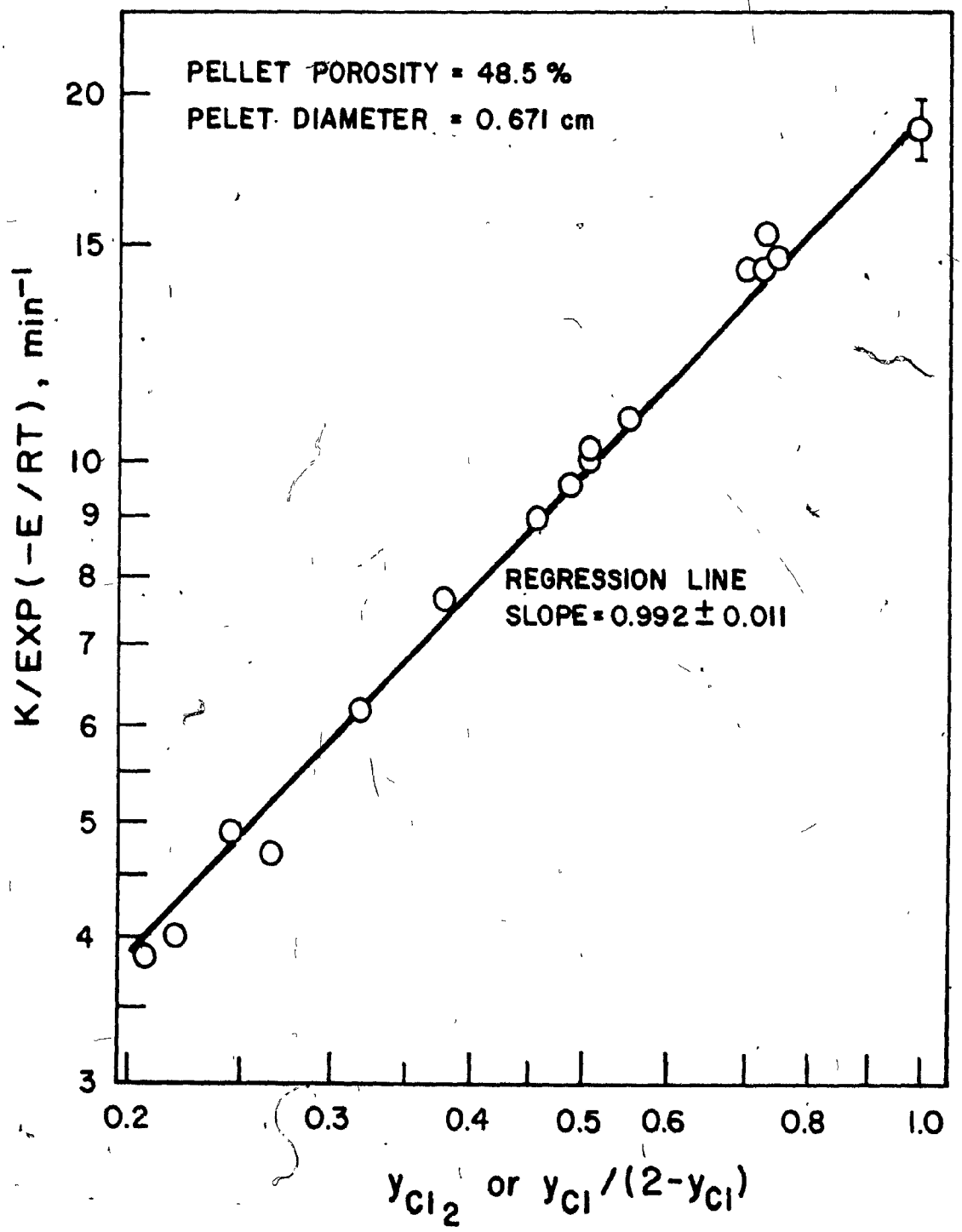
PELLET POROSITY = 48.5 %
PELET DIAMETER = 0.671 cm
REGRESSION LINE
SLOPE = 0.992 ± 0.011
K/EXP(-E/RT), min⁻¹
20
15
10
9
8
7
6
5
4
3
0.2
0.3
0.4
0.5
0.6
0.8
1.0
y_Cl2 or y_Cl/(2-y_Cl)

FIGURE 27

EFFECT OF CHLORINE CONCENTRATION

Pellet Porosity = 54.9 %

Pellet Diameter = 0.671 cm

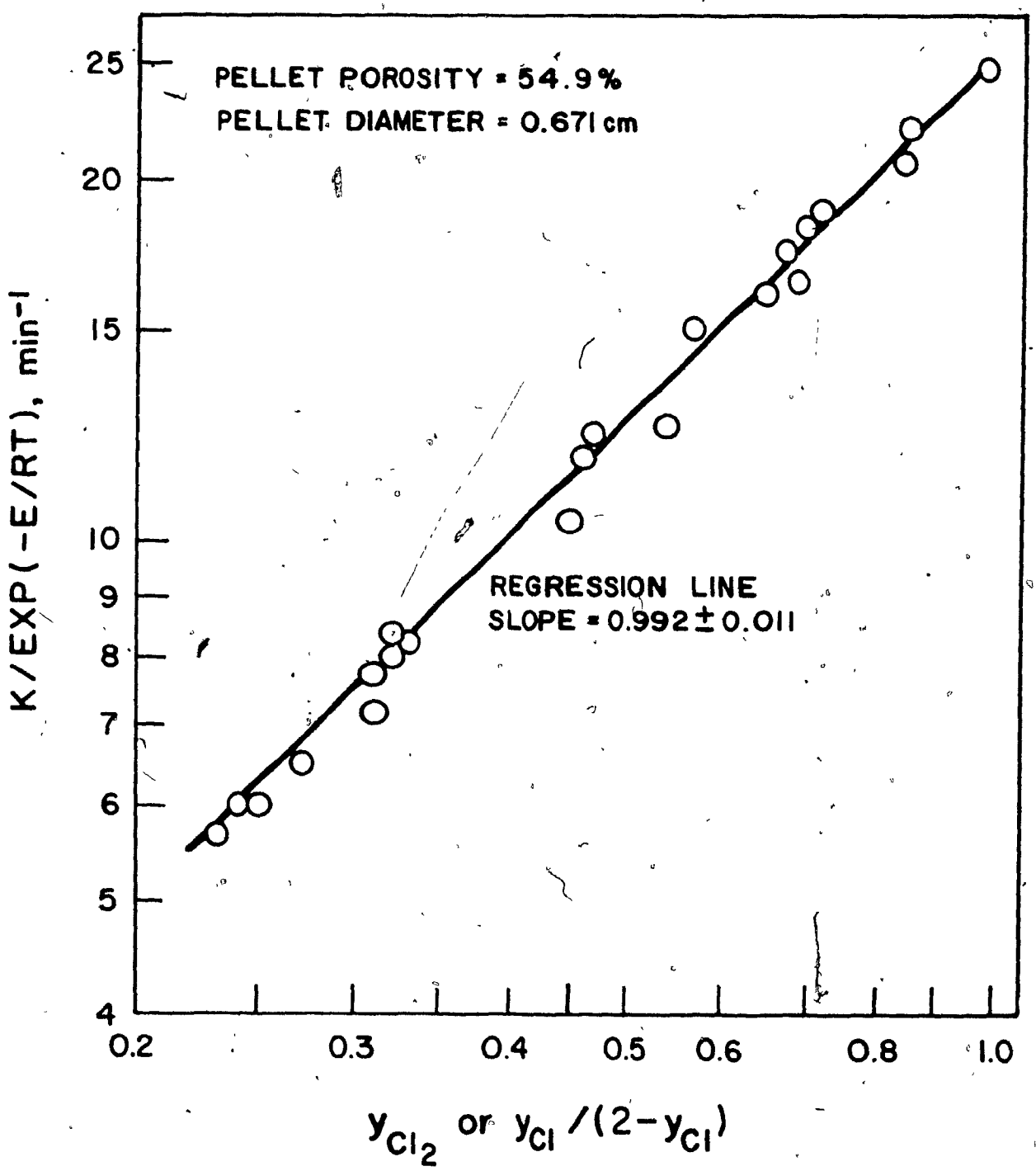
PELLET POROSITY = 54.9%
PELLET DIAMETER = 0.671 cm
REGRESSION LINE
SLOPE = 0.992 ± 0.011
K/EXP(-E/RT), min⁻¹
25
20
15
10
9
8
7
6
5
4
0.2
0.3
0.4
0.5
0.6
0.8
1.0
y_{Cl_2} or $y_{Cl}/(2-y_{Cl})$

expressed in Equation (103) was preferred over an exponential form ($y_{Cl}^{1.53}$) in calculations involving simultaneous mass transfer and chemical reaction resistances, since the former allowed an approximate time-conversion relationship as discussed in the Theoretical Analysis section, Equation (51), (without the need to solve a nonlinear differential equation which would have resulted with the latter).

Rate Expression for Chemical Reaction Control

From the theoretical formulation and the regression analysis of the experimental data, the following empirical expression for the rate of zirconium dioxide chlorination with chlorine alone has been obtained:

$$1-(1-X)^{1/3} = 3.313\exp(-12162/T)y_{Cl_2}(1-\varepsilon)^{-2}D^{-1}\,t_r \qquad (104)$$

where X is the fraction of zirconium dioxide reacted, T is the reaction temperature, y_{Cl_2} is the chlorine concentration in the bulk gas, ε is the void fraction of the pellet, D is the diameter of the pellet in cm, and t is the reaction time in minutes.

In Figure 28, the values of the reaction time calculated from Equation (104) are plotted against the experimental data for the chemical reaction controlled region ($T<1950$) including the effects of all individual parameters discussed previously. As can be seen, Equation (104) represents the experimental data fairly well, the scatter being within ± 10% of the reaction time. This

FIGURE 28

COMPARISON OF EXPERIMENTAL REACTION TIME

WITH VALUES PREDICTED BY EQUATION (104)

(CHEMICAL REACTION CONTROLLED REGION, T<1950 K)

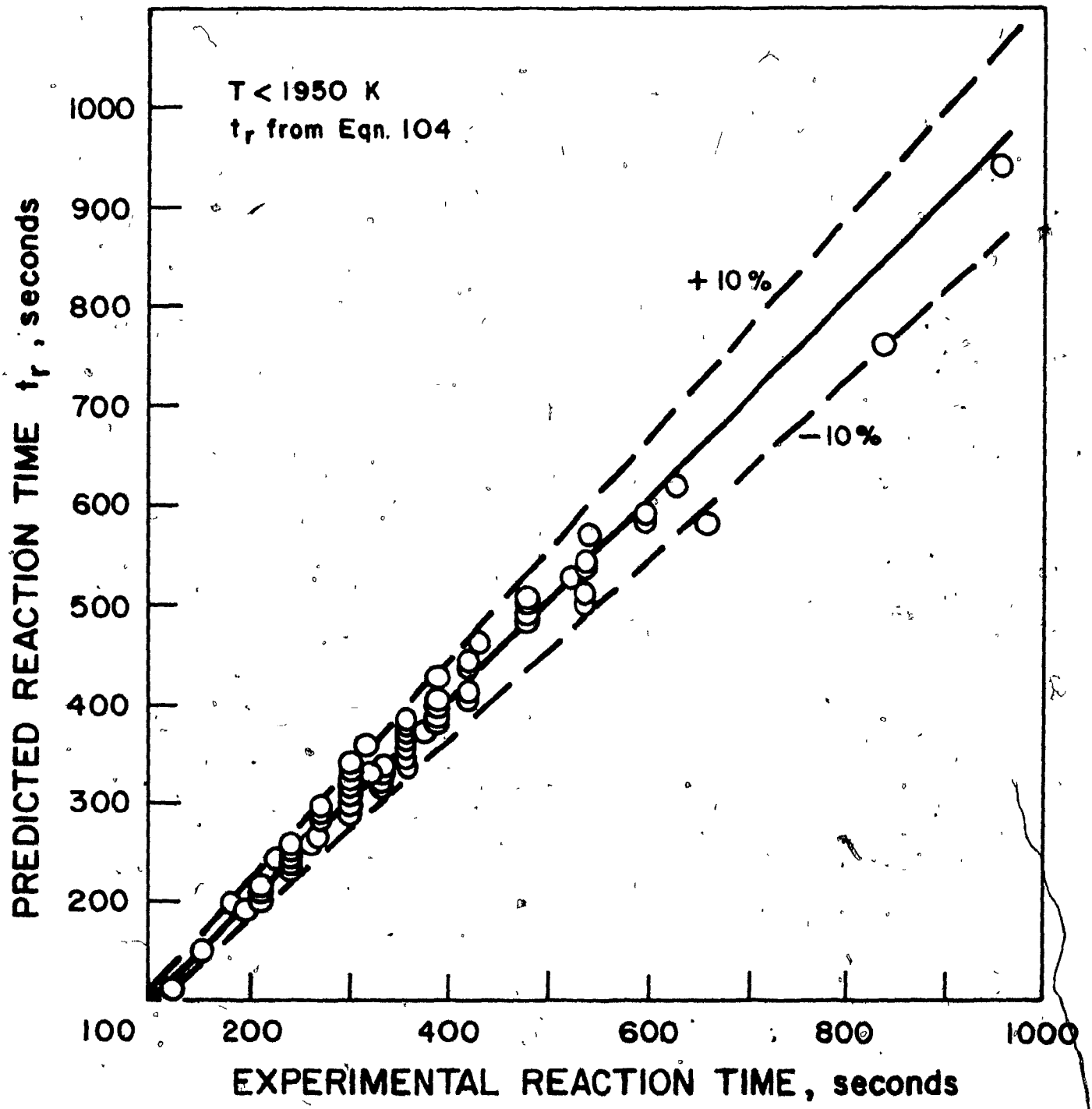
T < 1950 K
t_r from Eqn. 104
+10%
−10%
PREDICTED REACTION TIME t_r, seconds
EXPERIMENTAL REACTION TIME, seconds
100
200
300
400
500
600
700
800
900
1000

scatter seems to be reasonable in the light of the experimental difficulties encountered.

Combined Mass Transfer and Chemical Reaction Controlled Region (T>1950 K)

As was discussed earlier, Arrhenius plots of the experimental data (Figures 21-23) have shown that above about 1950 K gas film diffusion started to contribute some resistance. An approximate time-conversion expression has been derived in the Theoretical Analysis section and the reaction time has been shown to be approximated by:

$$t = t_r + t_m \tag{105}$$

where t_r is the time required to reach a conversion X in the absence of mass transfer resistances as calculated from Equation (104), t_m is the time required to reach the same conversion when the reaction is controlled purely by mass transfer as given by Equation (51).

Numerical calculations were carried out with the aid of a computer program (the listing is presented in Appendix III) to predict the contribution of mass transfer resistance at each experimental condition in the entire temperature range (1540 < T < 2480 K). A typical output from this program is presented in Appendix IV for the data given in Table I of Appendix II (pellet porosity of 48.5% and diameter of 0.671 cm).

In Figure 29, the influence of mass transfer, expressed as $t_m/(t_m + t_r)$, is plotted against the reaction temperature. The plot includes the complete experimental data except those of the chlorine concentration studies. This figure shows that the theoretically-predicted mass transfer contribution increases sharply above about 1950 K, whereas below this temperature this contribution is relatively small and within the limits of the experimental scatter. Thus, the previous conclusions with respect to the controlling mechanism seem to be confirmed. Furthermore, Figure 30, in which the values of the experimental reaction time are plotted against the ones predicted for the same conversions in the region of the combined resistances, shows that the theoretical formulation agrees reasonably well with the experimental results.

CONCLUSION

1. The kinetics of the reaction between zirconium dioxide and chlorine in the temperature range of 1540 - 2480 K in a radio-frequency chlorine plasma tail-flame were studied. The influences of such parameters as time, temperature, porosity, diameters, and chlorine concentration on the rate were determined experimentally, using a single stationary spherical pellet.

2. The microscopic examinations of partially-reacted pellets revealed that the reaction was confined to a very thin layer near the external surface. This was confirmed by the

FIGURE 29

THEORETICALLY PREDICTED MASS TRANSFER

CONTRIBUTIONS AT EXPERIMENTAL CONDITIONS

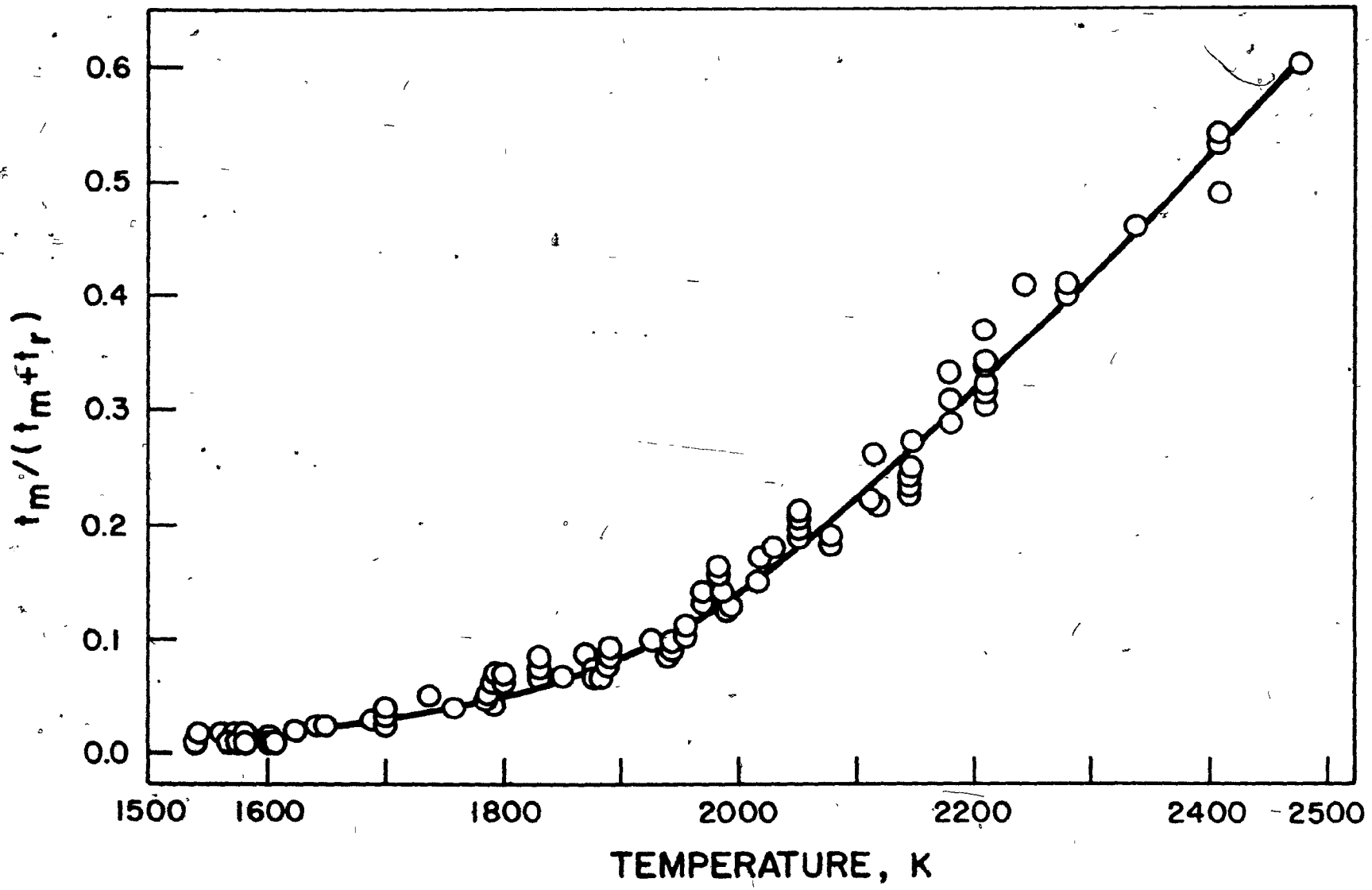
0.6
0.5
0.4
0.3
0.2
0.1
0.0
$t_m/(t_m+t_r)$
1500
1600
1800
2000
2200
2400
2500
TEMPERATURE, K

FIGURE 30

COMPARISON OF EXPERIMENTAL REACTION TIME WITH VALUES PREDICTED BY EQUATIONS (104) and (51)

(COMBINED CHEMICAL REACTION AND MASS TRANSFER CONTROLLED REGION, T>1950 K)

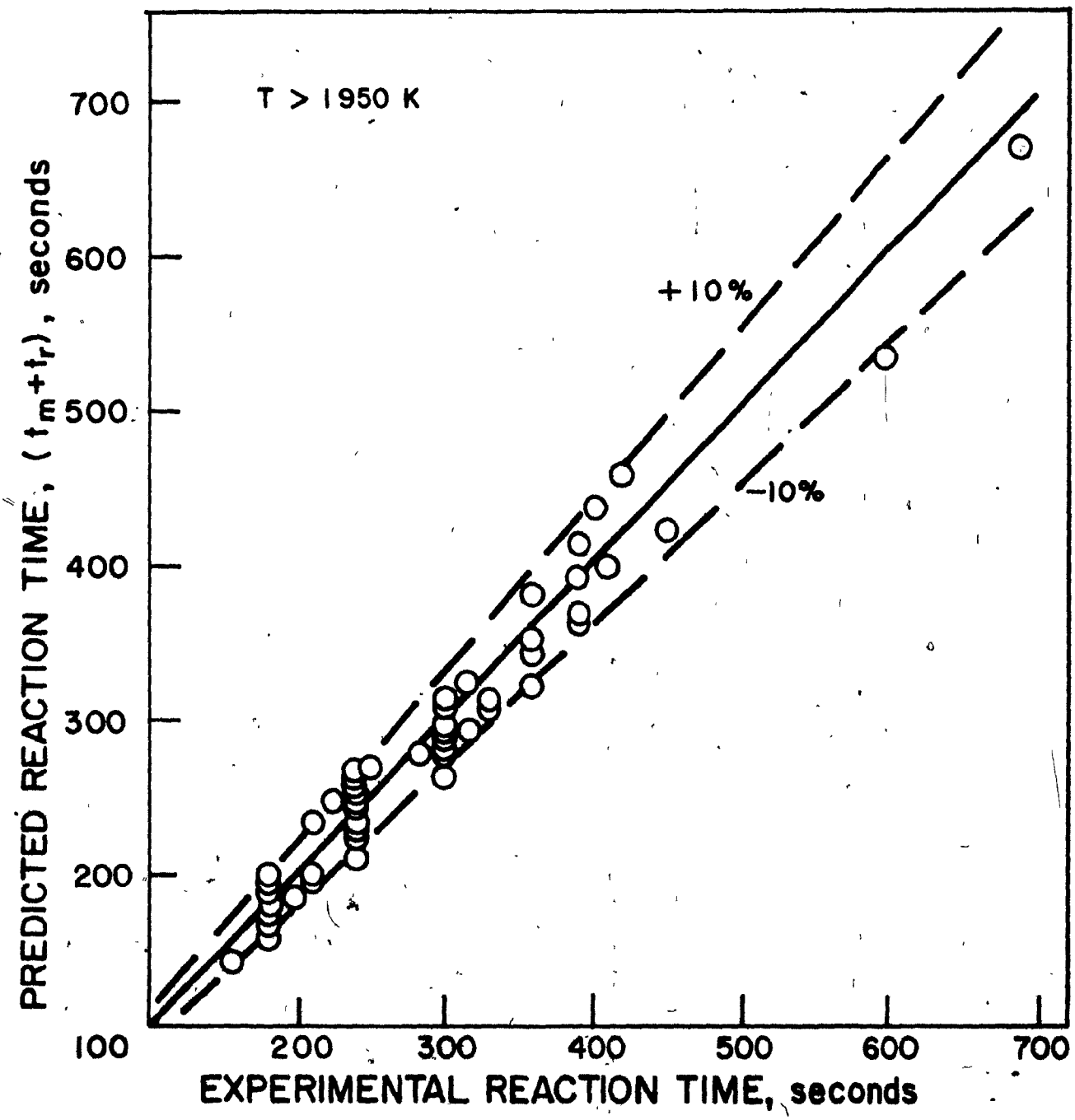
T > 1950 K
+10%
−10%
PREDICTED REACTION TIME, (t_m+t_r), seconds
EXPERIMENTAL REACTION TIME, seconds
100
200
300
400
500
600
700

experimental conversion-time data which fitted the shrinking-core model.

3. The Arrhenius plots of the experimental data indicated the existence of a gas film diffusion resistance above about 1950 K, below which the rate was controlled by chemical reaction. The activation energy of 101.2 kJ/mole (24.2 kcal/mole) obtained for the latter region did not change with the pellet porosity, thus supporting the conclusion with respect to the surface reaction.

4. The overall rate constant, however, showed a higher porosity dependence [proportional to $(1 - \varepsilon)^{-2}$] than that could be accounted for by the change of solid density [proportional to $(1 - \varepsilon)^{-1}$]. This was attributed to the existence of a thin fluffy layer near the external surfaces, resulting in a higher actual reacting area than the geometrical surface area on which the shrinking-core model is based.

5. The rate was found to be inversely proportional to the pellet diameter, in agreement with the theoretical formulation, Equation (14), again confirming the conclusion of chemical reaction resistance.

6. The rate was first order with respect to the gaseous reactant concentration when it was expressed in terms of molecular chlorine, or in terms of atomic chlorine in the form of $(y_{Cl}/2 - y_{Cl})$.

7. The empirical expression given by Equation (104) represented the experimental data reasonably well.

8. For the region of T>1950 K, where both the chemical and mass transfer resistances were important, the theoretical analysis showed that the total reaction time could be approximated by the summation of two terms: the time required to reach the same conversion in the absence of diffusional resistance, and that for pure mass transfer control. Theoretically calculated mass transfer resistances confirmed the experimental findings with respect to the controlling mechanisms. Furthermore, the predicted reaction time compared reasonably well with the experimental values.

NOMENCLATURE

NOMENCLATURE

A	-	Gaseous component in Equation (5)
A_T	-	Temperature decay constant for fully developed region
A_v	-	Velocity decay constant for fully developed region
a	-	Stoichiometric coefficient in Equation (5)
B	-	Solid reactant in Equation (5); second virial coefficient in Equation (65)
B^*	-	Lennard-Jones second virial coefficient
b_T	-	Temperature decay constant for the core and the transition region
b_v	-	Velocity decay constant for the core and the transition region
C	-	Constant in Equation (45)
c	-	Total gas concentration
D	-	Diameter of spherical reacting particle
D_{ij}	-	Binary diffusion coefficient
D_{im}	-	Effective binary diffusion coefficient of component i in mixture
d	-	Nozzle diameter
E	-	Activation energy
e	-	Spectral emissivity at wavelength, λ
ΔF_1	-	Free energy change for Equation (2)
ΔF_2	-	Free energy change for Equation (3)

ΔF_3	-	Free energy change for Equation (4)
f	-	Concentration function
f_1	-	Jet axial decay function
H_{Cl_2}	-	Molar enthalpy of gaseous chlorine
K	-	Overall rate constant
K_1	-	Jet axial velocity decay constant defined by Equation (70)
K_E	-	Equilibrium constant
k	-	Boltzmann's constant
k_m	-	Mass transfer coefficient
k_s	-	Surface reaction rate constant
M	-	Molecular weight
N	-	Molar flux
N_{Re}	-	Reynolds number
N^o_{Re}	-	Reynolds number based on initial particle diameter
N_{Sc}	-	Schmidt number
N_{Sh}	-	Sherwood number
n	-	Total number of gaseous components
P	-	Pressure
P_R	-	Ratio of power at the nozzle exit to the inlet (plate) power
q	-	Factor defined by Equation (65)
R	-	Initial radius of spherical particle
r_c	-	Radius of shrinking spherical particle
S	-	Swirl number
S_R	-	Ratio of swirl to radial gas in RF torch
T	-	Temperature

T^* - Dimensionless temperature ($T/\varepsilon/k$)

T_b - Brightness temperature (pyrometer reading)

T_c - Critical temperature

T_N - Nozzle exit gas temperature

t - Reaction time

t_m - Reaction time under mass transfer control

t_r - Reaction time under chemical reaction control

U - Gas velocity

U_N - Nozzle exit gas velocity

V_c - Critical volume

w - Weight of solid reactant

X - Fraction of solid reactant reacted at time t

x - Distance from nozzle exit

x_o - Distance of virtual origin of the fully developed jet from the nozzle exit

y - Mole fraction of gaseous component

z - Dimensionless radius of spherical particle $r/R = z = (1 - X)^{1/3}$

z_c - Dimensionless radius of spherical particle (r_c/R)

Greek Letters

α - Constant defined by Equation (33)

β - Constant defined by Equation (34)

γ - Constant defined by Equation (36)

ε - Void fraction; Lennard-Jones parameter

ϕ - Index for stoichimetric coefficient as defined by Equation (23)

Ψ - Mixture viscosity parameter as defined by Equation (62)

Ω_D - Collision integral for diffusion

Ω_v - Collision integral for viscosity

λ - Wavelength

ρ - Density of fluid

ρ_s - Molar density of reacting solid

σ - Lennard-Jones parameter

μ - Viscosity

Subscripts

e - Equilibrium

f - Gaseous film

i, j - Components i, j

mix - Mixture

o - Bulk fluid

s - Surface

∞ - Ambient

REFERENCES

REFERENCES

Babu, R.S., Chintamani, Vijay, P.L. and Subramanyam, R.B., 'Production of Nuclear-Grade Zirconium Sponge from Pure Zirconium Oxide,' India, At. Energy Comm., Bhabha At. Res. Cent., BARC-427, (1969)

Bayliss, R.K., Bryant, J.W. and Sayce, I.G., 'Plasma Dissociation of Zircon Sand,' 3rd. International Symposium on Plasma Chemistry, Paper No. S.5.2, Limoges, France, (1977)

Bhattacharyya, D. and Gauvin, W.H., 'Modelling of Heterogenous Systems in a Plasma Jet Reactor,' AIChE J., 21, (5), 879 (1975)

Bird, R.B., Stewart, W.E. and Lightfoot, E.N., Transport Phenomena, John Wiley & Sons, New York, (1960)

Bischoff, K.B., 'Further comments on the Pseudo-Steady State Approximation for Moving Boundary Problems,' Chem. Eng. Sci., 20, 783 (1965)

Bowen, J.R., 'Comments on the Pseudo-Steady State Approximation for Moving Boundary Problems,' Chem. Eng. Sci., 20, 712 (1965)

Branstetter, J.R., 'Some Practical Aspects of Surface Temperature Measurement by Optical and Ratio Pyrometers,' NASA TN D-3604, (1966)

Calvelo, A. and Cunningham, R.E., 'Kinetics of Gas-Solid Reactions - Influence of Surface Area and Effective Diffusivity Profile,' J. Catalysis, 17, 1 (1970)

Carnahan, B., Luther, H.A. and Wilkes, J.O., Applied Numerical Methods, John Wiley & Sons, New York, (1969)

Chigier, N.A. and Chervinsky, A., 'Experimental and Theoretical Study of Turbulent Swirling Jets Issuing from a Round Orifice,' Israel J. Tech., 4, (1), 44 (1966)

Chigier, N.A. and Chervinsky, A., 'Experimental Investigation of Swirling Vortex Motion in Jets,' Trans. ASME, J. Appl. Mech., 34, 443 (1967)

Chintamani, Vijay, P.L., Subramanyam, R.B. and Sundaram, C.V., 'Further Studies on the Pilot Plant Production of Reactor-Grade Zirconium Sponge,' India. At. Energy Comm., Bhabha At. Res. Cent., BARC-607, (1972)

Chizhikov, D.M., Deineka, S.S. and Makarova, V.N., 'Use of Plasmas in Chloride Metallurgy,' in Manual-Investigations of Processes in Metallurgy of Nonferrous and Rare Metals, Nauka, Mowcow, 136 (1969), Chem. Abst., 73:90192

Chizhikov, D.M., Tsvetkov, Yu. V., Panfilov, S.A., Deineka, S.S. and Taginov, I.K., 'Use of a Low-Temperature Plasma in the Metallurgy of Nonferrous and Rare Metals,' Nizkotemp. Plasma Tekhnol. Neorg. Veshchestv, Tr. Vses. Semin., 2nd. 1970, 86 (1971), Chem. Abst., 80:147764

Ciba Ltd., 'Finely Divided, Nonpyrophoric Metals,' Neth. Patent Appl. 6 608 844, (1966)

Costa, E.C. and Smith, J.M., 'Kinetics of Noncatalytic, Nonisothermal, Gas-Solid Reactions: Hydrofluorination of Uranium Dioxide,' AIChE J., 17, (4), 947 (1971)

Denisova, N.D. and Bystrova, O.N., 'Compressibility of Gaseous Zirconium and Hafnium Tetrachlorides,' Russian J. Phys. Chem., 46, (8), 1237 (1972)

Elger, G.W., 'Quality of Zirconium Prepared by Different Reductants,' U.S. Bureau of Mines RI-5933, U.S. Government Printing Office, Washington, (1962).

Fahim, M.A. and Ford, J.D., 'Kinetics of Hydrogen Reduction of Coablt Sulfide,' Can. J. Chem. Eng., 54, 578 (1976)

Fruehan, R.J. and Martonik, L.J., 'The Rate of Chlorination of Metal Oxides: Part III. The Rate of Chlorination of Fe_2O_3 and NiO in Cl_2 and HCl,' Metallurgical Trans., 4, 2793 (1973)

Garvie, R.C., 'Zirconia' in Refractory Materials. A Series of Monographs. High Temperature Oxides, Part II. Ed. Alper, A.M. Academic Press, (1970)

Gilles, H.L. and Clump, C.W., 'Reduction of Iron Ore with Hydrogen in a Direct Current Plasma Jet,' Ind. Eng. Chem. Process Des. Develop., 9, (2), 194 (1970)

Gragg, F.M., 'Production of Pure Zirconium by Use of a Radio-Frequency Plasma,' Ph.D. Dissertation, The University of Arizona, (1973)

Grain, C.F. and Garvie, R.C., 'Mechanism of the Monoclinic to Tetragonal Transofrmation of Zirconium Dioxide,' U.S. Bureau of Mines, RI-6619, U.S. Government Printing Office, Washington, (1965)

Hattikudur, U.R. and Thodos, G., 'Equations for the Collision Integrals $\Omega(^{1,1})^*$ and $\Omega(^{2,2})^*$,' J. Chem. Phys., 52, 4313 (1970)

Hirschfelder, J.O., Curtiss, C.F. and Bird, R.B., Molecular Theory of Gases and Liquids, John Wiley & Sons, New York, 166 (1954)

Hsu, H.W. and Bird, R.B., 'Multicomponent Diffusion Problems,' AIChE J., 6, (3), 516 (1960)

Huska, P.A. and Clump, C.W., 'Decomposition of Molybdenum Disulphide in an Induction-Coupled Argon Plasma,' Ind. Eng. Chem. Process Des. Develop., 6, (2), 238 (1967)

Ishida, M. and Wen, C.Y., 'Comparison of Kinetic and Diffusional Models for Gas-Solid Reactions,' AIChE J., 14, (2), 311 (1968)

JANAF Thermochemical Tables, Dow Chemical Company, Stull, D.R., Clearing House for Federal Scientific and Technical Information, (1967)

Kroll, W.J., Carmody, W.R. and Schlechten, A.W., 'High Temperature Experiments with Zirconium and Zirconium Compounds,' U.S. Bureau of Mines RI-4915, U.S. Government Printing Office, Washington, (1952)

Landsberg, A., Hoatson, C.L. and Block, F.E., 'The Chlorination Kinetics of Zirconium Dioxide in the Presence of Carbon and Carbon Monoxide,' Metall. Trans., 3, 517 (1972)

Levenspiel, O., Chemical Reaction Engineering, 2nd Ed., John Wiley & Sons, New York, (1972)

Lilley, D.G., 'Turbulent Swirling Flame Predictions,' AIAA J., 12, (2), 219 (1974)

Little, J.E., Wentzell, J.M. (Rio Algom Mines Ltd.), 'Reduction to a Refractory Metal by a Plasma Jet,' Belgium Patent: 668 600, (1965)

Luss, D., 'The Pseudo-Steady State Approximation for Gas-Solid Reactions,' Can. J. Chem. Eng., 46, (3), 154 (1968)

Manieh, A.A. and Spink, D.R., 'Chlorination of Zircon Sand,' Can. Met. Quart., 12, (3), 331 (1973)

Manieh, A.A., Scott, D.S. and Spink, D.R., 'Electrothermal Fluidized Bed Chlorination of Zircon,' Can. J. Chem. Eng., 52, 507 (1974)

Martinez, G.M. and Couch, D.E., 'Electrowinning of Zirconium from Zirconium Tetrachloride,' Metall. Trans., 3, 571 (1972)

Martinez, G.M., Shanks, D.E., Woodyard, J.R. and Wong, M.M., 'Investigation of a Cell Design for Electrowinning Zirconium Metal from Zirconium Tetrachloride,' U.S. Bureau of Mines RI-8125, U.S. Government Printing Office, Washington, (1976)

Miller, G.L., Metallurgy of the Rarer Metals - 2, Zirconium, Butterworths Scientific Publications, London, (1954)

Morris, A.J. and Jensen, R.F., 'Fluidized Bed Chlorination Rates of Australian Rutile,' Metall. Trans. B., 7B, 89 (1976)

Munz, R.J., 'The Decomposition of Molybdenum Disulphide in an Induction Plasma Tailflame,' Ph.D. Thesis, McGill University, Montreal, Canada, (1974)

Munz, R.J. and Gauvin, W.H., 'The Decomposition Kinetics of Molybdenite in an Argon Plasma,' AIChE J., 21, (6), 1132 (1975)

Neubauer, I. and Romwalter, A., 'Polymorph Phase - Numwandlung bis 1200 C in Technischen ZrO_2 mit CaO - Bahalt,' Rev. Int. Htes. Temp. et Refract., 14, (4), 208 (1977)

Nisel'son, L.A., Sokolova, T.D. and Stolyarov, V.I., 'The $ZrCl_4$ - H_fCl_4 System and Conditions of Separating Its Components by the Method of Rectification,' Dokadly Akademii Nauk SSSR, 168, (5), 1107 (1966)

O'Reilly, A.J., Doig, I.D. and Ratcliffe, J.S., 'The Kinetics of the Chlorination of Zirconium Dioxide in a Static Bed with Carbon and Chlorine,' Inorg. Nucl. Chem., 34, 2487 (1972)

Peterson, E.E., 'Reaction of Porous Solids,' AIChE J., 3, (4) 443 (1957)

Pogonina, L.N. and Ivashentsev, Ya. I., 'Investigation of the Chlorination of Titanium Dioxide, Zirconium Dioxide and Hafnium Dioxide by Chlorine,' Voprosy Khimii, (2), 47 (1974)

Pratte, B.D. and Keffer, J.F., 'The Swirling Turbulent Jet,' Trans. ASME, J. Basic Eng., 92, 739 (1972)

Rains, R.G. and Kadlec, R.H., 'The Reduction of Al_2O_3 to Aluminum in a Plasma,' Metall. Trans., 1, 1501 (1970)

Ramachandran, P.A. and Smith, J.M., 'A Single-Pore Model for Gas-Solid Noncatalytic Reactions,' AIChE J., 23, (3), 353 (1977)

Ranz, W.E. and Marshall, W.R., 'Evaporation from Drops,' CEP, 48, (3), 141 (1952)

Reid, R.C. and Sherwood, T.K., The Properties of Gases and Liquids, 2nd Ed., McGraw-Hill, New York, (1966)

Sampath, B.S., Ramachandran, P.A. and Hughes, R., 'Modelling of Noncatalytic Gas-Solid Reactions - I. Transient Analysis of the Particle-Pellet Model,' Chem. Eng. Sci., 30, 125 (1975)

Sayegh, N.N., 'Variable-Property Flow and Heat Transfer to Single Spheres in High Temperature Surroundings,' Ph.D. Thesis, McGill University, Montreal, Canada, (1977)

Sehra, J.C., 'Fluidized Bed Chlorination of Nuclear Grade ZrO_2 with CO and Cl_2,' Trans. Indian Inst. Metals, 27, (2), 93 (1974)

Semenenko, K.N., Felin, M.G. and Kostenko, A.L., 'Reaction of Atomic Hydrogen with Zirconium Halides in a Glow Discharge Plasma,' Vestn. Mosk. Univ. Khim., 16, (1), 39 (1975)

Shain, S.A., 'A Note on Multicomponent Diffusion,' AIChE J., 7, (1), 17 (1961)

Shelton, S.M., Kauffman, A.J., Roberson, A.H., Dilling, E.D., Beall, R.A., Hayes, E.T., Kato, H., McClain, J.H. and Halbrook, F., 'Zirconium - Its Production and Properties,' U.S. Bureau of Mines, Bulletin 561, U.S. Government Printing Office, Washington, (1956)

Shen, J. and Smith, J.M., 'Diffusional Effects in Gas-Solid Reactions,' Ind. Eng. Chem. Fundam., 4, (3), 293 (1965)

Sohn, H.Y. and Szekely, J., 'A Structural Model for Gas-Solid Reactions with a Moving Boundary - III. A General Dimensionless Representation of the Irreversible Reaction Between a Porous Solid and a Reactant Gas,' Chem. Eng. Sci., 27, 763 (1972)

Spink, D.R., 'Extractive Metallurgy of Zirconium and Hafnium,' CIM Bulletin, 70, (787), 145 (1977)

Starrat, F.W., 'Zirconium by Sodium Reduction,' J. Metals, 11, 441 (1959)

Stephens, W.W. and Gilbert, H.L., 'Chlorination of Zirconium Oxide,' Trans. AIME, J. Metals, 194, 733 (1952)

Svehla, R.A., 'Estimated Viscosities and Thermal Conductivities of Gases at High Temperatures,' NASA TR R-132, (1962)

Szekely, J. and Evans, J.W., 'A Structural Model for Gas-Solid Reactions with a Moving Boundary,' Chem. Eng. Sci., 25, 1091 (1970)

Szekely, J. and Evans, J.W., 'A Structural Model for Gas-Solid Reactions with a Moving Boundary - II. The Effect of Grain Size, Porosity and Temperature on the Reaction of Porous Pellets,' Chem. Eng. Sci., 26, 1901 (1971)

Szekely, J., Evans, J.W. and Sohn, H.Y., Gas-Solid Reactions, Academic Press, New York, (1976)

Tsirel'nikov, V.I., Kommissarova, L.N. and Spitsyn, V.I., 'Thermal Conductivity and Viscosity of Zirconium and Hafnium Tetrachloride Vapors at 300 - 700°,' Dokl. Akad. Nauk SSSR, 139, 1389 (1961)

Turevskii, E.N., Aleksandrov, I.A. and Dvoiris, A.D., 'Comparison of Methods for Calculating Diffusion in Multicomponent Gas Mixtures,' Khim. Tekhnol. Topl. Masel, 16, (4), 36 (1971)

Vasilenko, D.B. and Vol'skii, A.N., 'The Thermodynamics of Reaction of Chlorination of Zirconium Dioxide by Gaseous Chlorine,' Russian J. Inorg. Chem., 3, (7), 32 (1958)

Wang, S.C. and Wen, C.Y., 'Experimental Evaluation of Nonisothermal Solid-Gas Reaction Model,' AIChE J., 18, (6), 1231 (1972)

Wen, C.Y., 'Noncatalytic Heterogenous Solid-Fluid Reaction Models,' Ind. Eng. Chem., 60, (9), 34 (1968)

Wilke, C.R., 'Diffusional Properties of Multicomponent Gases,' CEP, 46, (2), 95 (1950a)

Wilke, C.R., 'A Viscosity Equation for Gas Mixtures,' J. Chem. Phys., 18, 517 (1950b)

Wilks, P.H., Ravinder, P., Grant, C.L., Pelton, P.A., Downe, R.R.J. and Talbot, M.C., 'Plasma Process for Zirconium Dioxide,' CEP, 68, 82 (1972)

Wilks, P.H., Ravinder, P., Grant, C.L., Pelton, P.A., Downe, R.R.J. and Talbot, M.C., 'Commercial Production of Submicron Zirconium Dioxide via Plasma,' Chem. Eng. World, 9, (3), Section 1, 59 (1974)

Williams, R.J.J., Calvelo, A. and Cunningham, R.E., 'A General Asymptotic Analytical Solution for Non-Catalytic Gas-Solid Reactions,' Can. J. Chem. Eng., 50, 486 (1972)

Yagi, S. and Kunii, D., 'Proposed Theory of Fluidized Roasting of Sulfide Ore with Uniform Size. I - Single Particle of Ore in the Fluidized Bed,' J. Chem. Soc. Japan, Ind. Chem. Sect., 56, 131 (1953)

Yagi, S. and Kunii, D., 'Fluidized-Solid Reactors for Particles with Decreasing Diameters,' Chem. Eng. Japan., 19, 500 (1955a)

Yagi, S. and Kunii, D., 'Combustion of Carbon Particles in Flames and Fluidized Beds,' Symposium on Combustion, 5th, Pittsburgh, 1954, Reinhold, New York, 231 (1955b)

PART II - CHLORINATION OF ZIRCONIUM DIOXIDE IN THE PRESENCE OF CARBON

INTRODUCTION

In contrast with the reaction of zirconium dioxide with chlorine alone, which has been studied in Part I of this work, the chlorination of ZrO_2 in the presence of a carbonaceous material is thermodynamically feasible, as shown in Figure 1 for the three reactions:

$$ZrO_2 + 2Cl_2 + C \rightarrow ZrCl_4 + CO_2 \quad (1)$$

$$ZrO_2 + 2Cl_2 + 2C \rightarrow ZrCl_4 + 2CO \quad (2)$$

$$ZrO_2 + 2Cl_2 + 2CO \rightarrow ZrCl_4 + 2CO_2 \quad (3)$$

Although these three reactions are all possible and probably occur simultaneously, it has been shown thermodynamically (Vasilenko and Vol'skii, 1958) that at equilibrium the ratios of carbon monoxide to carbon dioxide are about 12 and 330 at temperatures of 1075 and 1275 K, respectively. Hence the end product of the chlorination reaction is essentially carbon monoxide, rather than carbon dioxide, when the gaseous products remain in contact with an excess of unreacted carbon above about 1300 K. This can also be seen in Figure 1 in which Reaction (2) has the largest negative free energy values. As discussed in Part I, at experimental bulk gas temperature levels (3500 - 6000 K) used in this work, chlorine gas is expected to be in the atomic form. Hence the chlorination of

FIGURE 1

FREE ENERGIES OF ZrO_2 CHLORINATION REACTIONS

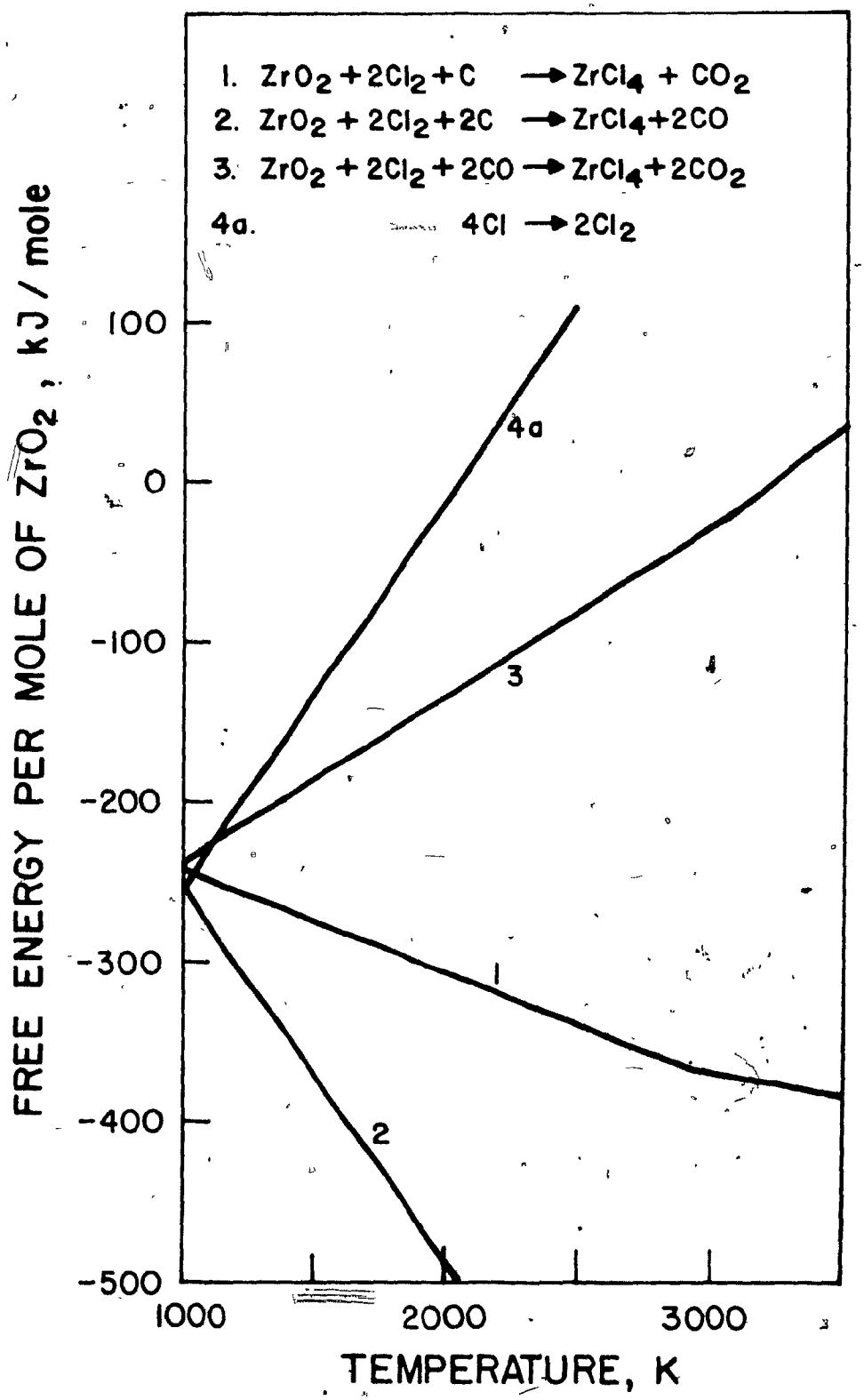
1. $ZrO_2 + 2Cl_2 + C \rightarrow ZrCl_4 + CO_2$
2. $ZrO_2 + 2Cl_2 + 2C \rightarrow ZrCl_4 + 2CO$
3. $ZrO_2 + 2Cl_2 + 2CO \rightarrow ZrCl_4 + 2CO_2$
4a. $4Cl \rightarrow 2Cl_2$
FREE ENERGY PER MOLE OF ZrO_2, kJ / mole
100
0
-100
-200
-300
-400
-500
1000
2000
3000
TEMPERATURE, K
4a
3
1
2

zirconium dioxide in the presence of carbon in a chlorine plasma may be represented by the following reaction:

$$ZrO_2 + 4Cl + 2C \rightarrow ZrCl_4 + 2CO \qquad (4)$$

The literature on chlorination of various metal oxides, including TiO_2 (Dunn, 1960), (Bergholm, 1961), (Seryakov et al., 1967, 1969, 1970), (Masterova and Levin, 1973), (Morris and Jensen, 1976), ThO_2 (Ivashentsev et al., 1975), Al_2O_3 (Landsberg, 1975, 1977), $ZrSiO_4$ (Manieh et al., 1973, 1974), (Sparling and Glastonbury, 1973) and ZrO_2 (Stephens and Gilbert, 1952), (O'Reilly et al., 1972), (Landsberg et al., 1972) with carbon as a reducing agent, has been limited to temperatures below 1400 K. The results of different workers on the same oxide (e.g., in the case of TiO_2 and ZrO_2) varied widely depending upon experimental conditions, the method of preparation of the samples, and the type of carbon reducing agent used. Landsberg et al. (1972) chlorinated disk pellets of zirconium dioxide surrounded by a loosely packed bed of carbon powder in the temperature range of 1120 - 1320 K. It was found that the reaction was taking place at the surface, was first order with respect to the chlorine concentration, and was chemically-controlled with an activation energy of 127.7 kJ/mole. The rate of reaction was lower with coarser carbon particles, suggesting the importance of carbon-metal oxide contact during the chlorination. The rate data reported by O'Reilly et al. (1972) also confirmed this fact, although it was not stated explicitly in their paper. They chlorinated uncompacted intimately mixed zirconium dioxide powder and petroleum coke (in a

weight ratio of one to four) in the temperature range of 940 - 1100 K. The conversion-time data fitted the shrinking-core model under chemical reaction control up to 30-80 percent conversions (depending upon the temperature level), above which the rate of reaction decreased significantly and deviated from the model. The order of reaction with respect to chlorine concentration, 0.64, and the value of the activation energy, 230.7 kJ/mole, reported by O'Reilly et al. did not agree with those of Landsberg et al. (1972).

In the present work, mixtures of zirconium dioxide and carbon powder were compacted into spherical pellets and were chlorinated in an R.F. chlorine plasma tail flame. Graphite was selected as the carbonaceous reducing agent due to its excellent compactibility in making the pellets. The kinetic study covered the particle temperature range between 1400 and 1950 K.

MATHEMATICAL MODELLING OF THE REACTION

The analytical treatment of a heterogenous reaction involving pellets composed of two solid components, such as zirconium dioxide and carbon, exhibits a higher degree of complexity than that of a single solid component reaction. The degree of contact between the solid constituents may influence the progress of the reaction due to a mechanistic behaviour of the solid reducing agent and the nature of the intermediate product (if it forms and exists during the reaction).

As seen in the Literature Review, the mechanism of different

metal oxide chlorination reactions in the presence of carbon has found the least degree of agreement among different investigators (Bergholm, 1961), (Stefanyuk and Morozov, 1965), (Seryakov et al., 1967, 1970), (Sparling and Glastonbury, 1973), (Manieh, Scott and Spink, 1974), (Ketov et al., 1974), (Ivashentsev et al., 1975), particularly among those who have studied the same system. Most of the proposed mechanistic models have been nearly entirely speculative. However, the majority of these investigators and also the kinetic data reported by others (Landsberg et al., 1972), (O'Reilly et al., 1972) have indicated the importance of the degree of contact between metal oxide and carbon particles. This was found to vary with the progress of the reaction and became the rate-limiting factor. Thus a simple shrinking-core model may not represent the progress of the reaction under conditions of chemical control, whereas it may well correlate the time-conversion data under purely mass transfer-controlled conditions.

A relatively simple approach is followed here in developing a time-conversion relationship for the chlorination of zirconium dioxide compacted with carbon. The model assumes that mass transfer resistance (ash diffusion) is absent or negligibly small, and that the rate is proportional to a contact area or to a distance of separation between the zirconium dioxide and the carbon particles. The latter in turn is assumed to be proportional to a functional form of initial carbon concentration in the pellet and also to the amount of unreacted zirconium dioxide left in the pellet. Mathematically the rate equation may be written as:

$$-\frac{dW}{dt} = k\ W\ f_1(x_c)\ f_2(y_{Cl_2}) \tag{5}$$

where $\underline{k}$ is the intrinsic rate constant, $\underline{W}$ is the weight of unreacted zirconium dioxide in the pellet at time $\underline{t}$, $\underline{x_c}$ is the initial concentration of carbon in the pellet, $\underline{y_{Cl_2}}$ is the concentration of chlorine in the bulk gas and $\underline{f_1}$, $\underline{f_2}$ are the functional relationships for the concentrations of carbon and chlorine, respectively.

Equation (5) may be rearranged and integrated to give:

$$-(\ell nW-\ell nW_o) = k\ f_1(x_c)\ f_2(y_{Cl_2})\ t \tag{6}$$

or

$$-\ell n(W/W_o) = K\ t \tag{7}$$

where $\underline{W_o}$ is the initial weight of zirconium dioxide in the pellet, and $\underline{K}$ is the overall rate constant defined as:

$$K = k\ f_1(x_c)\ f_2(y_{Cl_2}) \tag{8}$$

Equation (7) may be written in terms of fractional conversion of the zirconium dioxide, X, which is by definition:

$$X = (W_o-W)/W_o \tag{9}$$

and, thus:

$$(W/W_o) = 1-X \tag{10}$$

Insertion of Equation (10) into Equation (7) yields:

$$-\ln(1-X) = K\ t \qquad (11)$$

If Equation (11) represents the conversion-time relationships for the chlorination of zirconium dioxide-carbon pellets, the plot of $-\ln(1-X)$ versus time should yield a straight line. It should be noted that the overall rate constant K as defined by Equation (8) is not a function of the particle diameter, hence the conversion-time relationship given by Equation (11) will not be affected by variations in the particle diameter.

A relationship similar to Equation (11) was derived by Seryakov et al. (1970) on the basis of the transfer of an intermediate product from the surface of one solid phase to the other, as discussed in the Literature Review. They also assumed that the reaction stopped when the contact area approached zero, yielding the maximum amount of oxide that could be reacted. The extent of conversion was based on the latter rather than on the initial amount of metal oxide in the pellet, as defined in the present work. Later, Masterova and Levin (1973) correlated their data on the chlorination of titanium dioxide-carbon pellets with a similar logarithmic model, on a purely experimental basis.

EXPERIMENTAL

APPARATUS

A detailed description of the experimental system has been given in Part I. Briefly, it consisted of two main systems: A plasma

generating unit including a radio-frequency induction torch, a power supply and a control console, and a reactor system including a single-particle reactor, a set of heat exchangers to cool the gaseous exhaust, and a chlorine absorption and disposal unit. Schematic drawings of the overall set-up and of its individual components have been presented in Figures 7 through 11 of Part I.

The torch consisted of a quartz tube surrounded by a copper induction coil immersed in cooling water, a water-cooled gas distributor at the one end and a water-cooled monel nozzle (outlet) at the other end. The distributor allowed the introduction of the cold plasma-forming gas in axial, radial and tangential directions. The former was used for ignition only, and the normal operation was in the radial and tangential modes. The latter served the purpose of stabilizing the flow. The torch was started with argon and then switched over to chlorine with the proper power adjustments. A minimum power level of 7-10 kW was necessary to maintain the chlorine plasma. The maximum power was limited by the cooling rate of the nozzle.

The water-cooled single stationary particle reactor consisted of the reaction chamber (upper section) with a window for visual observation and particle temperature measurements, and of a lower section which housed the particle support system and provided the reactor outlet without disturbing the symmetry of the flow in the reaction chamber. The design of the bottom part of the reactor allowed the particle-supporting system to slide up and down under

leak-proof conditions.

The particle was mounted on an alumina sting 0.08 cm in diameter and 1.0 cm in length which itself was mounted on a larger alumina rod (0.48 cm in diameter and 30.5 cm in length). The lower part of the alumina rod was sheathed by an inconel tube to provide strength and tight sealing of the bottom. The particle-supporting system was connected to a laboratory jack which allowed positioning of the particle.

The chlorine gas, cooled down to 350 - 500 K at the outlet of the cooling system, was absorbed in a caustic solution. The gas had a minimum purity of 99.9% and was supplied from a commercial liquid chlorine cylinder.

MEASUREMENT TECHNIQUES AND ANALYSIS

Preparation of Spherical Pellets

As in Part I, the zirconium dioxide used in these experiments was optical grade, having a minimum purity of 99.8% and was supplied by Atomergic Chemetals Corp., Plainview, N.Y. Analysis of the material and the particle size distribution have been given in Table VII and Figure 12 of Part I. About 96 weight percent of the particles had an equivalent diameter less than about 44 microns and the mass median diameter corresponded to 6.6 microns.

Different carbonaceous materials such as coke, lamp black and graphite were tried to form spherical pellets from their

individual mixture with the zirconium dioxide. Trials with the former two were not successful due to their hardness. Graphite, on the other hand, due to its lubricating properties, improved the compactability of the zirconium dioxide particles. Graphite was therefore chosen as the carbon source in the chlorination study. The graphite used was by the J.T. Baker Company and was of technical grade, with a particle size less than 4.4 microns. It contained 2.69 wt % of ash, as determined by ASTM specification C 561. A semi-quantitative spectrographic analysis of the ash is given in Table I.

The die compaction method described in Part I was also used here to prepare spherical pellets from intimately-mixed zirconium dioxide and graphite powders. This method yielded a pellet of somewhat spherical shape having a disk portion around the equator. The difference in the diameters measured along the two axes of a pellet could be controlled within three percent of the shortest diameter.

Following the sintering process (at about 1275 K in an inert atmosphere for about four hours) a hole 0.08 cm in diameter was drilled to mount the pellet on the particle supporting system. Pellets of three different diameters (0.67, 0.826 and 1.000 cm) and five different carbon concentrations (18.0, 20.2, 23.1, 31.4, 42.5 wt %) were produced for the kinetic study.

Measurement of Particle Temperature

Particle temperature was measured with a high-resolution

TABLE I

ANALYSIS OF ASH IN GRAPHITE

ELEMENT	CONCENTRATION %
Si	30
Mg	10
Fe	10
Al	5
Na	1
Ca	1
Mn	1
Cu	0.5
Ni	0.05
Cr	0.05
Pb	0.01
Bi	0.002
Ag	0.002
As	not detected
Zn	not detected
Hg	not detected
Te	not detected
Sb	not detected
Ti	not detected
Cd	not detected

optical pyrometer (Pyro Micro-Optical Pyrometer) supplied by The Pyrometer Instrument Co. Inc., Northvale, N.J. Six interchangeable objective lenses permitted measurements to be made at distances varying from 12 cm to infinity with object sizes as small as 0.01 cm. Temperatures in the range of 1000 - 3500 K could be measured.

The temperatures of the reacting pellets were measured by focusing the pyrometer filament on the equator portion of the spheres. The brightness temperatures (the pyrometer ammeter readings) were then corrected for the emissivity of the reacting pellet (see Part I: Measurement of Particle Temperature) using an equation (Branstetter, 1966) of the form:

$$1/T - 1/T_b = (\lambda/1.438)\ln e \qquad (12)$$

In this equation e is the spectral emissivity, λ is the wavelength in angstroms x 10^{-8} (6500 x 10^{-8} for the present case), T and T_b are the blackbody and the brightness temperatures in degrees Kelvin, respectively.

The actual emissivity value was measured by providing a black body hole on the reacting pellets. It was found to have a constant value of 0.85. The exterior surface of the unreacted pellets was mostly covered by the graphite (due to its higher mobility during the compaction). Since the pellets contained the graphite in an amount in excess of the reaction (Equation 4) stoichiometry, the particle size did not change during the reaction. Therefore, the surface roughness did not change during the reaction

or from run to run (as it did in the chlorination of pure ZrO_2) to an extent appreciable enough to vary the emissivity of the pellet.

Amount of Reaction

The amount of zirconium dioxide reacted was calculated from the measured weight loss (due to the removal of zirconium tetrachloride as vapor, plus the removal of carbon as carbon monoxide) and the reaction stoichiometry (Equation 4) as follows:

$$\Delta W = \Delta W_p \, M_{ZrO_2} / (M_{ZrO_2} + 2 \, M_c) \tag{13}$$

where ΔW is the amount of ZrO_2 reacted, ΔW_p is the total weight loss on the pellet, M_{ZrO_2} and M_c are the molecular weights of zirconium dioxide and of carbon, respectively.

The excess carbon in the partially-reacted pellets was then burnt off in a muffle furnace, and the residue (unreacted ZrO_2) was weighed to obtain the degree of conversion, X, which was calculated from:

$$X = \Delta W / (\Delta W + W_f) \tag{14}$$

where W_f is the amount of unreacted zirconium dioxide.

The initial concentration of the zirconium dioxide in the pellet was also calculated through these weight measurements in order to check the variation of the ZrO_2 concentration among the pellets (hence the degree of mixing of the ZrO_2 and the carbon). This was calculated as:

$$x_{ZrO_2} = (\Delta W + W_f)/W_{po} \quad (15)$$

where, x_{ZrO_2} is the weight fraction of ZrO_2 in the unreacted pellet, W_{po} is the initial weight of the pellet, ΔW is the amount of ZrO_2 reacted. The maximum standard deviation of the ZrO_2 content of pellets among the five concentration groups studied (means: 82.0, 79.8, 76.9, 68.6, 57.5 wt %) was 0.8 wt % and at 95% confidence level, the value of each pellet was within ± 1.5 wt % of the respective mean concentration. The concentration data are included in Appendix V.

PROCEDURE

Following weighing, the pellet was mounted on the support and placed in the lower cool portion of the reactor which was then closed and purged for several minutes to remove any residual oxygen. The torch was started with argon while the particle was in the lower section of the reactor, thus preventing cracking of the particle due to thermal shock. Once smooth operation of the torch with an argon plasma was established, the particle was raised to a predetermined reaction position where it could be viewed through the reactor window. This was followed by switching from pure argon to pure chlorine plasma operation, with the adjustment of power to a predetermined level. A stopwatch was started as soon as the chlorine began to flow. This procedure differed from the one described in Part I where the particle was kept in the lower section of the reactor while switching from argon to chlorine plasma, and the timing

was started while positioning the particle. Since the chlorination of ZrO_2 + C mixture could take place at relatively much lower temperature than that of pure ZrO_2, the procedure followed in this section ensured the correct timing of the reaction duration.

Visual observations and pyrometric measurements were made during the reaction. After a predetermined length of time, the torch was turned off and the flow of chlorine gas was stopped. The system was purged with cold argon to remove the remaining chlorine so that the reactor could be opened safely. Meanwhile, the partially-reacted pellet cooled down. This was followed by its weight measurement, microscopic examination and micrographing. Finally, the excess carbon was burnt off in a muffle furnace and the unreacted zirconium dioxide was weighed in order to obtain the degree of conversion.

The temperature of the reacting pellet in the chlorine plasma was controlled by its emissivity, its position below the torch nozzle and the power and gas flow rates of the plasma torch. For a given temperature, an attempt was made to keep all these conditions constant to an extent allowed by the operation of the plasma-generating system. The experiments were designed to study time-conversion relationship, temperature and concentration dependence of the rate, and influences of the mass transfer on the chlorination rate. The latter was studied by reacting pellets of three different diameters (0.671, 0.826 and 1.00 cm) while the former were studied with a single pellet diameter of 0.826 cm.

RESULTS AND DISCUSSION

Microscopic Examinations

Measurement of the pellet diameter before and after reaction did not indicate any variation in the pellet size during the reaction. This was due to the presence of carbon in the pellet in an amount in excess of the reaction stoichiometry (Equation 4), which made the pellet maintain its initial shape and dimension. The surface of an unreacted pellet was smooth and relatively nonporous whereas a partially-reacted pellet exhibited a porous surface, as seen in the micrographs (x 4) in Figure 2, where the initial carbon concentrations were 23.1 and 31.4 wt % for Figure 2a and 2b, respectively. As seen the surface is less porous in the latter due to the higher carbon content. Also seen in these micrographs is the presence of unreacted zirconium dioxide in the bottom hemisphere in larger concentration than in the top where the temperature (hence the rate of reaction) was the highest.

Microscopic examinations of partially-reacted sectioned pellets showed a zirconium dioxide concentration gradient from the surface to the center of the pellet. The degree of this radial variation of the concentration was influenced by the reaction temperature, being less pronounced at low temperatures and more apparent at high temperatures. The progress of the reaction approached the shrinking-core type of behaviour (Levenspiel, 1972), (Szekely et al., 1976) at high temperatures, yielding almost a sharp interface between reacted and unreacted regions. This is illustrated

FIGURE 2

MICROGRAPHS (x 4) OF PARTIALLY-REACTED PELLETS

(0.826 cm DIAMETER)

		(a)	(b)
Reaction Temperature	(K)	1830	1830
Conversion	(%)	80.6	58.5
Initial Carbon Concentration	(wt%)	23.1	31.4

(a)

(b)

in Figures 3 and 4, which show micrographs (x 4) of typical sectioned partially-reacted pellets of the same diameter (0.826 cm) and the same initial carbon concentration (42.5 wt %). The pellets shown in Figure 3 were all reacted at 1540 K and those shown in Figure 4 at 1680 K but in each case to different conversions (3a to 28.7%, 3b to 44.6%, 3c to 87.1%, and 4a to 36.9%, 4b to 61.9, 4c to 87.1%).

As seen in these micrographs, the reacted region in each case is not truly free from zirconium dioxide, but the pellets reacted at high temperature (Figure 4) have relatively less unreacted zirconium dioxide left in the so-called 'ash-layer.' Although diffusion resistance through the ash layer becomes apparent at relatively high temperatures, this does not seem to be the rate-controlling factor for the given temperature range due to the highly porous nature of the reacted layer. The main contributor to the progress of the reaction is most probably the role of carbon, specifically the degree of contact between the carbon and the oxide particles. The presence of unreacted zirconium dioxide particles near the external surface of the pellets which have reacted to a conversion of 87% (Figures 3c and 4c) may substantiate this view. The comparison of the distribution of the zirconium dioxide particles in the partially-reacted pellets shown in Figures 3 and 4 may also suggest that the degree of contact is less important at high reaction temperatures, based on the fact that in the latter figure the ash layer contains relatively less unreacted zirconium dioxide. The foregoing discussion was supported by the experimental conversion-time data which are presented in the next section.

FIGURE 3

MICROGRAPHS (x4) OF PARTIALLY-REACTED SECTIONED PELLETS

Carbon Concentration	-	42.5 wt %
Pellet Diameter	-	0.826 cm
Reaction Temperature	-	1540 K
a) Conversion	-	28.7 wt %
b) Conversion	-	44.6 wt %
c) Conversion	-	87.1 wt %

(a)

(b)

(c)

FIGURE 4

MICROGRAPHS (x4) OF PARTIALLY-REACTED SECTIONED PELLETS

Carbon Concentration	-	42.5 wt %
Pellet Diameter	-	0.826 cm
Reaction Temperature	-	1680 K

a)	Conversion	-	36.9 wt %
b)	Conversion	-	61.9 wt %
c)	Conversion	-	87.1 wt %

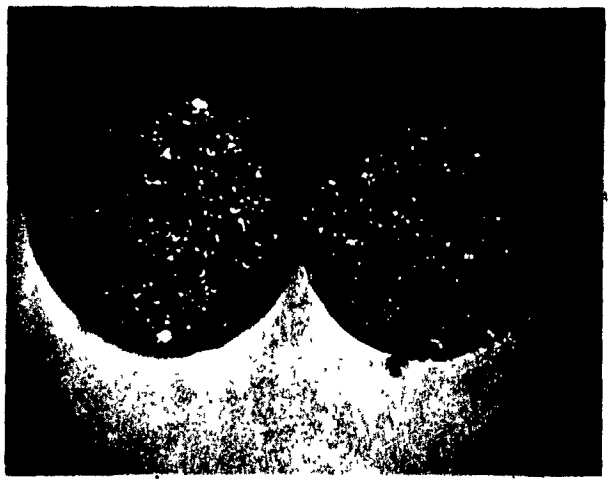

(a)

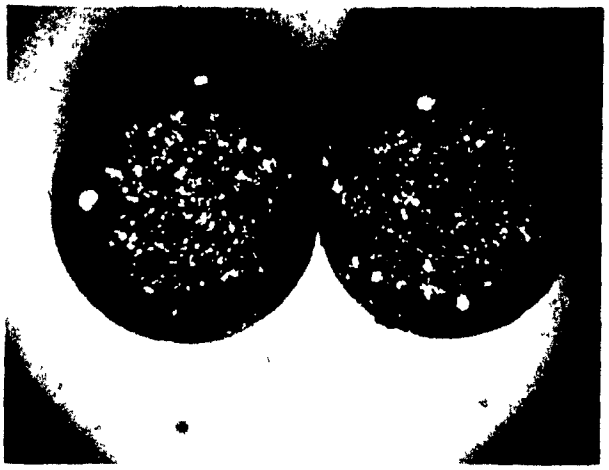

(b)

(c)

Conversion-Time Relationship

The discussion in the previous section led to the conclusion that the chlorination of zirconium dioxide-carbon pellets does not progress according to the shrinking-core model, that is, on a sharp reaction front, but rather that it takes place in an enlarging zone beginning from the pellet surface. The thickness of this zone and the concentration gradient of the zirconium dioxide in it changes with the reaction time and the temperature level. Based on these observations, the overall consumption of the ZrO_2 with time, under chemical-reaction control, has been represented by the logarithmic expression given by Equation (11) developed earlier.

A number of pellets of equal diameter and carbon concentration were reacted at a constant temperature for different lengths of time in order to verify the applicability of Equation (11). The experimental conversion-time data at different temperature levels are given in Figure 5. The mean carbon concentration of the pellets used in this series of experiments was 23.1 wt %. It is seen that the plots of time versus $-\ln(1-X)$ holds a linear relationship as expected, but only to a certain conversion level beyond which the rate of conversion is less than the model predictions. The fractional conversion at which the deviation from the logarithmic model occurs increases with the temperature. At 1440 K, the deviation starts at about 60% conversion and the reaction almost stops, whereas at 1660 K it takes place at 95% conversion and the reaction continues at a slower rate. From the fact that mass

FIGURE 5

CONVERSION-VERSUS-REACTION TIME AS

A FUNCTION OF TEMPERATURE

Carbon Concentration - 23.1 wt %

Pellet Diameter - 0.826 cm

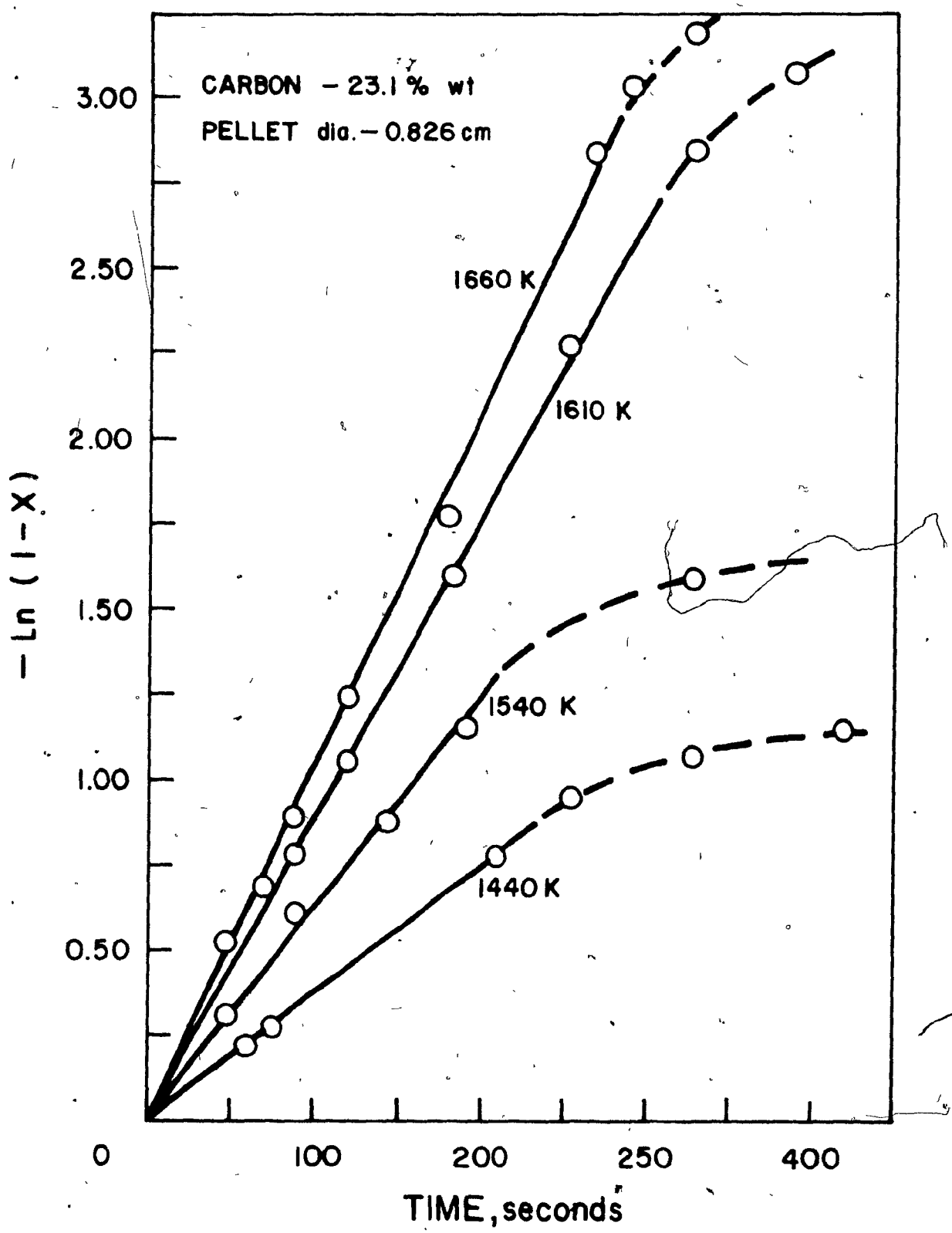
CARBON – 23.1 % wt
PELLET dia. – 0.826 cm
1660 K
1610 K
1540 K
1440 K
3.00
2.50
2.00
1.50
1.00
0.50
0
100
200
250
400
– Ln (1 – X)
TIME, seconds

transfer resistance through the ash layer theoretically becomes significant at high temperatures, e.g., at high reaction rates, one would expect the deviation from a chemical reaction control to occur at lower conversion levels as the temperature increases, if an ash diffusion resistance were influencing the progress of the reaction. Since in the present case the opposite is observed, an ash diffusional resistance may not be the influencing factor. This conclusion was supported by the micrographs of the sectioned partially-reacted pellets which contained unreacted zirconium dioxide near the external surface of the pellet at even 87% conversion (Figures 3c and 4c).

Figure 6 shows conversion-time data for pellets under conditions similar to those of Figure 5, but with a much higher carbon concentration of 42.5 wt %. The results are entirely different. No deviation from the logarithmic model takes place at all levels of temperature, for the fractional conversions covered in Figure 5. These results, together with the microscopic examination of the partially-reacted pellets, may suggest that a limiting distance between the zirconium dioxide and the carbon particles, which is a minimum in the fresh pellet and increases as the reaction progresses, is influencing the rate of chlorination. With higher initial carbon concentration, a higher degree of contact between the oxide and the carbon particles is possibly achieved at all times during the reaction. Thus the rate of conversion does not drop as

FIGURE 6

CONVERSION-VERSUS-REACTION TIME AS

A FUNCTION OF TEMPERATURE

Carbon Concentration - 42.5 wt %

Pellet Diameter - 0.826 cm

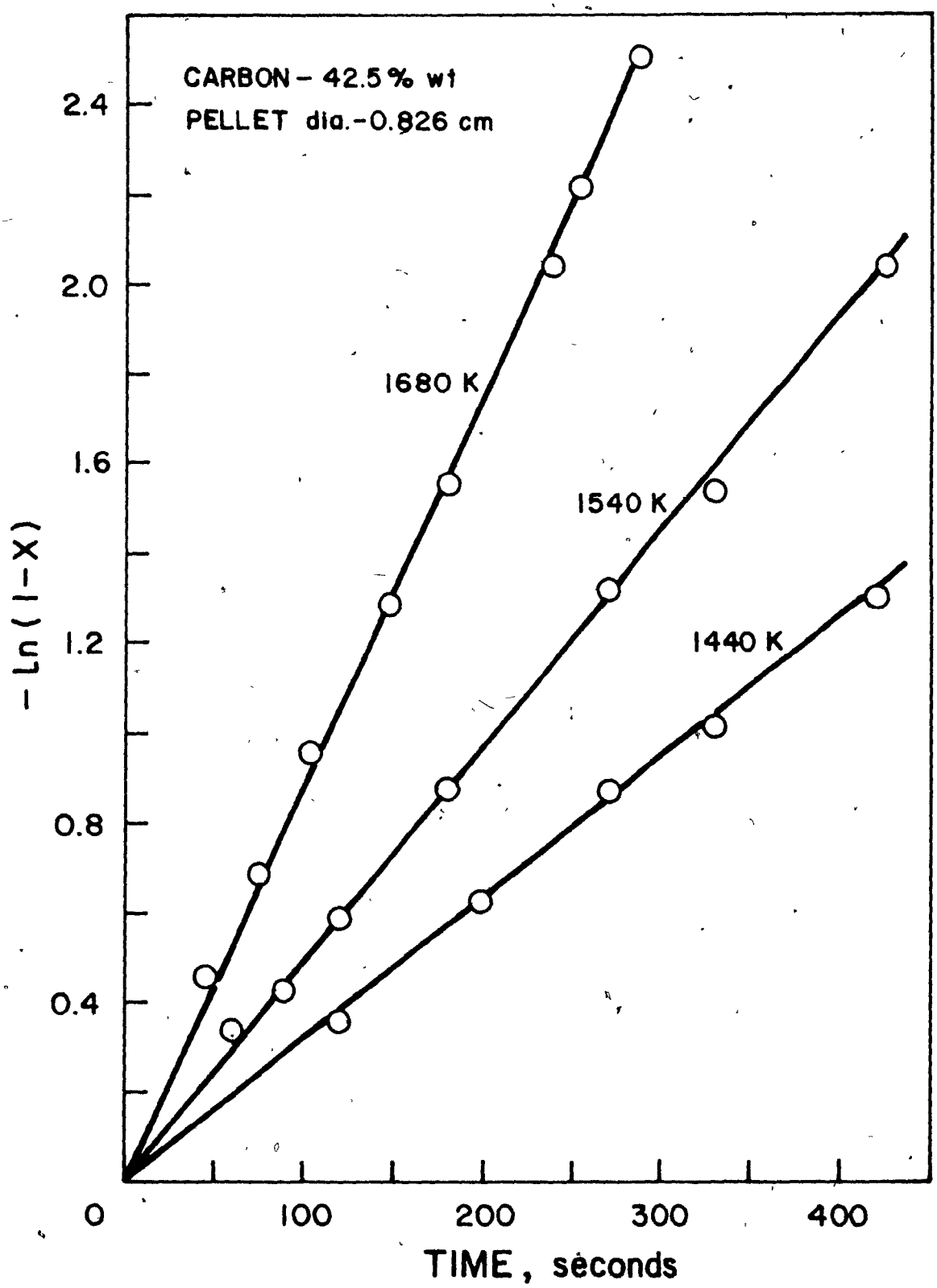
CARBON – 42.5% wt
PELLET dia.-0.826 cm
1680 K
1540 K
1440 K
2.4
2.0
1.6
1.2
0.8
0.4
0
100
200
300
400
– Ln (1–X)
TIME, seconds

the reaction progresses. As the mobility of the solid constituents of the pellet increases with temperature, the influence of the distance on the rate of conversion becomes less pronounced and approaches zero.

These important findings are supported by the work of Bergholm (1961) who studied the chlorination of titanium dioxide-carbon mixtures in both compacted and loose forms. Based on microscopic examinations, Bergholm concluded that direct contact between the grains was not required but a distance less than about 200 microns was necessary for the chlorination to proceed. He also found that the chlorination rate of compacted mixture was higher than that of loose mixture, but the difference in the rates of conversion decreased with increasing temperature, in agreement with the present work. Bergholm confirmed the importance of the close distance between the oxide and the carbon surfaces by further treating the residue of an experiment in which the reaction had stopped after a certain amount of conversion. The reaction could be carried out further after the residue had been thoroughly mixed. However, addition of more carbon did not cause a greater increase in the reaction rate than did mixing of the residue without new carbon.

The kinetic data reported by O'Reilly et al. (1972) who studied the chlorination of zirconium dioxide-carbon uncompacted mixture (1:4 wt ratio), also showed a drop in the rate of chlorination after a certain amount of conversion. Deviation from their model (shrinking-core) predictions occurred at a conversion

level as low as 30% (at 1000 K) even with the high carbon concentration they used.

Influence of Temperature

The effect of temperature on the rate of chlorination of zirconium dioxide-carbon compacts was studied with pellets of 0.826 cm in diameter in the range between 1400 and 1950 K. Since the conversion was based on the zirconium dioxide content of a pellet being as small as 57.5 wt %, pellets of smaller diameter would necessitate handling very small quantities of unreacted zirconium dioxide which would reduce the accuracy of the conversion measurements. Pellets of larger diameter, on the other hand, would experience a larger temperature gradient on the pellet. Thus the choice of 0.826 cm diameter was an optimum one and it was used for the majority of the experiments. The upper temperature was limited by the maximum power to the torch, by the arcing that took place between the plasma and the torch nozzle, and also by the excessive heating of the nozzle with consequent attack by the hot chlorine, whereas the lower temperature was that at which the chlorine plasma could be maintained at a given gas flow rate with a minimum power input, for a maximum distance from the nozzle exit (about 6 cm) at which a pellet could be viewed.

As in Part I of this study, the choice of the temperature levels was dictated by the plasma behaviour, that is, its stability and reproducibility. The overall rate constants corresponding to the linear portion of $-\ln(1-X)$-versus-time data were plotted according

to an Arrhenius-type relationship in Figures 7, 8 and 9 for pellets having initial carbon concentrations of 23.1, 31.4 and 42.5 wt %, respectively. The experimental data for each of these cases plus the results of another smaller number of runs with pellets of 18.0 and 20.0 wt % of carbon are presented in Tables A, B, C and D of Appendix V. When more than one set of conversion-time data at a constant temperature were available, the overall rate constant used in the Arrhenius plots were obtained from the slopes of the straight lines by least-squares fit. The results of these analyses are given in Table II.

The Arrhenius plots in Figures 7-9 show two separate temperature regions. Up to about 1700 K (the straight line portion), the reaction rate is sensitive to temperature, thus suggesting a chemical reaction controlling region. At temperatures higher than this, the rate is relatively insensitive to the temperature rise, showing that a physical factor (ash-diffusion) starts to influence the rate. As also seen in these figures, temperature sensitivity of the rate in the region above 1700 K decreases with increasing carbon concentration (in the order from Figures 7 to 9) due to a corresponding decrease in void fractions of the ash layer which raises the mass transfer resistance.

The data in these figures below 1700 K (corresponding to the chemical reaction-controlling region) were used in a multiple regression analysis using a statistical package program (STATPK, McGill University Computing Centre), in order to obtain the value

FIGURE 7

ARRHENIUS PLOT OF REACTION BETWEEN

ZrO_2-C MIXTURE AND CHLORINE

Carbon Concentration = 23.1 wt %

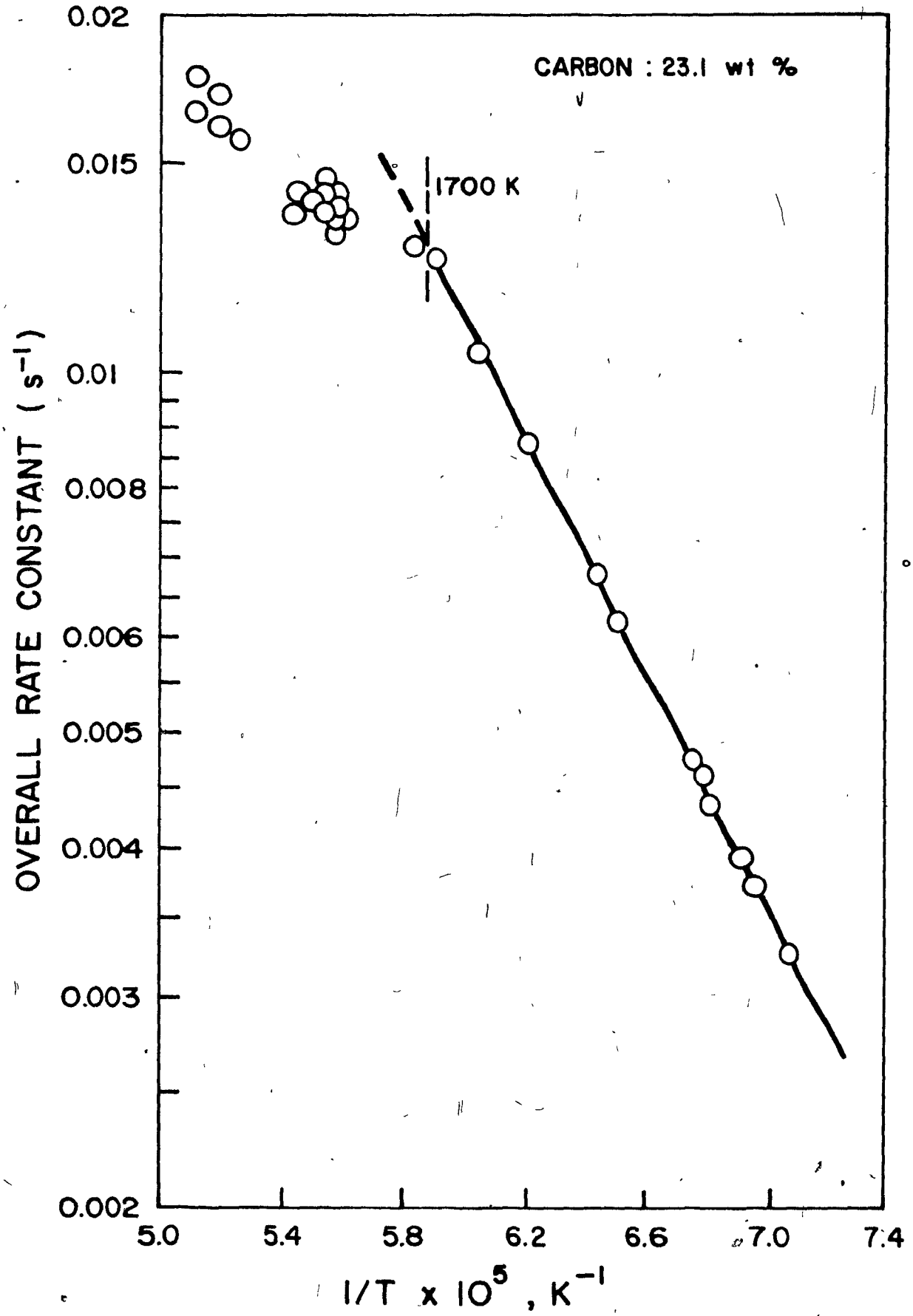
CARBON : 23.1 wt %
1700 K
OVERALL RATE CONSTANT (s⁻¹)
0.02
0.015
0.01
0.008
0.006
0.005
0.004
0.003
0.002
5.0
5.4
5.8
6.2
6.6
7.0
7.4
1/T x 10⁵ , K⁻¹

FIGURE 8

ARRHENIUS PLOT OF REACTION BETWEEN

ZrO_2-C MIXTURE AND CHLORINE

Carbon Concentration = 31.4 wt %

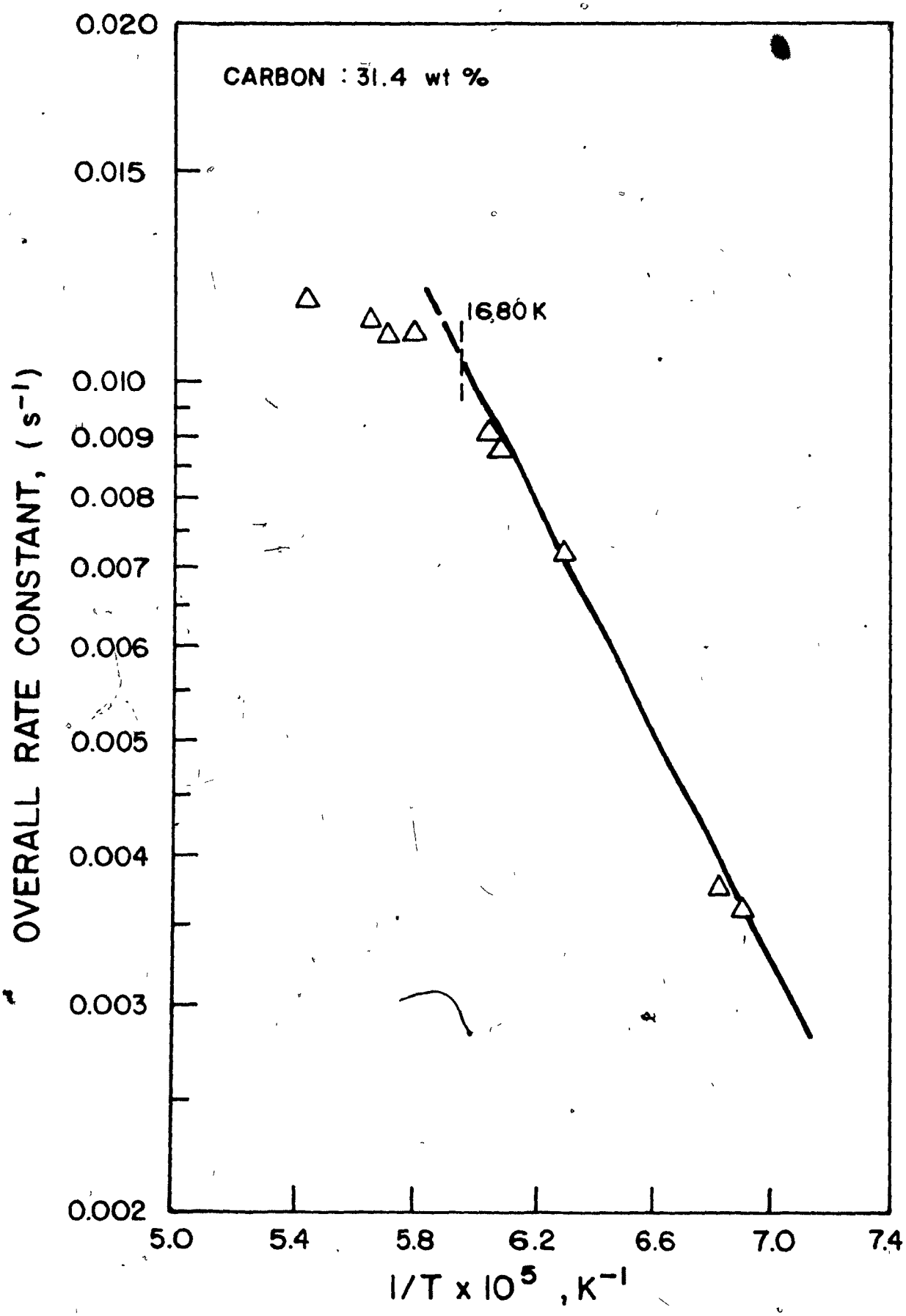
CARBON : 31.4 wt %
16,80 K
OVERALL RATE CONSTANT, (s⁻¹)
0.020
0.015
0.010
0.009
0.008
0.007
0.006
0.005
0.004
0.003
0.002
5.0
5.4
5.8
6.2
6.6
7.0
7.4
1/T x 10⁵ , K⁻¹

FIGURE 9

ARRHENIUS PLOT OF REACTION BETWEEN

ZrO_2-C MIXTURE AND CHLORINE

Carbon Concentration = 42.5 wt %

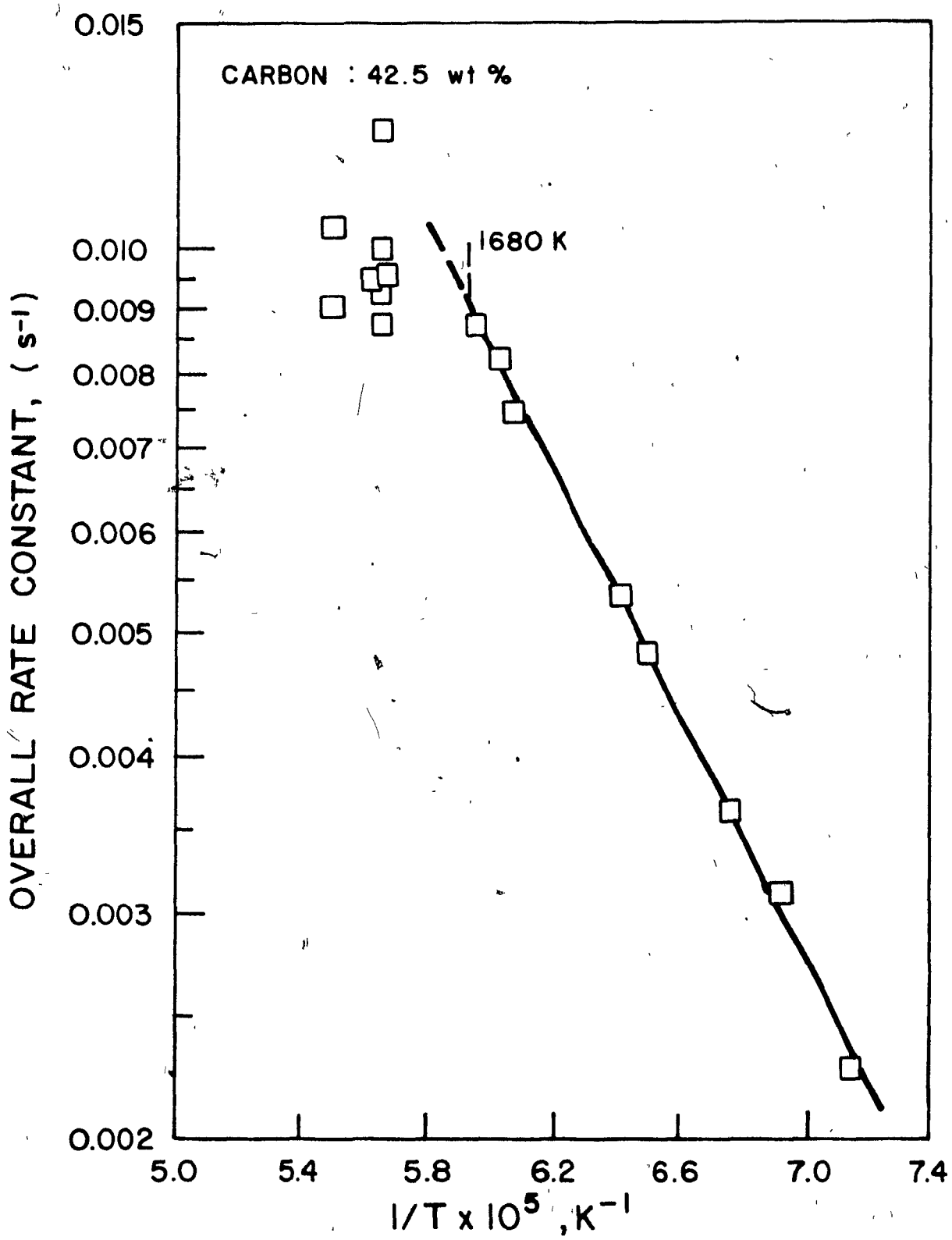
CARBON : 42.5 wt %
1680 K
OVERALL RATE CONSTANT, (s-1)
0.015
0.010
0.009
0.008
0.007
0.006
0.005
0.004
0.003
0.002
5.0
5.4
5.8
6.2
6.6
7.0
7.4
1/T x 10^5 , K^-1

TABLE II

OVERALL RATE CONSTANT FROM THE SLOPE OF $-\ell n(1-X)$ VERSUS t

Carbon (wt %)	Pellet Diameter (cm)	Temperature (K)	Number Of Data Points In Linear Portion	Overall Rate Constant $K \times 10^5$ (sec^{-1})
23.1	0.826	1440	4	371
23.1	0.826	1480	2	486
23.1	0.826	1540	4	618
23.1	0.826	1550	3	678
23.1	0.826	1610	5	877
23.1	0.826	1660	7	1045
23.1	0.826	1690	2	1245
31.4	0.826	1585	3	719
42.5	0.826	1440	5	311
42.5	0.826	1535	7	480
42.5	0.826	1560	2	531
42.5	0.826	1680	8	869
23.1	0.671	1480	2	480
23.1	0.671	1500	3	530
23.1	0.671	1690	2	1210
23.1	0.671	1810	2	1750
23.1	0.671	1840	2	2050
23.1	1.000	1640	2	850
23.1	1.000	1650	2	940

of the activation energy together with the chlorine and carbon concentration dependence which will be discussed separately. The least squares fit yielded an activation energy of 93.325 ± 1.272 kJ/mole (22.300 ± 0.304 kcal/mole) with a corresponding partial correlation coefficient of 0.993. The straight lines in Figures 7-9 are the resulting regression lines which fitted the rate data corresponding to each carbon concentration level perfectly well. The fact that the values of the activation energy (the slopes of the Arrhenius plots) did not change with increasing carbon content of the pellets confirmed the absence of ash diffusion resistance in this region. Since a higher carbon concentration means a reacted layer of lesser void fraction, a smaller activation energy value would have resulted with the pellets of 42.5% carbon content if there had been a mass transfer resistance through the reacted layer. This was also supported by the microscopic examination of the sectioned partially-reacted pellets as discussed earlier. A different set of experimental data confirming the above conclusion will be discussed subsequently.

Ash Diffusion Versus Pellet Diameter

As mentioned earlier in the development of the conversion-time relationship, the overall rate constant, $\underline{K}$, as defined by Equation (8), was not expected to be influenced by the change in pellet diameter under chemical reaction control. Accordingly, an Arrhenius plot of the rate constants of different pellet diameters is expected to yield a single straight line, if ash diffusion is not contributing. Otherwise, the overall rate constant would decrease

with increasing pellet diameter due to a corresponding increase in the diffusion resistance.

In order to confirm that the value of the activation energy reported in the previous section was an intrinsic one, a number of kinetic runs were carried out with pellets of 1.000 and 0.671 cm in diameters, in addition to that of 0.826 cm used in the previous experiments. The kinetic data of these runs are presented in Tables E and F of Appendix V. Figure 10 includes Arrhenius plots for the three pellet diameters. As seen, the data for both 0.826 and 0.671-cm pellet diameters fell on the same line, up to about 1700 K, and had the same activation energy value (93.325 kJ/mole). Furthermore, ash diffusion did not start to influence the rate up to about 1850 K with the pellet of 0.671-cm diameter, whereas deviation from chemical reaction control began at a relatively lower temperature (about 1700 K) with the larger pellet diameter (0.826 cm), in agreement with the ash diffusion phenomenon. On the other hand, the value of the overall rate constant for the pellets of 1.00-cm diameter was lower than those with smaller diameters at all temperature levels. All of these observations confirm the conclusion previously stated. That is, ash diffusion was not contributing to the progress of the reaction when the reacting pellet diameters were 0.826 cm and smaller, and thus the reported activation energy was an intrinsic value.

Influence of Chlorine Concentration

The experiments to determine the effect of chlorine partial

FIGURE 10

ARRHENIUS PLOT OF REACTION BETWEEN ZrO_2-C MIXTURE AND CHLORINE FOR DIFFERENT PELLET DIAMETERS

Carbon Concentration = 23.1 wt %

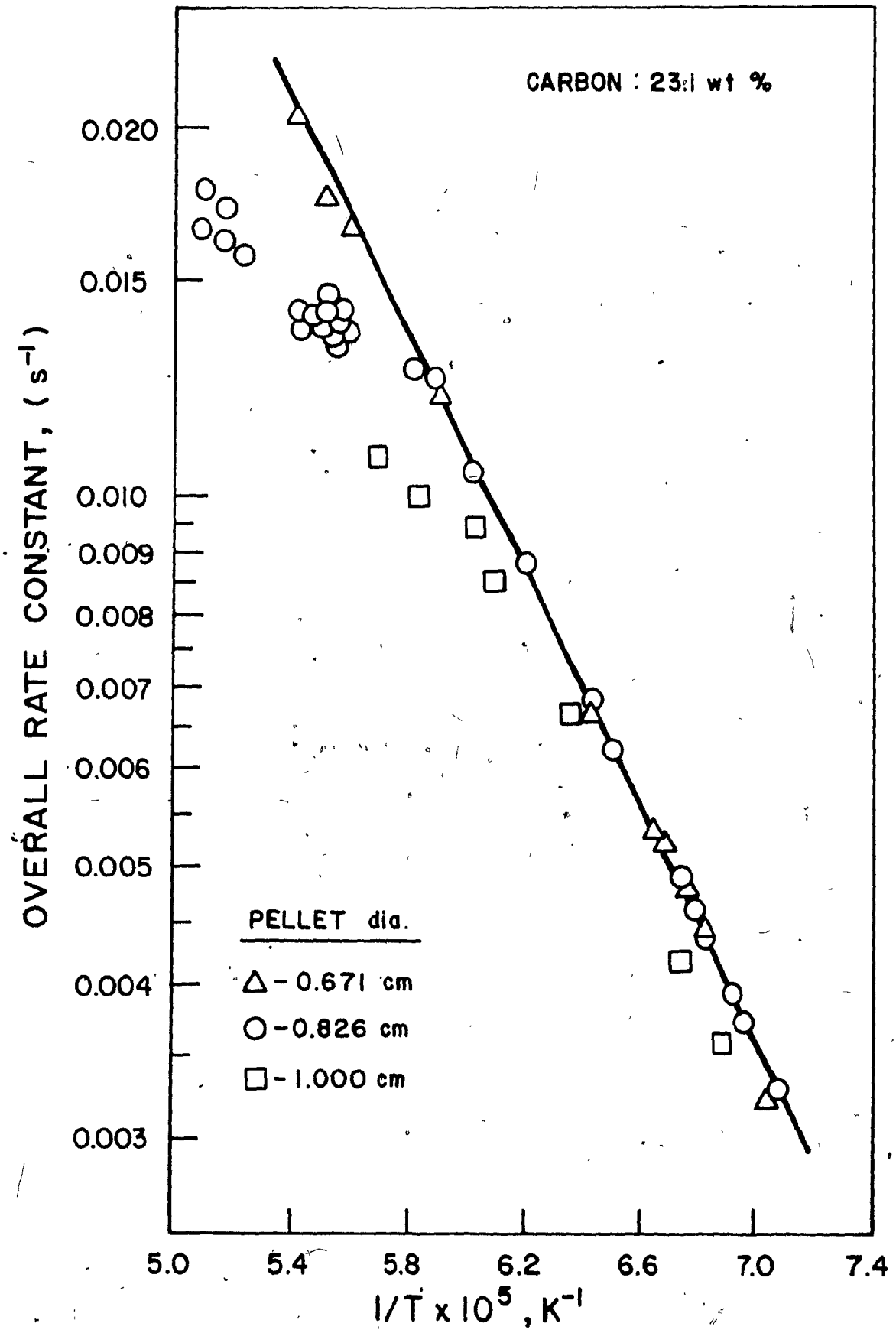
CARBON : 23.1 wt %
0.020
0.015
0.010
0.009
0.008
0.007
0.006
0.005
0.004
0.003
OVERALL RATE CONSTANT, (s^{-1})
PELLET dia.
△ - 0.671 cm
○ - 0.826 cm
□ - 1.000 cm
5.0
5.4
5.8
6.2
6.6
7.0
7.4
$1/T \times 10^5$, K^{-1}

pressure on the overall rate constant were performed with pellets of 0.826-cm diameter containing 23.1 wt % carbon. Chlorine gas was diluted with argon in both the radial and the swirl flows of the torch in the same proportion, to ensure uniform mixing. An attempt was made to react the pellets at the same temperature, but this required a considerable trial-and-error approach in finding the appropriate power input and pellet position at different concentration levels. Although this was achieved in some cases, on the whole the temperature varied from run to run. Hence the analysis was done by correcting the overall rate constant for the temperature by using the value of the activation energy reported earlier. The experimental data of these runs are presented in Table G of Appendix V, and in their corrected form in Figure 11.

The regression analysis of these data together with the rest of the data presented earlier resulted in an exponent of 0.79 ± 0.03 for the mole fraction of molecular chlorine, y_{Cl_2}, indicating that the order of the reaction with respect to the chlorine concentration is 0.79.

The fractional order of the reaction found in this study agrees with the order of metal oxide chlorinations reported in the Literature. An order of 0.64 and 1.0 was reported by O'Reilly et al. (1972) and Landsberg et al. (1972), respectively, for the chlorination of zirconium dioxide. Seryakov et al. (1970) found the order of TiO_2 chlorination varied from 0.63 to 0.71 with respect to the type of carbon used. For the chlorination of the same oxide,

FIGURE 11

EFFECT OF CHLORINE CONCENTRATION

ON THE RATE

Carbon Concentration = 23.1 wt %

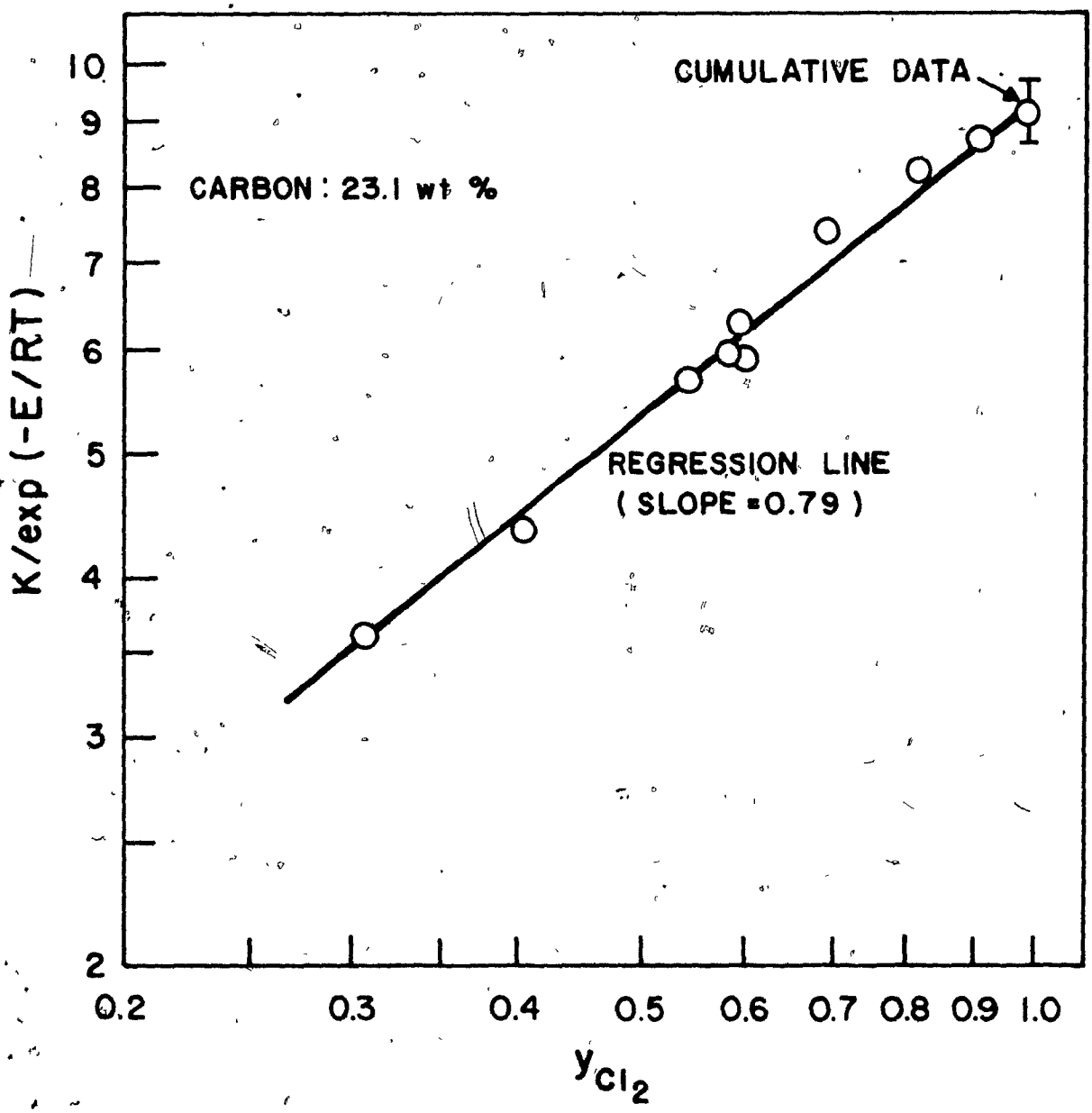
CUMULATIVE DATA
CARBON : 23.1 wt %
REGRESSION LINE
(SLOPE = 0.79)
K/exp (-E/RT)
10
9
8
7
6
5
4
3
2
0.2
0.3
0.4
0.5
0.6
0.7
0.8
0.9
1.0
y_{Cl_2}

Morris and Jensen (1976) found an order of 0.69, whereas Masterova and Levin (1973) reported a range between 0.62 and 0.87.

Influence of Carbon Concentration

Analysis of the kinetic data with respect to the carbon concentration was based on the carbon content of the individual pellets, rather than the average values of the five concentration groups discussed earlier. The experimental runs covered a carbon concentration range between about 17.5 and 45 wt %. The lower limit was the one close to the amount required by the reaction stoichiometry, (16.3 wt %, Equation 4). As in the previous cases, only those data corresponding to the straight line portion of the time-conversion expression (Equation 11) were considered.

The overall rate constants were corrected for temperature using the previously-obtained activation energy value, and were then plotted in Figure 12 in their corrected form against the pellet carbon concentration. The data were best fitted by an expression of the following form:

$$K/\exp(-E/RT) = 4.17/x_c^{0.696}\exp(0.0029/x_c^3) \qquad (16)$$

where $\underline{K}$ is the overall rate constant, $\underline{E}$ is the activation energy, $\underline{T}$ is the pellet temperature, $\underline{x_c}$ is the weight fraction of carbon in the pellet. The resulting regression curve is also plotted in Figure 12. The rate of chlorination is seen to be highest within a certain carbon concentration range. Outside of this range, any increase or decrease in the carbon content of the pellet reduces

FIGURE 12

EFFECT OF CARBON CONCENTRATION ON THE RATE

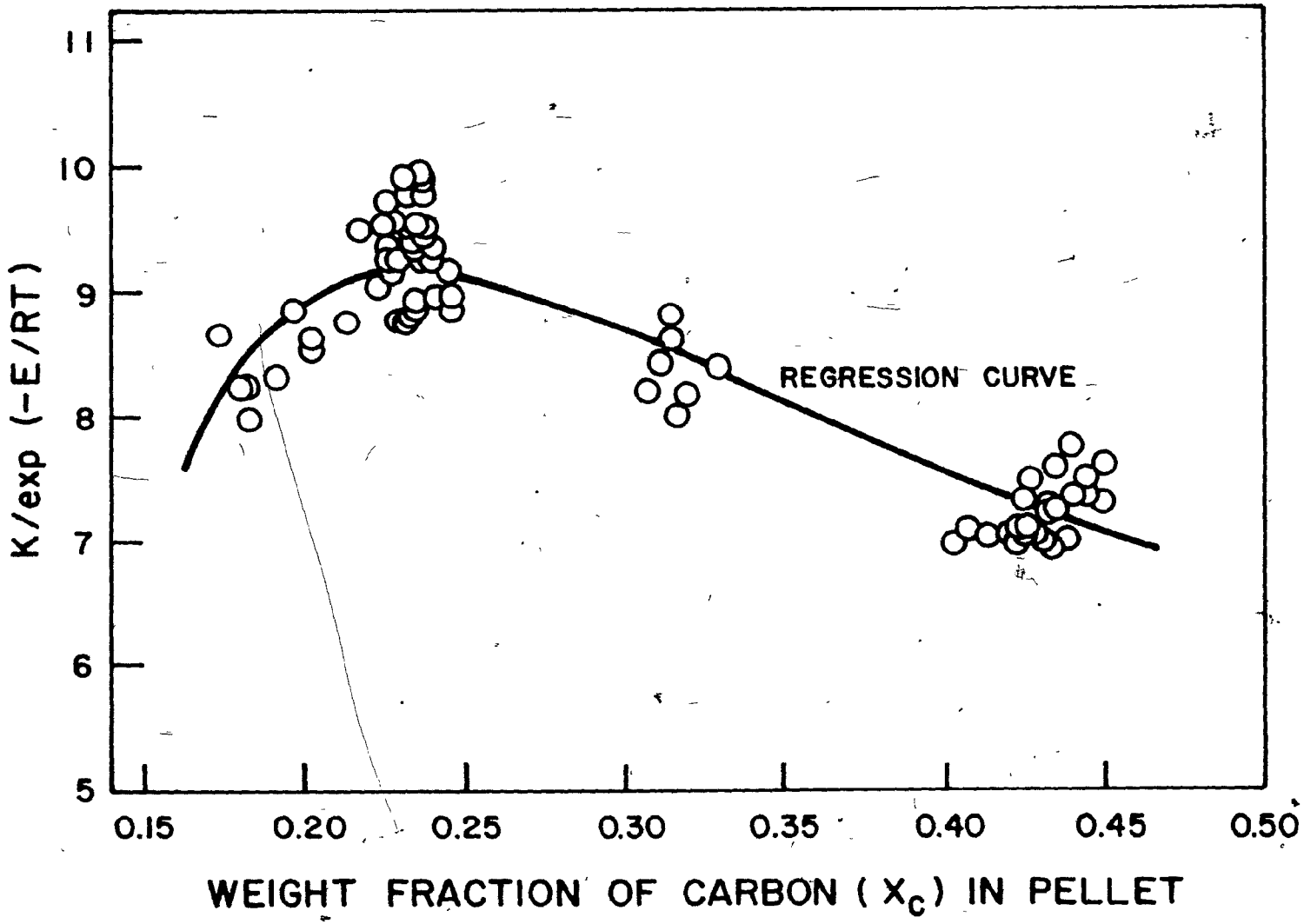
K/exp (-E/RT)
11
10
9
8
7
6
5
0.15
0.20
0.25
0.30
0.35
0.40
0.45
0.50
REGRESSION CURVE
WEIGHT FRACTION OF CARBON (X_c) IN PELLET

the rate. This observation may be attributed to the existence of an optimum ratio of zirconium dioxide-to-carbon in the original mix, yielding a maximum contact area per unit volume, and consequently a maximum chlorination rate. This ratio depends on the relative sizes and shape of the solid particles. For example, if the zirconium dioxide and the carbon particles are both spherical and of equal size, the carbon content corresponding to equal volumes of both gives the maximum contact area per unit volume of a pellet.

Since the results presented above were based on the data corresponding to the straight line portion of the time-conversion relationship presented earlier, the foregoing discussion should be interpreted with caution. A drop in the rate of conversion (deviation from Equation 11 as presented in Figure 5) may take place when the distance between the oxide and the carbon particle surfaces increases to a critical value after a certain amount of conversion (the level of which increases with the reaction temperature). Therefore, the range of carbon concentration yielding the highest conversion rate in Figure 12 is valid either for low conversion levels if the temperature is low, or up to high conversion levels if the reaction is carried out at high temperatures (for complete conversion at about 1700 K). In other words, a decrease in the reaction temperature should be compensated by a higher carbon content in the pellet in order to maintain the conversion rate predicted by Equation (11).

Rate Expression for Chemical Reaction Control

From the theoretical formulation and the regression analysis of the complete experimental data presented up to now, the following empirical expression for the rate of zirconium dioxide chlorination with chlorine in the presence of carbon has been developed:

$$-\ln(1-X) = 4.17\exp(-11223/T)y_{Cl_2}^{0.79}t/x_c^{0.696}\exp(0.0029/x_c^3) \quad (17)$$

where X is the fraction of zirconium dioxide reacted at time t (sec), T is the reaction temperature, y_{Cl_2} is the chlorine concentration in the bulk gas, x_c is the weight fraction of carbon in the mix. The multiple correlation coefficient of 0.993 and a probability associated with 'F' value being unity indicates that the excellent fit was not due to chance.

Figure 13 shows the experimental and the predicted (from Equation 17) reaction times for the chemical reaction-controlled region, not deviating from the logarithmic model. As can be seen, Equation (17) represents the experimental data fairly well. The scatter, being within ± 10% of the reaction time, seems to be reasonable for a chlorine plasma system.

CONCLUSION

1- The kinetics of the chlorination of compacts of zirconium dioxide and carbon were studied in the temperature range of 1400 - 1950 K in a radio-frequency chlorine plasma tailflame.

FIGURE 13

COMPARISON OF EXPERIMENTAL REACTION TIME

WITH VALUES PREDICTED FROM EQUATION (17)

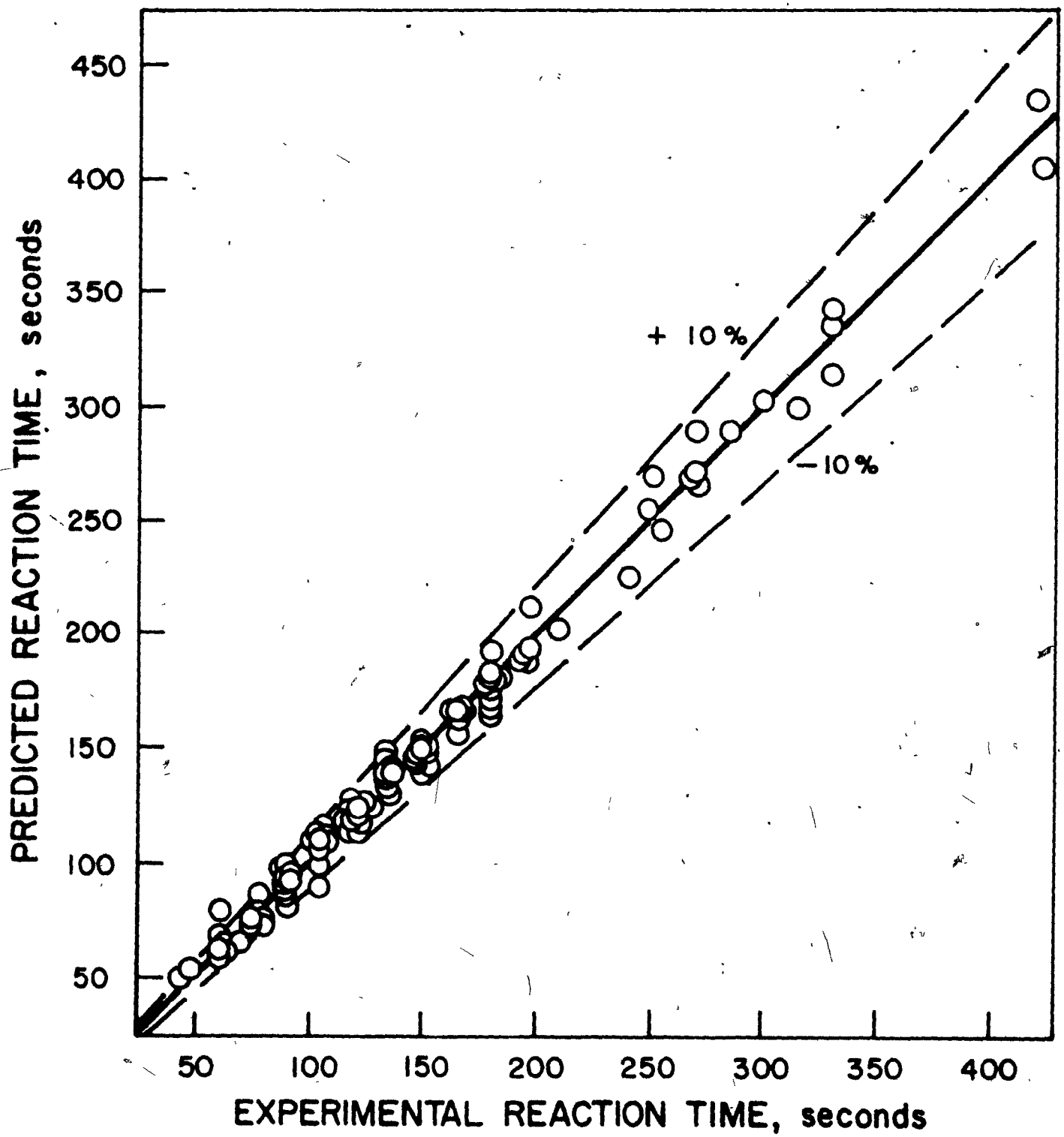
PREDICTED REACTION TIME, seconds
450
400
350
300
250
200
150
100
50
+ 10 %
−10 %
50
100
150
200
250
300
350
400
EXPERIMENTAL REACTION TIME, seconds

Influences of time, temperature, chlorine concentration and pellet carbon content on the rate were determined experimentally, using a single stationary pellet composed of zirconium dioxide and graphite particles.

2- The microscopic examination of sectioned partially-reacted pellets showed that the reaction did not progress according to the shrinking-core model but rather that it took place in an enlarging reaction zone beginning from the pellet surface. The presence of unreacted zirconium dioxide particles near the external surface of pellets (reacted up to about 90% conversion) suggested the importance of a close distance between the oxide and the carbon particles for the progress of the reaction.

3- The overall consumption of zirconium dioxide with time under chemical reaction control was represented by a logarithmic expression (Equation 11) based on the volumetric reaction model. For pellets having a carbon concentration less than about 32 wt %, the rate of conversion was less than the model predictions above a conversion level which increased with the reaction temperature. The pellets of higher carbon concentrations showed no such deviations. This behaviour was attributed to the limit imposed on the reaction rate by the degree of contact between the constituent particles, as was also indicated by the microscopic examinations of partially-reacted pellets. Ash diffusion resistance could not be the reason for the above behaviour, since it would have caused a lower rate of conversion than the model predictions for the pellets of high carbon

concentrations, rather than low ones due to the lower ash layer porosity associated with the former.

4- The Arrhenius plots of the experimental data indicated the existence of an ash diffusion resistance above about 1700 K (for a pellet diameter of 0.826 cm), below which the rate was controlled by chemical reaction. The value of the activation energy (93.325 kJ/mole) obtained for the latter region did not change with the pellet carbon content (hence with the porosity of the reacted layer) which supported the conclusion with respect to the controlling mechanism (e.g., absence of ash diffusion resistance below 1700 K).

5- The role of ash diffusion on the rate of chlorination was further confirmed by the Arrhenius plots of rate constants for different pellet diameters. The pellets of 0.671 and 0.826 cm yielded the same rate constants below 1700 K, whereas those of 1.00 cm diameters resulted in the lower rate constants at all temperature levels (>1400 K), showing that mass transfer started to contribute when the pellet diameter was larger than 0.826 cm. Furthermore, in agreement with the mass transfer phenomena, the pellets of 0.671 cm did not deviate from the Arrhenius straight line up to about 1850 K (in comparison with 1700 K with the pellets of 0.826 cm).

6- The order of reaction with respect to the molecular chlorine concentration was 0.79.

7- Influence of carbon concentrations on the chlorination rate was expressed by a functional relationship given by Equation

(16). Experimental data indicated the existence of an optimum ratio of the zirconium dioxide and the carbon in the original mix yielding a maximum contact area per unit volume, consequently, a maximum chlorination rate.

8- The empirical expression given by Equation (17) for the chlorination rates of zirconium dioxide-carbon compacts represented the experimental data (those having no deficiency in oxide-carbon contact area) reasonably well.

9- The results obtained in this work suggest that:

a- When low carbon concentration is used, the chlorinator should be operated at high temperatures (∿1700 K), so that the limiting oxide-carbon distance required for the progress of the reaction would be tolerable enough not to affect the rate.

b- Any reduction in chlorinator temperature should be compensated by an increase in initial carbon content of the pellet, so that the degree of contact between the oxide and the carbon particles would be maintained at all times.

c- Chlorination of dense compacts of fine-grained zirconium dioxide and carbon should be preferred over that of loose stationary mixtures for low temperature operations.

d- Since the contact between the oxide and carbon is less critical at high temperatures (∿1700 K), a fluidized bed reactor may be a more natural choice (to eliminate ash diffusion resistance). A fluidized bed operation below 1700 K may require higher carbon-to-zirconium dioxide ratio than the operation with compacts for the same reaction rate.

NOMENCLATURE

NOMENCLATURE

E	–	Activation energy
e	–	Spectral emissivity at wavelength λ
f_1	–	Functional relationship for x_c
f_2	–	Functional relationship for y_{Cl_2}
K	–	Overall rate constant
k	–	Intrinsic rate constant
M	–	Molecular weight
R	–	Gas constant
T	–	Reaction temperature; pellet blackbody temperature
T_b	–	Pellet brightness temperature (pyrometer reading)
t	–	Reaction time
W	–	Weight of unreacted ZrO_2 at time t
W_p	–	Total weight of pellet at time t
X	–	Weight fraction of ZrO_2 reacted at time t
x_i	–	Initial weight fraction of solid component i in pellet
y_i	–	Mole fraction of gaseous component i in bulk gas

Greek Letters

λ	–	Wavelength

Subscripts

c - Carbon

Cl_2 - Chlorine

f - Final

o - Initial

p - Pellet

ZrO_2 - Zirconium dioxide

REFERENCES

REFERENCES

Bergholm, A., 'Chlorination of Rutile,' Trans. Metall. Soc. AIME, 221, 1121 (1961)

Branstetter, J.R., 'Some Practical Aspects of Surface Temperature Measurement by Optical and Ratio Pyrometers,' NASA TN D-3604, (1966)

Dunn, W.E. Jr., 'High-Temperature Chlorination of TiO_2 Bearing Minerals,' Trans. Metall. Soc. AIME, 218, 6 (1960)

Ketov, A.N., Gaisinovich, M.S., Burmisurova, E.V., Fedorov, A.A., and Shlingerskii, A.S., 'Mechanism of Chlorination of Metal Oxides in the Solid State,' Chem. Abs., 83 : 103907, (1974)

Ivashentsev, Ya. I., Gol'tsova, T.F. and Bezgreshaya, N.P., 'Chlorination of Thorium Dioxide in Trichloro-Methane Vapor,' J. Appl. Chem. USSR, 48, (11), 2543 (1975)

Landsberg, A., 'Chlorination Kinetics of Aluminum Bearing Minerals,' Metall. Trans., 6B, 207 (1975)

Landsberg, A., 'Some Factors Affecting the Chlorination of Kaolinic Clay,' Metall. Trans., 8B, 435 (1977)

Landsberg, A., Hoatson, C.L., and Block, F.E., 'The Chlorination Kinetics of Zirconium Dioxide in the Presence of Carbon and Carbon Monoxide,' Metall. Trans., 3, 517 (1972)

Levenspiel, O., Chemical Reaction Engineering, 2nd Ed., John Wiley and Sons, New York, 357 (1972)

Manieh, A.A., and Spink, D.R., 'Chlorination of Zircon Sand,' Can. Metall. Quart., 12, (3), 331 (1973)

Manieh, A.A., Scott, D.S., and Spink, D.R., 'Electrothermal Fluidized Bed Chlorination of Zircon,' Can. J. Chem. Eng.,' 52, 507 (1974)

Masterova, A.P., and Levin, M.I., 'Study of Kinetic Relationships in Chlorination of Granules Made from Titanium-Containing Concentrate and Coke,' J. Appl. Chem. USSR, 46, (6), 1286 (1973)

Morris, A.J., and Jensen, R.F., 'Fluidized-Bed Chlorination Rates of Australian Rutile,' Metall. Trans., 7B, 89 (1976)

O'Reilly, A.J., Doig, I.D., and Ratcliffe, J.S., 'The Kinetics of the Chlorination of Zirconium Dioxide in a Static Bed with Carbon and Chlorine,' Inorg. Nucl. Chem., 34, 2487 (1972)

Seryakov, G.V., Baks, S.A., Zheltova, V.V., and Strashun, E.P., 'Mechanism of the Chlorination of Titanium Dioxide by Chlorine in the Presence of Carbon,' Russian J. Inorg. Chem., 12, (1), 3 (1967)

Seryakov, G.V., Baks, S.A., Strashun, E.P., and Tulyakov, N.V., 'Kinetics of the Chlorination of Briquettes from a Mixture of Titanium Concentrate and a Carbonaceous Reducing Agent,' J. Appl. Chem. USSR, 42, (1), 150 (1969)

Seryakov, G.V., Baks, S.A., Strashun, N.E., and Tulyakov, N.V., 'Nature of the Limiting Step in the Chlorination of Titanium Dioxide Briquetted with Carbon,' J. Appl. Chem. USSR, 43, (8), 1653 (1970)

Sparling, D.W., and Glastonbury, J.R., 'Kinetics and Mechanism of Zircon Chlorination,' Pap. West. Aust. Conf., Australas. Inst. Min. Metall. May 10, 455 (1973)

Stefanyuk, S.L., and Morozov, I.S., 'Kinetics and Mechanism of Chlorination of Minerals (Loparite, Pyrochlore, Zircon and Euxenite),' J. Appl. Chem. USSR, 38, (4), 729 (1965)

Stephens, W.W., and Gilbert, H.L., 'Chlorination of Zirconium Oxide,' Trans. AIME, J. Metals, 194, 733 (1952)

Szekely, J., Evans, J.W., and Sohn, H.Y., Gas-Solid Reactions, Academic Press, New York, (1976)

Vasilenko, D.B., and Vol'skii, A.N., 'The Thermodynamics of Reactions of Chlorination of Zirconium Dioxide by Gaseous Chlorine,' Russian J. Inorg. Chem., 3, (7), 32 (1958)

CONTRIBUTIONS TO KNOWLEDGE

1- A plasma of pure chlorine has been generated successfully and its use for a chlorination kinetic study has been demonstrated.

2- A reactor system complete with all auxiliary units was designed and constructed to provide the required kinetic data as well as to handle hot and extremely corrosive chlorine. This system with its versatile design will be suitable for studying kinetics of a wide variety of heterogenous reactions in a plasma tailflame (of even highly corrosive gases).

3- The chlorination of zirconium dioxide has been an important intermediate production step in the manufacture of zirconium metal. The present work provided the kinetic data in the temperature range of 1400 - 2480 K which were not available in the literature.

4- The reaction of zirconium dioxide and chlorine was shown to take place in the absence of reducing agent above about 20 m/s atomic chlorine velocity and 1540 K. From the theoretical formulation and the regression analysis of the experimental data an empirical rate equation for the chemically controlled region (<1950 K) was developed.

For the region (>1950 K) where both gas film diffusion and chemical reaction influenced the rate, a separate time-conversion

relationship was developed theoretically and the experimental measurements confirmed the theoretical predictions.

5- As part of the theoretical analysis:

a) A set of empirical equations was developed for the plasma jet centreline velocity and temperature profiles which allowed the estimation of plasma flame velocity and temperature at the position of a reacting particle from the plasma torch operating parameters.

b) The unknown Lennard-Jones potential parameters of $ZrCl_4$ vapor were evaluated for the calculation of transport properties from empirical equations reported in the literature. Reasonable agreement obtained between the experimental measurements and the theoretical analysis confirmed the values of potential parameters reported in this work.

6- A comprehensive kinetic data for the chlorination of zirconium dioxide in the presence of carbon as reducing agent were provided for the temperature range of 1400 - 1950 K. An empirical rate expression was developed based on theoretical formulation and regression analysis of the experimental data.

7- The kinetic data resulting from this work provided important information to help to design and operate the chlorinator under optimum conditions. It can be concluded from the study that the presence of a reducing agent is necessary to obtain the rates of conversion necessary for commercial applications.

RECOMMENDATIONS FOR FUTURE WORK

I. KINETIC STUDIES

1. The technology of zirconium production has only marginally improved since the Second World War. With the development of the CANDU reactors as the source of nuclear energy for Canada, the need for a Canadian source of zirconium metal appears to be obvious. This presents an excellent opportunity to review critically the existing methods of production and to develop new ones. The production of zirconium tetrachloride which has been studied in this thesis is an example of this approach. A study of the iodination of ZrO_2 to produce the tetraiodide should be a natural follow-up to the present investigation, in view of the possibility of using this halide in a novel process in conjunction with a simplified process of hafnium separation, as has been mentioned in the Literature Review. It is known that the decomposition of the tetraiodide is easier to achieve than that of the tetrachloride, to obtain zirconium directly by a plasma process. On the other hand, it is also known that a higher temperature level is required for the conversion of ZrO_2 to the tetraiodide under conditions of equal reaction rates. These higher temperatures are, however, well within the range of commercial plasma-generating devices.

2. The present study has amply demonstrated that, although the

chlorination of zirconia is possible in the presence of chlorine gas alone, the rate of the reaction is considerably enhanced if a reducing agent is also present. There is a good possibility that CO might be as good or better a reducing agent than the solid carbon used in the present study. In addition, the use of a gaseous reductant such as gaseous CO should avoid the problem of feed preparation, and simplify the design of the reactor.

II. EXPERIMENTAL TECHNIQUES

It is believed that the reactor system which has been designed and tested in this study is ideally suited for kinetic investigations of heterogeneous systems at high temperatures. To increase its applicability, simplify its operation and improve the accuracy of the results, it is recommended that:

a) A measurement technique be devised to allow continuous recording of the reacting particle temperature. An optical pyrometer was used in the present work, since it was not affected by the high r.f. noise level associated with the induction plasma torch. The readings from this instrument are not continuous and depend on the emissivity of the surface, which may change with the degree of conversion and reaction temperature. A measurement technique not influenced by emissivity and/or having capability of continuous recording would lead to data of high precision and accuracy, and probably would reduce the experimental difficulties.

b) A technique should be developed to obtain continuous

conversion-time data which would greatly reduce the number of experimental runs and also improve the accuracy and precision of individual experiments.

c) Measurement techniques should be developed for determining the temperature and velocity of the plasma jet surrounding the reacting particle more accurately in the temperature range between 2000 and 6000 K.

APPENDICES

APPENDIX I

Integration of $x\,dx/(1 + ax^{1/2})$ (1)

for $1 < x < x_c$

Define:

$$y = 1 + ax^{1/2} \tag{2}$$

Derivative of Equation (2) is:

$$dy = 1/2\ ax^{-1/2}\ dx \tag{3}$$

Solving Equations (2) and (3) for x and dx, respectively, and substituting in Equation (1) gives:

$$xdx/(1 + ax^{1/2}) = 2(y - 1)^3 dy/a^4 y$$

$$= 2/a^4(y^2 - 3y + 3 - y^{-1})\ dy \tag{4}$$

Integration of Equation (4) gives:

$$\int_1^{x_c} xdx/(1 + ax^{1/2}) = 2/a^4(y^3/3 - 3y^2/2 + 3 - \ell ny)\Big|_1^{x_c}$$

Inserting Equation (2) into right hand side of Equation (5) gives: (5)

$$= 2/a^4[1/3(1 + ax^{1/2})^3 - 3/2(1 + ax^{1/2})^2 + 3(1 + ax^{1/2}) - \ell n(1 + ax^{1/2})]\Big|_1^{x_c} \tag{6}$$

or:

$$= 2/a^4[1/3 + ax^{1/2} + a^2x + a^3x^{3/2}/3 - 3/2 - 3ax^{1/2} - 3a^2x/2 + 3 + 3ax^{1/2} - \ell n(1 + ax^{1/2})]\Big|_1^{x_c} \tag{7}$$

or:

$$= 2/a^4[ax^{1/2} + a^3x^{3/2}/3 - a^2x/2 - \ell n(1 + ax^{1/2}) + 11/16]\Big|_1^{z_c} \tag{8}$$

APPENDIX I

(Continued)

Applying the integral limits to Equation (8) and rearranging it results in:

$$\int_{1}^{x_c} x\, dx/(1 + ax^{1/2}) = -2(1 - x_c^{3/2})/3a + (1 - x_c)/a^2 -$$

$$2(1 - x_c^{1/2})/a^3 + 2\, \ln[(1 + a)/(1 + ax_c^{1/2})]/a^4 \qquad (9)$$

APPENDIX II

EXPERIMENTAL DATA FOR PART I

Nomenclature for Table headings:

m_g	–	Gas mass velocity
P_R	–	Ratio of power at nozzle exit to plate (inlet) power
S_R	–	Ratio of swirl to radial gas in RF torch
T_N	–	Gas temperature at nozzle exit (based on atomic chlorine)
T_P	–	Pellet reaction temperature
t	–	Reaction time
V_N	–	Gas velocity at nozzle exit (based on atomic chlorine)
X	–	Weight percent of ZrO_2 reacted at time t
x	–	Distance between pellet and nozzle exit plane
y_{Cl_2}	–	Plasma chlorine concentration

TABLE II-A

Pellet Void Fraction = 0.485
Pellet Diameter = 0.671 cm
Chlorine Concentration = 100 %

No.	x (mm)	S_R	P_R	m_g (g/s)	V_N (m/s)	T_N (K)	T_P (K)	t (s)	X (%)
1	42	0.448	0.286	1.69	22.8	2914	1538	120	3.8
2	67	0.428	0.269	1.31	23.6	3896	1538	600	18.8
3	67	0.478	0.279	1.39	24.5	3819	1538	540	17.2
4	66	0.483	0.281	1.50	24.5	3539	1538	330	10.7
5	42	0.448	0.286	1.66	22.8	2970	1538	840	23.9
6	64	0.439	0.277	1.54	25.9	3639	1568	270	10.9
7	63	0.451	0.262	1.48	25.1	3671	1568	360	14.4
8	67	0.483	0.279	1.42	25.5	3876	1568	480	18.6
9	66	0.483	0.286	1.54	27.8	3883	1568	420	16.3
10	64	0.451	0.281	1.52	27.0	3853	1623	540	24.3
11	61	0.451	0.231	1.56	30.1	4180	1673	240	15.8
12	20	0.448	0.271	1.70	31.3	3973	1673	540	28.9
13	65	0.463	0.248	1.38	30.5	4785	1673	210	13.4
14	34	0.441	0.285	1.73	30.5	3813	1673	960	49.8
15	65	0.498	0.245	1.34	26.0	4171	1673	390	23.2
16	65	0.478	0.238	1.35	29.3	4688	1701	546	36.2
17	65	0.463	0.241	1.33	29.6	4792	1701	360	25.6
18	65	0.439	0.235	1.45	29.0	4305	1701	360	25.7
19	45	0.472	0.208	1.29	27.1	4534	1756	390	31.8
20	41	0.438	0.279	1.49	27.8	4031	1791	300	27.6
21	28	0.448	0.254	1.61	33.3	4470	1791	660	49.4
22	28	0.441	0.233	1.61	34.3	4602	1791	1200	79.6
23	28	0.448	0.233	1.59	34.7	4714	1791	360	31.4
24	40	0.398	0.229	1.40	29.6	4563	1882	330	40.6
25	40	0.438	0.244	1.57	31.6	4348	1882	240	32.2
26	34	0.441	0.239	1.63	41.8	5544	1939	240	34.9
27	34	0.441	0.257	1.63	40.6	5395	1939	360	48.0
28	34	0.448	0.257	1.61	40.2	5387	1939	600	71.9
29	25	0.412	0.242	1.41	31.4	4801	1952	300	46.8
30	34	0.451	0.247	1.60	34.3	4641	1952	360	53.0
31	19	0.384	0.231	1.43	25.9	3903	1952	240	39.2
32	34	0.438	0.253	1.59	37.1	5027	1990	240	40.3
33	19	0.398	0.221	1.49	30.6	4431	2016	240	40.2
34	34	0.448	0.219	1.59	39.4	5351	2016	240	41.6
35	18	0.438	0.235	1.54	34.5	4822	2081	300	54.3
36	18	0.425	0.221	1.57	38.5	5287	2081	180	36.3

TABLE II-A

(Continued)

No.	x (mm)	S_R	P_R	m_g (g/s)	V_N (m/s)	T_N (K)	T_P (K)	t (s)	X (%)
37	18	0.438	0.223	1.53	34.9	4928	2114	240	47.4
38	19	0.464	0.216	1.49	33.6	4865	2147	360	63.8
39	26	0.448	0.208	1.65	42.7	5590	2147	450	73.2
40	18	0.437	0.221	1.61	38.6	5171	2147	240	46.6
41	19	0.457	0.216	1.51	33.8	4821	2147	300	52.5
42	26	0.448	0.179	1.66	39.1	5092	2147	690	91.9
43	19	0.449	0.215	1.53	33.7	4763	2179	180	37.5
44	26	0.448	0.197	1.65	41.0	5366	2212	315	59.7
45	19	0.385	0.237	1.55	37.1	5155	2212	156	32.8
46	19	0.451	0.231	1.50	39.0	5625	2212	240	49.0
47	26	0.448	0.186	1.67	38.7	4998	2212	195	41.0
48	18	0.423	0.222	1.69	37.1	4730	2278	180	38.1
49	18	0.451	0.223	1.63	36.6	4835	2278	180	38.9
50	18	0.437	0.200	1.64	39.9	5260	2411	300	57.9
51	18	0.448	0.201	1.70	51.4	6525	2411	600	90.6
52	18	0.437	0.217	1.67	41.7	5413	2411	330	64.5
53	18	0.437	0.198	1.64	41.8	5517	2411	390	72.3
54	18	0.437	0.229	1.68	45.5	5856	2478	285	58.4

TABLE II-B

Pellet Void Fraction = 0.549
Pellet Diameter = 0.671 cm
Chlorine Concentration = 100 %

No.	x (mm)	S_R	P_R	m_g (g/s)	V_N (m/s)	T_N (K)	T_P (K)	t (s)	X (%)
55	42	0.429	0.263	1.39	21.7	3361	1598	300	16.5
56	38	0.427	0.266	1.48	24.1	3525	1622	300	18.7
57	38	0.448	–	1.25	–	–	1622	150	9.9
58	38	0.439	0.253	1.57	26.3	3619	1639	420	28.8
59	37	0.439	0.249	1.54	26.4	3691	1686	300	24.2
60	37	0.467	0.247	1.57	25.7	3531	1686	300	23.0
61	37	0.439	0.239	1.53	24.9	3528	1686	540	42.0
62	41	0.339	0.224	1.33	18.9	3082	1735	390	37.5
63	42	0.318	0.248	1.19	17.6	3189	1735	480	46.0
64	39	0.498	0.259	1.52	28.5	4062	1779	330	35.9
65	41	0.430	0.257	1.30	22.5	3751	1800	300	36.6
66	35	0.279	0.198	1.35	22.3	3654	1800	360	45.1
67	36	0.384	0.223	1.44	27.5	4139	1823	318	43.2
68	31	0.318	0.218	1.34	27.9	4485	1836	240	35.7
69	35	0.327	0.184	1.36	24.9	3955	1836	180	28.0
70	35	0.347	0.184	1.35	24.9	3992	1836	390	53.6
71	38	0.492	0.229	1.47	25.3	3727	1836	430	57.6
72	37	0.501	0.244	1.45	26.8	3997	1836	270	39.2
73	38	0.442	0.235	1.40	23.8	3672	1836	300	41.6
74	39	0.362	0.269	1.41	22.1	3393	1836	240	34.2
75	36	0.362	0.259	1.37	24.2	3820	1874	240	39.6
76	35	0.405	0.249	1.42	26.7	4083	1874	300	47.1
77	37	0.439	0.246	1.56	26.6	3688	1874	360	52.4
78	37	0.451	0.247	1.55	34.9	4853	1926	300	51.3
79	32	0.480	0.231	1.57	32.2	4442	1952	360	63.3
80	24	0.516	0.216	1.46	30.1	4439	1971	240	47.7
81	24	0.507	0.220	1.50	27.6	3988	1971	180	37.9
82	24	0.516	0.213	1.46	26.8	3947	2016	249	52.2
83	28	0.457	0.213	1.47	29.7	4377	2049	240	53.2
84	28	0.464	0.222	1.57	31.1	4286	2049	300	60.8
85	20	0.522	0.203	1.62	32.4	4324	2179	240	55.5
86	21	0.467	0.221	1.58	32.9	4496	2179	300	66.2
87	18	0.427	0.229	1.48	32.7	4785	2179	360	74.2
88	20	0.442	0.214	1.43	28.6	4321	2179	240	55.1
89	18	0.512	0.211	1.53	33.1	4675	2212	410	82.6
90	18	0.467	0.213	1.54	35.5	4986	2212	300	65.8
91	22	0.514	0.227	1.76	44.0	5387	2212	210	51.2
92	19	0.463	0.237	1.53	36.6	5159	2278	360	75.0
93	18	0.540	0.202	1.55	35.0	4870	2344	240	57.9

TABLE II-C

Pellet Void Fraction = 0.590
Pellet Diameter = 0.671 cm
Chlorine Concentration = 100 %

No.	x (mm)	S_R	P_R	m_g (g/s)	V_N (m/s)	T_N (K)	T_P (K)	t (s)	X (%)
94	38	0.478	0.260	1.32	19.6	3190	1598	240	16.3
95	30	0.355	0.240	1.24	18.0	3148	1604	360	23.1
96	38	0.478	0.260	1.32	19.6	3190	1604	480	31.9
97	39	0.343	0.259	1.32	19.4	3185	1604	300	20.6
98	30	0.325	0.221	1.06	17.9	3632	1698	300	29.7
99	39	0.331	0.232	1.14	19.0	3602	1800	300	42.1
100	36	0.382	0.251	1.23	19.1	3368	1800	630	71.6
101	42	0.339	–	1.14	–	–	1800	210	32.2
102	36	0.382	0.251	1.23	19.1	3368	1800	240	37.2
103	20	0.478	0.223	1.33	18.4	3006	1830	390	57.9
104	34	0.398	0.251	1.55	29.7	4134	1830	360	54.3
105	28	0.362	0.244	1.40	29.8	4611	1887	300	53.4
106	35	0.398	0.226	1.45	25.7	3860	1900	360	62.3
107	35	0.447	0.246	1.53	29.1	4099	1900	195	39.5
108	35	0.398	0.224	1.45	25.7	3860	1900	240	45.5
109	34	0.451	0.248	1.61	31.2	4182	1932	240	49.7
110	30	0.425	0.250	1.58	29.7	4058	1932	300	59.2
111	27	0.425	0.217	1.46	28.7	4246	1984	180	42.8
112	33	0.438	0.253	1.61	34.6	4633	1984	390	76.3
113	27	0.398	0.231	1.45	25.9	3875	1984	360	71.7
114	30	0.425	0.262	1.57	34.6	4754	2029	300	64.1
115	24	0.425	0.220	1.45	31.2	4642	2049	390	79.7
116	29	0.439	0.243	1.57	31.1	4283	2049	240	55.4
117	24	0.425	0.207	1.46	28.9	4260	2049	180	45.2
118	28	0.425	0.234	1.59	30.1	4083	2068	210	50.4
119	22	0.425	0.213	1.57	32.0	4401	2144	300	66.2
120	22	0.491	0.235	1.53	36.7	5196	2212	390	83.2
121	19	0.451	0.235	1.63	35.0	4657	2212	180	48.0
122	20	0.425	0.221	1.59	31.4	4257	2245	240	60.7
123	22	0.451	0.234	1.63	34.9	4619	2245	240	59.7
124	18	0.451	0.235	1.63	35.3	4690	2278	300	72.3

TABLE II-D

Pellet Void Fraction = 0.505
Pellet Diameter = 0.494 cm
Chlorine Concentration = 100 %

No.	x (mm)	S_R	P_R	m_g (g/s)	V_N (m/s)	T_N (K)	T_P (K)	t (s)	X (%)
125	41	0.398	-	1.30	-	-	1592	360	21.6
126	41	0.446	-	1.30	-	-	1604	330	21.5
127	30	0.446	-	1.30	-	-	1789	270	38.8
128	44	0.398	0.252	1.30	19.3	3207	1857	300	50.0
129	41	0.350	0.237	1.19	18.5	3363	1871	225	41.6
130	30	0.354	-	1.10	-	-	1871	240	41.9
131	29	0.430	0.233	1.28	19.2	3257	1887	300	54.9
132	33	0.425	0.233	1.50	30.8	4434	1939	255	52.5
133	27	0.398	0.194	1.33	27.3	4439	1990	210	50.8
134	22	0.384	0.223	1.45	28.4	4237	2081	225	61.1
135	25	0.464	0.222	1.46	31.4	4640	2147	240	65.7

Pellet Void Fraction = 0.500
Pellet Diameter = 0.826 cm
Chlorine Concentration = 100 %

136	37	0.405	0.230	1.37	22.4	3535	1836	375	34.5
137	43	0.425	0.270	1.55	26.6	3702	1849	330	32.8
138	30	0.457	0.216	1.58	32.3	4426	1952	330	43.3
139	17	0.412	0.202	1.33	28.6	4641	1984	315	41.0
140	19	0.398	0.222	1.43	31.4	4744	2003	420	56.3
141	19	0.504	0.230	1.59	35.9	4876	2016	405	56.0
142	21	0.462	0.226	1.57	35.4	4859	2081	330	46.1
143	19	0.504	0.221	1.48	34.1	4977	2179	300	48.1

Pellet Void Fraction = 0.498
Pellet Diameter = 1.000 cm
Chlorine Concentration = 100 %

144	37	0.459	0.254	1.36	28.3	4506	1816	525	37.7
145	37	0.405	0.234	1.37	22.4	3546	1874	420	37.5
146	37	0.405	0.234	1.42	22.5	3420	1881	264	24.9
147	28	0.464	0.216	1.55	31.7	4400	1984	435	48.1
148	19	0.504	0.248	1.57	38.6	5304	2173	420	50.2

TABLE II-E

INFLUENCE OF CHLORINE CONCENTRATION

Pellet Void Fraction = 0.485
Pellet Diameter = 0.671 cm

No.	S_R	m_g (g/s)	y_{Cl_2}	T_p (K)	t (s)	[illegible] (%)
149	0.466	1.56	0.741	1686	300	15.4
150	0.455	1.08	0.207	1789	480	10.0
151	0.502	1.20	0.486	1803	300	16.0
152	0.464	1.31	0.458	1816	300	15.7
153	0.425	1.20	0.553	1816	360	22.3
154	0.410	1.37	0.705	1823	300	25.0
155	0.472	1.20	0.319	1823	300	11.3
156	0.531	1.18	0.246	1829	300	9.2
157	0.498	1.48	0.588	1849	315	25.3
158	0.522	1.19	0.266	1849	420	13.1
159	0.399	1.29	0.379	1856	300	15.5
160	0.438	1.53	0.732	1856	360	32.7
161	0.458	1.51	0.729	1856	300	29.5
162	0.466	1.55	0.507	1856	300	20.3
163	0.496	1.57	0.510	1856	300	20.1
164	0.527	1.09	0.218	1952	360	13.5
		Pellet Void Fraction = 0.549 Pellet Diameter = 0.671 cm				
165	0.391	1.38	0.647	1769	300	23.0
166	0.497	1.14	0.231	1782	240	7.2
167	0.431	1.38	0.472	1782	300	18.7
168	0.432	1.20	0.320	1782	360	14.8
169	0.473	1.17	0.250	1803	420	14.0
170	0.432	1.19	0.321	1803	300	14.0
171	0.462	1.38	0.464	1803	300	19.2
172	0.463	1.44	0.683	1803	300	27.6
173	0.486	1.46	0.568	1803	300	24.2
174	0.485	1.14	0.243	1810	360	12.4
175	0.447	1.47	0.708	1810	300	29.5
176	0.450	1.21	0.329	1816	300	14.5
177	0.533	1.20	0.271	1816	360	13.7
178	0.382	1.46	0.853	1823	330	37.5
179	0.458	1.51	0.734	1823	300	31.7
180	0.448	1.52	0.861	1823	300	36.5
181	0.432	1.16	0.312	1843	300	15.0
182	0.430	1.35	0.450	1913	300	24.7
183	0.453	1.16	0.307	1919	300	17.9
184	0.472	1.36	0.536	1919	300	29.6
185	0.433	1.48	0.694	1939	240	32.8

APPENDIX III

LISTING OF COMPUTER PROGRAM

FOR MASS TRANSFER CALCULATIONS

```
C       ***********  MAIN PROGRAM  **************
C       ********  COMBINED CHEMICAL REACTION AND GAS FILM DIFFUSION CONTROLLING
C
C
C
        DIMENSION YB(4),YS(4),YAV(4),DIM(4),D(4,4),VIS(4),A(4),XK(4)
        DIMENSION XEK(4),SIGMA(4),TIME(4),SC(4),XMW(4),XKM(4)
        DATA YB/1.0,0.0,0.0,0.0/
        DATA A/4.0,1.0,1.0,0.0/
        DATA XK/1.0,-1.0,-1.0,0.0/
        DATA XMW/35.46,233.03,32.0,70.92/
        DATA XEK/130.8,582.4,106.7,316.0/
        DATA SIGMA/3.613, 5.616,3.467,4.217/
C
C       NC : NUMBER OF GASEOUS COMPONENTS
C       AA : FREQUENCY FACTOR
C       ER : ACTIVATION ENERGY/GAS CONSTANT
C       EPS : SOLID VOLUME FRACTION
C       DP : PARTICLE DIAMETER ,CM
C       YB : BULK GAS COMPOSITION
C       A  : STOICHIOMETRIC COEFFICIENTS
C       XK : STOICHIOMETRIC COEFFICIENT INDEX
C       XEK,SIGMA : LENNARD - JONES POTENTIAL PARAMETERS
C
        NC=3      ;      P=1.
 1500   FORMAT(1H1)
        AA=3.314
        ER=12162.3
 1      CONTINUE
        NO=0
        READ(5,1000,END=2000)DP,EPS
        WRITE(6,1500)
        ROS=5.73*EPS/123.22
        P=DP/2.
 1000   FORMAT(2F10.4)
C
C       ROS = MOLAR DENSITY OF ZRO2 PELLET
 10     CONTINUE
        READ(5,1001)ID,DIST,S,CR,PCL,VGN,TGN,TP,CON,TIM
 1001   FORMAT(A4,1X,F6.2,3F7.4,F6.2,2F7.1,F7.4,F6.2)
        IF(TIM.EQ.0.0) GO TO 1
        NO=NO+1
        VGN=VGN*100.
        TIM=TIM*60.
```

```
C       GAS VELOCITY AND TEMP. AT (DIST) CM FROM NOZZLE EXIT
        CALL VELTEM(DIST,TGN,VGN,S,CP,373.,2.54,TG,VG)
        TAV=(TP+TG)/2.
        CNEW=.5
        N=0
C       ITERATION FOR SURFACE CONCENTRATIONS
   12   CONTINUE
        C=CNEW
C       EQUILIBRIUM CONCENTRATIONS
        CALL THERMO(TP,C,YS,NC)
C       GAS-FILM PROPERTIES
        DO 14 J=1,NC
   14   YAV(J)=(YS(J)+YB(J))/2.
        XMWMIX=0.0
        DO 15 J=1,NC
   15   XMWMIX=XMWMIX+YAV(J)*XMW(J)
        ROMIX=P*XMWMIX/82.0567/TAV
        CALL VISDIF(TAV,XEK,SIGMA,XMW,YAV,VIS,D,VMIX,NC)
        CALL DIMIX(A,XK,D,YAV,DIM,NC)
        REN=.3*(2.*R*VG*ROMIX/VMIX)**.5/(1.-CON)**.166666
        DO 18 I=2,3
        SC(I)=VMIX/ROMIX/DIM(I)
   18   XKM(I)=DIM(I)/(1.-CON)**.33333+DIM(I)*SC(I)**.33333*REN
        CNEW=XKM(2)/XKM(3)*(1.+2.*YS(3))/(1.+2.*YS(2))
        ERROR=ABS(CNEW-C)/C
        IF(N.GT.5) GO TO 19
        N=N+1
        IF(ERROR.GT..01) GO TO 12
   19   CONTINUE
C       TIME FOR PURE MASS TRANSFER CONTROL (CALCULATES FOR EACH OF NC COMPONENTS)
        CALL MASST(A,XK,R,VG,TAV,YS,YB,CON,VMIX,DIM,TIME,REND,SC,EPS,ROMIX
       1,NC)
C       TIME FOR PURE CHEMICAL REACTION CONTROL
        REACT=(1.-(1.-CON)**(1./3.))/AA/EXP(-ER/TP)/PCL*DP*EPS**2.0
        REACT=REACT*60.
        DO 20 I=1,NC
   20   VIS(I)=VIS(I)*100.
        VMIX=VMIX*100.
        ROMIX=ROMIX*1000.
        WRITE(6,1505)
 1505   FORMAT(1X,113('='),/,              1X,'ID',3X,'DIST',1X,'SW/RAD',1X
       1,'PN/PPL',2X,'YCL2',4X,'REN',3X,'V-NOZ',3X,'V-DIST',3X,'T-NOZ',2X,
       2'T DIST',2X,'T-PART',2X,'CONV', 8X,'TIME (SEC)',/,6X,'(CM)',30X,
       3'CM/S',5X,'CM/S',6X,'K',6X,'K',7X,'K',13X,'EXPER',7X,'CACULATED',
```

```
      4/,97X,'CHEM-R',3X,'MAS-TR',/,1X,113('-')}
       WRITE(6,1600)NO,DIST,S,CR,PCL,RENO,VGN,VG,TGN,TG,TP,CON,TIM,REACT
     .1,TIME(1)
 1600 FORMAT(1X,'I ',I2,1X,F4.1,2F7.4,F6.3,6F8.0,F7.4,F7.0,3X,F7.0,2X,
     1F7.0,/)
       WRITE(6,1501)
 1501 FORMAT(/,2(29X,'CL',5X,'ZRCL4',4X,'O2',13X),/)
       ERROR=ERROR*100.
       WRITE(6,1502)(D(1,J),J=1,NC),(YS(I),I=1,NC),(D(2,J),J=1,NC)
     1,(YAV(I),I=1,NC),(D(3,J),J=1,NC),(SC(I),I=1,NC),(VIS(I),I=1,NC)
     2,ROMIX,VMIX,(DIM(I),I=1,NC),ERROR
 1502 FORMAT(1X,'BINARY DIFFUSION COEF.  :',3F8.4,
     110X,'SURFACE CONCENTRATION   :',3F8.4,/,6X,'(SQ-CM/SEC)',9X,3F8.4
     2,10X,'AV. FILM CONCENTRATION  :',3F8.4,/,26X,3F8.4,
     310X,'SCHMIT NUMBER            :',3F8.4,/,/,
     41X,'VISCOSITY (CENTI-POISE) :',3F8.4,10X,'FILM-DENSX1000,VISCOSITY
     5:',2F8.4,/,/,1X,'EFFECTIVE DIFF. COEFF.  :',3F8.4,
     610X,'% CONVERGENCE ERROR     :',F8.4,/,/,/)
C      DATA ENDS WITH A BLANK CARD
       GO TO 10
 2000 CONTINUE
       WRITE(6,1500)
       STOP
       END


       SUBROUTINE VELTEM(X,TGN,VGN,S,CR,TINF,DN,TG,VG)
C
C      THIS SUBROUTINE CALCULATES CENTER-LINE TEMP. AND VELOCITY AT 'X'
C      DISTANCE(CM) AWAY FROM NOZZLE EXIT.
       AV=1.826/(1.+.922*S-.027*(S/CR**2.))
       BV=(.555-9.234*S*CR)/100.
       AT=9.364+.567/CR**2.
       BT=(.273-17.221*CR**2.-2.360*S**3.)/100.
C      TEMPERATURE
C      A- TRANSITION REGION
       TG=(AT**(BT*(X/DN)**2.))*TGN
C      B- DEVELOPED REGION
       TGD=(AT*(1./(2.3+X/DN))**2.)*TGN
       IF(TG.GT.TGD)TG=TGD
C      VELOCITY
```

```
C     A  TRANSITION REGION
      VG=((AV*(TG/TINF)**.5)**(BV*(X/DN)**3.))*VGN
C     B  DEVELOPED REGION
      VGD=((AV*(TG/TINF)**.5)*(1./(X/DN+2.3)))*VGN
      IF(VG.GT.VGD)VG=VGD
      RETURN
      END


      SUBROUTINE VISDIF(T,XEK,SIGMA,XMW,Y,VIS,D,VMIX,NC)
      DIMENSION XEK(4),SIGMA(4),XMW(4),VIS(4),D(4,4),Y(4),PHI(4,4)
      DO 5 I=1,NC
      TV=T/XEK(I)
      GAMAV=1.155/TV**.1462+.3945/EXP(.6672*TV)+2.05/EXP(2.168*TV)
      VIS(I)=26.692E-06*(XMW(I)*T)**.5/GAMAV/SIGMA(I)**2.
    5 CONTINUE
      VMIX=0.0
      DO 20 I=1,NC
      SUM=0.0
      DO 10 J=1,NC
      XEK12=(XEK(I)*XEK(J))**.5
      SIGM12=(SIGMA(I)+SIGMA(J))/2.
      TD=T/XEK12
      GAMAD=1.069/TD**.158+.3445/EXP(.6537*TD)+1.556/EXP(2.099*TD)
      D(I,J)=0.001858*T**1.5*((XMW(I)+XMW(J))/XMW(I)/XMW(J))**.5/GAMAD/
     1SIGM12**2.
      PHI(I,J)=1./8.**.5/(1.+XMW(I)/XMW(J))**0.5*(1.+(VIS(I)/VIS(J))**.5
     1*(XMW(J)/XMW(I))**.25)**2.
      SUM=SUM+Y(J)*PHI(I,J)
   10 CONTINUE
      VMIX=VMIX+Y(I)*VIS(I)/SUM
   20 CONTINUE
      RETURN
      END


      SUBROUTINE THERMO(T,C,Y,NC)
C     CALCULATES SURFACE CONCENTRATIONS USING EQUILIBRIUM.
```

```
C     DF1  :  2CL--> CL2
C     DF2  :  ZRO2+2CL2 --> ZRCL4+O2
C     DF3  :  ZRO2+4CL  --> ZRCL4+O2
C     T  :  PARTICLE TEMP.
C     YS(I) :  SURFACE CONCENT.
C     NC  :  NUMBER OF COMPONENTS
      DIMENSION YS(4),Y(4)
      DF1=-59628.79+28.182*T+229.798E-06*T**2.
      DF2=51625.92-15.983*T+203.475E-06*T**2.
      DF3=2.*DF1+DF2
      EQK=EXP(-DF3/1.987/T)
      EQ=EQK**.5
      B=C**.5/(1.+C)
      Y(1)=(-B+(B**2.+4.*EQ*B)**.5)/2./EQ
      Y(2)=(1.-Y(1))/(1.+C)
      Y(3)=C*Y(2)
      RETURN
      END
```

```
      SUBROUTINE MASST(A,XK,R,V,T,YS,YB,X,VMIX,DIM,TIME,RENO,SC,ROS
     1,ROMIX,NC)
      DIMENSION A(4),XK(4),YS(4),YB(4),DIM(4),TIME(4),SC(4)
C     X  D  FRACTION OF ZRO2 REACTED
C     R  :  PARTICLE RADIUS (CM)
C     V  D  BULK GAS VELOCITY
C     T:  AVERAGE FILM TEMP.
C     DIM  : EFFECTIVE BINARY DIFFUSION COEFF. OF COMPONENT I IN THE MIX
C     TIME  :  CALCULATED REACTION TIME BASED ON PURE MASS TRANSFER.
      XX=1.-X
      DO 20 I=1,3
      RENO=2.*R*V*ROMIX/VMIX
      SC(I)=VMIX/ROMIX/DIM(I)
      F=.3*SC(I)**(1./3.)*RENO**.5
      BETA=DIM(I)/82.0567/T
      SUM=0.0
      DO 10 J=1,NC
   10 SUM=SUM+XK(J)*A(J)/A(I)/XK(I)
      GAMA=(YS(I)-YB(I))/R**2./XK(I)/A(I)/ROS/(1.-YS(I)*SUM)
      TIME(I)=-(2./3./F*(1.-XX**.5)-(1.-XX**(1./3.))/F**2.+2./F**3.*
```

```
     1(1.-XX**(1./6.))-2./F**4.*ALOG((1.+F)/(1.+F*XX**(1./6.))))/GAMA/
     2BETA
20   CONTINUE
     RETURN
     END


     SUBROUTINE DIMIX(A,XK,D,Y,DMIX,NC)
C    A   :  STOICHIOMETRIC COEFF. NOT INCLUDING SOLID WHOSE COEFF. IS 1
C    XK  :  SIGN OF STOICH COEFF.  :  1. --> REACTANT , -1. --> PRODUCTS
C    D   :  BINARY DIFFUSION COEF. OF COMPONENTS I,J
C    Y   :  AVERAGE FILM CONCENTRATIONS
C    NC  :  TOTAL NO. OF COMPONENTS
C    DMIX : EFFECTIVE BINARY DIFFUSION COEF. OF COMPONENT I IN THE MIX
     DIMENSION A(4),XK(4),Y(4),D(4,4),DMIX(4)
     DO 20 I=1,3
     SUM1=0.0    ;    SUM2=0.0
     DO 10 J=1,NC
     SUM1=SUM1+XK(J)*A(J)/A(I)/XK(I)
     SUM2=SUM2+(Y(J)-Y(I)*A(J)/A(I)*XK(J)/XK(I))/D(I,J)
10   CONTINUE
     DMIX(I)=(1.-Y(I)*SUM1)/SUM2
20   CONTINUE
     RETURN
     END
```

APPENDIX IV

COMPUTER OUTPUT OF MASS TRANSFER CALCULATIONS

FOR THE DATA OF

TABLE-A OF APPENDIX II

(TABLE II-A)

ID	DIST (CM)	SW/RAD	PN/PPL	YCL2	REN	V-NOZ CM/S	V-DIST CM/S	T-NOZ K	T-DIST K	T-PART K	CONV	TIME (SEC) EXPER	CACULATED CHEM-R	CACULATED MAS-TR
I- 1	4.2	0.4479	0.2860	1.000	962.	2282.	2197.	2914.	2629.	1538.	0.0376	120.	111.	1.

	CL	ZRCL4	O2
BINARY DIFFUSION COEF. (SQ-CM/SEC)	4.6581	1.9201	5.0625
	1.9201	0.5717	2.1096
	5.0625	2.1096	5.4994
VISCOSITY (CENTI-POISE)	0.0721	0.0592	0.0767
EFFECTIVE DIFF. COEFF.	2.5543	1.9046	4.3812

	CL	ZRCL4	O2
SURFACE CONCENTRATION	0.3830	0.4394	0.1777
AV. FILM CONCENTRATION	0.6915	0.2197	0.0888
SCHMIT NUMBER	0.5999	0.8046	0.3498
FILM-DENSX1000,VISCOSITY	0.4594	0.0704	
% CONVERGENCE ERROR	0.9320		

ID	DIST (CM)	SW/RAD	PN/PPL	YCL2	REN	V-NOZ CM/S	V-DIST CM/S	T-NOZ K	T-DIST K	T-PART K	CONV	TIME (SEC) EXPER	CACULATED CHEM-R	CACULATED MAS-TR
I- 2	6.7	0.4276	0.2695	1.000	802.	2358.	1914.	3896.	2744.	1538.	0.1881	600.	587.	7.

	CL	ZRCL4	O2
BINARY DIFFUSION COEF. (SQ-CM/SEC)	4.8719	2.0090	5.2948
	2.0090	0.5993	2.2069
	5.2948	2.2069	5.7517
VISCOSITY (CENTI-POISE)	0.0734	0.0604	0.0780
EFFECTIVE DIFF. COEFF.	2.6714	1.9927	4.5795

	CL	ZRCL4	O2
SURFACE CONCENTRATION	0.3828	0.4400	0.1772
AV. FILM CONCENTRATION	0.6914	0.2200	0.0886
SCHMIT NUMBER	0.5999	0.8042	0.3499
FILM-DENSX1000,VISCOSITY	0.4475	0.0717	
% CONVERGENCE ERROR	0.9436		

ID	DIST (CM)	SW/RAD	PN/PPL	YCL2	REN	V-NOZ CM/S	V-DIST CM/S	T-NOZ K	T-DIST K	T-PART K	CONV	TIME (SEC) EXPER	CACULATED CHEM-R	CACULATED MAS-TR
I- 3	6.7	0.4777	0.2795	1.000	831.	2448.	1875.	3819.	2603.	1538.	0.1720	540.	533.	7.

	CL	ZRCL4	O2
BINARY DIFFUSION COEF. (SQ-CM/SEC)	4.6101	1.9001	5.0103
	1.9001	0.5655	2.0877
	5.0103	2.0877	5.4426
VISCOSITY (CENTI-POISE)	0.0718	0.0590	0.0764
EFFECTIVE DIFF. COEFF.	2.5270	1.8847	4.3334

	CL	ZRCL4	O2
SURFACE CONCENTRATION	0.3828	0.4399	0.1772
AV. FILM CONCENTRATION	0.6914	0.2200	0.0886
SCHMIT NUMBER	0.5995	0.8039	0.3496
FILM-DENSX1000,VISCOSITY	0.4626	0.0701	
% CONVERGENCE ERROR	0.9424		

ID	DIST (CM)	SW/RAD	PN/PPL	YCL2	REN	V-NOZ CM/S	V-DIST CM/S	T-NOZ K	T-DIST K	T-PART K	CONV	TIME (SEC) EXPER	CACULATED CHEM-R	CACULATED MAS-TR
I- 4	6.6	0.4834	0.2808	1.000	866.	2454.	1828.	3539.	2442.	1539.	0.1074	330.	325.	4.

	CL	ZRCL4	O2		CL	ZRCL4	O2
BINARY DIFFUSION COEF. (SQ-CM/SEC) :	4.3156	1.7776	4.6902	SURFACE CONCENTRATION :	0.3829	0.4398	0.1773
	1.7776	0.5275	1.9534	AV. FILM CONCENTRATION :	0.6914	0.2199	0.0887
	4.6902	1.9534	5.0950	SCHMIT NUMBER :	0.5991	0.8035	0.3492
VISCOSITY (CENTI-POISE) :	0.0700	0.0572	0.0744	FILM-DENSX1000,VISCOSITY:	0.4813	0.0682	
EFFECTIVE DIFF. COEFF. :	2.3645	1.7631	4.0567	% CONVERGENCE ERROR :	0.9406		

ID	DIST (CM)	SW/RAD	PN/PPL	YCL2	REN	V-NOZ CM/S	V-DIST CM/S	T-NOZ K	T-DIST K	T-PART K	CONV	TIME (SEC) EXPER	CACULATED CHEM-R	CACULATED MAS-TR
I- 5	4.2	0.4479	0.2859	1.000	941.	2278.	2192.	2970.	2680.	1538.	0.2392	840.	761.	9.

	CL	ZRCL4	O2		CL	ZRCL4	O2
BINARY DIFFUSION COEF. (SQ-CM/SEC) :	4.7521	1.9592	5.1647	SURFACE CONCENTRATION :	0.3829	0.4396	0.1775
	1.9592	0.5838	2.1524	AV. FILM CONCENTRATION :	0.6915	0.2198	0.0887
	5.1647	2.1524	5.6104	SCHMIT NUMBER :	0.5999	0.8044	0.3498
VISCOSITY (CENTI-POISE) :	0.0727	0.0598	0.0773	FILM-DENSX1000,VISCOSITY:	0.4541	0.0710	
EFFECTIVE DIFF. COEFF. :	2.6059	1.9433	4.4686	% CONVERGENCE ERROR :	0.9368		

ID	DIST (CM)	SW/RAD	PN/PPL	YCL2	REN	V-NOZ CM/S	V-DIST CM/S	T-NOZ K	T-DIST K	T-PART K	CONV	TIME (SEC) EXPER	CACULATED CHEM-R	CACULATED MAS-TR
I- 6	6.4	0.4393	0.2774	1.000	874.	2592.	2081.	3639.	2621.	1568.	0.1087	270.	283.	4.

	CL	ZRCL4	O2		CL	ZRCL4	O2
BINARY DIFFUSION COEF. (SQ-CM/SEC) :	4.6983	1.9368	5.1061	SURFACE CONCENTRATION :	0.4153	0.4156	0.1691
	1.9368	0.5769	2.1279	AV. FILM CONCENTRATION :	0.7076	0.2078	0.0845
	5.1061	2.1279	5.5468	SCHMIT NUMBER :	0.6175	0.8311	0.3589
VISCOSITY (CENTI-POISE) :	0.0724	0.0595	0.0769	FILM-DENSX1000,VISCOSITY:	0.4435	0.0708	
EFFECTIVE DIFF. COEFF. :	2.5864	1.9218	4.4495	% CONVERGENCE ERROR :	0.8607		

ID	DIST (CM)	SW/RAD	PN/PPL	YCL2	REN	V-NOZ CM/S	V-DIST CM/S	T-NOZ K	T-DIST K	T-PART K	CONV	TIME (SEC) EXPER	CACULATED CHEM-R	CACULATED MAS-TR
I 7	6.3	0.4512	0.2620	1.000	824.	2506.	2129.	3671.	2831.	1568.	0.1435	360.	379.	6.

	CL	ZRCL4	O2		CL	ZRCL4	O2
BINARY DIFFUSION COEF. (SQ-CM/SEC) :	5.0948	2.1016	5.5371	SURFACE CONCENTRATION :	0.4152	0.4158	0.1690
	2.1016	0.6281	2.3084	AV. FILM CONCENTRATION :	0.7076	0.2079	0.0845
	5.5371	2.3084	6.0149	SCHMIT NUMBER :	0.6180	0.8315	0.3594
VISCOSITY (CENTI-POISE) :	0.0747	0.0616	0.0794	FILM-DENSX1000,VISCOSITY:	0.4224	0.0732	
EFFECTIVE DIFF. COEFF. :	2.8059	2.0854	4.8249	% CONVERGENCE ERROR :	0.8627		

ID	DIST (CM)	SW/RAD	PN/PPL	YCL2	REN	V-NOZ CM/S	V-DIST CM/S	T-NOZ K	T-DIST K	T-PART K	CONV	TIME (SEC) EXPER	CACULATED CHEM-R	CACULATED MAS-TR
I- 8	6.7	0.4834	0.2793	1.000	819.	2554.	1967.	3876.	2644.	1568.	0.1857	480.	498.	8.

	CL	ZRCL4	O2		CL	ZRCL4	O2
BINARY DIFFUSION COEF. (SQ-CM/SEC) :	4.7414	1.9547	5.1530	SURFACE CONCENTRATION :	0.4152	0.4159	0.1689
	1.9547	0.5825	2.1475	AV. FILM CONCENTRATION :	0.7076	0.2079	0.0845
	5.1530	2.1475	5.5977	SCHMIT NUMBER :	0.6174	0.8308	0.3590
VISCOSITY (CENTI-POISE) :	0.0726	0.0597	0.0772	FILM-DENSX1000,VISCOSITY:	0.4412	0.0711	
EFFECTIVE DIFF. COEFF. :	2.6099	1.9395	4.4892	% CONVERGENCE ERROR :	0.8654		

ID	DIST (CM)	SW/RAD	PN/PPL	YCL2	REN	V-NOZ CM/S	V-DIST CM/S	T-NOZ K	T-DIST K	T-PART K	CONV	TIME (SEC) EXPER	CACULATED CHEM-R	CACULATED MAS-TR
I- 9	6.6	0.4834	0.2858	1.000	893.	2775.	2140.	3883.	2638.	1568.	0.1633	420.	434.	6.

	CL	ZRCL4	O2		CL	ZRCL4	O2
BINARY DIFFUSION COEF. (SQ-CM/SEC) :	4.7306	1.9502	5.1413	SURFACE CONCENTRATION :	0.4153	0.4156	0.1691
	1.9502	0.5811	2.1426	AV. FILM CONCENTRATION :	0.7076	0.2078	0.0846
	5.1413	2.1426	5.5849	SCHMIT NUMBER :	0.6176	0.8311	0.3590
VISCOSITY (CENTI POISE) :	0.0726	0.0596	0.0771	FILM-DENSX1000,VISCOSITY:	0.4417	0.0710	
EFFECTIVE DIFF. COEFF. :	2.6043	1.9351	4.4802	% CONVERGENCE ERROR :	0.8605		

ID	DIST (CM)	SW/RAD	PN/PPL	YCL2	REN	V-NOZ CM/S	V-DIST CM/S	T-NOZ K	T-DIST K	T-PART K	CONV	TIME (SEC) EXPER	CACULATED CHEM-R	MAS-TR
I-10	6.4	0.4512	0.2807	1.000	809.	2703.	2203.	3853.	2747.	1623.	0.2430	540.	513.	10.

	CL	ZRCL4	O2		GL	ZRCL4	O2
BINARY DIFFUSION COEF. (SQ-CM/SEC)	5.0391	2.0785	5.4766	SURFACE CONCENTRATION	0.4757	0.3712	0.1532
	2.0785	0.6209	2.2831	AV. FILM CONCENTRATION	0.7378	0.1856	0.0766
	5.4766	2.2831	5.9492	SCHMIT NUMBER	0.6535	0.8854	0.3778
VISCOSITY (CENTI-POISE)	0.0744	0.0613	0.0790	FILM-DENSX1000,VISCOSITY	0.4008	0.0732	
EFFECTIVE DIFF. COEFF.	2.7962	2.0638	4.8171	% CONVERGENCE ERROR	0.7228		

ID	DIST (CM)	SW/RAD	PN/PPL	YCL2	REN	V-NOZ CM/S	V-DIST CM/S	T-NOZ K	T-DIST K	T-PART K	CONV	TIME (SEC) EXPER	CACULATED CHEM-R	MAS-TR
I-11	6.1	0.4512	0.2309	1.000	697.	3013.	2759.	4180.	3601.	1673.	0.1581	240.	258.	6.

	CL	ZRCL4	O2		CL	ZRCL4	O2
BINARY DIFFUSION COEF. (SQ-CM/SEC)	6.8833	2.8438	7.4808	SURFACE CONCENTRATION	0.5297	0.3315	0.1388
	2.8438	0.8594	3.1218	AV. FILM CONCENTRATION	0.7649	0.1657	0.0694
	7.4808	3.1218	8.1263	SCHMIT NUMBER	0.6900	0.9404	0.3972
VISCOSITY (CENTI-POISE)	0.0840	0.0702	0.0893	FILM-DENSX1000,VISCOSITY	0.3141	0.0835	
EFFECTIVE DIFF. COEFF.	3.8512	2.8256	6.6905	% CONVERGENCE ERROR	0.5992		

ID	DIST (CM)	SW/RAD	PN/PPL	YCL2	REN	V-NOZ CM/S	V-DIST CM/S	T-NOZ K	T-DIST K	T-PART K	CONV	TIME (SEC) EXPER	CACULATED CHEM-R	MAS-TR
I-12	2.0	0.4479	0.2713	1.000	719.	3125.	3112.	3973.	3890.	1673.	0.2894	540.	498.	12.

	CL	ZRCL4	O2		CL	ZRCL4	O2
BINARY DIFFUSION COEF. (SQ-CM/SEC)	7.5184	3.1070	8.1710	SURFACE CONCENTRATION	0.5297	0.3315	0.1388
	3.1070	0.9415	3.4103	AV. FILM CONCENTRATION	0.7649	0.1658	0.0694
	8.1710	3.4103	8.8761	SCHMIT NUMBER	0.6902	0.9407	0.3974
VISCOSITY (CENTI-POISE)	0.0869	0.0728	0.0924	FILM-DENSX1000,VISCOSITY	0.2978	0.0865	
EFFECTIVE DIFF. COEFF.	4.2073	3.0871	7.3077	% CONVERGENCE ERROR	0.5998		

ID	DIST (CM)	SW/RAD	PN/PPL	YCL2	REN	V-NOZ CM/S	V-DIST CM/S	T-NOZ K	T-DIST K	T-PART K	CONV	TIME (SEC) EXPER	CACULATED CHEM-R	CACULATED MAS-TR
I-13	6.5	0.4632	0.2484	1.000	642.	3047.	2670.	4785.	3760.	1673.	0.1337	210.	216.	6.

	CL	ZRCL4	O2		CL	ZRCL4	O2
BINARY DIFFUSION COEF. (SQ-CM/SEC)	7.2303	2.9876	7.8579	SURFACE CONCENTRATION	0.5297	0.3316	0.1387
	2.9876	0.9043	3.2794	AV. FILM CONCENTRATION	0.7648	0.1658	0.0693
	7.8579	3.2794	8.5360	SCHMIT NUMBER	0.6900	0.9404	0.3973
VISCOSITY (CENTI-POISE)	0.0856	0.0716	0.0910	FILM-DENSX1000,VISCOSITY	0.3050	0.0851	
EFFECTIVE DIFF. COEFF.	4.0454	2.9685	7.0267	% CONVERGENCE ERROR	0.6026		

ID	DIST (CM)	SW/RAD	PN/PPL	YCL2	REN	V-NOZ CM/S	V-DIST CM/S	T-NOZ K	T-DIST K	T-PART K	CONV	TIME (SEC) EXPER	CACULATED CHEM-R	CACULATED MAS-TR
I-14	3.4	0.4410	0.2850	1.000	[illegible]61.	3045.	2979.	3813.	3568.	1673.	0.4976	960.	948.	22.

	CL	ZRCL4	O2		CL	ZRCL4	O2
BINARY DIFFUSION COEF. (SQ-CM/SEC)	6.8110	2.8138	7.4022	SURFACE CONCENTRATION	0.5297	0.3317	0.1387
	2.8138	0.8500	3.0889	AV. FILM CONCENTRATION	0.7648	0.1658	0.0693
	7.4022	3.0889	8.0409	SCHMIT NUMBER	0.6898	0.9401	0.3971
VISCOSITY (CENTI-POISE)	0.0836	0.0699	0.0889	FILM-DENSX1000,VISCOSITY	0.3162	0.0831	
EFFECTIVE DIFF. COEFF.	3.8101	2.7958	6.6187	% CONVERGENCE ERROR	0.6034		

ID	DIST (CM)	SW/RAD	PN/PPL	YCL2	REN	V-NOZ CM/S	V-DIST CM/S	T-NOZ K	T-DIST K	T-PART K	CONV	TIME (SEC) EXPER	CACULATED CHEM-R	CACULATED MAS-TR
I-15	6.5	0.4976	0.2449	1.000	623.	2595.	2252.	4171.	3324.	1673.	0.2322	390.	390.	11.

	CL	ZRCL4	O2		CL	ZRCL4	O2
BINARY DIFFUSION COEF. (SQ-CM/SEC)	6.2939	2.5994	6.8402	SURFACE CONCENTRATION	0.5296	0.3319	0.1385
	2.5994	0.7832	2.8539	AV. FILM CONCENTRATION	0.7648	0.1659	0.0693
	6.8402	2.8539	7.4305	SCHMIT NUMBER	0.6894	0.9395	0.3968
VISCOSITY (CENTI-POISE)	0.0811	0.0675	0.0862	FILM-DENSX1000,VISCOSITY	0.3317	0.0805	
EFFECTIVE DIFF. COEFF.	3.5197	2.5827	6.1150	% CONVERGENCE ERROR	0.6070		

ID	DIST (CM)	SW/RAD	PN/PPL	YCL2	REN	V-NOZ CM/S	V-DIST CM/S	T-NOZ K	T-DIST K	T-PART K	CONV	TIME (SEC) EXPER	CACULATED CHEM-R	CACULATED MAS-TR
I-16	6.5	0.4777	0.2382	1.000	577.	2925.	2566.	4689.	3844.	1701.	0.3624	546.	571.	17.

	CL	ZRCL4	O2		CL	ZRCL4	O2
BINARY DIFFUSION COEF. (SQ-CM/SEC) :	7.4790	3.0907	8.1282	SURFACE CONCENTRATION :	0.5593	0.3104	0.1304
	3.0906	0.9364	3.3924	AV. FILM CONCENTRATION :	0.7796	0.1552	0.0652
	8.1282	3.3924	8.8296	SCHMIT NUMBER :	0.7105	0.9715	0.4080
VISCOSITY (CENTI-POISE) :	0.0868	0.0727	0.0922	FILM-DENSX1000,VISCOSITY:	0.2896	0.0864	
EFFECTIVE DIFF. COEFF. :	4.2003	3.0719	7.3153	% CONVERGENCE ERROR :	0.5452		

ID	DIST (CM)	SW/RAD	PN/PPL	YCL2	REN	V-NOZ CM/S	V-DIST CM/S	T-NOZ K	T-DIST K	T-PART K	CONV	TIME (SEC) EXPER	CACULATED CHEM-R	CACULATED MAS-TR
I-17	6.5	0.4632	0.2413	1.000	581.	2960.	2609.	4792.	3877.	1701.	0.2562	360.	385.	12.

	CL	ZRCL4	O2		CL	ZRCL4	O2
BINARY DIFFUSION COEF. (SQ-CM/SEC) :	7.5538	3.1217	8.2095	SURFACE CONCENTRATION :	0.5593	0.3102	0.1305
	3.1217	0.9461	3.4264	AV. FILM CONCENTRATION :	0.7796	0.1551	0.0652
	8.2095	3.4264	8.9179	SCHMIT NUMBER :	0.7106	0.9717	0.4080
VISCOSITY (CENTI-POISE) :	0.0871	0.0730	0.0926	FILM-DENSX1000,VISCOSITY:	0.2878	0.0868	
EFFECTIVE DIFF. COEFF. :	4.2428	3.1027	7.3896	% CONVERGENCE ERROR :	0.5425		

ID	DIST (CM)	SW/RAD	PN/PPL	YCL2	REN	V-NOZ CM/S	V-DIST CM/S	T-NOZ K	T-DIST K	T-PART K	CONV	TIME (SEC) EXPER	CACULATED CHEM-R	CACULATED MAS-TR
I-18	6.5	0.4393	0.2351	1.000	637.	2898.	2611.	4305.	3578.	1701.	0.2570	360.	387.	12.

	CL	ZRCL4	O2		CL	ZRCL4	O2
BINARY DIFFUSION COEF. (SQ-CM/SEC) :	6.8935	2.8480	7.4919	SURFACE CONCENTRATION :	0.5594	0.3100	0.1306
	2.8480	0.8607	3.1264	AV. FILM CONCENTRATION :	0.7797	0.1550	0.0653
	7.4919	3.1264	8.1384	SCHMIT NUMBER :	0.7106	0.9718	0.4079
VISCOSITY (CENTI-POISE) :	0.0840	0.0702	0.0893	FILM-DENSX1000,VISCOSITY:	0.3041	0.0836	
EFFECTIVE DIFF. COEFF. :	3.8716	2.8308	6.7448	% CONVERGENCE ERROR :	0.5385		

ID	DIST (CM)	SW/RAD	PN/PPL	YCL2	REN	V-NOZ CM/S	V-DIST CM/S	T-NOZ K	T-DIST K	T-PART K	CONV	TIME (SEC) EXPER	CACULATED CHEM-R	CACULATED MAS-TR
I-19	4.5	0.4718	0.2083	1.000	487.	2708.	2620.	4534.	4225.	1756.	0.3182	390.	394.	16.

	CL	ZRCL4	O2		CL	ZRCL4	O2
BINARY DIFFUSION COEF. (SQ-CM/SEC) :	8.4786	3.5046	9.2145	SURFACE CONCENTRATION :	0.6143	0.2704	0.1153
	3.5046	1.0656	3.8463	AV. FILM CONCENTRATION :	0.8072	0.1352	0.0576
	9.2145	3.8463	10.0097	SCHMIT NUMBER :	0.7521	1.0353	0.4296
VISCOSITY (CENTI-POISE) :	0.0911	0.0766	0.0968	FILM-DENSX1000,VISCOSITY:	0.2525	0.0911	
EFFECTIVE DIFF. COEFF. :	4.7978	3.4857	8.3993	% CONVERGENCE ERROR :	0.4311		

ID	DIST (CM)	SW/RAD	PN/PPL	YCL2	REN	V-NOZ CM/S	V-DIST CM/S	T-NOZ K	T-DIST K	T-PART K	CONV	TIME (SEC) EXPER	CACULATED CHEM-R	CACULATED MAS-TR
I-20	4.1	0.4379	0.2790	1.000	561.	2777.	2677.	4031.	3674.	1784.	0.2762	300.	301.	15.

	CL	ZRCL4	O2		CL	ZRCL4	O2
BINARY DIFFUSION COEF. (SQ-CM/SEC) :	7.2839	3.0098	7.9162	SURFACE CONCENTRATION :	0.6416	0.2504	0.1081
	3.0098	0.9112	3.3038	AV. FILM CONCENTRATION :	0.8208	0.1252	0.0540
	7.9162	3.3038	8.5993	SCHMIT NUMBER :	0.7744	1.0699	0.4410
VISCOSITY (CENTI-POISE) :	0.0859	0.0719	0.0913	FILM-DENSX1000,VISCOSITY:	0.2680	0.0859	
EFFECTIVE DIFF. COEFF. :	4.1372	2.9947	7.2650	% CONVERGENCE ERROR :	0.3681		

ID	DIST (CM)	SW/RAD	PN/PPL	YCL2	REN	V-NOZ CM/S	V-DIST CM/S	T-NOZ K	T-DIST K	T-PART K	CONV	TIME (SEC) EXPER	CACULATED CHEM-R	CACULATED MAS-TR
I-21	2.8	0.4479	0.2541	1.000	569.	3331.	3295.	4471.	4308.	1791.	0.4940	660.	582.	26.

	CL	ZRCL4	O2		CL	ZRCL4	O2
BINARY DIFFUSION COEF. (SQ-CM/SEC) :	8.7588	3.6206	9.5190	SURFACE CONCENTRATION :	0.6487	0.2453	0.1060
	3.6206	1.1018	3.9735	AV. FILM CONCENTRATION :	0.8244	0.1227	0.0530
	9.5190	3.9736	10.3405	SCHMIT NUMBER :	0.7805	1.0791	0.4443
VISCOSITY (CENTI-POISE) :	0.0923	0.0777	0.0981	FILM-DENSX1000,VISCOSITY:	0.2378	0.0925	
EFFECTIVE DIFF. COEFF. :	4.9809	3.6027	8.7497	% CONVERGENCE ERROR :	0.3570		

ID	DIST (CM)	SW/RAD	PN/PPL	YCL2	REN	V-NOZ CM/S	V-DIST CM/S	T-NOZ K	T-DIST K	T-PART K	CONV	TIME (SEC) EXPER	CACULATED CHEM-R	CACULATED MAS-TR
I-22	2.8	0.4410	0.2329	1.000	564.	3430.	3400.	4602.	4460.	1791.	0.7964	1200.	1179.	49.

	CL	ZRCL4	O2		CL	ZRCL4	O2
BINARY DIFFUSION COEF. (SQ-CM/SEC) :	9.1233	3.7715	9.9152	SURFACE CONCENTRATION :	0.6485	0.2460	0.1055
	3.7715	1.1489	4.1391	AV. FILM CONCENTRATION :	0.8242	0.1230	0.0527
	9.9152	4.1391	10.7709	SCHMIT NUMBER :	0.7799	1.0778	0.4441
VISCOSITY (CENTI-POISE) :	0.0937	0.0790	0.0996	FILM-DENSX1000,VISCOSITY:	0.2323	0.0940	
EFFECTIVE DIFF. COEFF. :	5.1862	3.7527	9.1074	% CONVERGENCE ERROR :	0.3708		

ID	DIST (CM)	SW/RAD	PN/PPL	YCL2	REN	V-NOZ CM/S	V-DIST CM/S	T-NOZ K	T-DIST K	T-PART K	CONV	TIME (SEC) EXPER	CACULATED CHEM-R	CACULATED MAS-TR
I-23	2.8	0.4479	0.2329	1.000	553.	3468.	3436.	4714.	4567.	1791.	0.3136	360.	338.	15.

	CL	ZRCL4	O2		CL	ZRCL4	O2
BINARY DIFFUSION COEF. (SQ-CM/SEC) :	9.3848	3.8797	10.1994	SURFACE CONCENTRATION :	0.6488	0.2451	0.1061
	3.8797	1.1826	4.2577	AV. FILM CONCENTRATION :	0.8244	0.1226	0.0530
	10.1994	4.2577	11.0795	SCHMIT NUMBER :	0.7807	1.0793	0.4444
VISCOSITY (CENTI-POISE) :	0.0948	0.0799	0.1007	FILM-DENSX1000,VISCOSITY:	0.2280	0.0950	
EFFECTIVE DIFF. COEFF. :	5.3378	3.8606	9.3766	% CONVERGENCE ERROR :	0.3538		

ID	DIST (CM)	SW/RAD	PN/PPL	YCL2	REN	V-NOZ CM/S	V-DIST CM/S	T-NOZ K	T-DIST K	T-PART K	CONV	TIME (SEC) EXPER	CACULATED CHEM-R	CACULATED MAS-TR
I-24	4.0	0.3981	0.2295	1.000	443.	2958.	2903.	4563.	4305.	1882.	0.4063	330.	329.	27.

	CL	ZRCL4	O2		CL	ZRCL4	O2
BINARY DIFFUSION COEF. (SQ-CM/SEC) :	8.9678	3.7071	9.7462	SUPFACE CONCENTRATION :	0.7267	0.1894	0.0838
	3.7071	1.1288	4.0684	AV. FILM CONCENTRATION :	0.8634	0.0947	0.0419
	9.7462	4.0684	10.5872	SCHMIT NUMBER :	0.8523	1.1900	0.4815
VISCOSITY (CENTI-POISE) :	0.0931	0.0784	0.0990	FILM-DENSX1000,VISCOSITY:	0.2129	0.0935	
EFFECTIVE DIFF. COEFF. :	5.1562	3.6926	9.1256	% CONVERGENCE ERROR :	0.2183		

ID	DIST (CM)	SW/RAD	PN/PPL	YCL2	REN	V-NOZ CM/S	V-DIST CM/S	T-NOZ K	T-DIST K	T-PART K	CONV	TIME (SEC) EXPER	CACULATED CHEM-R	CACULATED MAS-TR
I 25	4.0	0.4379	0.2437	1.000	503.	3164.	3080.	4348.	4058.	1882.	0.3217	240.	250.	20.

	CL	ZRCL4	O2
BINARY DIFFUSION COEF. (SQ-CM/SEC)	8.3830	3.4650	9.1106
	3.4650	1.0533	3.8029
	9.1106	3.8029	9.8968
VISCOSITY (CENTI-POISE)	0.0907	0.0763	0.0964
EFFECTIVE DIFF. COEFF.	4.8204	3.4515	8.5331

	CL	ZRCL4	O2
SURFACE CONCENTRATION	0.7269	0.1891	0.0840
AV. FILM CONCENTRATION	0.8634	0.0946	0.0420
SCHMIT NUMBER	0.8527	1.1908	0.4817
FILM-DENSX1000,VISCOSITY	0.2216	0.0911	
% CONVERGENCE ERROR	0.2129		

ID	DIST (CM)	SW/RAD	PN/PPL	YCL2	REN	V-NOZ CM/S	V DIST CM/S	T-NOZ K	T-DIST K	T-PART K	CONV	TIME (SEC) EXPER	CACULATED CHEM-R	CACULATED MAS-TR
I-26	3.4	0.4410	0.2394	1.000	459.	4176.	4103.	5544.	5281.	1939.	0.3490	240.	228.	23.

	CL	ZRCL4	O2
BINARY DIFFUSION COEF. (SQ-CM/SEC)	11.5840	4.7897	12.5895
	4.7897	1.4662	5.2559
	12.5895	5.2559	13.6759
VISCOSITY (CENTI-POISE)	0.1029	0.0871	0.1093
EFFECTIVE DIFF. COEFF.	6.7028	4.7737	11.9095

	CL	ZRCL4	O2
SURFACE CONCENTRATION	0.7684	0.1597	0.0719
AV. FILM CONCENTRATION	0.8842	0.0798	0.0360
SCHMIT NUMBER	0.8953	1.2572	0.5039
FILM-DENSX1000,VISCOSITY	0.1725	0.1035	
% CONVERGENCE ERROR	0.1503		

ID	DIST (CM)	SW/RAD	PN/PPL	YCL2	REN	V-NOZ CM/S	V-DIST CM/S	T-NOZ K	T-DIST K	T-PART K	CONV	TIME (SEC) EXPER	CACULATED CHEM-R	CACULATED MAS-TR
I-27	3.4	0.4410	0.2573	1.000	464.	4060.	3979.	5395.	5104.	1939.	0.4801	360.	335.	33.

	CL	ZRCL4	O2
BINARY DIFFUSION COEF. (SQ-CM/SEC)	11.1181	4.5969	12.0831
	4.5969	1.4062	5.0444
	12.0831	5.0444	13.1258
VISCOSITY (CENTI-POISE)	0.1012	0.0857	0.1076
EFFECTIVE DIFF. COEFF.	6.4327	4.5815	11.4292

	CL	ZRCL4	O2
SURFACE CONCENTRATION	0.7684	0.1598	0.0719
AV. FILM CONCENTRATION	0.8842	0.0799	0.0359
SCHMIT NUMBER	0.8954	1.2571	0.5039
FILM-DENSX1000,VISCOSITY	0.1769	0.1019	
% CONVERGENCE ERROR	0.1520		

ID	DIST (CM)	SW/RAD	PN/PPL	YCL2	REN	V-NOZ CM/S	V-DIST CM/S	T-NOZ K	T-DIST K	T-PART K	CONV	TIME (SEC) EXPER	CACULATED CHEM-R	MAS-TR
I-28	3.4	0.4479	0.2572	1.000	460.	4020.	3937.	5387.	5095.	1939.	0.7193	600.	590.	55.

	CL	ZRCL4	O2		CL	ZRCL4	O2
BINARY DIFFUSION COEF. (SQ-CM/SEC) :	11.0929	4.5865	12.0557	SURFACE CONCENTRATION :	0.7682	0.1601	0.0717
	4.5865	1.4029	5.0330	AV. FILM CONCENTRATION :	0.8841	0.0801	0.0358
	12.0557	5.0330	13.0960	SCHMIT NUMBER :	0.8949	1.2563	0.5038
VISCOSITY (CENTI-POISE) :	0.1012	0.0856	0.1075	FILM-DENSX1000,VISCOSITY:	0.1773	0.1018	
EFFECTIVE DIFF. COEFF. :	6.4167	4.5710	11.3993	% CONVERGENCE ERROR :	0.1581		

ID	DIST (CM)	SW/RAD	PN/PPL	YCL2	REN	V-NOZ CM/S	V-DIST CM/S	T-NOZ K	T-DIST K	T-PART K	CONV	TIME (SEC) EXPER	CACULATED CHEM-R	MAS-TR
I-29	2.5	0.4118	0.2418	1.000	397.	3136.	3118.	4801.	4679.	1952.	0.4683	300.	311.	36.

	CL	ZRCL4	O2		CL	ZRCL4	O2
BINARY DIFFUSION COEF. (SQ-CM/SEC) :	10.0600	4.1592	10.9332	SURFACE CONCENTRATION :	0.7770	0.1538	0.0692
	4.1592	1.2698	4.5642	AV. FILM CONCENTRATION :	0.8885	0.0769	0.0346
	10.9332	4.5642	11.8767	SCHMIT NUMBER :	0.9050	1.2720	0.5089
VISCOSITY (CENTI-POISE) :	0.0974	0.0822	0.1035	FILM-DENSX1000,VISCOSITY:	0.1858	0.0980	
EFFECTIVE DIFF. COEFF. :	5.8268	4.1457	10.3610	% CONVERGENCE ERROR :	0.1435		

ID	DIST (CM)	SW/RAD	PN/PPL	YCL2	REN	V-NOZ CM/S	V-DIST CM/S	T-NOZ K	T-DIST K	T-PART K	CONV	TIME (SEC) EXPER	CACULATED CHEM-R	MAS-TR
I-30	3.4	0.4512	0.2465	1.000	460.	3434.	3371.	4641.	4406.	1952.	0.5301	360.	365.	41.

	CL	ZRCL4	O2		CL	ZRCL4	O2
BINARY DIFFUSION COEF. (SQ-CM/SEC) :	9.3812	3.8782	10.1954	SURFACE CONCENTRATION :	0.7770	0.1537	0.0693
	3.8782	1.1822	4.2561	AV. FILM CONCENTRATION :	0.8885	0.0768	0.0346
	10.1954	4.2561	11.0752	SCHMIT NUMBER :	0.9054	1.2727	0.5091
VISCOSITY (CENTI-POISE) :	0.0948	0.0799	0.1007	FILM-DENSX1000,VISCOSITY:	0.1937	0.0953	
EFFECTIVE DIFF. COEFF. :	5.4339	3.8657	9.6634	% CONVERGENCE ERROR :	0.1407		

ID	DIST (CM)	SW/RAD	PN/PPL	YCL2	REN	V-NOZ CM/S	V-DIST CM/S	T-NOZ K	T-DIST K	T-PART K	CONV	TIME (SEC) EXPER	CACULATED CHEM-R	CACULATED MAS-TR
I 31	1.9	0.3844	0.2312	1.000	410.	2590.	2585.	3903.	3853.	1952.	0.3918	240.	250.	32.

	CL	ZRCL4	O2		CL	ZRCL4	O2
BINARY DIFFUSION COEF. (SQ-CM/SEC) :	8.0671	3.3343	8.7674	SURFACE CONCENTRATION :	0.7770	0.1537	0.0693
	3.3343	1.0124	3.6595	AV. FILM CONCENTRATION :	0.8885	0.0769	0.0346
	8.7674	3.6595	9.5239	SCHMIT NUMBER :	0.9057	1.2731	0.5092
VISCOSITY (CENTI-POISE) :	0.0893	0.0750	0.0950	FILM-DENSX1000,VISCOSITY:	0.2122	0.0898	
EFFECTIVE DIFF. COEFF. :	4.6718	3.3234	8.3093	% CONVERGENCE ERROR :	0.1417		

ID	DIST (CM)	SW/RAD	PN/PPL	YCL2	REN	V-NOZ CM/S	V-DIST CM/S	T-NOZ K	T-DIST K	T-PART K	CONV	TIME (SEC) EXPER	CACULATED CHEM-R	CACULATED MAS-TR
I-32	3.4	0.4379	0.2534	1.000	433.	3707.	3638.	5027.	4765.	1990.	0.4033	240.	230.	32.

	CL	ZRCL4	O2		CL	ZRCL4	O2
BINARY DIFFUSION COEF. (SQ-CM/SEC) :	10.3756	4.2898	11.2762	SURFACE CONCENTRATION :	0.8018	0.1358	0.0625
	4.2898	1.3105	4.7075	AV. FILM CONCENTRATION :	0.9009	0.0679	0.0312
	11.2762	4.7075	12.2493	SCHMIT NUMBER :	0.9341	1.3177	0.5239
VISCOSITY (CENTI-POISE) :	0.0986	0.0833	0.1047	FILM-DENSX1000,VISCOSITY:	0.1759	0.0992	
EFFECTIVE DIFF. COEFF. :	6.0345	4.2775	10.7585	% CONVERGENCE ERROR :	0.9409		

ID	DIST (CM)	SW/RAD	PN/PPL	YCL2	REN	V-NOZ CM/S	V-DIST CM/S	T-NOZ K	T-DIST K	T-PART K	CONV	TIME (SEC) EXPER	CACULATED CHEM-R	CACULATED MAS-TR
I-33	1.9	0.3981	0.2207	1.000	390.	3061.	3055.	4431.	4377.	2016.	0.4022	240.	212.	36.

	CL	ZRCL4	O2		CL	ZRCL4	O2
BINARY DIFFUSION COEF. (SQ-CM/SEC) :	9.4697	3.9149	10.2916	SURFACE CONCENTRATION :	0.8166	0.1255	0.0579
	3.9149	1.1936	4.2963	AV. FILM CONCENTRATION :	0.9083	0.0627	0.0290
	10.2916	4.2963	11.1797	SCHMIT NUMBER :	0.9521	1.3458	0.5333
VISCOSITY (CENTI-POISE) :	0.0951	0.0802	0.1011	FILM-DENSX1000,VISCOSITY:	0.1821	0.0957	
EFFECTIVE DIFF. COEFF. :	5.5188	3.9045	9.8527	% CONVERGENCE ERROR :	0.8528		

ID	DIST (CM)	SW/RAD	PN/PPL	YCL2	REN	V-NOZ CM/S	V-DIST CM/S	T-NOZ K	T-DIST K	T-PART K	CONV	TIME (SEC) EXPER	CACULATED CHEM-R	CACULATED MAS-TR
I-34	3.4	0.4479	0.2188	1.000	412.	3939.	3881.	5351.	5132.	2016.	0.4159	240.	220.	34.

	CL	ZRCL4	O2		CL	ZRCL4	O2
BINARY DIFFUSION COEF. (SQ-CM/SEC)	11.3955	4.7117	12.3847	SURFACE CONCENTRATION	0.8167	0.1254	0.0579
	4.7117	1.4419	5.1704	AV. FILM CONCENTRATION	0.9083	0.0627	0.0290
	12.3847	5.1704	13.4534	SCHMIT NUMBER	0.9515	1.3449	0.5330
VISCOSITY (CENTI-POISE)	0.1022	0.0865	0.1086	FILM-DENSX1000,VISCOSITY	0.1628	0.1029	
EFFECTIVE DIFF. COEFF.	6.6422	4.6992	11.8572	% CONVERGENCE ERROR	0.8420		

ID	DIST (CM)	SW/RAD	PN/PPL	YCL2	REN	V-NOZ CM/S	V-DIST CM/S	T-NOZ K	T-DIST K	T-PART K	CONV	TIME (SEC) EXPER	CACULATED CHEM-R	CACULATED MAS-TR
I-35	1.8	0.4379	0.2351	1.000	374.	3445.	3437.	4822.	4760.	2081.	0.5430	300.	255.	59.

	CL	ZRCL4	O2		CL	ZRCL4	O2
BINARY DIFFUSION COEF. (SQ-CM/SEC)	10.5940	4.3801	11.5136	SURFACE CONCENTRATION	0.8495	0.1027	0.0478
	4.3801	1.3386	4.8066	AV. FILM CONCENTRATION	0.9247	0.0513	0.0239
	11.5136	4.8066	12.5071	SCHMIT NUMBER	0.9934	1.4101	0.5548
VISCOSITY (CENTI-POISE)	0.0994	0.0840	0.1056	FILM-DENSX1000,VISCOSITY	0.1622	0.1000	
EFFECTIVE DIFF. COEFF.	6.2040	4.3705	11.1080	% CONVERGENCE ERROR	0.6434		

ID	DIST (CM)	SW/RAD	PN/PPL	YCL2	REN	V-NOZ CM/S	V-DIST CM/S	T-NOZ K	T-DIST K	T-PART K	CONV	TIME (SEC) EXPER	CACULATED CHEM-R	CACULATED MAS-TR
I-36	1.8	0.4246	0.2211	1.000	375.	3853.	3845.	5287.	5226.	2081.	0.3633	180.	155.	35.

	CL	ZRCL4	O2		CL	ZRCL4	O2
BINARY DIFFUSION COEF. (SQ-CM/SEC)	11.8196	4.8871	12.8455	SURFACE CONCENTRATION	0.8495	0.1026	0.0479
	4.8871	1.4965	5.3628	AV. FILM CONCENTRATION	0.9248	0.0513	0.0240
	12.8455	5.3628	13.9540	SCHMIT NUMBER	0.9930	1.4097	0.5546
VISCOSITY (CENTI-POISE)	0.1037	0.0878	0.1102	FILM-DENSX1000,VISCOSITY	0.1518	0.1043	
EFFECTIVE DIFF. COEFF.	6.9226	4.8764	12.3945	% CONVERGENCE ERROR	0.6218		

ID	DIST (CM)	SW/RAD	PN/PPL	YCL2	REN	V-NOZ CM/S	V-DIST CM/S	T-NOZ K	T-DIST K	T-PART K	CONV	TIME (SEC) EXPER	CACULATED CHEM-R	CACULATED MAS-TR
I-37	1.8	0.4379	0.2233	1.000	359.	3491.	3484.	4928.	4870.	2114.	0.4742	240.	196.	54.

	CL	ZRCL4	O2
BINARY DIFFUSION COEF. (SQ-CM/SEC)	10.9631	4.5328	11.9147
	4.5328	1.3862	4.9741
	11.9147	4.9741	12.9428
VISCOSITY (CENTI-POISE)	0.1007	0.0852	0.1070
EFFECTIVE DIFF. COEFF.	6.4339	4.5238	11.5343

	CL	ZRCL4	O2
SURFACE CONCENTRATION	0.8637	0.0928	0.0435
AV. FILM CONCENTRATION	0.9319	0.0464	0.0217
SCHMIT NUMBER	1.0124	1.4399	0.5647
FILM-DENSX1000,VISCOSITY	0.1555	0.1013	
% CONVERGENCE ERROR	0.5466		

ID	DIST (CM)	SW/RAD	PN/PPL	YCL2	REN	V-NOZ CM/S	V-DIST CM/S	T-NOZ K	T-DIST K	T-PART K	CONV	TIME (SEC) EXPER	CACULATED CHEM-R	CACULATED MAS-TR
I-38	1.9	0.4645	0.2164	1.000	341.	3359.	3350.	4865.	4801.	2147.	0.6383	360.	268.	87.

	CL	ZRCL4	O2
BINARY DIFFUSION COEF. (SQ-CM/SEC)	10.8698	4.4942	11.8133
	4.4942	1.3742	4.9318
	11.8133	4.9318	12.8327
VISCOSITY (CENTI-POISE)	0.1004	0.0849	0.1067
EFFECTIVE DIFF. COEFF.	6.3908	4.4860	11.4698

	CL	ZRCL4	O2
SURFACE CONCENTRATION	0.8765	0.0841	0.0394
AV. FILM CONCENTRATION	0.9382	0.0420	0.0197
SCHMIT NUMBER	1.0302	1.4675	0.5740
FILM-DENSX1000,VISCOSITY	0.1533	0.1009	
% CONVERGENCE ERROR	0.4934		

ID	DIST (CM)	SW/RAD	PN/PPL	YCL2	REN	V-NOZ CM/S	V-DIST CM/S	T-NOZ K	T-DIST K	T-PART K	CONV	TIME (SEC) EXPER	CACULATED CHEM-R	CACULATED MAS-TR
I-39	2.6	0.4479	0.2076	1.000	372.	4266.	4241.	5590.	5467.	2147.	0.7323	450.	331.	95.

	CL	ZRCL4	O2
BINARY DIFFUSION COEF. (SQ-CM/SEC)	12.6509	5.2310	13.7490
	5.2310	1.6035	5.7401
	13.7490	5.7401	14.9354
VISCOSITY (CENTI-POISE)	0.1065	0.0903	0.1132
EFFECTIVE DIFF. COEFF.	7.4382	5.2215	13.3490

	CL	ZRCL4	O2
SURFACE CONCENTRATION	0.8765	0.0841	0.0394
AV. FILM CONCENTRATION	0.9382	0.0420	0.0197
SCHMIT NUMBER	1.0293	1.4663	0.5735
FILM-DENSX1000,VISCOSITY	0.1399	0.1071	
% CONVERGENCE ERROR	0.4957		

ID	DIST (CM)	SW/RAD	PN/PPL	YCL2	REN	V-NOZ CM/S	V-DIST CM/S	T-NOZ K	T-DIST K	T-PART K	CONV	TIME (SEC) EXPER	CACULATED CHEM-R	CACULATED MAS-TR
I-40	1.8	0.4364	0.2212	1.000	365.	3858.	3850.	5171.	5110.	2147.	0.4660	240.	176.	56.

	CL	ZRCL4	O2
BINARY DIFFUSION COEF. (SQ-CM/SEC)	11.6835	4.8309	12.6977
	4.8309	1.4790	5.3011
	12.6977	5.3011	13.7934
VISCOSITY (CENTI-POISE)	0.1032	0.0874	0.1097
EFFECTIVE DIFF. COEFF.	6.8701	4.8221	12.3306

	CL	ZRCL4	O2
SURFACE CONCENTRATION	0.8766	0.0839	0.0395
AV. FILM CONCENTRATION	0.9383	0.0419	0.0198
SCHMIT NUMBER	1.0300	1.4675	0.5739
FILM-DENSX1000,VISCOSITY	0.1467	0.1038	
% CONVERGENCE ERROR	0.4604		

ID	DIST (CM)	SW/RAD	PN/PPL	YCL2	REN	V-NOZ CM/S	V-DIST CM/S	T-NOZ K	T-DIST K	T-PART K	CONV	TIME (SEC) EXPER	CACULATED CHEM-R	CACULATED MAS-TR
I-41	1.9	0.4568	0.2161	1.000	347.	3378.	3369.	4821.	4759.	2147.	0.5252	300.	205.	68.

	CL	ZRCL4	O2
BINARY DIFFUSION COEF. (SQ-CM/SEC)	10.7597	4.4487	11.6937
	4.4487	1.3600	4.8818
	11.6937	4.8818	12.7028
VISCOSITY (CENTI-POISE)	0.1000	0.0845	0.1062
EFFECTIVE DIFF. COEFF.	6.3264	4.4406	11.3547

	CL	ZRCL4	O2
SURFACE CONCENTRATION	0.8765	0.0840	0.0395
AV. FILM CONCENTRATION	0.9383	0.0420	0.0197
SCHMIT NUMBER	1.0304	1.4679	0.5741
FILM-DENSX1000,VISCOSITY	0.1542	0.1005	
% CONVERGENCE ERROR	0.4755		

ID	DIST (CM)	SW/RAD	PN/PPL	YCL2	REN	V-NOZ CM/S	V-DIST CM/S	T-NOZ K	T-DIST K	T-PART K	CONV	TIME (SEC) EXPER	CACULATED CHEM-R	CACULATED MAS-TR
I-42	2.6	0.4479	0.1785	1.000	378.	3907.	3893.	5092.	5007.	2147.	0.9187	690.	527.	145.

	CL	ZRCL4	O2
BINARY DIFFUSION COEF. (SQ-CM/SEC)	11.4105	4.7179	12.4010
	4.7179	1.4438	5.1772
	12.4010	5.1772	13.4711
VISCOSITY (CENTI-POISE)	0.1023	0.0866	0.1087
EFFECTIVE DIFF. COEFF.	6.7074	4.7092	12.0362

	CL	ZRCL4	O2
SURFACE CONCENTRATION	0.8765	0.0843	0.0392
AV. FILM CONCENTRATION	0.9383	0.0422	0.0196
SCHMIT NUMBER	1.0295	1.4663	0.5737
FILM-DENSX1000,VISCOSITY	0.1490	0.1029	
% CONVERGENCE ERROR	0.5636		

ID	DIST (CM)	SW/RAD	PN/PPL	YCL2	REN	V-NOZ CM/S	V-DIST CM/S	T-NOZ K	T-DIST K	T-PART K	CONV	TIME (SEC) EXPER	CACULATED CHEM-R	CACULATED MAS-TR
I-43	1.9	0.4495	0.2153	1.000	342.	3369.	3361.	4763.	4703.	2179.	0.3749	180.	124.	50.

	CL	ZRCL4	O2
BINARY DIFFUSION COEF. (SQ-CM/SEC)	10.6993	4.4237	11.6280
	4.4237	1.3522	4.8544
	11.6280	4.8544	12.6315
VISCOSITY (CENTI-POISE)	0.0997	0.0843	0.1060
EFFECTIVE DIFF. COEFF.	6.3021	4.4164	11.3233

	CL	ZRCL4	O2
SURFACE CONCENTRATION	0.8882	0.0759	0.0359
AV. FILM CONCENTRATION	0.9441	0.0379	0.0180
SCHMIT NUMBER	1.0473	1.4945	0.5829
FILM-DENSX1000,VISCOSITY	0.1519	0.1003	
% CONVERGENCE ERROR	0.3918		

ID	DIST (CM)	SW/RAD	PN/PPL	YCL2	REN	V-NOZ CM/S	V-DIST CM/S	T-NOZ K	T-DIST K	T-PART K	CONV	TIME (SEC) EXPER	CACULATED CHEM-R	CACULATED MAS-TR
I-44	2.6	0.4479	0.1970	1.000	356.	4099.	4078.	5366.	5259.	2212.	0.5968	315.	206.	88.

	CL	ZRCL4	O2
BINARY DIFFUSION COEF. (SQ-CM/SEC)	12.2607	5.0696	13.3249
	5.0696	1.5533	5.5630
	13.3249	5.5630	14.4748
VISCOSITY (CENTI-POISE)	0.1052	0.0892	0.1118
EFFECTIVE DIFF. COEFF.	7.2332	5.0620	13.0075

	CL	ZRCL4	O2
SURFACE CONCENTRATION	0.8987	0.0687	0.0326
AV. FILM CONCENTRATION	0.9493	0.0344	0.0163
SCHMIT NUMBER	1.0619	1.5174	0.5905
FILM-DENSX1000,VISCOSITY	0.1376	0.1057	
% CONVERGENCE ERROR	0.3460		

ID	DIST (CM)	SW/RAD	PN/PPL	YCL2	REN	V-NOZ CM/S	V-DIST CM/S	T-NOZ K	T-DIST K	T-PART K	CONV	TIME (SEC) EXPER	CACULATED CHEM-R	CACULATED MAS-TR
I-45	1.9	0.3853	0.2375	1.000	336.	3706.	3698.	5155.	5084.	2212.	0.3284	156.	98.	46.

	CL	ZRCL4	O2
BINARY DIFFUSION COEF. (SQ-CM/SEC)	11.7877	4.8740	12.8109
	4.8740	1.4924	5.3483
	12.8109	5.3483	13.9164
VISCOSITY (CENTI-POISE)	0.1036	0.0877	0.1101
EFFECTIVE DIFF. COEFF.	6.9544	4.8667	12.5067

	CL	ZRCL4	O2
SURFACE CONCENTRATION	0.8987	0.0686	0.0326
AV. FILM CONCENTRATION	0.9494	0.0343	0.0163
SCHMIT NUMBER	1.0623	1.5180	0.5907
FILM-DENSX1000,VISCOSITY	0.1409	0.1041	
% CONVERGENCE ERROR	0.3303		

ID	DIST (CM)	SW/RAD	PN/PPL	YCL2	REN	V-NOZ CM/S	V-DIST CM/S	T-NOZ K	T-DIST K	T-PART K	CONV	TIME (SEC) EXPER	CACULATED CHEM-R	CACULATED MAS-TR
I-46	1.9	0.4512	0.2310	1.000	319.	3895.	3883.	5625.	5544.	2212.	0.4900	240.	158.	71.

	CL	ZRCL4	O2
BINARY DIFFUSION COEF. (SQ-CM/SEC)	13.0458	5.3943	14.1782
	5.3943	1.6543	5.9192
	14.1782	5.9193	15.4016
VISCOSITY (CENTI-POISE)	0.1078	0.0914	0.1145
EFFECTIVE DIFF. COEFF.	7.6963	5.3863	13.8400

	CL	ZRCL4	O2
SURFACE CONCENTRATION	0.8987	0.0687	0.0326
AV. FILM CONCENTRATION	0.9493	0.0344	0.0163
SCHMIT NUMBER	1.0615	1.5168	0.5903
FILM-DENSX1000,VISCOSITY	0.1326	0.1083	
% CONVERGENCE ERROR	0.3506		

ID	DIST (CM)	SW/RAD	PN/PPL	YCL2	REN	V-NOZ CM/S	V-DIST CM/S	T-NOZ K	T-DIST K	T-PART K	CONV	TIME (SEC) EXPER	CACULATED CHEM-R	CACULATED MAS-TR
I-47	2.6	0.4479	0.1856	1.000	365.	3873.	3857.	4998.	4908.	2212.	0.4099	195.	127.	58.

	CL	ZRCL4	O2
BINARY DIFFUSION COEF. (SQ-CM/SEC)	11.3208	4.6808	12.3034
	4.6808	1.4323	5.1364
	12.3034	5.1364	13.3651
VISCOSITY (CENTI-POISE)	0.1020	0.0863	0.1084
EFFECTIVE DIFF. COEFF.	6.6790	4.6738	12.0116

	CL	ZRCL4	O2
SURFACE CONCENTRATION	0.8987	0.0686	0.0327
AV. FILM CONCENTRATION	0.9494	0.0343	0.0163
SCHMIT NUMBER	1.0626	1.5185	0.5909
FILM-DENSX1000,VISCOSITY	0.1444	0.1025	
% CONVERGENCE ERROR	0.3251		

ID	DIST (CM)	SW/RAD	PN/PPL	YCL2	REN	V-NOZ CM/S	V-DIST CM/S	T-NOZ K	T-DIST K	T-PART K	CONV	TIME (SEC) EXPER	CACULATED CHEM-R	CACULATED MAS-TR
I-48	1.8	0.4230	0.2221	1.000	353.	3707.	3700.	4730.	4676.	2278.	0.3813	180.	99.	65.

	CL	ZRCL4	O2
BINARY DIFFUSION COEF. (SQ-CM/SEC)	10.8866	4.5012	11.8316
	4.5012	1.3763	4.9394
	11.8316	4.9394	12.8526
VISCOSITY (CENTI-POISE)	0.1004	0.0849	0.1067
EFFECTIVE DIFF. COEFF.	6.4401	4.4956	11.6007

	CL	ZRCL4	O2
SURFACE CONCENTRATION	0.9167	0.0563	0.0270
AV. FILM CONCENTRATION	0.9584	0.0281	0.0135
SCHMIT NUMBER	1.0906	1.5623	0.6054
FILM-DENSX1000,VISCOSITY	0.1436	0.1009	
% CONVERGENCE ERROR	0.2333		

ID	DIST (CM)	SW/RAD	PN/PPL	YCL2	REN	V-NOZ CM/S	V-DIST CM/S	T-NOZ K	T-DIST K	T-PART K	CONV	TIME (SEC) EXPER	CACULATED CHEM-R	CACULATED MAS-TR
I-49	1.8	0.4512	0.2225	1.000	340.	3657.	3649.	4835.	4776.	2278.	0.3886	180.	101.	66.

	CL	ZRCL4	O2
BINARY DIFFUSION COEF. (SQ-CM/SEC)	11.1483	4.6094	12.1160
	4.6094	1.4100	5.0582
	12.1160	5.0582	13.1615
VISCOSITY (CENTI-POISE)	0.1014	0.0858	0.1077
EFFECTIVE DIFF. COEFF.	6.5948	4.6038	11.8792

	CL	ZRCL4	O2
SURFACE CONCENTRATION	0.9167	0.0563	0.0270
AV. FILM CONCENTRATION	0.9584	0.0282	0.0135
SCHMIT NUMBER	1.0904	1.5619	0.6053
FILM-DENSX1000.VISCOSITY	0.1416	0.1018	
% CONVERGENCE ERROR	0.2380		

ID	DIST (CM)	SW/RAD	PN/PPL	YCL2	REN	V-NOZ CM/S	V-DIST CM/S	T-NOZ K	T-DIST K	T-PART K	CONV	TIME (SEC) EXPER	CACULATED CHEM-R	CACULATED MAS-TR
I-50	1.8	0.4366	0.2004	1.000	314.	3994.	3987.	5260.	5209.	2411.	0.5785	300.	125.	147.

	CL	ZRCL4	O2
BINARY DIFFUSION COEF. (SQ-CM/SEC)	12.6668	5.2376	13.7663
	5.2376	1.6055	5.7473
	13.7663	5.7473	14.9542
VISCOSITY (CENTI-POISE)	0.1065	0.0903	0.1132
EFFECTIVE DIFF. COEFF.	7.5228	5.2331	13.5810

	CL	ZRCL4	O2
SURFACE CONCENTRATION	0.9429	0.0385	0.0186
AV. FILM CONCENTRATION	0.9715	0.0192	0.0093
SCHMIT NUMBER	1.1323	1.6277	0.6272
FILM-DENSX1000.VISCOSITY	0.1255	0.1069	
% CONVERGENCE ERROR	0.1400		

ID	DIST (CM)	SW/RAD	PN/PPL	YCL2	REN	V-NOZ CM/S	V-DIST CM/S	T-NOZ K	T-DIST K	T-PART K	CONV	TIME (SEC) EXPER	CACULATED CHEM-R	CACULATED MAS-TR
I-51	1.8	0.4479	0.2011	1.000	315.	5139.	5129.	6525.	6460.	2411.	0.9060	600.	273.	258.

	CL	ZRCL4	O2
BINARY DIFFUSION COEF. (SQ-CM/SEC)	16.2986	6.7396	17.7133
	6.7396	2.0720	7.3953
	17.7133	7.3953	19.2419
VISCOSITY (CENTI-POISE)	0.1175	0.0999	0.1249
EFFECTIVE DIFF. COEFF.	9.6785	6.7338	17.4707

	CL	ZRCL4	O2
SURFACE CONCENTRATION	0.9428	0.0387	0.0185
AV. FILM CONCENTRATION	0.9714	0.0194	0.0092
SCHMIT NUMBER	1.1299	1.6241	0.6260
FILM-DENSX1000.VISCOSITY	0.1079	0.1180	
% CONVERGENCE ERROR	0.1880		

ID	DIST (CM)	SW/RAD	PN/PPL	YCL2	REN	V-NOZ CM/S	V-DIST CM/S	T-NOZ K	T-DIST K	T-PART K	CONV	TIME (SEC) EXPER	CACULATED CHEM-R	CACULATED MAS-TR
I-52	1.8	0.4366	0.2173	1.000	318.	4173.	4164.	5413.	5352.	2411.	0.6451	330.	146.	166.

	CL	ZRCL4	O2		CL	ZRCL4	O2
BINARY DIFFUSION COEF. (SQ-CM/SEC)	13.0641	5.4019	14.1981	SURFACE CONCENTRATION	0.9429	0.0385	0.0186
	5.4019	1.6566	5.9276	AV. FILM CONCENTRATION	0.9715	0.0193	0.0093
	14.1981	5.9276	15.4233	SCHMIT NUMBER	1.1320	1.6273	0.6271
VISCOSITY (CENTI-POISE)	0.1078	0.0915	0.1146	FILM-DENSX1000,VISCOSITY	0.1232	0.1082	
EFFECTIVE DIFF. COEFF.	7.7587	5.3973	14.0067	% CONVERGENCE ERROR	0.1440		

ID	DIST (CM)	SW/RAD	PN/PPL	YCL2	REN	V-NOZ CM/S	V-DIST CM/S	T-NOZ K	T-DIST K	T-PART K	CONV	TIME (SEC) EXPER	CACULATED CHEM-R	CACULATED MAS-TR
I 53	1.8	0.4366	0.1985	1.000	312.	4182.	4175.	5517.	5464.	2411.	0.7229	390.	174.	194.

	CL	ZRCL4	O2		CL	ZRCL4	O2
BINARY DIFFUSION COEF. (SQ-CM/SEC)	13.3787	5.5320	14.5399	SURFACE CONCENTRATION	0.9429	0.0386	0.0185
	5.5320	1.6971	6.0703	AV. FILM CONCENTRATION	0.9715	0.0193	0.0093
	14.5399	6.0703	15.7946	SCHMIT NUMBER	1.1318	1.6269	0.6269
VISCOSITY (CENTI-POISE)	0.1088	0.0924	0.1157	FILM-DENSX1000,VISCOSITY	0.1214	0.1092	
EFFECTIVE DIFF. COEFF.	7.9453	5.5273	14.3433	% CONVERGENCE ERROR	0.1535		

ID	DIST (CM)	SW/RAD	PN/PPL	YCL2	REN	V-NOZ CM/S	V-DIST CM/S	T-NOZ K	T-DIST K	T-PART K	CONV	TIME (SEC) EXPER	CACULATED CHEM-R	CACULATED MAS-TR
I-54	1.8	0.4366	0.2291	1.000	308.	4548.	4537.	5856.	5783.	2478.	0.5835	285.	111.	168.

	CL	ZRCL4	O2		CL	ZRCL4	O2
BINARY DIFFUSION COEF. (SQ-CM/SEC)	14.4838	5.9891	15.7410	SURFACE CONCENTRATION	0.9524	0.0320	0.0155
	5.9891	1.8391	6.5718	AV. FILM CONCENTRATION	0.9762	0.0160	0.0078
	15.7410	6.5718	17.0993	SCHMIT NUMBER	1.1476	1.6519	0.6352
VISCOSITY (CENTI-POISE)	0.1122	0.0953	0.1193	FILM-DENSX1000,VISCOSITY	0.1139	0.1126	
EFFECTIVE DIFF. COEFF.	8.6145	5.9848	15.5644	% CONVERGENCE ERROR	0.1054		

APPENDIX V

EXPERIMENTAL DATA FOR PART II

TABLE V-A

Average Carbon Content = 23.1 ± 0.1 % wt
Pellet Diameter = 0.826 cm
Chlorine Concentration = 100 %

No.	Gas (g/s)	Swirl/ Radial	ZrO_2 Content (wt %)	Pellet Temperature (K)	Reaction Time (s)	Conversion (wt %)
1	1.44	0.434	75.4	1415	165	41.7
2	1.45	0.405	76.7	1437	60	19.2
3	1.41	0.421	76.4	1437	75	23.8
4	1.43	0.413	75.2	1437	330	65.6
5	1.42	0.413	75.1	1437	420	68.3
6	1.40	0.459	75.3	1437	255	61.5
7	1.38	0.478	75.4	1437	210	53.9
8	1.38	0.478	76.1	1446	120	37.7
9	1.46	0.434	76.4	1466	120	40.8
10	1.43	0.434	76.3	1471	150	49.9
11	1.43	0.434	76.4	1483	90	35.3
12	1.44	0.434	76.5	1483	135	48.1
13	1.44	0.434	76.3	1522	105	47.4
14	1.45	0.405	76.2	1537	144	58.5
15	1.45	0.442	76.3	1537	48	27.0
16	1.42	0.413	76.2	1537	90	45.7
17	1.47	0.434	76.1	1537	192	68.8
18	1.43	0.413	75.8	1537	330	79.6
19	1.42	0.428	75.5	1537	180	64.6
20	1.44	0.442	75.8	1551	255	74.9
21	1.39	0.391	77.3	1551	60	38.8
22	1.38	0.391	76.7	1551	420	81.9
23	1.47	0.463	76.9	1551	90	47.5
24	1.40	0.384	76.7	1551	300	79.3
25	1.39	0.391	76.6	1551	150	61.1
26	1.43	0.434	77.4	1551	90	47.0
27	1.38	0.494	77.3	1608	90	54.2
28	1.37	0.478	78.2	1608	120	65.2
29	1.38	0.494	77.1	1608	186	79.8
30	1.47	0.434	76.6	1608	252	89.8
31	1.47	0.434	76.4	1608	330	94.2
32	1.42	0.376	76.8	1608	390	95.4
33	1.36	0.478	76.6	1659	90	58.9
34	1.48	0.463	77.1	1659	180	83.1
35	1.44	0.434	76.9	1659	120	69.3

TABLE V-A

(Continued)

No.	Gas (g/s)	Swirl/ Radial	ZrO_2 Content (wt %)	Pellet Temperature (K)	Reaction Time (s)	Conversion (wt %)
36	1.40	0.510	77.2	1659	120	71.1
37	1.48	0.463	78.6	1659	69	49.2
38	1.47	0.434	77.4	1659	48	41.0
39	1.48	0.434	76.3	1659	270	94.2
40	1.48	0.434	76.5	1659	351	95.3
41	1.47	0.434	76.3	1659	290	95.4
42	1.46	0.434	76.4	1659	330	95.6
43	1.49	0.463	77.2	1693	90	67.6
44	1.45	0.434	77.2	1693	60	51.6
45	1.45	0.434	77.6	1710	90	68.2
46	1.47	0.427	76.9	1733	180	87.0
47	1.46	0.427	77.1	1750	135	80.1
48	1.41	0.434	77.1	1750	180	87.5
49	1.54	0.425	77.5	1780	75	63.8
50	1.44	0.434	77.7	1790	60	56.2
51	1.44	0.427	76.7	1796	90	71.2
52	1.58	0.579	77.7	1796	83	69.1
53	1.44	0.427	77.4	1796	60	55.1
54	1.44	0.427	76.6	1796	120	79.2
55	1.52	0.507	77.0	1807	78	66.8
56	1.50	0.478	77.9	1807	57	54.4
57	1.48	0.463	76.7	1807	102	76.7
58	1.52	0.507	77.6	1807	78	67.8
59	1.44	0.434	77.2	1836	90	72.3
60	1.46	0.434	76.9	1836	116	80.6
61	1.46	0.434	77.0	1836	45	48.5
62	1.42	0.405	77.3	1836	120	80.3
63	1.55	0.565	77.3	1900	120	84.7
64	1.58	0.579	77.0	1925	105	81.8
65	1.62	0.579	77.9	1925	30	40.6
66	1.56	0.590	77.6	1950	45	55.3
67	1.56	0.590	77.6	1950	72	69.7

TABLE V-B

Average Carbon Content = 31.4 ± 0.5 % wt
Pellet Diameter = 0.826 cm
Chlorine Concentration = 100 %

No.	Gas (g/s)	Swirl/ Radial	ZrO_2 Content (wt %)	Pellet Temperature (K)	Reaction Time (s)	Conversion (wt %)
68	1.45	0.420	67.2	1449	180	47.8
69	1.46	0.434	68.3	1466	135	39.9
70	1.46	0.434	68.6	1585	135	63.9
71	1.37	0.462	68.5	1585	180	72.6
72	1.40	0.362	68.8	1585	165	68.7
73	1.41	0.510	69.2	1642	135	69.3
74	1.47	0.434	68.0	1653	102	60.5
75	1.47	0.434	69.4	1653	105	61.4
76	1.47	0.434	69.3	1721	90	62.9
77	1.47	0.434	67.9	1750	75	56.4
78	1.47	0.434	69.8	1767	105	69.4
79	1.47	0.434	67.7	1830	75	58.5

TABLE V-C

Average Carbon Content = 42.5 ± 0.4 % wt
Pellet Diameter = 0.826 cm
Chlorine Concentration = 100 %

No.	Gas (g/s)	Swirl/ Radial	ZrO_2 Content (wt %)	Pellet Temperature (K)	Reaction Time (s)	Conversion (wt %)
80	1.46	0.434	56.2	1398	195	35.8
81	1.47	0.434	57.9	1443	120	29.8
82	1.46	0.420	55.2	1443	198	46.5
83	1.46	0.420	56.1	1443	270	58.1
84	1.47	0.420	55.4	1443	330	63.7
85	1.46	0.420	55.7	1443	420	72.7
86	1.46	0.434	56.6	1477	180	47.9
87	1.46	0.434	56.6	1535	120	44.6
88	1.43	0.420	57.2	1535	190	34.5
89	1.47	0.434	57.6	1535	180	58.5
90	1.47	0.434	56.6	1535	60	28.7
91	1.44	0.405	59.4	1535	426	87.1
92	1.47	0.434	56.8	1535	330	78.5
95	1.47	0.434	56.7	1535	270	73.3
96	1.20	0.531	59.8	1558	150	53.8
97	1.47	0.434	56.6	1558	135	52.5
98	1.44	0.405	57.7	1642	141	65.3
99	1.45	0.405	60.7	1642	90	47.9
100	1.39	0.362	56.0	1653	120	62.9
101	1.46	0.405	58.2	1653	120	63.0
102	1.45	0.405	57.9	1676	45	36.9
103	1.44	0.405	57.0	1676	150	72.4
104	1.44	0.405	57.9	1676	240	87.1
105	1.45	0.405	57.2	1676	180	78.8
106	1.46	0.434	58.6	1676	315	93.5
107	1.45	0.405	57.6	1676	255	89.2
108	1.44	0.405	57.4	1676	75	49.9
109	1.40	0.376	57.5	1676	105	61.9
110	1.45	0.405	59.6	1761	105	63.3
111	1.45	0.405	58.9	1761	84	54.1
112	1.45	0.405	58.3	1761	60	45.3
113	1.44	0.405	57.1	1761	240	87.7
114	1.44	0.405	59.2	1761	150	75.8
115	1.44	0.405	57.5	1761	30	31.6
116	1.45	0.405	57.2	1807	57	44.9
117	1.45	0.405	58.8	1807	210	84.9

TABLE V-D

Average Carbon Content = 18.0 ± 0.4 % wt
Pellet Diameter = 0.826 cm
Chlorine Concentration = 100 %

No.	Gas (g/s)	Swirl/ Radial	ZrO_2 Content (wt %)	Pellet Temperature (K)	Reaction Time (s)	Conversion (wt %)
118	1.39	0.421	81.6	1437	180	43.1
119	1.36	0.429	81.7	1446	135	36.8
120	1.40	0.383	82.0	1457	75	24.3
121	1.42	0.420	81.9	1545	120	49.9
122	1.44	0.413	82.6	1548	60	31.0

Average Carbon Content = 20.2 ± 0.7 % wt
Pellet Diameter = 0.826 cm
Chlorine Concentration = 100 %

123	1.47	0.434	78.6	1437	180	43.0
124	1.45	0.434	80.9	1449	77	24.0
125	1.42	0.376	79.7	1449	120	35.4
126	1.46	0.434	79.8	1539	150	58.3
127	1.45	0.405	80.2	1539	60	30.2

TABLE V-D

Average Carbon Content = 18.0 ± 0.4 % wt
Pellet Diameter = 0.826 cm
Chlorine Concentration = 100 %

No.	Gas (g/s)	Swirl/ Radial	ZrO_2 Content (wt %)	Pellet Temperature (K)	Reaction Time (s)	Conversion (wt %)
118	1.39	0.421	81.6	1437	180	43.1
119	1.36	0.429	81.7	1446	135	36.8
120	1.40	0.383	82.0	1457	75	24.3
121	1.42	0.420	81.9	1545	120	49.9
122	1.44	0.413	82.6	1548	60	31.0

Average Carbon Content = 20.2 ± 0.7 % wt
Pellet Diameter = 0.826 cm
Chlorine Concentration = 100 %

123	1.47	0.434	78.6	1437	180	43.0
124	1.45	0.434	80.9	1449	77	24.0
125	1.42	0.376	79.7	1449	120	35.4
126	1.46	0.434	79.8	1539	150	58.3
127	1.45	0.405	80.2	1539	60	30.2

TABLE V-E

Average Carbon Content = 23.1 % wt
Pellet Diameter = 0.671 cm
Chlorine Concentration = 100 %

No.	Gas (g/s)	Swirl/ Radial	ZrO_2 Content (wt %)	Pellet Temperature (K)	Reaction Time (s)	Conversion (wt %)
128	1.36	0.429	76.7	1420	165	40.9
129	1.44	0.434	75.4	1466	120	40.9
130	1.34	0.406	76.5	1480	165	53.4
131	1.44	0.434	76.0	1480	105	40.9
132	1.45	0.405	76.5	1494	135	50.3
133	1.47	0.434	75.1	1500	180	62.7
134	1.47	0.434	77.7	1500	120	47.1
135	1.46	0.434	76.4	1500	78	36.3
136	1.47	0.434	75.9	1500	270	69.6
137	1.47	0.434	77.2	1500	360	72.2
138	1.43	0.405	76.7	1556	150	62.9
139	1.44	0.405	76.9	1687	108	73.3
140	1.45	0.405	77.3	1687	78	61.2
141	1.47	0.434	77.1	1778	78	72.6
142	1.45	0.405	77.1	1807	75	71.7
143	1.45	0.434	76.3	1807	105	85.7
144	1.44	0.405	76.6	1836	75	77.1
145	1.47	0.434	77.1	1836	135	94.6

TABLE V-F

Average Carbon Content = 23.1 % wt
Pellet Diameter = 1.00 cm
Chlorine Concentration = 100 %

No.	Gas (g/s)	Swirl/ Radial	ZrO_2 Content (wt %)	Pellet Temperature (K)	Reaction Time (s)	Conversion (wt %)
146	1.47	0.434	76.1	1454	150	41.4
147	1.41	0.405	76.0	1483	150	46.4
148	1.40	0.405	76.2	1557	135	59.1
149	1.44	0.434	76.0	1636	165	76.5
150	1.44	0.434	76.5	1636	165	74.4
151	1.44	0.405	77.0	1653	105	61.7
152	1.48	0.434	77.3	1653	135	72.4
153	1.47	0.434	76.7	1653	126	69.6
154	1.47	0.573	76.8	1710	100	63.0
155	1.48	0.434	77.1	1750	104	67.0

TABLE V-G

Average Carbon Content = 23.1 % wt

Pellet Diameter = 0.826 cm

No.	Gas (g/s)	Swirl/ Radial	ZrO_2 Content (wt %)	Pellet Temp. (K)	Chlorine Concent. (mole%)	Reaction Time (s)	Conversion (wt %)
156	1.13	0.420	77.2	1562	59.0	150	48.2
157	1.30	0.450	77.6	1636	69.4	135	65.1
158	1.00	0.391	77.6	1642	54.6	300	83.9
159	1.39	0.458	77.5	1647	82.0	107	62.3
160	0.77	0.515	78.3	1653	31.1	165	48.8
161	1.11	0.419	77.9	1653	60.0	60	34.8
162	1.11	0.419	77.7	1653	60.0	195	72.5
163	1.12	0.410	77.6	1653	58.7	150	63.3
164	1.51	0.447	78.3	1676	91.4	105	67.8
165	0.84	0.400	77.7	1687	40.7	150	56.9